Expression of factors within tumours to reverse immune suppression

Phil Jakeman

Biochemistry, B.Sc. A.R.C.S (Imperial College London)

Linacre College

University of Oxford

A thesis submitted for the degree of Doctor of Philosophy

to the Department of Oncology, University of Oxford.

Michaelmas Term 2015

Supervisors: Dr. Kerry Fisher and Dr. Shisong Jiang

Expression of factors within tumours to reverse immune suppression

Phil Jakeman

Linacre College, University of Oxford

A thesis submitted for the degree of Doctor of Philosophy,
to the Department of Oncology University of Oxford.

Michaelmas Term 2015

Abstract

Macrophages are important immune cells that play central roles in both health and disease. They display a broad phenotypic diversity, although for simplicity two distinct subtypes have been denoted 'M1' and 'M2'. While this nomenclature is overly simple, it does provide a useful framework for classifying different macrophages. M1 macrophages are largely characterised by their pro-inflammatory, disease-fighting functions, whereas M2 macrophages are involved in wound healing, tissue remodelling and immune suppression. Macrophages are often present at high numbers within solid tumours, and although this was historically expected to correlate with a good prognosis, in fact, most 'tumour-associated macrophages' (TAMs) are more M2-like and can support tumour development and growth. This thesis aims to assess the plasticity of TAMs and to determine whether and how TAMs might be 're-educated' to become more M1-like, potentially thereby switching from their tumour-supporting role to a tumour-killing function. The overarching purpose is to develop an oncolytic adenovirus capable of killing tumour cells but genetically 'armed' to express biological mediators locally to re-educate TAMs and activate their tumour-killing activities.

A variety of human and murine macrophages were studied in this thesis, including cell lines and primary cells from malignant ascites. Macrophage polarisation was measured,

and the potential for re-education from M2 to M1 was assessed using gamma interferon (IFN-γ) with and without lipopolysaccharide (LPS). Morphological (e.g. Major histocompatibility complex (MHC) class II expression) and functional re-education (e.g. production of nitric oxide, NO) were both achieved using IFN-γ alone, although this was more effective when the original M2-polarising environment was removed. Interestingly only M1-polarised macrophages showed the ability to cross present antigens, both as free peptides and as tumour-associated proteins. An oncolytic group B adenovirus was synthesised, based on ColoAd1, expressing IFN-γ (murine and human versions for different applications) and the effect of exposing macrophages to virus particles or to the lysates of virus-infected cancer cells was explored. Virus alone showed an intriguing ability to functionally re-educate M2 macrophages, assessed by NO production, although this was dramatically enhanced when it encoded IFN-γ. The IFN-γ-expressing virus also showed greater re-education activity than free IFN-γ, probably reflecting the short *in vitro* half-life of IFN-γ when given as a free cytokine, which can be overcome by continual production from virus-infected tumour cells. This might be coupled with the intrinsic ability of the virus to stimulate pro-inflammatory macrophage responses. Overall this thesis shows a high level of plasticity between macrophage subtypes, and a clear potential for re-education of M2 macrophages to a more pro-inflammatory phenotype using genetically modified oncolytic viruses.

Acknowledgements

I would like to thank my supervisors Dr. Kerry Fisher and Dr. Shisong Jiang for their support during my D.Phil. and for making it such a fun experience. I am thoroughly indebted to Professor Len Seymour for affording me the opportunity to study in his lab all those years ago, and for his continued support and guidance throughout the D.Phil. project and the writing of the thesis. Without doubt, I would not have had the same experience in Oxford and would not have been able to have such an engaging and exciting project were it not for Len.

I would like to thank the all the Seymour lab members for their encouragement and friendship over the years, with a particular mention to Dr. Tom Hills, Dr. Clemens Thoma, Dr. Aliaa Alamoudi and Dr. Gray Kueberuwa whose lively scientific discussions made the science so much fun from the start of my time in the lab. I would like to thank Christina Woodward for her continued support, and never-ending help throughout the years.

I wish to thank Hege for keeping me sane and providing me all the support I needed to get through the final year and the writing of my thesis. I couldn't have been able to do it without you.

This thesis however, is dedicated to my parents. Their never-ending encouragement, love, inspiration and support have made me everything that I am today. They nurtured a curious mind from a very young age and have only ever encouraged me to follow my passions in life.

Table of contents

ABSTRACT 2

ACKNOWLEDGEMENTS 4

TABLE OF CONTENTS 5

LIST OF FIGURES 9

LIST OF ABBREVIATIONS 14

INTRODUCTION 17

1.1 Background and context to the thesis 18

1.2 Macrophages 23

1.2.1 Macrophage Polarisation and classification 23
1.2.2 Macrophages in wound healing, repair and homeostasis 26
1.2.3 Macrophages in the immune system 27

1.3 Macrophages in tumours 30

1.3.1 Tumour-promoting functions of macrophages 30
1.3.1.1 Promotion of tumour growth and metastasis 31
1.3.1.2 Stimulation of angiogenesis 35
1.3.1.3 Macrophages in hypoxic regions of tumours 36
1.3.1.4 Mediation of immune suppression 42
1.3.1.5 Interactions of TAMs with anti-cancer therapies 48
1.3.2 Anti-tumour functions of macrophages 51

1.4 TAMs as a therapeutic target 55

1.4.1 Inhibition of macrophage recruitment 55
1.4.2 Depletion of TAMs 59
1.4.3 Inhibition the suppressive funciton of TAMs 62
1.4.4 “Re-education” of TAMs 64

1.5 Oncolytic viruses 72

1.5.1 Oncolytic virus specificity: cancer cell receptors 73

1.5.2 Oncolytic virus specificity: genetic engineering to exploit cancer signalling 73
1.5.3 Oncolytic virus specificity: defective interferon signalling in tumours 75
1.5.4 ColoAd1 78

1.6 Thesis aims and hypothesis 82

1.6.1 Thesis aims 82
1.6.2 Thesis hypothesis 82

2 MATERIALS AND METHODS 83

2.1 Cell lines 84

2.1.1 Cell line maintenance and sub-culturing 84
2.1.2 Mycoplasma testing 86

2.2 *In vivo* experimentation 87

2.2.1 Housing conditions 87
2.2.2 Intraperitoneal tumour injection and sample collection 88
2.2.3 *In vivo* treatment of ovarian ascites 89
2.2.4 *Ex vivo* treatment of murine ovarian ascites 89

2.3 Patient samples 90

2.3.1 *Collection and processing* 91
2.3.2 *Ex vivo* culturing 92

2.4 Production of IFN-γ-expressing ColoAd1 92

2.4.1 Molecular biology techniques for ColoAd-1 cloning 92
2.4.2 Cloning of human and murine IFN-γ into ColoAd1 97
2.4.3 Growth and purification of ColoAd1-h IFN-γ and ColoAd1-m-IFN-γ 99
2.4.4 Characterisation of IFN-γ-expressing ColoAd1 102

2.5 Cellular Assays 103

2.5.1 MTS viability assay 103
2.5.2 Flow cytometry 104
2.5.3 Enzyme-linked immunosorbent assay (ELISA) 116

2.6 Data processing and statistical analysis 118

3 PRODUCTION OF COLOAD1 VIRUSES "ARMED" WITH HUMAN AND MURINE IFN-γ 119

3.1 Introduction 120

3.1.1 Chapter aims 120

3.2 Results 121

3.2.1 Production of ColoAd1 viruses armed with human or murine IFN-γ virus 121

3.2.2 *In vitro* characterisation of virus 126

3.3 Discussion of results 135

4 USE OF CELL PHENOTYPE TO ASSESS MACROPHAGE POLARISATION AND PLASTICITY 139

4.1 Introduction 140

4.1.1 Chapter aims 143

4.2 Results 144

4.2.1 Studying murine macrophage polarisation 144

4.2.2 Studying human macrophage polarisation 150

4.2.3 Polarising THP-1 macrophages using tumour cell lines 165

4.2.4 Developing a co-culture model for more realistic studies of macrophage polarisation and re-education 171

4.3 Discussion of results 179

5 FUNCTIONAL OUTCOMES OF MACROPHAGE POLARISATION 184

5.1 Introduction 185

5.1.1 Chapter aims 188

5.2 Results 189

5.2.1 Nitric Oxide production 189

5.2.2 Phagocytosis is an effective functional marker of macrophage polarisation 203

5.2.3 Cross presentation of antigen by differentially polarised macrophages 210

5.3 Discussion of results **234**

6 STUDIES OF MACROPHAGE POLARISATION AND RE-EDUCATION USING TRANSLATIONAL MODELS **246**

6.1 Introduction **247**

6.1.1 Chapter aims 250

6.2 Results **251**

6.2.1 Developing a murine xenograft mode of ovarian peritoneal ascites 251

6.2.2 Studies into human macrophage polarisation using the ascitic fluid from patients with ovarian cancer 263

6.2.3 *Ex vivo* treatments of human ovarian ascites 275

6.2.4 Short term *ex vivo* infection of ascitic cells from patients 281

6.3 Discussion of results **288**

7 GENERAL DISCUSSION AND CONCLUSIONS **298**

7.1 Principal findings **298**

7.2 General discussion **299**

7.3 Future work **301**

7.4 Conclusions **304**

8 REFERENCES **305**

List of figures

Figure 1.1 Tumour-mediated Immunosuppression 22

Figure 1.2 The M1 / M2 paradigm of macrophage polarisation 25

Figure 1.3 The tumour-promoting functions of TAMs 32

Figure 2.1 ColoAd1 Cloning overview 98

Figure 2.2 Rescue of ColoAd1 viruses expressing murine and human IFN-γ 99

Figure 2.3 Removing dead cell from flow cytometric analysis 106

Figure 2.4 Studying cellular phagocytosis by flow cytometry 111

Figure 2.5 Optimisation of SIINFEKL cross-presentation using murine dendritic cells 113

Figure 2.6 Gating strategy for cross-presentation of SW480 lysate 115

Figure 3.1 Cloning strategy for inserting IFN-γ into ColoAd1 123

Figure 3.2 Sub-cloning of murine and human IFN-γ into the ColoAd1 backbone 125

Figure 3.3 Concentrations of engineered ColoAd1 viruses 127

Figure 3.3 Oncolysis of IGROV-1 cells by ColoAd1-IFN-γ 128

Figure 3.4 Production of IFN-γ by ColoAd1 armed with murine or human IFN-γ 130

Figure 3.5 Infecting human and murine macrophages with ColoAd1 132

Figure 3.6 Assessing production of IFN-γ following virus infection 134

Figure 4.1 Differentially polarised murine macrophages display varied receptor expression 145

Figure 4.2 M2 murine macrophages can be re-educated using IFN-γ *in vitro* 148

Figure 4.3 Re-educated murine macrophages exhibit changes in TNF-α production 149

Figure 4.4 PMA differentiation of THP-1 monocytes into macrophages 151

Figure 4.5 Experimental strategy for creation of differentially polarised THP-1 macrophages over a 24-hour exposure 153

Figure 4.6 Differentially polarised THP-1 macrophages display varied receptor expression and cytokine production after 24 hours 155

Figure 4.7 Experimental strategy for creation of differentially polarised THP-1 macrophages over 48 hours using two consecutive 24-hour exposures 156

Figure 4.8 Receptor expression by macrophages differentially polarised using the 48 hour exposure protocol 157

Figure 4.9. Experimental strategy for creation of differentially polarised macrophages over 48 hours using two consecutive 24 hour exposures 158

Figure 4.10 Receptor expression by macrophages differentially polarised using the 48 hours exposure protocol 159

Figure 4.11 Schematic of *in vitro* re-education of M2-polarised macrophages 161

Figure 4.12 *In vitro* re-education of M2-polarised macrophages 162

Figure 4.13 Comparison of "re-education" in the presence or absence of M2 media 163

Figure 4.14 Comparison of TNF-α expression in "re-educated" macrophages 164

Figure 4.15 Polarisation of human macrophages by supernatants 166

Figure 4.16 Schematic for re-education of tumour supernatant polarised macrophages 168

Figure 4.17 Re-education of tumour supernatant polarised macrophages 168

Figure 4.18 Re-education of tumour supernatant polarised macrophages; TNF-α readout 169

Figure 4.19 Development of a IGROV :macrophage co-culture model 172

Figure 4.20 Re-polarising THP-macrophages in co-culture with tumour cells using ColoAd1 , ColoAd1-hIFNγ or hIFNγ 174

Figure 4.21 Co-culture of SW80 and THP-1 polarises toward an M2 type macrophage 176

Figure 4.22 Re-polarising THP-macrophages in co-culture with SW480 cells using ColoAd1 , ColoAd1-hIFNγ or hIFNγ 177

Figure 5.1 Nitric Oxide production by differentially polarised macrophages 191

Figure 5.2 NO production by differentially polarised human and mouse macrophages 192

Figure 5.3 Schematic for re-education of M2 polarised murine macrophages using NO as a readout 194

Figure 5.4 NO can demonstrate re-education of M2 polarised murine macrophages 195

Figure 5.5 NO can demonstrate re-education of human macrophages 197

Figure 5.6 ColoAd1 can induce NO production in human macrophages 200

Figure 5.7 ColoAd1 treated macrophages show increased NO production 202

Figure 5.8 Uptake of zymosan by differentially polarised murine macrophages 205

Figure 5.9 Uptake of Dextran by differentially polarised macrophages of murine and human origin 207

Figure 5.10 Uptake of OVA by mouse and human macrophages 209

Figure 5.11 Cross-presentation of SIINFEKL by peritoneal-derived mouse macrophages 212
Figure 5.12 Antigen presentation of SIINFEKL by IC-21 murine macrophages 215
Figure 5.13 Processing of OVA antigen by murine macrophages 217
Figure 5.14 Cross-presentation of full-length OVA by murine dendritic cells 219
Figure 5.15 IC-21 macrophages do not cross-present full length OVA 220
Figure 5.16 Generation of polyclonal anti-OVA serum 221
Figure 5.17 Uptake of OVA by mouse and human macrophages 223
Figure 5.18 IC21 cannot cross present full length OVA, even when opsonised 224
Figure 5.19 M1-polarised macrophages can cross-present B16OVA tumour antigen 227
Figure 5.20 Polarisation of IC-21 macrophages determines the ability to phagocytose B16-OVA cells 229
Figure 5.21 Phagocytosis of virus-infected p53-positive tumour cells 232
Figure 5.22 Cross presentation of virus-infected p53-positive tumour cells 233
Figure 6.1 Development of a peritoneal IGROV-1 xenograft model 252
Figure 6.2 Phenotype of peritoneal macrophages during ascites formation 254
Figure 6.3 Cellular composition of murine peritoneal ascites 256
Figure 6.4 *Ex vivo* treatment of peritoneal ascites 258
Figure 6.5 Effects of *in vivo* treatment on the composition of murine peritoneal ascites 260
Figure 6.6 Phenotype of murine ascitic macrophages after treatment *in vivo* 262
Figure 6.7 Receptor profiles of macrophages polarised with ovarian ascitic fluid 264
Figure 6.8 Re-education of ascites polarised macrophages 267
Figure 6.9 Re-education of ascites-polarised THP-1 macrophage with supernatant from virus- lysed tumour cells 270
Figure 6.10 Ascites polarised macrophages display a similar functional behaviour profile to that of M2 macrophages 272
Figure 6.11 Virus can mediated macrophage re-education from ascites treated macrophages through NO induction 274
Figure 6.12 Fluid from malignant ascites inhibits infection of A549 cells 276
Figure 6.13 Inhibitory effects of ascites are concentration dependent 278
Figure 6.14 Inhibitory effects are mediated through neutralisation and pre-conditioning of cells 280

Figure 6.15 Immune profiling of Ascitic cells 282

Figure 6.16 GFP infection of patient samples 284

Figure 6.17 IFNγ production by infection of patient samples with ColoAd-hIFNγ 285

Figure 6.18 Immune modulation of macrophage phenotypes *ex vivo* 286

List of tables

Table 1. Common strategies for targeting TAM 56

Table 2.1. Cell lines 86

Table 2.2. Patient samples 91

Table 2.3. DNA ligation reaction composition 95

Table 2.4 Primers for addition of restriction endonuclease sites 96

Table 2.5 PCR Protocol 96

Table 2.6 Recipe for virus banding dialysis buffer 100

Table 2.7 List of antibodies used for flow cytometry 108

Table 3.1 Concentrations of engineered ColoAd1 viruses 127

Table 4.1 Major immunomodulatory receptors of macrophages 142

List of abbreviations

ABC	ATP-binding cassette
ADCC	Antibody-dependent cellular cytotoxicity
ADCP	Antibody-dependent cellular phagocytosis
Ad5	Adenovirus serotype 5
Ad11	Adenovirus serotype 11
ATF-4	Activating transcription factor-4
APC	Antigen presenting cell
BAL	Bronchoalveolar lavage
Bp	Base pairs
CAR	Coxsackie and adenovirus receptor
CCL-22	Chemokine (C-C motif) ligand 22
CPA	Cyclophosphamide
CPE	Cytopathic effect
dH_2O	De-ionised H_2O
DAMP	Danger-associated molecular pattern
DMEM	Dulbecco's modified essential medium
EGF	Epidermal growth factor
EGR-1	Early growth response -1
ER	Endoplasmic reticulum
ERAP-1	Endoplasmic reticulum amino-peptidase
ECM	Extra-cellular matrix
EDTA	Ethylenediaminetetracetic acid
Fc	Fragment crystalisable
FBS	Fetal bovine serum
FITC	Fluorescein Isothiocyanate
GILT	Gamma-interferon-inducible lysosomal thiol-reductase
Gp33	glycoprotein 33, from lymphocytic choreomeningitis virus
Gy	Gray units of absorbed radiation
HIF	Hypoxia inducible factor
HRP	Horse radish peroxidase
IFN	Interferon

IFN-α	Interferon-alpha
IFN-β	Interferon-beta
IFN-γ	Interferon-gamma
IL-10	Interleukin-10
ISG	Interferon-stimulated genes
I-κB	Inhibitor of kappa-light chain enhancer of activated B cells
iNOS	Inducible Nitric Oxide synthase
I.P.	Intra-peritoneal
I.T.	Intra-tumoural
I.V.	Intra-venous
JAK-STAT	Janus kinase-signal transducers and activators of transcription factor
Kb	Kilo base
L-Arg	L-arginine
LB	Luria Bertani
LCMV	Lymphocytic choreomeningitis virus
LDI	Low dose irradiation
LPS	lipopolysaccharide
MCP-1	Macrophage chemoattractant protein 1
M-CSF	Macrophage colony stimulating factor
MHC	Major histocompatibility complex
mmHg	Millimeter of Mercury
NF-κB	Nuclear factor -kappa-light chain enhancer of activated B cells
NIR	Near-infra red
NK	Natural Killer
NO	Nitric oxide
PAMP	Pathogen-associated molecular pattern
PBS	Phosphate buffered saline
PFU	Particle forming units
PGE-2	Prostaglandin E2
PKR	Protein kinase RNA-activated
Poly I:C	Polyinosinic: polycytidylic acid
PS	Phosphatidylserine
PSA	Prostate-specific antigen

$Rag^{-/-}$	Recombination activation gene-deficient mice
RANTES	Regulated on activation, normal T cell expressed and secreted
Rb	Retinoblastoma protein
RPM	Revolutions per minute
SCF	Stem cell factor
SD	Standard deviation
SDF	Stromal cell derived factor
SOC	Super optimal broth media
SOCS	Suppressor or cytokine signalling
STAT	Signal transducers and activators of transcription factor
TAM	Tumour-associated macrophage
TAMs	Tumour-associated macrophages
TAP	Transporter-associated with antigen processing
TCA	Tri-carboxylic acid
TGF-β	Transforming growth factor-beta
TLR	Toll like receptor
TNF-α	Tumour necrosis factor-alpha
Treg	Regulatory T cells
UV	Ultraviolet
VEGF	Vascular endothelial growth factor
Vp	Virus particles
VPC	Virus particles per cell
Vp /mL	Virus particles per mL
w/v	Weight per volume

Chapter 1

Introduction

Introduction

1.1 Background and context to the thesis

Cancer is a disease with a significant burden of morbidity and mortality; in the United Kingdom, it impacts the quality of life of close to half the population and is the underlying cause of death for around one in every three people (Sasieni et al., 2011). The prevalence of cancer is partly the inevitable consequence of an aging population living in a society where other illnesses are managed more successfully. Early diagnosis, surgery and lifestyle changes can push back the time that cancer impacts on quality of life, but ultimately cancers are likely to arise in any individual, given enough time. With this in mind, disease management, as much as disease cure, needs to be at the center of our approaches to intervene and care for those afflicted. Where cancer has advanced beyond the point of curative surgery, understanding the structure and composition of tumours becomes very important for treatment.

Tumours are made up of multiple cell populations all of which are derived from the host making distinguishing 'self' from 'non-self' extremely difficult (Zou, 2005). In advanced cancer, transformed cells may only be contributing to a proportion of the tumour mass, frequently less than 50%, with the remainder comprised of stromal cells such as leukocytes, fibroblasts and endothelial cells (Fridman et al., 2012). Within both the transformed cells and the stromal compartments there can be multiple populations with adaptations to cope with metabolic stress such as hypoxia, facilitating metastasis on a background of a wide range of differentiation states.

With complexity and diversity being central to disease progression, it is unsurprising that efforts to develop highly specific drugs against individual pathways have largely failed to provide durable responses in the clinic (Hait, 2010). Resistance and outgrowth of cell populations under therapeutic selection pressures is the all too frequent outcome, especially during single or repeated application of the same therapeutic agent.

An alternative approach to highly specific drug targets is to focus on broadly applicable 'hallmarks' of cancer (Hanahan and Weinberg, 2000). Regardless of transforming mutations or cell of origin, cancers exhibit the same set of overarching characteristics such as cell cycle dysregulation and the circumvention of immune responses. Interventions that impact on one of these underlying features can have dramatic therapeutic effects, but equally can cause severe side effects. Cell cycle-selective chemotherapy, for example, remains a central theme in the treatment of colorectal cancer using platinum drugs and antimetabolites such as 5-Fluorouracil. However these agents act simply to cause toxicity to rapidly growing cells, either by interfering with synthesis of thymidine (required for DNA but not RNA) or causing sufficient DNA damage to trigger apoptosis. Non-transformed normal cells that require rapid or continuous turnover are also exposed to toxicity, and this includes cells such as the bone marrow (where the immune system is highly active in maintaining a continuous defence against pathogens) and also in rapid-turnover epithelial surfaces. Hence, with little to distinguish an active tumour cell from a dividing normal cell, broad cytotoxic activity goes hand-in-hand with toxicities to mucosal surfaces and bone marrow

Tumour-induced immune suppression and the associated evasion of tumour immunosurveillance is central to tumour progression (*Figure 1.1)* The immune environment, however, is one hallmark of cancer that can in principle be broadly

exploited across different tumour cell populations while maintaining a selective capability (Hanahan and Weinberg, 2011). Utilising the adaptive immune system to combat cancer is an intensive area of research with emerging technologies including Chimeric Antigen Receptor- (CAR-) T cells, bispecific molecules (Immune mobilising monoclonal T cell receptors against cancer (ImmTACs), Bispecific T cell engagers (BiTEs) etc) and checkpoint inhibitor antibodies designed to facilitate or enable cytotoxic destruction of transformed cells (Naidoo et al., 2014). While these approaches are finding success in certain tumour subtypes, it is unlikely that reliance on the adaptive immune response alone will be sufficient for treating most cancers. The innate immune response underlies the adaptive immunological response in cancer patients, and it is the innate immune system that really defines the general immune environment within diseased areas. Innate immune cells mediate multiple functions that can impact on tumour progression, from direct tumouricidal activity through to facilitation of tumour growth and metastasis (Gajewski et al., 2006).

Macrophages in particular appear to play an important role in cancer initiation, development and progression (Solinas et al., 2009). In late stage disease, macrophages are usually associated with poor outcomes and the suppression of functional immune responses (Petrillo et al., 2015; Ruffell et al., 2012b; Sica and Mantovani, 2012). Macrophages can be highly specialised in their role in healthy tissue and in disease, but they are also known to be somewhat plastic and capable of changing phenotype, depending on circumstance (Biswas et al., 2008).

The central purpose of this thesis is to identify the extent to which tumour macrophages can be 're-educated' towards an anti-cancer activity, starting from a phenotype that is, at

best, indifferent to cancer growth but, at worse, facilitates tumour progression. The strategy employed here to mediate re-education of tumour-associated macrophages is based on the use of oncolytic viruses encoding interferon gamma (IFN-γ), designed to express IFN-γ only when the cancer-selective virus replicates within tumour cells, secreting IFN-γ into the extracellular tumour microenvironment where it can act on local macrophages.

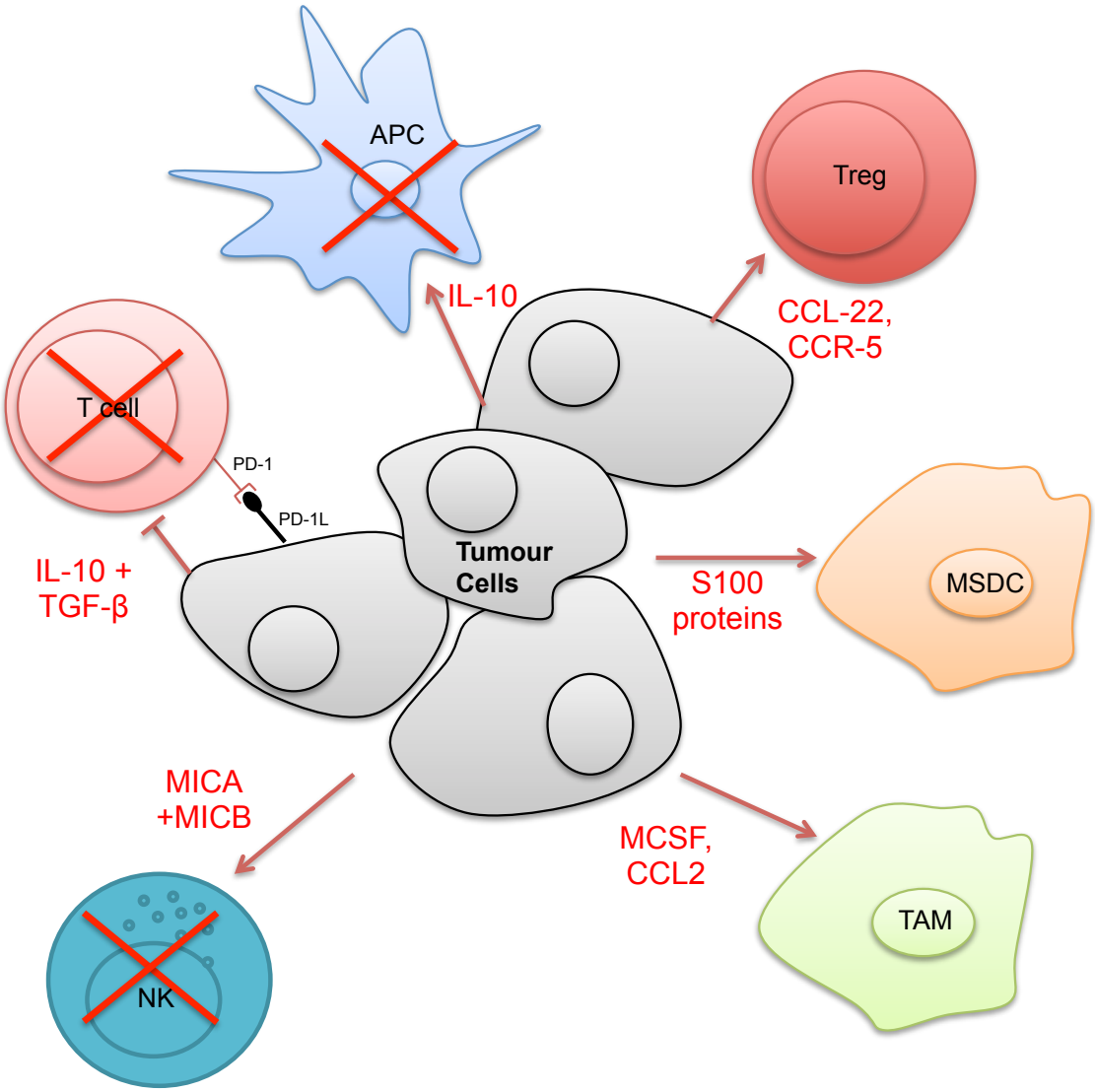


Figure 1.1 Tumour-mediated Immunosuppression

Tumours mediate a number of immunosuppressive strategies. Immunosuppressive cytokines such as IL-10 and TGF-β can inhibit CD8 T cell function and suppress antigen presenting cell function. Chemokines such as CCL2 and CCL22 can recruit suppressive cell types such as regulatory T cells (Treg) and tumour –associated macrophages (TAM). Release of soluble stress ligand MICA and MICB inhibit natural killer (NK) cell function, whilst soluble pro-inflammatory S100 family proteins facilitate myeloid derived suppressor cell (MDSC) accumulation.

1.2 Macrophages

1.2.1 Macrophage Polarisation and classification

Macrophages represent one of the most pleiotropic cell types in the human body, attributed with a range of functions central to basic homeostasis. The original characterisation of macrophage activation was studied using a stimulation with IFN-γ and TNF-α, which in turn generated a population of macrophages with high anti-microbial/-bacterial capacity, characterised by high levels of pro-inflammatory cytokines such as IL-1, IL-6 and TNF-α along with increased reactive oxygen species (Mosser and Edwards, 2008). These "classically activated" macrophages were shown to elicit potent anti- microbial functions and are central in orchestrating pro-inflammatory immune responses to infection and other pathologies (Martinez et al., 2008). Lipopolysaccharide (LPS) has largely replaced TNF-α as the second stimulant used in cocktails of cytokines for classical activation although it acts largely through the same mechanism; binding and signalling through TLR-4 induces MyD88 signalling to stimulate TNF-α production in macrophages which acts in an autocrine manner to signal through TNF-receptors on macrophages (Allavena et al., 2011). Subsequently classically activated macrophages have been shown to be characterised by other pro-inflammatory cytokine secretion such as high IL-12 and IL-23 and additional functions such as the ability to present antigen in high capacity (Martinez et al., 2009).

"Alternative" macrophage activation was based on the work by Gordon *et al*. who showed that stimulation of macrophages with IL-4 induced signalling through the common IL-4 receptor chain to induce expression of the mannose receptor (Stein et al.,

1992). Importantly this work identified a distinct population of macrophages characterised by increased receptor expression, production of high levels of arginase instead of nitric oxide (NO) and as such, demonstrated significantly impaired ability to resolve microbial infection (Goerdt and Orfanos, 1999; Mosser, 2003; Rutschman et al., 2001).

On the basis of the functional differences between these two activation types, these differentially polarised macrophages were described as "M1" or "M2" respectively in analogy to the Th1/Th2 paradigm of CD4 T cell help. M2 macrophages were further subdivided, as it was shown that stimulation with IL-4/IL-13 ("M2a"), immune complexes in the presence of TLR ligands ("M2b") and IL-10 ("M2c") all induced M2 cells with slightly different functions (*Figure 1.2*) . Whilst all seemed capable of immunoregulation, M2a could resolve parasite infection, M2b promoted Th2 responses and M2c facilitated matrix remodeling (Mantovani et al., 2012). Despite such observations, these subtypes are commonly assumed to possess equivalent phenotype and function, and are grouped together as "alternative" macrophages despite noticeable differences between these M2 subsets. At the level of receptor expression, M2a express high levels of mannose and other scavenger receptors whilst M2b express CD86 and M2c predominately express CD163 (Martinez and Gordon, 2014). Generally, M2-type macrophages are defined by reduced expression of pro-inflammatory cytokines however, M2b present an exception as they produce high levels of IL-10 with simultaneous release of pro-inflammatory cytokines (Mantovani et al., 2004). Another example is the case of arginase, which demonstrates enhanced expression in M2a and M2c-type macrophages, but does not for M2b-type macrophages, which can have functional consequences such as in the case of for T cell interaction (Mosser, 2003).

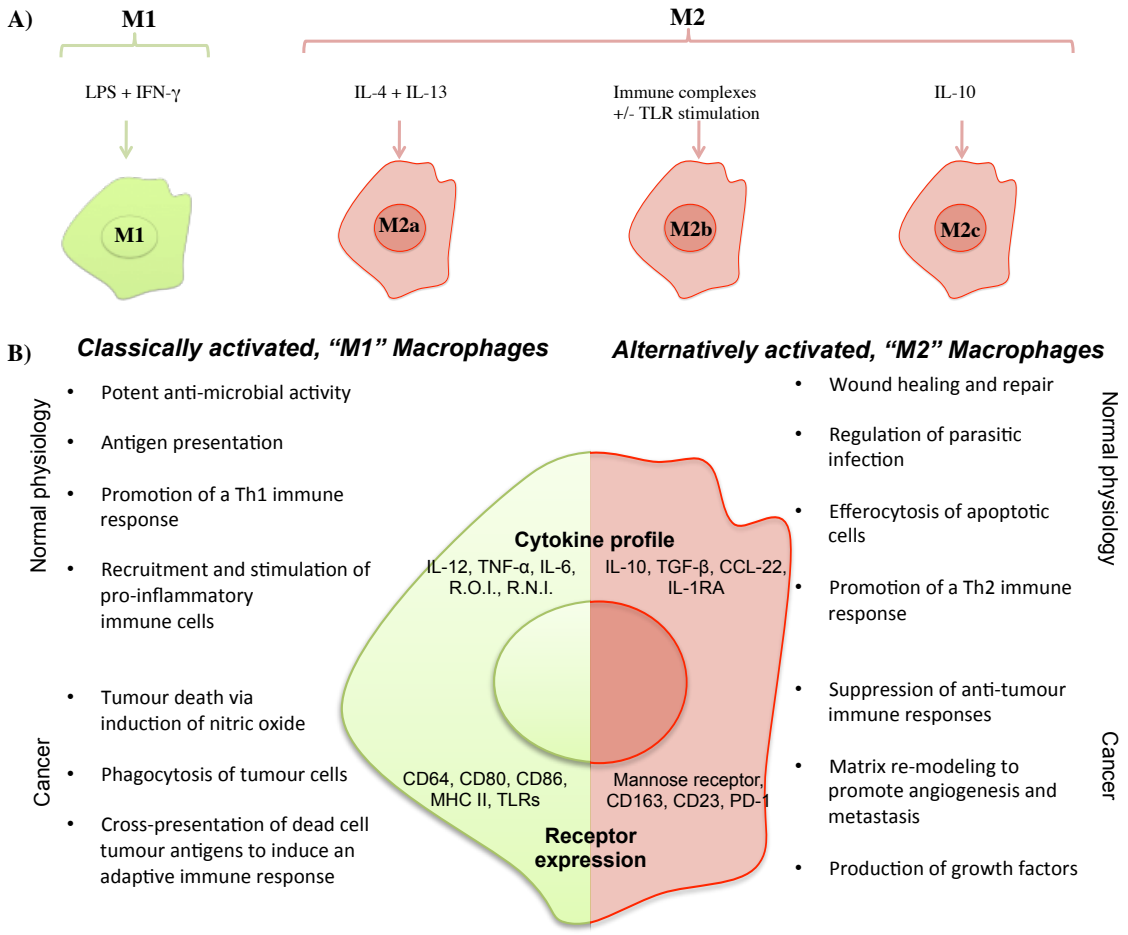


Figure 1.2 The M1 / M2 paradigm of macrophage polarisation.

A) Defined polarisation conditions yield distinct populations of macrophages, the "classically" activated M1 macrophage and the major M2 macrophage subtypes. **B)** A summary of the main functions of M1 and M2 type macrophages, including common cytokine and receptor profiles used to distinguish them

The M1 / M2 characterisation is most certainly a simplification, but it is a useful oversimplification that provides a framework which attempts to encapsulate the vast diversity of these cells. The task of characterising such a vast array of cell types is compounded by the plethora of stimuli to which macrophages are exposed and the ability of these cells to sequentially change phenotype in response to changing microenvironment (Stout et al., 2005). It is important to remember that "M1" and "M2" are macrophages generated by defined cytokines, in defined conditions and represent the extremes of macrophage polarisation (Martinez and Gordon, 2014). As such, the M1 and M2 designations should be thought of as broad distinctions of a more pro-inflammatory and a more anti-inflammatory/suppressive phenotype respectively (Biswas and Mantovani, 2010).

1.2.2 Macrophages in wound healing, repair and homeostasis

Macrophages are central in the regulation and maintenance of homeostasis, with some of their most documented roles linked to their function as profession phagocytes. The enhanced phagocytic ability of macrophages, and in particular M2-type macrophages, is of utmost importance in the clearance of dying cells throughout the body. Clearance of these cells is better described as efferocytosis, and is responsible for the removal of the apoptotic "corpses" of dying cells generated in the range of billions of cells daily. Macrophages are recruited by "find me" signals released by dying cells such as ATP and UTP, and subsequently stimulated to phagocytose by "eat me" signals such as phosphatidylserine exposure on the cell surface (Ravichandran, 2010). Importantly, the

M2 polarisation of these macrophages is central to making this an immunologically silent death through the production of immunosuppressive molecules such as PGE-2, VEGF, IL-10 and TGF-β, which act to dampen inflammation and recruit Tregs (Poon et al., 2014).

The induction of an immunosuppressive cytokine profile in M2 macrophages is critical for the regulatory functions of macrophages; both at the level of immune cell development but also at the regulation of wound healing and induction of repair processes. Here, the expression of matrix re-modeling proteases such as MMP-7 and MMP-7 facilitates repair, whilst the immunosuppressive cytokines such as IL-10 and TGF-β are able to prevent excessive inflammation (Mantovani et al., 2012). The integral nature of macrophage repair functions are exemplified in the case of chronic venous ulcers, where an absence of macrophages or dysfunction in macrophages prevents the resolution of inflammation and worsens the pathology (Sindrilaru et al., 2011).

1.2.3 Macrophages in the immune system

The diversity of macrophage function is well illustrated in their role played in the immune system, where macrophages interact with both innate and adaptive cells to initiate and regulate immune responses (Biswas and Mantovani, 2010). Chemokines represent a large component of the secreted soluble mediators release by macrophages. Chemokines such as CCL20 and CXCL 10 can attract other innate cells to the site of an infection, creating an influx and inflammatory cells within the infected area. Such cells

include natural killer (NK) and dendritic cells (DC), which upon their arrival can be further activated through the production of pro-inflammatory cytokines such as TNF-α, IFN-α, IL-6 and IL-12 (Biswas and Mantovani, 2010). Importantly, the recruitment and activation of other innate cells such as NK and DCs sustain pro-inflammatory signalling in a reciprocal fashion; activated NK cells can produce IFN-γ and IL-15 which can continue to activate macrophages, whilst production of IFN-α, IFN-β and IL-12 can stimulate NK cell function (Lapaque et al., 2009; Mortier et al., 2009) .

Macrophages might be considered analogous in their function to dendritic cells in that they possess the ability to co-ordinate- and interact with- both innate and adaptive arms of the immune system. As mentioned, the wide repertoire of cytokines and chemokines that macrophages possess endows them with a potent chemoattractant capacity. Macrophage-derived CXCL9, CCL15 and CCL20 are among some of the better documented chemokines with well defined roles in lymphocyte recruitment and lymphoid trafficking (Mantovani and Sica, 2010). CXCL9 has been associated with the induction of immune responses to acute infection (Hardison et al., 2006). For example, in a model of Chagas disease it was shown that CXCL9, CXCL10 and CCL5 predominate the chemokine profile in response to acute infection with *Trypanosoma cruzi*, with macrophages identified as the primary source of these cytokines. Antagonism of macrophages or macrophage-derived CXCL9 by neutralising antibodies in this setting caused an increased parasite load, attributed to decreased inflammatory cytokine production and decreased infiltration of CD8 T cells (Hardison et al., 2006). The CCL20-CCR6 axis has been described as a potent chemo-attractant for TH17 and Treg cells (Cook et al., 2014; Yamazaki et al., 2008), and is implicated in the pathogenesis of a number of inflammatory disorders such as ulcerative colitis, irritable

bowel syndrome and Crohn's disease (Lee et al., 2013). In a study cohort of patients with gastritis, chemotaxis assays were used to demonstrate that T cells isolated from tissue biopsies selectively migrated towards CCL20 and later confirmed that the majority of these CD3-positive T cells were also positive for CCR6 (Wu et al., 2007). CCL20 has also been shown to be important in the recruitment of dendritic cell subsets. In a study by He et. al., macrophage inflammatory protein MIP-1α was administered intravenously into B6 mice to stimulate CCL20 production from macrophages, which in turn caused recruitment of CCR6+ dendritic cell precursors from peripheral blood (He et al., 2008). Importantly, the authors demonstrate that these recruited dendritic cells can become potent antigen presenters in the presence of appropriate stimuli, as culturing with IL-4 or GM-CSF was able to simulate proliferation of allogeneic T cells in a mixed lymphocyte reaction. Macrophages might further be considered analogous to dendritic cells in their capacity and ability to present antigen, stimulating and activating T cell proliferation (Hume, 2008). Indeed, whilst macrophages were long considered "non-professional" antigen-presenting cells, recent reports have dispelled the antigen presenting superiority of dendritic cells as a potential artifact of *in vitro* experimentation, as *in vivo* studies have demonstrated that macrophages have an equal capacity to induce CD8 proliferation *in vivo* (Pozzi et al., 2005). In a paper by Pozzi et. al., it was shown that macrophages possess the ability to migrate to lymphoid organs and stimulate T cells (Pozzi et al., 2005). Using an adoptive transfer model, CFSE-labeled transgenic T cells specific for the gp33 peptide of lymphocytic choreomeningitis virus (LCMV) were transferred into Rag $^{-/-}$ mice. Mice were immunized with bone marrow derived macrophages or dendritic cells pulsed with gp33 peptide, with the draining lymph nodes removed after a number of days later to isolate T cells and assess proliferation by flow cytometry. Such experimentation demonstrated that macrophages

and dendritic cells can stimulate T cell proliferation of equal magnitude, with the peak frequency of T cell proliferation occurring earlier in mice immunised with macrophages as compared to those immunised with dendritic cells (day three compared to day four, for the highest dose of pulsed peptide). In a reciprocal manner however, T cells can be crucial in macrophage activation. During infection, presence of Th1 cells can fully activate macrophages to up-regulate lysosomal proteases for efficient destruction of microbes through production of IFN-γ, but also through CD40 receptor engagement to sensitise macrophages to further IFN-γ (Biswas and Mantovani, 2010).

1.3 Macrophages in tumours

1.3.1 Tumour-promoting functions of macrophages

Macrophages can promote tumour progression in a number of different ways (*Figure 1.3*). The wound-healing properties of macrophages can be exploited by tumour cells to encourage invasion, angiogenesis and metastasis. In parallel the immune modulation characteristics can be co-opted to suppress immune rejection. Finally macrophages can hinder therapeutic interventions or aid recovery of tumours following damage. These different characteristics are described in more detail below.

1.3.1.1 Promotion of tumour growth and metastasis

Central to tumour growth and invasion is the reciprocal production of stimulatory factors between tumour and immune cells. Such reciprocal signalling is mediated, for example, by epidermal growth factor (EGF) and colony-stimulating factor (CSF), produced by macrophages and tumour cells respectively in a paracrine loop. Macrophage-produced EGF interacts with the high affinity EGF receptor on tumour cells (EGFR1), where it has been demonstrated to regulate proliferation and migration (Condeelis and Pollard, 2006). Elevated CSF concentrations in tumours have been correlated with increased macrophage accumulation and skewed polarisation towards an M2 phenotype. Production of extracellular matrix (ECM)-modulating enzymes such as cathepsin and MMPs by such macrophages are known to be involved in ECM degradation and membrane disruption, which are the main processes macrophages use to facilitate tumour invasion (Mantovani et al., 2012).

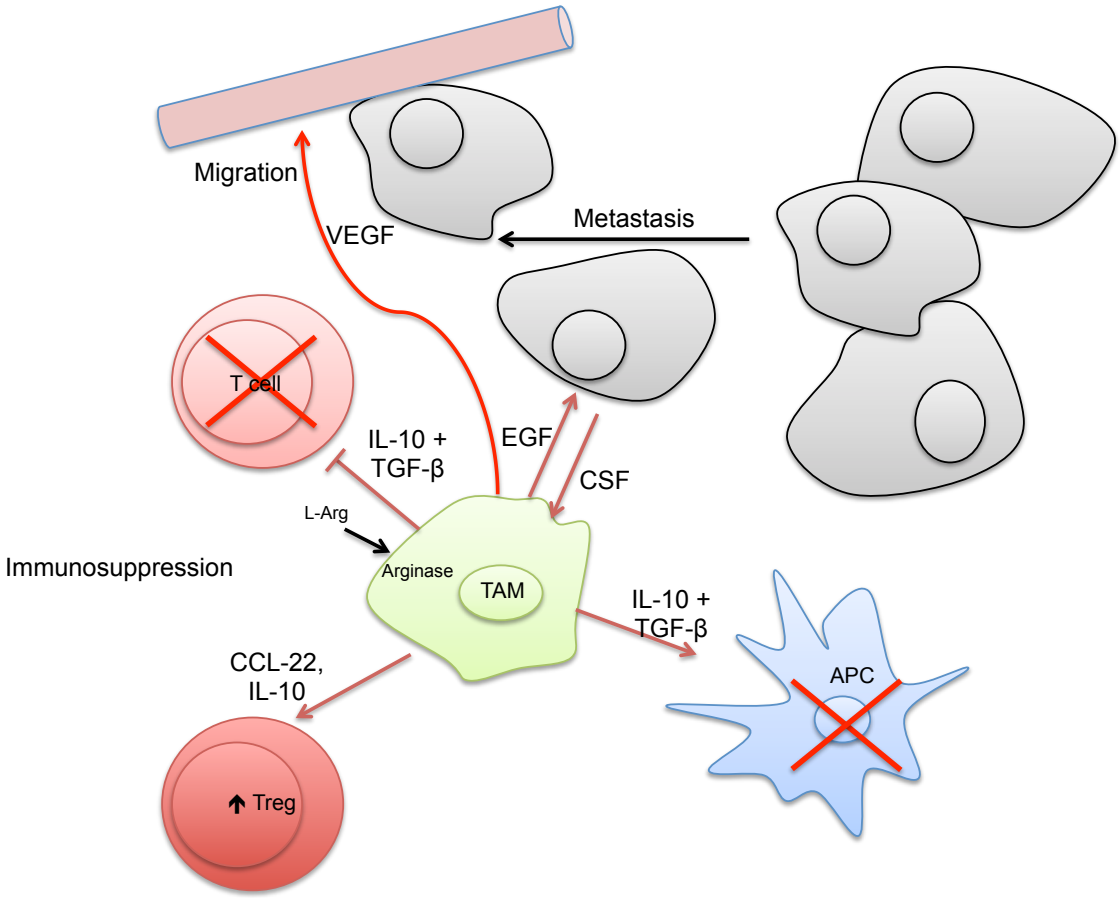


Figure 1.3 The tumour-promoting functions of TAMs

Macrophages facilitate tumour growth by a reciprocal interaction with cancer cells; macrophages are recruited and polarised by tumour CSF, and in turn provide EGF growth factor. TAM VEGF production has been identified as a key factor in tumour angio- and lymph-angiogenesis and is attributed with facilitating the spread of tumour cells. TAM also foster immunosuppression, inhibiting T cells directly through Arginase and IL-10 / TGF-β, whilst recruiting suppressive Treg through CCL22 production. Inhibitory cytokine production by TAM can also inhibit effective antigen presentation and foster anergic signalling

The implication that TAMs might regulate tumour metastasis has been strongly supported by clinical correlation data. High numbers of macrophages have been demonstrated at the early stages of metastasis formation in a range of cancer types (Lewis et al., 2006). For example, a study of over 60 tumour samples from patients with bladder cancer identified a significantly increased macrophage presence in more invasive tumour sub-types, correlating with an increased incidence of distant metastases (Hanada et al., 2000).

A mechanism by which macrophages mediate metastasis through the CSF:EGF interaction was perhaps best demonstrated in a paper by Wyckoff et. al. Here, the authors studied the impact of CSF-1:CSF-receptor signalling using a mammary tumour model with macrophages genetically manipulated to express GFP following stimulation of the CSF receptor (CSF-R); so called "c-fms" mice (Wyckoff et al., 2007). EGF-producing macrophages were shown to be responsible for increased tumour cell motility, directing tumour cell migration toward perivascular macrophages. Further, macrophage density at such tumour vessels appeared to facilitate the intra-vasation of tumour cells which resulted in increased tumour growth, invasion and the formation of metastases (Wyckoff et al., 2007). Characterising the phenotype of the TAMs, they showed that macrophages (identified by F4/80-positivity) within the tumour stroma were all positive for dextran (labeled with Texas red) unlike their granulocytic counterparts. Interestingly, macrophages only phagocytose dextran in the presence of the tumour stroma, not in the blood, suggesting an increased expression of scavenger receptors indicative of an M2 phenotype (Chao et al., 2012; Wyckoff et al., 2007; Yan et al., 2015). Accordingly a number of strategies have aimed to deplete macrophages or

antagonise the CSF:EGF interaction as a means to inhibit tumour growth and metastases in a number of mouse models (Lin et al., 2001; Solinas et al., 2009; Wyckoff et al., 2007). In preclinical models of glioblastoma for example, antagonism of CSF signalling using the CSF-1 receptor inhibitor BLZ945 was able to increase long term survival of mice with established platelet-derived growth factor gliomas (PDG mice), halting tumour growth and inducing tumour regression (>30% of tumour volume) in a third of the mice treated. Intriguingly, on investigating the mechanism behind the success of the treatment, the authors found that the antibody did not reduce macrophage infiltration into the brain. Rather, BLZ945 treatment reduced the number of macrophages polarised towards an M2 phenotype (arginase^{+}/mannose receptor ^{high}/CD163 ^{high}). This M2 phenotype was correlated with an impaired ability to phagocytose glioma cells and thus, blockade of M2 macrophage formation by BLZ945 was able to elicit an anti-tumour effector function by stimulating phagocytosis of tumour cells by macrophages (Pyonteck et al., 2013). In another example of therapeutic CSF receptor antagonism, Wyckoff et. al. extended their studies in the murine mammary model to demonstrate the therapeutic potential of targeting CSF-1 receptor. Using a monoclonal antibody that blocks the function of the CSF-1 receptor to treat mice with MMTV (mammary mouse tumour virus) tumours, the authors demonstrated that they could reduce macrophage infiltration by over 80% on average (Wyckoff et al., 2007). With their previous work demonstrating the critical the role of macrophages in facilitating tumour invasion and metastasis, they showed that the CSF-R1 antibody-mediated reduction in TAMs also correlated with a 6 fold-decrease in tumour burden in the bloodstream relative to the control treated group (Wyckoff et al., 2007).

1.3.1.2 Stimulation of angiogenesis

The most compelling evidence for the role of TAMs in tumour angiogenesis comes from clinical observations, with accumulation of TAMs having been shown to correlate with vascularity in a range of tumours such as breast (Leek et al., 1996), glioma (Nishie et al., 1999) prostate (Lissbrant et al., 2000) and many others (Lewis et al., 2006; Solinas et al., 2009). Characterisation of TAMs indicate that they are well equipped to modulate angiogenesis, producing VEGF-A, -C, -D and angiogenesis-related molecules such as MMP-7, -9,-12, FGF and TGF-β (Murdoch et al., 2008). Macrophage production of VEGF-A provides the principal pro-angiogenic mechanism, through secretion of VEGF to bind VEGFR-1 on endothelial cells. Indeed, the association of VEGF-producing macrophages with highly-vascularised tumours has been demonstrated in a number of human cancers. For example, in a study by Leek et. al. VEGF-positive TAMs were identified in over 80% of human lung cancer patients studied (Leek et al., 1996). To elucidate the precise mechanism by which TAMs might drive tumour neovascularization, a number of murine studies have been performed. In a murine model of ovarian cancer for example, infiltrating macrophages were shown to express high levels of MMP-9 and FGF, however it was their VEGF production that determined the extent of angiogenesis within the tumours (Huang et al., 2002). Indeed infiltration by VEGF-producing TAMs has been shown to be one of principal drivers of angiogenesis in a murine breast cancer model (Lin et al., 2006). Here, Lin et. al. used a CSF-1 overexpressing transgenic model to show that pre-malignant lesions extensively infiltrated with macrophages significantly enhanced angiogenesis , relative to non-transgenic mice which contained 6-fold fewer macrophages; an effect that was attributed to macrophage VEGF production (Lin et al., 2006). Further, TAM production

of MMP-9 which is associated with mobilization of VEGF, provides an additional mechanism to stimulate angiogenesis through increased substrate availability for VEGFR-1 (Ruffell et al., 2012a).

1.3.1.3 Macrophages in hypoxic regions of tumours

Tumour hypoxia is widespread among solid tumours, characterised by persistent exposure to "chronic" levels of hypoxia (Harris, 2002; Van Overmeire et al., 2014). Whilst the extent of hypoxia within solid tumours varies between patient, cancer stage and tumour type, hypoxia is characterised by a significant reduction in the oxygenation of the tumour relative to surrounding normal tissue, with typical partial oxygen pressures (pO_2) in the range of 1-15 mmHg (Brown and Wilson, 2004). To put in context, median partial oxygen pressure in pancreatic cancer is 2.7 mmHg, whilst the corresponding normal tissue experiences 51.6 mmHg pO_2 (Koong et al., 2000). Tumour hypoxia is a result of abnormal vasculature that fails to keep pace with a tumour that outgrows its blood supply (Nagy et al., 2009). Both existing vasculature and new vessel formation within the tumour are irregular and disorganised, lacking defined branching, containing arterio-venous shunts and incomplete endothelial linings, all of which contribute to a "leaky" flow of blood and an inadequate perfusion of tumours (Brown and Giaccia, 1998; Nagy et al., 2009).

A link between hypoxia and macrophages has been demonstrated for a number of tumour types including from patients with breast, ovarian and prostate cancer, where macrophages have shown an increased accumulation within hypoxic regions of the tumours (Lewis and Murdoch, 2005; Negus et al., 1997; Talks et al., 2000). Indeed, a

positive correlation is observed in number of liver metastasis between the levels of hypoxia within tumours and the extent of TAM accumulation (Stessels et al., 2004). The explanation for increased macrophage accumulation at such poorly vascularised sites can in part be explained by the mechanisms through which hypoxia influences macrophage migration; facilitating initial recruitment then "trapping" macrophages once at the site of hypoxia (Van Overmeire et al., 2014).

Recruitment of macrophages into hypoxic areas of the tumour is thought to be at least in part a result of their clearance role in homeostasis. Hypoxic areas of tumours are frequently found adjacent to necrotic areas, as one would expect for areas of such low oxygen tension. As such, dying cells in addition to release of molecules associated with dying cells are thought to act as chemoattractants into hypoxic regions of tumours (Murdoch et al., 2004). A number of chemoattractants have been reported to regulate macrophage infiltration such as CCL2 and CSF1 and are discussed elsewhere in this thesis. Of particular note for hypoxia however is VEGF, which, in addition to stimulating new vessel formation, can also act as a chemoattractant for monocytes and macrophages (Barleon et al., 1996). In breast cancer, elevated levels of VEGF are reported to correlate with regions of hypoxia and further, with accumulation of macrophages, suggesting that macrophages can act as a source of VEGF both to facilitate angiogenesis and to enhance macrophage migration into regions of hypoxia. (Leek et al., 1996; 2000). Macrophage accumulation was shown to be significantly higher in breast cancer within poorly vascularized regions (as evidenced by low positivity for the blood vessel marker CD31). Staining of tumour sections for VEGF demonstrated positivity in distinct foci that associated with CD68-positivity (Lewis et

al., 2000). Further, analysis of the hypoxic areas of tumours indicated that there was significant up-regulation of HIF-2α within CD68 positive cells (Talks et al., 2000).

Adaptations of macrophages to hypoxic regions

Once attracted into these regions of low oxygen it has been suggested that hypoxia increases the retention of these macrophages through the down-regulation of proteins that influence their motility such as macrophage-chemoattractant protein 1 (MCP-1) (Turner et al., 1999). Further, hypoxia can influence the responsiveness of macrophages to chemoattractants through down-regulation of chemokine receptors. In one such example, macrophages isolated from patients with ovarian cancer were shown to exhibit decreased expression of the MCP-1 receptor, CCR 2 (Sica et al., 2000). Using migration assays the authors were able to demonstrate that these TAMs experienced significant reductions in the ability to respond to MCP-1 to other chemoattractants such as CCL-4 and C5a.

Upon exposure to hypoxia, macrophages quickly alter their metabolism in order to survive a lower oxygen environment, switching from aerobic to anaerobic glycolysis. Whilst transcription factors such as activating transcription factor-4 (ATF-4) and early growth response-1 (EGR-1) have been shown to become activated in response to hypoxia, it is the hypoxia-inducible transcription factors HIF -1α and HIF -2α that drive many of the central adaptions to hypoxia in macrophages (Kelly and O'Neill, 2015; Lewis and Murdoch, 2005). For example, HIF -1α up-regulates the levels of lactate de-hydrogenase, catalysing the conversion of pyruvate into lactate, to inhibit acetyl CoA availability for the TCA (tri-carboxylic acid) cycle (Semenza et al., 1996). Similarly,

HIF -1α up-regulates the glucose transporter, GLUT-1, to increase the availability of glucose to feed into anaerobic glycolysis and generate ATP (Chen et al., 2001).

Influence of hypoxia on macrophage phenotype

The phenotype of macrophages within hypoxic regions of tumours has largely been aligned with that of M2 / TAM polarised macrophages. Hypoxic macrophages in tumours express increased levels of mannose receptor, CD163, IL-4 receptor and arginase activity, combined with decreased NO production and reduced levels of MHC II, a phenotype resembling the alternatively polarised M2 macrophages (Van Overmeire et al., 2014). Recently however, experimentation has aimed to more precisely characterise the phenotype and function of macrophages localised to areas of hypoxia. In particular, attempts have been made to distinguish the specific impact of hypoxia on TAM phenotype from other tumour-associated factors that drive TAM formation. In one such example, Leblond et. al. studied the influence of hypoxia on macrophage phenotype *in vivo* by comparing the TAMs generated from orthotopic injection of the human glioblastoma cell lines U87 or U251, known to generate negligible, or significant areas of hypoxia respectively (Leblond et al., 2016). Using positron emission tomography ([^{18}F]-FMISO PET) to identify the onset and degree of hypoxia within the tumours, the authors were able to characterise TAMs from established tumours before and after the onset of hypoxia to isolate the effect of low oxygen availability. The results demonstrated that in the non-hypoxic U87 tumour model, macrophages were found to be positive for iNOS and negative for arginase, indicating a more M1-biased phenotype. In the pre-hypoxic U251 tumours, the authors report a mixed phenotype of arginase-negative, iNOS-positive and -negative macrophages. After the onset of

hypoxia however, all the macrophages in the U251 tumours are iNOS negative, arginase-positive and pre-dominantly co-localise to areas of hypoxia (Leblond et al., 2016). A recent paper by Movahed et. al. sought to better characterise the phenotype of TAMs in hypoxic regions, by isolating macrophages from tumours that co-localised with the hypoxic marker pimonidazole, in a murine model of mammary adenocarcinoma (Movahedi et al., 2010). The authors found that macrophages localised to areas of hypoxia displayed significantly reduced expression of MHC II relative to TAMs from the rest of the tumour. Further, whilst these MHC II ^{low} macrophages exhibited expression of a number of prototypic M2 signatures such as MMP-9 and VEGF, they appeared distinct from other TAMs within the tumour as they demonstrated increased expression of mannose receptor, arginase 1 and CD163 relative to the other macrophages. The authors were also able to demonstrate functional differences between the hypoxic, MHC II ^{low} cells TAMs and other macrophages in the tumour. Whilst MHC II ^{high} and MHC II^{low} macrophages were both poor antigen presenters, there was a marked difference in the pro-angiogenic capacity of these cells; MHC II ^{high} and MHC II ^{low} TAMs were isolated, sorted and compared in their ability to induce angiogenesis using the CAM (Chorioallantoic membrane) assay. Here, the authors demonstrated that MHC II^{low} macrophages increased vessel formation two-fold higher than their respective MHC II ^{high} TAMs.

Tie-2 –expressing macrophages

Arguably, the best studied hypoxic macrophages are TEMs, the Tie-2 expressing macrophages, a subset of macrophage defined by their expression of the angiopoietin receptor, Tie -2 (Murdoch et al., 2007). TEMs have been identified in a range of

cancers, with a recent study demonstrating TEM-positivity in lung, pancreatic kidney, colorectal and breast tumours (Venneri et al., 2007). Further, analyzing the total leukocyte content in these samples illustrates the pre-dominance of TEMs within the tumour, with up to 73% of the monocytic/macrophage infiltrate in the tumour identified as Tie2-positive.

Hypoxia has been shown to up-regulate both the number of cells positive to Tie2, and the intensity of expression (Murdoch et al., 2007). Akin to surface markers associated with an M2 phenotype, hypoxia markedly alters the cytokine profile of the macrophages. Human macrophages exposed to chronic hypoxia (0.1% O_2) exhibit significant reductions in the levels of TNF-α and CCL2 (Murdoch et al., 2007). If these hypoxic macrophages are exposed further to angiopoietin 2, a growth factor found up-regulated in a number of tumours, the inhibition of TNF-α and CCL2 is accentuated, with additional decreases in the levels of IL-12 observed (Murdoch et al., 2007). It has been demonstrated using mouse models that TEMs are a central player in tumour angiogenesis and survival. De Palma et. al. generated a conditional knockout system for studying the impact of TEMs, using lentiviruses to make Tie 2-positive cells co-express thymidine kinase, thereby sensitising them to ganciclovir treatment (De Palma et al., 2005). The authors were able to use their conditional knock out system in a mammary tumour model, were they showed that challenging mice with murine N202 cancer cells in the absence of TEMs could inhibit tumour formation. Further, they demonstrated that depletion of TEMs once N202 tumours were established could induce regression. To discriminate the central role of TEMs in tumour angiogenesis from the pro-angiogenic functions of other myeloid cells known to secrete angiogenic factors within tumours, the authors repeated the experiments with CD11b cells that are Tie2+ cell depleted,

demonstrating that tumour angiogenesis was not enhanced by addition of TEM-depleted myeloid cells. Translating such findings into more humanized models, Venneri et. al demonstrated that human TEMs appear capable of exerting similar pro-angiogenic effects as their murine counterparts (Venneri et al., 2007). Here, U87 human glioma cells were xenografted into nude mice and co-injected with either Tie2-positive or – negative human monocytes. Upon sacrificing the mice, tumours were found to be significantly larger and more vascularised in the tumours co-injected with TEMs (Venneri et al., 2007). In addition to their pro-angiogenic functions, TEMs have been shown to exhibit immunosuppressive functions akin to TAMs, suppressing T cell activity (Coffelt et al., 2011; Venneri et al., 2007). In a study by Coffelt et. al., human CD3+ T cells were co-cultured with TEMs to demonstrate that TEMs could inhibit the polyclonal activation and proliferation of T cells in an IL 10-dependent manner (Coffelt et al., 2011). The authors further demonstrated that angiopoietin treated TEMs co-cultured with CD4 T cells were able to expand Treg subsets *in vitro*, validating the *in vivo* significance of these findings by showing that angiopoietin-2 overexpressing tumours displayed significantly higher levels of Tregs than in wild-type tumours.

1.3.1.4 Mediation of immune suppression

Of all the tumour-promoting functions of macrophages, arguably the most significant interest has been focused on how TAMs mediate immune suppression, particularly suppression of the adaptive immune system within tumours (Figure 1.5). Their important role in this phenomenon likely reflects the pleiotropic nature of the cytokines

expressed by macrophages, which enables their interaction with a wide range of immune cells, including T- and B- cells, neutrophils, mast cells, NK and NKT cells (Biswas and Mantovani, 2010; Mantovani and Sica, 2010).

In the context of cancer immunotherapy, the best characterised of these interactions has been that of the TAM and the T cell, with significant research centered on understanding the role macrophages may play in cancer-associated suppression of T cell activity (Biswas and Mantovani, 2010; Jiang et al., 2015).

The cytokine profile associated with TAM includes a number of immunosuppressive cytokines and mediators including IL-4, IL-10, TGF-β, CCL-2, CCL-18, CCL-22, PGE-2, MMP-7 and VEGF. Suppressive cytokines such as IL-10 and TGF-β, produced by macrophages, are largely responsible for the ability of TAM to suppress T cell function and they can do so at a number of different levels (Biswas and Mantovani, 2010). Macrophage produced IL-10 and TGF-β can act in an autocrine or paracrine manner to stimulate the expression of a number of inhibitory co-receptors for T cell activation; notably, members of the B7 family (N. L. Harris et al., 1999). In particular, TAMs have been shown to over-express B7-H1 and B7-H4 in various cancers to elicit T cell suppression in a mode of action analogous to CTLA-4 (Kryczek et al., 2006; Kuang et al., 2009). This mechanism has been particularly well studied in ovarian cancer ascites where IL-10 drives B7-H4 expression in TAMs. For example, in a study of TAMs from ovarian cancer patients (n=12) over 70% were positive for B7-H4 expression (Kryczek et al., 2006). The authors profiled immunomodulatory cytokines within the tumour microenvironment of these patients to identify high levels of IL-6 and IL-10, which the authors could demonstrate were crucial cytokines for the induction of B7-H4 expression

on TAMs. To assay the ability of these macrophages to suppress tumour-antigen specific T cell proliferation, an *ex-vivo* T cell stimulation assay was established. HLA-$A2^+$ dendritic cells from healthy donors were pulsed with Her-2/neu peptide, into which $CD3^+$, $CD25^-$ T cells isolated from the ascites from HLA-$A2^+$ ovarian cancer patients were added; Proliferation of any Her-2/neu-specific T cell was then assessed using thymidine incorporation. $B7H4^+$ and $B7H4^-$ TAMs (from the same T cell donor) were isolated and sorted, then co-cultured with these dendritic cells and T cells to assess their ability to suppress Her-2 specific T cell activation and proliferation. The authors demonstrated that B7-$H4^+$ TAMs induced 6-fold more T cell suppression than their $B7H4^-$ counterparts – an effect which could be blocked by pre-treating TAMs with B7-H4 anti-sense oligonucleotides to disrupt B7-H4 expression. B7-$H4^+$ positive macrophages also exhibited high positivity of B7-H1 receptor and arginase activity, suggesting complementary mechanisms by which these TAMs may mediate their immunosuppression. However, in neutralising the activity of B7-H1 (by blocking antibody) and inhibiting arginase (through pre-treatment with the hydroxylated arginine analogue, nor-LOHA) the authors were unable to significantly decrease the immunosuppressive activity of the TAMs relative to the effect seen following disruption of B7-H4 expression. Such findings demonstrated that T cell suppression by ovarian cancer TAMs is principally mediated through physical interaction of B7-H4 with cognate receptors on T cells. As such, the mechanism of tumour antigen-specific suppression was considered analogous to the action of Treg cells. However, given that such macrophages constitute a larger proportion of immune cells than Treg (>30% more), their ability to induce T cell suppression may be even more significant (Kryczek et al., 2006).

In an extension of this work, the interaction between Tregs and TAMs was shown to be of particular importance. Tregs were shown to induce TAM production of IL-10 which acted in an auto- and para-crine manner, stimulating B7H4 expression on TAM and supporting suppressive activity of Tregs. In this way, the suppressive environment of ovarian ascites promotes Treg and TAM subsets, which can then act together to perpetuate suppressive activity. The significance of such findings is best illustrated by clinical correlations. In a study of over 100 patients with advanced ovarian cancer, a two-fold increase in B7H4 expression was shown to corresponded with an increase in FIGO (International Federation of Gynecology and Obstetrics) grading from 3 to 4, correlating with a >60% decrease in response to chemotherapy (Kryczek et al., 2007).

Induction of inhibitory signalling receptors on TAM is one mechanism by which T cells can be suppressed. However, down-regulation of stimulatory receptors presents an equally important mechanism for inhibition; IL-10 and TGF-β down-regulate a number of integral receptors such as CD80 and CD86 on the surface of macrophages. TAM are proficient in tumour antigen uptake and processing, but in the absence of stimulatory receptors, they can actively suppress both CD4 and CD8 T cells in an anergic fashion (Movahedi et al., 2010).

Macrophage-mediated inhibition of T cell function is not limited to receptor expression at the cell surface. For example, TAM produced IL-10 and TGF-β can induce transcriptional changes in T cells, polarising the cytokine profiles of the cells towards a more regulatory phenotype. IL-10 producing macrophages have been identified in renal cell carcinoma, where they have been shown to promote T cell exhaustion and induce a

shift in the phenotype of infiltrating CD4 T cells from IL-2 producing cells to those more suppressive cytokines and receptor expression such as IL-4, IL-10, TGF-β, TIM-3 and PD-1 (Dannenmann et al., 2014). Such shifts in T cell phenotype correlate with reduced survival and increased incidence of metastases.

The pattern of reciprocal interaction between T cells and TAMs is commonly observed; suppressive macrophages or T cells frequently induce expression of IL-10/TGF-β in their counterpart, which in turn promotes their own immunosuppressive phenotype. A clear example of this is evidenced by Ibe et. al., who show that infiltrating macrophages can have their pro-inflammatory, IFN-γ producing phenotype rapidly suppressed by tumour-associated T cells to induce a more immunosuppressive IL-10 producing macrophage subset. This IL-10 can then act in paracrine manner to further suppress other infiltrating macrophages but also maintain the suppressive state of resident T Cells (Ibe et al., 2001)

Such transcriptional changes in CD4+ T cells often include the induction of FoxP3 expression, increasing the presence of Tregs within tumours (Curiel et al., 2004; Daurkin et al., 2011; Denning et al., 2007; Savage et al., 2008). Thus, TAM induction of Tregs represents a powerful way to increase immune suppression within the tumour. These data further lay support for the "induced Treg" model (iTreg), with TAM-produced IL-10 driving FoxP3 expression in peripheral CD4 T cells from the memory T cell pool (as characterised by lower expression of CD25), relative to higher CD25 expression associated with natural Tregs (Savage et al., 2008).

Arginine is a non-essential amino acid that regulates T cell proliferation through expression of the CD3-zeta chain. Arginase expression by TAM has been well

documented and has been attributed with inhibition of T cell function through depletion of arginine availability in a number of cancer subtypes (Doedens et al., 2010; Fletcher et al., 2015).

Further, TAMs can regulate the levels of death-inducing ligands on the surface of tumour cells through proteolysis. For example, TAM expression of MMP-7 results in the cleavage of Fas-ligand on tumours cells, inhibiting the cytotoxic activity of T cells (Vargo-Gogola et al., 2002).

In a more indirect manner, production of chemokines by TAMs can facilitate T cell inhibition by the recruitment other immune cells that help foster immune suppression. One such example is in the TAM production of CCL18, a chemokine responsible for the recruitment of naïve T cells. In the context of a tumour, recruitment of naïve T cells provides a means to induce tolerance by exposing such cells to tumour antigen in the absence of sufficient co-stimulation (Gajewski et al., 2006; Mantovani et al., 2002).

The best-characterised of these examples however is in the TAM-mediated recruitment of Tregs using chemokines such as CCL-22. In models of ovarian cancer, increased Treg numbers were seen in both ascites and primary tumours from patients with more advanced ovarian carcinomas (FIGO stages 3 and 4), and the recruitment of these Tregs was dependent on CCL-22 production by macrophages (Curiel et al., 2004; Zou, 2005)

1.3.1.5 Interactions of TAMs with anti-cancer therapies

Clinical associations of reduced responses to chemo- and radio-therapy with high macrophage densities in tumours, suggest that TAMs may significantly impact on the efficacy of conventional cancer therapies (Petrillo et al., 2015; Zhang et al., 2012). In part, this may be mediated by the therapeutics themselves. The highly plastic nature of macrophages makes them sensitive to micro-environmental changes within the tumour (Mantovani and Sica, 2010). As a cell type that resolves excessive inflammation in tissue damage, it has been suggested that macrophages maybe adopt a phenotype suited for tissue repair in response to anti-cancer therapy which may inadvertently facilitate tumour progression (Mantovani et al., 2012; Mantovani and Allavena, 2015).

In a number of settings, chemo- and radio-therapy have been shown to increase macrophage accumulation with tumours. For example, paclitaxel has been shown to increase TAM infiltration, in part through increased production of macrophage chemokines such as CCL2 whilst simultaneously driving suppressive polarisation through concomitant increases in CSF (Mantovani and Allavena, 2015). In mouse models of breast and lung cancer, significant myeloid cell infiltration has been observed post-radiotherapy and was associated with relapse to treatment. Here, macrophages were shown to display an M2 phenotype as confirmed by high Tie-2 positivity, implicating that radio-resistance observed might be mediated through vascular changes by macrophages (Kozin et al., 2010). Further support for such a hypothesis can be found in models of glioblastoma, where radiation-induced macrophage infiltration accompanied increases in vasculogenesis and the induction of radio-resistance (Kioi et al., 2010). This was mediated through local induction of HIF-1α in hypoxic regions,

which drove the accumulation and stabilisation of macrophages by increases in stromal cell derived factor -1 (SDF-1). This, with the associated vasculogenesis, was attributed with an important role in the radio-resistance observed (Kioi et al., 2010).

Tie-2-positive macrophages have also been associated with relapses after conventional chemotherapy. Following cyclophosphamide (CPA) treatment, significant increases in VEGF-A-positive macrophages were induced in the tumour via increased CXCR4 chemokine signalling and were shown to induce angiogenesis and subsequent relapse to therapy (Hughes et al., 2015). Here, the polarisation state of these macrophages was shown to determine chemo-sensitivity and was illustrated by adoptive transfer experiments. Simulating the chemotherapy-induced myeloid infiltration, adoptive transfer of mannose receptor-positive M2 macrophages following CPA was able to replicate the relapsing phenotype, whilst M1 macrophage transfer inhibited tumour re-growth.

Macrophages with similar M2 profiles have also been shown to limit the efficacy of chemotherapy through production of cathepsins (Mantovani and Allavena, 2015). In a murine model of breast cancer, treatment with paclitaxel doubled the number of TAMs present with tumours, correlating with significant increases in cathepsins (cathepsin B and C). TAM-derived cathepsins were identified as the causal agent for the reduced efficacy of paclitaxel, as chemo-sensitisation could be restored using a pan-cathepsin inhibitor (Shree et al., 2011). Similar patterns have also been observed with other common chemotherapeutic agents such as gemcitabine and 5-fluorouracil, where induction of cathepsin production has diminished the effect of treatments.

An unresolved question is how differing dosages might impact on macrophage responses to chemo- and radio-therapy. A recent paper by Klug et. al. demonstrated that, in contrast to similar studies in the field, low-dose radiotherapy was able to normalise tumour vasculature in a mechanism involving macrophages (Klug et al., 2013). In this study the authors showed that there was increased T cell infiltration into tumours following low dose irradiation (LDI), which correlated both with tumour reduction but also re-vascularisation. Here, Klug et. al. found that T cell infiltration and re-vascularisation only occurred in tumours that were co-infiltrated with macrophages. Such an effect was confirmed by macrophage depletion experiments, showing that the effects of vascular normalisation and T cell infiltration were both abrogated when LDI was combined with macrophage depletion by clodronate-loaded liposomes. To examine the effects of LDI (2Gy) on macrophage phenotype and function, the authors isolated peritoneal macrophages from mice subject to whole body LDI, showing that these cells exhibited a reduction in classical M2 markers such as arginase and Fizz-1, whilst showing an increased M1 phenotype evidenced by iNOS induction. This M1 phenotype was confirmed in pancreatic tumours in RT5 mice that were subject to LDI, where infiltrating macrophages were shown to be iNOS+, IL-4^{low}, IL-10 ^{low} and IL-13 ^{low} relative to non-irradiated control TAMs. Importantly, this induction of an M1 phenotype by LDI was accompanied by infiltration of CD8 T cells and vascular normalisation (evidenced by a reduction in haemorrhagic lesions and decrease total CD31^{+} vessel area) and was dependent on iNOS induction, as inhibition of iNOS abrogated the vascular and immune effects observed. Further investigation showed that iNOS was central to the immunomodulatory effects observed, as inhibition of iNOS in these cells reduced expression of the T cell chemoattractant RANTES (regulated on activation, normal T cell expressed and secreted), which was suggested to mediate the

observed T cell infiltration (Klug et al., 2013). Such data suggest promising synergies between radiotherapy and macrophage polarisation may exist however, further experimentation will be required to define their full significance and suitability for incorporation into therapeutic approaches (Mantovani and Allavena, 2015).

1.3.2 Anti-tumour functions of macrophages

The term "tumour-associated macrophage", is normally synonymous with "suppressive macrophages" owing to the vast quantity of literature that describes the pro-tumoural functions of macrophages. However, much of the original work describing macrophages in tumours centered on the tumouricidal functions of macrophages infiltrating tumours (Keller et al., 1990). Here it was thought that the toxic bacteriostatic effector functions of classically activated macrophages responding to infections would translate into tumoricidal activity. Such work therefore demonstrated the impact of classically activated macrophages on tumour growth.

Early studies into the tumouricidal functions of macrophages focused on the production of nitric oxide (NO) and TNF-α by classically activated macrophages (Hibbs et al., 1987). Inducible nitric oxide synthase (iNOS) is induced in classical activation of macrophages, characterised by a rapid and profound generation of NO and highly toxic radical species such as nitrite and peroxynitrite. When co-cultured with tumour cells, macrophage-produced NO was shown to induce cytotoxicity as a result of DNA damage

in a number of different cancer types (Hibbs et al., 1987; MacMicking et al., 1997). Further, NO has been shown to induce apoptosis in tumours, even in cell lines previously thought resistant (Xu et al., 2002). In this sense, NO can be both direct tumoricidal but can also mediate sensitisation of tumour cells to other modes of killing, such as Fas-induced apoptosis (Garbán et al., 1999). The importance of macrophage NO has been reaffirmed in recent attempts to activate TAM in tumours. For example, agonistic antibodies for macrophage CD40 have shown promise in stimulating anticancer effects of previously suppressive TAMs (Beatty et al., 2011). Although production of TNF-α by macrophages activated in this way has been attributed with the induction of apoptosis in tumour cells, concurrent increase in NO play an important role in mediating the tumouristatic effects which often underpin the anticancer efficacy of this approach (Lum et al., 2006).

The effects of macrophage-induced NO appear not to be constrained to direct effects on tumour cells but may also act via the adaptive immune system. In contrast to other reports suggesting that iNOS induction may be detrimental to T cell function, a recent report by Miguel et. al. demonstrated a pivotal role for NO in immune therapy of glioma. Here, effective induction of a tumour-specific CD8 T cell response was insufficient to mediate tumour elimination without additional changes to the microenvironment to overcome the existing local immune suppression (Miguel et al., 2010). Activating TAMs towards a pro-inflammatory M1 phenotype induced NO production and facilitated tumour elimination; an effect that could be reversed by inhibiting iNOS activity.

The production of matrix-remodelling proteins is a function of macrophages normally attributed to M2-polarised cells, where they can promote tissue repair and frequently, facilitate metastatic growth of cancer (Mantovani et al., 2012). Expression of matrix metalloproteinase 12 (MMP-12) however, has been shown to play a role in the antagonism of angiogenesis in models of liver and lung cancer (Bingle et al., 2002; O'Reilly et al., 1994). Here, the proteolytic activity of macrophage produced MMP-12 was shown to facilitate the generation of angiostatin, an anti-angiogenic peptide derived from enzymatic cleavage of plasminogen, reducing angiogenesis and metastasis of lung tumours.

Relieving local immunosuppression of T cells has recently been a central focus of tumour immunology, as evidenced by the growth of antibodies used as checkpoint blockade inhibitors in pre-clinical cancer research and in the oncology clinics. Natural killer (NK) cells are typically attributed with mediating antibody-dependent functions such as antibody-dependent cellular cytotoxicity (ADCC), however macrophages are similarly able to perform ADCC and, in addition, can mediate antibody-dependent cellular phagocytosis (ADCP) (Karagiannis et al., 2007). The therapeutic importance of these mechanisms has been demonstrated clearly in preclinical systems, with ADCP-mediated tumour killing by macrophages showing efficacy in models of breast cancer and lymphoma, with antibodies targeting CD142 and CD40 respectively (Grugan et al., 2012; Josephs et al., 2015; Minard-Colin et al., 2008). In recent studies examining the mechanism of action of the antibody checkpoint inhibitor ipilimumab, antagonism of CTLA-4 signalling was accompanied by Treg depletion (Simpson et al., 2013). Here it was uncovered that macrophages can mediate phagocytosis of opsonised Treg, and while this is probably not the only mechanism of ipilimumab in the clinic, this does

demonstrate a likely central role for macrophages in current immunotherapeutic approaches (Selby et al., 2013).

In accordance with the immunosurveillance hypothesis put forward by Thomas and Burnet (Lanier and Lanier, 2001), macrophages have recently been shown to play a central role in regulation of tumour development (Jaiswal et al., 2010). These findings come from the recently uncovered role of CD47 and its interaction with macrophages (Oldenborg et al., 2001). CD47, a prominent 'don't eat me' anti-apoptotic signal has found to be up-regulated on a number of different tumours, suggesting that cancer co-opts this normal process of marking healthy "self" cells as a resistance mechanism to prevent clearance of tumour cells by macrophages. Binding of CD47 to its receptor on macrophages, SIRP-1α, has been shown to induce inhibitory signalling in the macrophage to prevent cellular phagocytosis (Chao et al., 2012). Antagonism of the CD47-SIRP interaction however has been shown to re-establish phagocytosis of tumour cells by macrophages, which recognise them as "altered self" (Chao et al., 2010; Theocharides et al., 2012; Zhao et al., 2011). Such studies highlight that cellular phagocytosis may be a central tumoricidal mechanism that macrophage possess, but one that is often subverted by tumours during the process of tumour evolution (Vonderheide, 2015).

These examples all illustrate the fact that macrophages possess the potential to be highly effective tumouricidal cells, yet during the tumour development, their pro-inflammatory functions are quickly disrupted and they re-polarise towards tumorigenic phenotypes.

1.4 TAMs as a therapeutic target

The numerous ways by which TAMs can promote tumour growth and inhibit conventional chemo- and radio-therapy make them an attractive target for therapeutic intervention. A number of strategies and approaches aimed at attenuating the negative impact of TAMs have been explored, of which the most common and well-developed are presented here (*Table 1*).

1.4.1 Inhibition of macrophage recruitment

A range of chemokines and cytokines have been implicated in the migration of monocytes and macrophages into tumour tissues including IL-1, CCL-5, CXCL-8 , CXCL-12 and VEGF (Sica et al., 2008). Two such molecules, M-CSF and CCL-2 have attracted particular attention:

M-CSF has been a central focus of the inhibition of macrophage recruitment (Hume et al., 2012). Indeed, clinical correlations have implicated M-CSF with worsening prognosis for liver cancer, where high M-CSF levels are attributed with the high influx of macrophages and poor survival rates (Zhu et al., 2008). Additionally, M-CSF has been shown to induce a transcriptional profile far closer to the alternative polarisation than to classically activated cells (Fleetwood et al., 2007).

Function	Therapeutic agent	Mechanism of action
Depletion	Trabectedin	Trabectedin has been shown to antagonise the production of CCL2 expression from number of cells within tumours including TAM(Germano et al., 2013). Trabectedin has been shown to inhibit recruitment of TAMs and further, deplete existing TAMs within tumours.
	Clodronate	Clodronate liposomes can be utilised to selectively target macrophages by exploiting their phagocytic functions. Encapsulation of bisphosphonates within such liposomes proves toxic once phagocytosed by TAMs (Zeisberger et al., 2006)
	Immuno-toxin	Folate receptor-β has been shown to be up-regulated in TAMs from a number of tumours including glioblastoma; engineering of a recombinant immunotoxin comprising anti-folate receptor conjugated with *Pseudomonas* exotoxin A selectively targets TAMs and initiates their apoptosis in experimental murine models of glioblastoma (Nagai et al., 2009).
Inhibition of recruitment	Anti-CCL2	The CCR2-CCL2 interaction is central for macrophage chemotaxis and migration. Inhibition of CCL2 secreted from tumours by antibody therapy has been shown to reduce the number of macrophages infiltrating tumours, and further prevents the formation of distant metastases initiated by macrophages (Bonapace et al., 2014).
Inhibiting suppressive TAM functions	STAT-3 inhibition	Hydrazinocurcumin, a polyphenolic compound has been shown to suppress the phosphorylation of STAT3 within TAMs (X. Zhang et al., 2013). Liposomes were loaded with Hydrazinocurcumin to facilitate delivery and targeting to macrophages (via external Legumain on the surface of liposomes). In a co-culture model with breast cancer cells, macrophages treated with hydrazinocurcumin in this manner were able to inhibit proliferation and induce apoptosis in these cancer cells (X. Zhang et al., 2013).
Macrophage activation of tumouricidal function	Anti-CD40 Monoclonal antibody	Stimulates macrophage activation through CD40 ligation that can activate M1 associated features such as iNOS and TNF-α. Localised production of NO and TNF-α by macrophages activated by CD40 stimulation can halt tumour proliferation and induce apoptosis (Lum et al., 2006).
	IFN-γ	IFN-γ has been shown to restore the M1-associated phenotype of TAMs, shifting the balance of cytokines produced by reducing VEGF and IL-10 expression and increasing IL-12 levels. Further, by up-regulating levels of co-stimulatory molecules such as CD86, IFN-γ can re-store the antigen presenting functions of TAMs (Duluc et al., 2009)
	IL-12	Treatment with IL-12 has been shown to activate the pro-inflammatory transcription factor NF-ϰB, increasing the production of iNOS and IFN-γ and a reduction in TNF production and reduces IL-10 (Schindler et al., 2001).

Table 1. Common strategies for targeting TAM

A number of strategies are utilised for targeting TAM. This figures details some of the more common examples used in the field to antagonise TAM functions

Antagonism of M-CSF by anti-M-CSF antibodies has proven an effective means to reduce macrophage infiltration within tumours, with numerous studies reporting macrophage reductions in the range of 50-60% (Paulus et al., 2006; Priceman et al., 2010). The decrease in macrophage number by this approach has resulted in the inhibition of tumour growth and the attenuation of many tumour-associated functions. For example, as TAM are known producers of VEGF, anti-M-CSF therapy reduced the levels of tumour angiogenesis and lymphangiogenesis. Clinically, blockade of tumour angiogenesis is achieved through antagonism of VEGF or its respective receptors, VEGF receptors 1-3 (Ellis and Hicklin, 2008). The best example of the former is bevacizumab, a humanised monoclonal antibody that binds VEGF thereby blocking its signalling function (Papadopoulos et al., 2012). Examples of the latter include sunitinib and sorafenib, small molecule inhibitors which target tyrosine kinases down-stream of VEGF receptors 1-3, to inhibit VEGF signalling (Castillo-Avila et al., 2009; Li et al., 2014). Unlike the mechanism of action of bevacizumab which binds directly to VEGF specifically, the targeting of a ubiquitous kinase downstream of the target receptors causes these small molecule inhibitors to target additional receptors upstream of tyrosine kinases including platelet-derived growth factor receptor-β, stem cell factor receptor (KIT) and Fms-like tyrosine kinase-3 (FLT-3). Whilst there is evidence demonstrating clinical efficacy for these angiogenesis inhibitors as anti-cancer therapeutics, there are significant adverse effects associated with systemic VEGF inhibition including haemorrhage, proteinuria and cardiac complications, exemplified by hypertension (Ellis and Hicklin, 2008). VEGF signalling in endothelial cells stimulates up-regulation of endothelial nitric oxide synthase and a subsequent release of NO which regulates vascular tone, maintaining normal dilation of blood vessels (Hood et al., 1998). As such, antagonism of VEGF might result in a level of systemic

vasoconstriction and increased blood pressure, perhaps explaining the high prevalence of hypertension in patients with cancer receiving therapies such as bevacuzizumab, sorafenib and sunitinib (Kamba and McDonald, 2007). Further, there is evidence that these adverse effects can be exacerbated when anti-angiogenic therapy is used in combination with chemotherapy. For example, in a trial of patients with non-squamous-cell-carcinoma the addition of bevacizumab to paclitaxel treatment significantly increased the number of deaths from adverse effects including lung hemorrhage and neutropenia-induced infection (Sandler et al., 2006). As macrophages represent a large source of VEGF within tumours, the ability to selectively target TAMs represents an attractive alternative anti-angiogenic strategy which, by acting locally, could circumvent some of the toxicities associated with existing anti-VEGF therapies. Further, inhibition of macrophage infiltration has been correlated with increased responses to conventional cancer therapy, with M-CSF antagonism increasing sensitivity to radiotherapy and overcoming resistance to chemotherapy; the exact mechanism behind this response remains to be identified (Ahn et al., 2010; Paulus et al., 2006).

Another chemokine of significant interest for macrophage infiltration is CCL-2. CCL-2 has been shown to increase macrophage recruitment into a number of tumours and is associated with enhanced tumour growth, increased angiogenesis and tumour metastasis in a number of mouse models (Deshmane et al., 2009; Ehling et al., 2014; Mizutani et al., 2009). In analogy to M-CSF, high CCL2 levels have been shown to induce a transcriptional profile typical of M2-polarised cells, with classical markers of alternatively polarised macrophages such as mannose receptor being expressed (Roca et al., 2009; Sierra-Filardi et al., 2014). In this respect, CCL-2 and M-CSF seem responsible not only for high macrophage infiltration, but for polarisation toward a

suppressive cell type that facilitates tumour growth. Depletion of CCL-2 or M-CSF by monoclonal antibody was studied in models of glioma, where modest increases in survival were observed for mice treated in combination with CCL-2 blockade and chemotherapy (Zhu et al., 2008).

Whilst studies antagonising macrophage recruitment show promising data, it should be noted that these approaches work best at the earlier stages of tumour formation. Reduced efficacy of such strategies in more developed tumour models are most likely explained by the pre-existing TAMs exerting their suppressive functions.

1.4.2 Depletion of TAMs

A more clinically relevant approach would be to deplete the macrophages from tumours that are already well-established. A large amount of work in this field has focused on the use of clodronate, a bis-phosphonate drug, encapsulated by liposomal particles to facilitate their engulfment by macrophages (Zeisberger et al., 2006). Clodronate-depletion of macrophages has been shown to inhibit tumour growth, angiogenesis and metastases (Hiraoka et al., 2008; Kimura et al., 2007). However, whilst these studies are encouraging, a number of other studies have demonstrated that depletion of macrophages does not result in tumour regression, but can in fact increase tumour growth (Galarneau et al., 2007; König et al., 2014). This appears counterintuitive to the notion of TAMs as key players in the development and maintenance of tumours (Fritz et al., 2014; König et al., 2014). Such mixed and contradictory findings most likely highlight the heterogeneity of TAMs. For example, whilst the majority of macrophages in tumours may be deleterious to patient outcome, it has been demonstrated that the

mixed population of macrophages within tumours can also contain cells with tumouricidal functions; strategies that deplete all macrophages are therefore removing sources of both pro- and anti-tumoural cells. Certainly, macrophages within different tumour types or isolated from different regions of the same tumours have been shown to display functional variety and differences in gene or receptor expression, although the 'average' phenotype has been one of a suppressive, tumour-promoting, TAM (Lewis et al., 2006; Movahedi et al., 2010). As such, TAM-depletion studies showing different outcomes may in fact reflect depletion of different macrophage populations. These might include, for example, improperly defined M1 type macrophages, supporting the view that M1 rather than M2-type macrophage are tumouricidal and critical to suppression of tumour growth. For example, in a murine model of glioma the depletion of TAMs by ganciclovir (following genetic modification with a mutated thymidine kinase) increased tumour growth (Galarneau et al., 2007; Gowing et al., 2006). Whilst these macrophages were indeed tumour-associated, phenotypic characterisation of these TAMs revealed strong expression of MCP-1 and IL-1β, with low expression of IL-4, IL-10 and TGF-β; a phenotype that would be typically classified as M1. As such, depletion strategies have evolved to try and specifically target suppressive, M2-like TAMs by a number of means.

In one approach the bisphosphonate, zoledronic acid has been shown to deplete macrophages in a similar fashion to clodronate, however it is used in a non-liposomal form and has been shown to target M2-type macrophages such as those expressing MMP-9 (Giraudo et al., 2004; Sabatino et al., 2014). In murine models of cervical carcinoma and liver cancer, zoledronic acid attenuated tumour progression, angiogenesis and metastasis by depletion of M2-type macrophages, although its

maximal effects were seen in combination with sorafenib (Giraudo et al., 2004; Zhang et al., 2010).

Another common approach has been to use immune-toxin conjugates directed against M2 markers as means to deplete TAMs. A number of models have been used to evaluate targeting of immunotoxins such *Pseudomonas* endotoxin A to commonly used M2 markers including folate or scavenger receptors (Bak et al., 2007; Nagai et al., 2009) . Whilst depletion of M2 macrophages usually provides positive results, the result is often delayed, or attenuated tumour growth as opposed to regression, or the engagement of anti-tumour immunity (Bak et al., 2007; Nagai et al., 2009; Wu et al., 2014). These results may represent the incomplete depletion of the suppressive TAM population, as many of these strategies hinge on the ability to identify TAMs by single markers. This is possibly best illustrated by Nagai et. al. where a >90% killing of folate receptor-positive macrophages, only constituted a 40% decrease in total TAMs (Nagai et al., 2009). An alternative interpretation of these results could be that removing the suppression induced by TAMs is insufficient to induce an anti-tumour response automatically, and needs to be accompanied by activation of the adaptive immune system.

1.4.3 Inhibiting the suppressive functions of TAMs

As an alternative to depletion of TAMs, another strategy utilised by several researchers has been to attenuate the suppressive functions of macrophages within tumours. Such strategies have relied on the increasing amount of research in the field that is studying the molecular determinants of TAM polarisation, identifying key regulators of the suppression functions within the cells themselves that may be amenable to therapeutic intervention.

Central to the TAM phenotype, is the suppression of many Th1-type, pro-inflammatory cytokines such as TNF-α, IL-12, IL-6 and IFN-γ. NF-κB is a major transcriptional regulator of pro-inflammatory cytokines within macrophages. Following engagement of pattern recognition receptors or stimulation by inflammatory cytokines such as TNF-α, a signalling cascade results in phosphorylation of the NF-κB inhibitor, I-κB, to enable nuclear localisation of the p65:p50 heterodimer and binding to its promoter to induce pro-inflammatory gene expression (Hagemann et al., 2009). As NF-κB activation is central to the production of major pro-inflammatory mediators, its expression is well regulated. One mechanism of regulation is at the level of competition for DNA binding; homodimers of p50 subunits can actively block binding of the activatory p65:p50 heterodimer. Recent findings identified that selective up-regulation and accumulation of p50 homodimers are present in TAMs and may provide a mechanism for the suppression of M1-type cytokine expression (Porta et al., 2009). Genetic deletion of p50 has validated the targeting of these homodimers, with such approaches being able to restore the typical IL-12^{high} IL-10^{low} cytokine profile associated

with M1 type macrophages (Saccani et al., 2006). However, the ubiquitous nature of NF-κB has made macrophage–specific targeting difficult to achieve and has limited its translation as a therapeutic option (Hagemann et al., 2009).

Acting in a similar manner to NF-κB, the signal transducers and activators of transcription family (STAT) of transcription factors integrate signals from cytokine stimulation of cell surface receptors via JAK-STAT signalling, to direct transcriptional profiles within immune cells. Of particular importance to TAM are STAT-3 and -6, which respond to IL-10 and IL-4 respectively to induce a number of suppressive molecules associated with TAM function (e.g. arginase) and to antagonise pro-inflammatory STAT-1 or NF-κB signalling (Hagemann et al., 2009). Studies looking to inhibit the activity STAT-3 and -6 have shown some promise. For example in a model of renal cell carcinoma the tyrosine kinase inhibitor sunitinib has been shown to reduce levels of STAT-3 in macrophages, correlating with some increases in inflammatory surface markers such as CD80 (Xin et al., 2009). Genetic deletion of STAT-6 has also been shown to be of utmost importance in TAMs, generating M1-type macrophages and enabling tumour rejection (Sinha et al., 2005); therapeutic means to selectively target STAT-6 in macrophages are still lacking. Combining the receptor targeting strategies described earlier with the antagonism of M2 signalling discussed here, one group has recently tried a TAM-targeted approach to STAT inhibition. Nanoparticles loaded with hydrazinocurcumin, (a turmeric derivative previous demonstrated to inhibit STAT-3 and -6) were targeted to suppressive macrophages using legumain, a lysosomal protease overexpressed on M2-polarised cells (Wang et al., 2011) . The authors demonstrated that this approach was able to suppress STAT-3 activation in macrophages, which were then able to exert tumouristatic effects on breast cancer cells (Zhang et al., 2013).

1.4.4 "Re-education" of TAMs

Strategies to deplete or inhibit TAMs have showed varying degrees of success, but are still hindered by a number of factors; prevalence of macrophages in well-established tumours can often negate the effects of inhibiting further macrophage recruitment, whilst the diversity of M2 type receptors often limits specific targeting of those macrophages once resident in the tumour. Further, previous studies demonstrate that antagonism of the suppressive effects of macrophages may not be sufficient to induce an anti-tumour response (Nagai et al., 2009).

The ability of macrophages to sequentially change phenotypes in response to changing microenvironments underpins their functional diversity and facilitates their tissue- and organ- specific roles within the body (Stout et al., 2009). It is this malleable, plastic nature that is harnessed by tumours to subvert macrophages towards a suppressive, tumorigenic phenotype (Biswas et al., 2008). However, in principle, this same plasticity could be utilised therapeutically to re-polarise TAMs back towards a pro-inflammatory phenotype.

Such re-polarisation of TAMs towards a more M1-like, tumouricidal phenotype has been termed "re-education" and is a fast-developing area of research, with a number of advantages over other approaches:

- First, the high level of macrophage infiltration in tumours becomes a major advantage for this approach, having all the potential effector cells required

already present within tumours, needing no depletion or recruitment of other macrophages.

- Second, re-programming TAMs simultaneously would remove one of the largest sources of immunosuppression within a tumour whilst creating a large source of pro-inflammatory cytokines to increase tumoricidal activity.

A number of studies have demonstrated therapeutic activation of macrophages, resulting in expression of markers associated with M1 macrophages and cytotoxic activity against tumour cells (Tang et al., 2013). Further, the range of different activation strategies utilised suggests that there are a great number of means by which macrophages may be activated toward tumouricidal activity including cytokine stimulation (Cao et al., 2009; Duluc et al., 2009; Roca et al., 2009; Watkins et al., 2007; Xu et al., 2015)(e.g. IL-21, IL12, IL-6, IL-2, TNF-α), antibody treatment (Lum et al., 2006) (e.g. anti-CD40) or TLR-stimulation (Kees et al., 2011; Sarkar et al., 2013)(e.g. Poly I:C, LPS) to name but some of the more common approaches. However, far fewer studies however have actually utilised the plasticity of these cells. Indeed, in many cases of "re-education" described, very few examples involve macrophages that have first been polarised towards a suppressive phenotype. These studies provide excellent examples of activation of naïve macrophages toward M1-type polarisations, but do not accurately describe the change in macrophage phenotype from one end of the polarisation spectrum to the other, which is likely to be required for successful re-education of TAMs.

Nevertheless, there have been some elegant examples of re-education of TAMs from a suppressive phenotype to a more M1-type. For example, in a model of more-developed

prostate cancer, Yin et. al. were able to examine the plasticity of macrophages that were already suppressed by their tumour microenvironment (Yin et al., 2013). They showed that sub-curative chemotherapy treatments enhanced cancer progression by fostering an immunosuppressive environment, mediated by phosphatidylserine (PS) exposure on the tumour cell surface. The authors identified that chemotherapy induced PS exposure, which engaged PS receptors on macrophages, inhibiting inflammatory responses and driving polarisation toward a TAM phenotype. Therapeutic re-education was performed using chemotherapy in combination with an anti-PS antibody to antagonise the PS-PS receptor interaction, whilst concurrently stimulating macrophages through activatory F_C receptor binding. The results of this study demonstrated changes to the phenotype of the previously suppressive TGF-β^{high}, IL-10^{high}, arginase^{high} TAMs to IL-12^{high}, TNF-α^{high}, iNOS^{high} macrophages (Yin et al., 2013). Further, the dramatic shift towards an M1 phenotype changed the receptor profile of the cells to increase CD80 and MHC II expression, suggestive of an acquired ability to present antigen. Increased NO production was shown to endow macrophages with direct tumoricidal capacity and in association with decreased VEGF, was attributed with decreased tumour angiogenesis.

Activation of CD40 by anti-CD40 antibody in combination with chemotherapy and TLR 9 stimulation has been shown to be able to re-educate TAMs (Buhtoiarov et al., 2005). In a model of established melanoma, this treatment regimen was able to induce tumour regression, in a mechanism attributed to a change in macrophage polarisation. Upon treatment, TAM phenotype shifted away from IL-10^{high}/IL-4^{high}, towards an IL-12^{high}/ TNF-α^{high}/ IFN-γ^{high} profile. Tumour cell cytotoxicity was principally as a result of increased TNF-α and NO production, inhibiting tumour cell proliferation and inducing apoptosis. Further, the change in TAM phenotype was shown to correlate with

a restoration in T cell function within the tumour (Buhtoiarov et al., 2010). The tumoricidal mechanism of CD40 ligation was largely attributed to the up-regulation of TNF-α and NO, both of which were dependent upon the induction of IFN-γ during treatment (Lum et al., 2006).

In another re-education study, a combination of CCL-16, CPG and anti-IL-10 antibody was shown to induce tumour regressions in a model of colon cancer that was attributed with change in macrophage phenotype. IL-10 producing macrophages were converted to M1-type macrophages, characterised by NO production and tumour shrinkage and decreased metastases (Guiducci et al., 2005). Importantly, the change in phenotype of these macrophages was linked to the induction of anti-tumour immunity. Within a week of treatment, tumour-specific CD8 cells were observed and correlated with rejection of tumours in 85% of cases. Such studies highlight that changes the suppressive tumour microenvironment by altering TAM can directly induce tumour lysis and induce tumour rejection alone (<30%), the main implication is the induction the adaptive immune system, overcoming inhibition microenvironments that attenuate anti-tumour T cell immunity.

These examples show that TAMs can be re-educated to reduce tumour growth, by direct tumoricidal activity, inhibiting essential processes for tumour growth (e.g. tumour angiogenesis) or engaging anti-tumour immunity. However, typically several different agents have been required in combination in these studies to induce a change in polarisation of TAM. Nevertheless most of these strategies converge in the production of IFN-γ which can act in a paracrine manner to direct macrophages toward a more M1-type phenotype.

Indeed, IFN-γ represents one of the most promising candidates for macrophage re-education and has been shown in a number of settings to be critical for activation and stimulation of the tumoricidal functions of macrophages (Schreiber, 1984; Schroder et al., 2003; Zaidi et al., 2011). As a monotherapy, IFN-γ has been shown to re-polarise macrophages isolated from the ascites of patients with ovarian cancer and re-establish the prototypic IL-12^{high}, IL-10^{low} phenotype, alongside up-regulation of co-stimulatory molecules and restoration T cell function (Duluc et al., 2009). Indeed, IFN-γ is reported to enhance antigen presentation through up-regulation of MHC I and MHC II surface expression in a range of cell types, but its functions in antigen presentation extend far beyond MHC expression; for example it can play significant roles in the processing and transport of antigen within an antigen-presenting cell (Arellano-Garcia et al., 2014; Kaplan et al., 1998; Keskinen et al., 1997). Some of the best-reported examples of IFN-γ improving antigen transport and processing are described in the context of the MHC I pathway. In the cytosol, peptides capable of binding into the MHC I cleft are generated through degradation by immunoproteasomes. The switch from the constitutive protease activity of the proteasome to the higher catalytic activity exhibited by the immunoproteasome is mediated by an IFN-γ-stimulated change in catalytic subunits of the 20S catalytic core; from the constitutively active β1, β2 and β5 subunits to the immunoproteasome-associated LMP-2, LMP-7 and MECL-1 (Aki et al., 1994). Peptide trafficking into the proteasome is often limited by the 19S regulatory caps, which recognise ubiquitin-tagged proteins and control their proteasomal degradation (Groettrup et al., 1995). IFN-γ increases the proteasome activator complex PA28, which provides an alternative cap for the 20S core to increase peptide entry and exit, a process that has been attributed with increased antigenicity (Boes et al., 1994; de Graaf

et al., 2011; Groettrup et al., 1995). Following processing by the immunoproteasome, peptides enter the endoplasmic reticulum (ER) by ATP-binding cassette (ABC) transporters. Production of these transporters-associated with antigen processing (TAP) is up regulated rapidly in response to IFN-γ. Increases in TAP-1 expression are mediated in a STAT-1 dependent manner in response to IFN-γ, concurrent with increases in MHC I surface expression levels (Brucet et al., 2004; Cramer and Klemsz, 1997). Processing of peptides continues beyond the levels of degradation by the immunoproteasome, as many antigenic peptides reach the ER in an amino-terminal extended pre-cursor form that require additional processing to shorter 8-10 amino acid length peptides to enable binding into the MHC-I cleft. A central protease identified in performing this role is the ER amino-peptidase, ERAP-1, whose expression is induced by IFN-γ (Saric et al., 2002). Importantly, immunoproteasome and ERAP activity act in concert to regulate antigen presentation via MHC I; basal levels of antigen processing by ERAP can down-regulate antigen presentation, trimming peptides excessively (>6 amino acid residues) such that they cannot fit in the MHC I cleft (Kloetzel and Ossendorp, 2004). IFN-γ can act to increase antigen presentation by increasing immunoproteasome activity to generate increased amino-extended peptides, which are then amenable to appropriate trimming by ERAP-1 (York et al., 2002). In this way, IFN-γ is able to increase both the production of antigenic peptides and their transport into the ER for loading onto nascent MHC I complexes. IFN-γ plays an equally important part in the antigen presentation of MHC II-restricted peptides. During lysosome-endosome fusion, IFN-γ up-regulates GILT, the γ-interferon-inducible lysosomal thiol-reductase, an enzyme involved in reducing di-sulphide bonds from endocytosed peptides to enable their optimal degradation (West and Cresswell, 2013). The importance of GILT is not limited solely to the MHC II pathway however. For

example, GILT up-regulation may be of particular importance for cross-presentation to CD8 T cells through MHC I, and has been demonstrated for virus glycoproteins that are rich in disulphide bonds, such as glycoprotein B from herpes simplex virus (Singh and Cresswell, 2010).

Such results have been validated in the clinic, where intra-peritoneally delivered IFN-γ has been shown to induce a change in polarisation of macrophages from patients with ovarian cancer (Allavena et al., 1990).

The potency and strength of IFN-γ signalling is particular attractive for re-education, where any potential therapeutic agent will need to overcome the existing suppressive signalling in place. Anti-inflammatory cytokines such as IL-4, IL-10 and TGF-β are prevalent suppressive mediators in tumours and have all been shown to induce TAM -/ M2- polarisation of macrophages, by increasing the immunosuppressive regulators of signalling, STAT-3 and -6 (Allavena and Mantovani, 2012). In the cases of IL-4 and TGF-β polarisation, IFN-γ can inhibit such suppressive signalling through up-regulation of SOCS-1 (Dickensheets et al., 1999). Whilst IFN-γ doesn't inhibit IL-10 signalling, it instead subverts IL-10 stimulated pathways to signalling through STAT-1 instead of STAT-3 (Herrero et al., 2003). The potency of IFN-γ is strengthened further by Duluc et. al, who screened common inflammatory cytokines for their ability to active tumour-associated macrophages, showing that only IFN-γ was capable of inducing significant macrophage activation (Duluc et al., 2009). Combined, these data make a strong case for the use of IFN-γ as an agent with which to re-educate tumour associated macrophages.

However this cytokine is an exemplar not only for the opportunities for re-education, but also as for the practical limitations to this approach; delivery and prolonged stimulation. In all the examples of re-education discussed thus far, the delivery of therapeutic regimen has largely been administered in situations very different from the clinical setting; frequently using *in vitro* models or sub-cutaneous tumours *in vivo*, easily treated by intra-tumoural injection (I.T.). Were these agents to be delivered in a more realistic setting, such as intravenous (I.V.) injection, a number of these approaches would become unfeasible as drug without efficient targeting to the tumour or shielding from clearance in the blood stream. IFN-γ is likely among the worst for delivery because of its short half-life, reported as less than 2 hours in the circulation, severely limiting its therapeutic application (Lortat-Jacob et al., 1996).

Such issues with delivery would be compounded by the need for repeated administration. The plastic nature of macrophages would most likely require a significant and sustained change to the microenvironment in order to facilitate re-education. Without it, macrophages would most likely revert back to the TAM phenotype. In conclusion, whilst re-education is an attractive option for the therapeutic treatment of TAM, its utility will be limited by the ability to deliver sustained levels of a candidate re-educating agent. A possible solution to this problem, which forms a central tenet of this thesis, is that superior delivery of IFN-γ can be achieved by encoding it within an oncolytic virus, allowing for its selective and sustained expression within the tumour microenvironment.

1.5 Oncolytic viruses

Oncolytic viruses are a novel anticancer therapeutic that amplify within cancer cells and lyse them, enabling spread to infect adjacent cells (Russell et al., 2012). Oncolytic viruses are highly selective and are an attractive therapeutic because of their ability to encode biological molecules including radiotherapeutic-sensitisers and cytokines. Oncolytic viruses are currently being utilised as 'oncolytic vaccines', encoding immunomodulatory agents such as IL-12 or GM-CSF in order to elicit an anti-tumour immune response (Melcher et al., 2011) such as herpes virus-based T-Vec (talimogene laherparepvec). Cancer-selective replication of most current oncolytic viruses is achieved by removing key functionalities from the virus, rendering it unable to thrive in its normal environment yet allowing transcomplementation of its activity by the tumour phenotype. The key to this is that many of the 'hallmarks of cancer' are similar to the features of a virus-infected cell, and judicious virus engineering allows production of genetically modified (attenuated) viruses that can only replicate successfully in cancer cells and therefore show impressive cancer-selectivity. Examples of this approach include T-Vec (which is engineered to exploit deficiencies in interferon defences in tumour cells), Jx594 (which also exploits the availability of phosphorylated thymidine in cancer cells) and Onyx-015 (designed to exploit deficiencies in P53-mediated apoptosis in cancer cells, but actually exploiting efficient nuclear export of late virus mRNA in tumour cells) (Kaufman et al., 2015; O'Shea et al., 2004). There are many such viruses now under clinical development, but work in this thesis will focus on making genetically modified versions of the oncolytic adenovirus ColoAd1.

1.5.1 Oncolytic virus specificity: cancer cell receptors

The first level of selectivity for oncolytic viruses may arise by differential transductional targeting. Tumour cells up-regulate the expression of a number of receptors compared to non-transformed cells in the same tissue. Some of these overexpressed receptors may constitute uptake receptors for oncolytic viruses. For example, adenovirus serotype 5 (Ad-5) utilises the coxsackie and adenovirus receptor (CAR) as its primary uptake receptor, which is up-regulated on a number of tumour types including colon, lung and liver (Reeh et al., 2013; Wunder et al., 2013). Another example is the complement regulatory protein CD46, which forms one of the principal virus uptake receptors for Measles virus and adenovirus serotype 11 (Ad-11), which is similarly up-regulated in a number of tumours including bladder, liver and breast cancer (Kinugasa et al., 1999; Thorsteinsson et al., 1998; Varela et al., 2008). As such, many viruses have innate tropism for cancer cells owing to the high expression of virus uptake receptors present on the surface of tumours.

1.5.2 Oncolytic virus specificity: genetic engineering to exploit cancer signalling

The next level of selectivity is usually at the level of selective replication. Genetic manipulations of the virus genome can endow selectivity via specific mechanisms. Akin to broad-spectrum chemo- and radio-therapies which often utilise rapidly proliferating cancer cells for selectivity, viruses can be engineered to target tumour cells with deregulated cell cycle. For example, oncolytic adenovirus was engineered with selectivity for cells with mutated or absent retinoblastoma protein (Rb) by partial

deletion of adenoviral E1A protein (Fueyo et al., 2000). Adenoviral E1A has been shown to bind Rb, an interaction that prevents Rb binding to- and inhibiting transcription factor activity of- E2F. (Zamanian and La Thangue, 1992). Thus, E1A can facilitate cell cycle progression by reversing Rb-mediated inhibition of E2F. Deletion of a 24-base pair sequence within the Rb-binding region of the E1A protein was demonstrated to inhibit formation of Rb-E1A complexes (Whyte et al., 1989), and was translated into a therapeutic through the engineering of an oncolytic adenovirus lacking this Rb-binding domain (Ad Δ24), enabling selective replication in cells that lack functional Rb, including tumour cells (Jiang et al., 2014). Similar strategies have been utilised in other oncolytic viruses such as with vaccinia virus and the deletion of the vaccinia thymidine kinase. Viral thymidine kinase improves the ability of viruses to replicate within cells that are not actively proliferating, by providing a source of phosphorylated thymidine required for virus DNA synthesis. Deletion of this gene in vaccinia virus allows selective replication in tumour cells and other cycling cells, which have a large external pool of thymidine (McCart et al., 2001). Arguably one of the best-documented cases of virus engineering to exploit deregulated tumour signalling is evidenced in the case of the oncolytic adenovirus H101 (Oncorine™), which gained product license in China for its specific replication in tumour cells lacking functional p53. Oncorine™ was developed from the earlier work of a similar oncolytic adenovirus, ONYX-015, which had the adenoviral E1B-55k protein deleted from its genome. E1B-55k binds p53 to inhibit its growth suppressing functions (Martin and Berk, 1998). As such, ONYX-015 was engineered as an oncolytic adenovirus that would selectively replicate and lyse tumour cells with defective p53. However, in the case of ONYX-015, it was later shown that the tumour-selective function was not due to compensation of a lost ability to inhibit p53, but instead related to the late viral RNA export functions that

E1B-55k possessed. Selectivity was in fact endowed in tumours which had de-regulated RNA export and could therefore export late virus RNA, an ability lost upon deletion of E1B-55k (O'Shea et al., 2004). Oncolytic viruses can also exploit over-active promoters found in highly proliferative tumours as a means to restrict virus replication and lysis to cancer cells. One of the most developed examples of such a strategy is in the case of CG7870, an oncolytic adenovirus that demonstrates prostate cancer-selective replication (Small et al., 2006). This virus exploits the up-regulated expression of PSA (prostate-specific antigen) in prostate cancer cells, with the early virus genes (E1B) placed under transcriptional control of a PSA promoter-enhancer, restricting virus replication to cells with overexpressed PSA (Small et al., 2006).

1.5.3 Oncolytic virus specificity: Defective interferon signalling in tumours

An additional mechanism of selectivity has been proposed to be at the level of antiviral defence signalling (Zhang et al., 2010). Upon recognition of virus, cells produce high levels of type I interferon. Interferons, so named for their ability to interfere with virus replication, are one of the principal orchestrators of anti-viral responses. For DNA viruses such as adenovirus and herpes virus, virus double-stranded DNA is recognised in the cytoplasm by cGAS, cyclic GMP-AMP synthase. Upon binding virus DNA, cGAS catalyses the production of cGAMP (cyclic GMP-AMP), which initiates a cascade of signalling that results in the production of IFN; cGAMP is able to activate STING (stimulator of IFN genes), which in turn activates NF-κB or IRF-3, which enables their translocation into the nucleus to bind ISGEs and initiate IFN production. Intracellular recognition of cytoplasmic viral RNA is mediated principally through PKR and RIG-I-like receptors (RLRs) such as RIG-1 and MDA-5, which possess helicase

domains for RNA binding and CARD (caspase activation and recruitment) domains to initiate signalling following the binding of viral RNA. MDA-5 has been shown to control recognition of picornaviruses, whilst RIG-1 is central in binding negative- and positively-stranded virus RNA such as those of influenza and reovirus, respectively. Once activated by virus RNA, MDA-5 and RIG-1 are able to interact with the adaptor protein MAVS (mitochondrial antiviral signalling complex). The activation of MAVS subsequently results in the activation of TBK-1 and/or IKKε, resulting in the phosphorylation and subsequent nuclear translocation of IRFs-3 and -7 to stimulate type I and III IFN production. Additionally, activation of MAVS can result in activation of the NF-κB pathway through phosphorylation of IKK-β, which in turn phosphorylates the inhibitory IκB subunit, to enable translocation of the p50/p65 heterodimer, and transcription of pro-inflammatory cytokines.

In non-transformed cells, signalling through type I interferon (IFN) receptors by IFN-α and –β causes a number of downstream cellular responses. Signals from the type I IFN receptor are transduced by the tyrosine kinases Tyk-2 and JAK-1, which subsequently phosphorylate the transcription factors STAT-1 or STAT-2, enabling their nuclear translocation as hetero- or homo-dimers of STAT-1/2 (Platanias, 2005). Once in the nucleus these STAT dimers can complex with IRF-9 and bind interferon-stimulated response elements to activate transcription of a number of Interferon-stimulated genes (ISGs). One function of the ISGs is to up-regulate prominent sensors of virus nucleic acid that can sense the presence of virus DNA or RNA and shut-down host translation. One of the most documented examples of such an ISG is protein kinase RNA-activated, PKR, a sensor of double-stranded RNA (dsRNA) (Klampfer et al., 2003). PKR becomes activated in response to dsRNA by way of an auto-phosphorylation event. This enables

PKR to subsequently phosphorylate the translation initiation factor eIF2, to inhibit its nucleotide exchange function and thereby inhibit further host translation to prevent virus replication. Another main function of IFN signalling and ISG induction is to induce production of type I IFNs. These IFNs are then able to act in an autocrine manner to reinforce anti-viral signalling and paracrine manner to restrict virus growth in neighbouring cells (Sadler and Williams, 2008). As such, the interferon response represents a potent anti-viral cellular defence.

Type I IFN have also been shown to promote tumour immunosurveillance through activation of dendritic cells, preventing death of anti-tumour CD8 T cells following their activation and increasing NK tumour cell killing (Hiroishi et al., 2000; Hoshino et al., 2002; Swann et al., 2007). As such, during the immunoediting phase of cancer development, many tumours aim to disrupt effective IFN signalling as a means to evade anti-tumour immune responses. This is best evidenced by the fact that over 60% of human cancer cell lines demonstrate a defective interferon response (Ilkow et al., 2014; Stojdl et al., 2003). Alterations to tumour IFN signalling have been reported at many locations within the IFN signalling pathway; Prostate cancer cells have been shown to lack JAK1 (Dunn et al., 2005), bladder cells can exhibit down-regulation of type I interferon receptor (Zhang et al., 2010) and STAT-1 is found impaired in a number of cancers including melanoma (Lesinski et al., 2007), lymphoma (Wu et al., 2015) and colorectal (Klampfer et al., 2003).

Such defects to anti-viral interferon responses in tumours provide an additional layer of selectivity for oncolytic viruses, restricting replication to tumour cells as intact antiviral signalling in non-transformed cells would prevent virus replication. One of the best

studied examples of selective replication in IFN-defective cells is with oncolytic reovirus (Ilkow et al., 2014). Transformation of cells is often associated with Ras mutation, which can negatively regulate IFN-β production: Oncolytic reovirus infection is therefore often restricted to cells with mutated Ras, which have defective IFN signalling (Shmulevitz et al., 2010).

1.5.4 ColoAd1

ColoAd1, also know by the INN pharmaceutical name Enadenotucirev (EnAd), is a chimeric Ad11p/Ad3 adenovirus, selected from a library of chimeric adenoviruses for the ability to replicate and exit rapidly from tumour cells (Kuhn et al., 2008). EnAd is able to lyse a broad range of carcinoma cell lines killing cells more quickly than wild type Ad11p, Ad3 or Ad5. In normal human cells in culture ColoAd1 activity is either negligible or highly attenuated (Di et al., 2014; Kuhn et al., 2008).

The specificity of ColoAd1 for cancer cells is most likely a reflection on how the virus was generated, using a process of "directed evolution" rather than rational design (Kuhn et al., 2008); a library of adenoviruses were serially passaged over a range of colorectal cancer cell lines, infecting at high multiplicities of infection to promote recombination of virus genomes. The resulting ColoAd1 virus shows potent killing of human carcinoma cell lines, with limited evidence of cytotoxicity in normal epithelial or endothelial cells (Kuhn et al., 2008). Partial selectivity of ColoAd1 for tumour cells can be explained by its composition; as a chimeric Ad11p/Ad3 (largely Ad11p), ColoAd1

utilises CD46 as its primary virus uptake receptor which has been demonstrated to be up-regulated in a number of cancers including bladder, breast and colorectal (Thorsteinsson et al., 1998; Varela et al., 2008). Relative to wild type Ad11p, ColoAd1 has a large deletion in the E3 region and a small deletion in E4or4F; E3 gene products are largely associated with evading the immune system, enabling the virus to escape anti-viral immune responses. The adenovirus E3-gp19K protein is among the best documented of these E3 gene products and acts to inhibit antigen presentation by interfering with MHC I, both through antagonising the loading of antigenic peptides into the cleft and by inhibiting MHC I-peptide complexes trafficking to the cell surface (Bennett et al., 1999). The deletion of these immune evading functions in the E3 region has been suggested to represent a potential mechanism by which ColoAd1 will elicit an immunogenic cell death and induce anti-tumour immune responses (Seymour and Fisher, 2016). Additionally however, E3 deletion should confer tumour selectivity as the absence of viral immune-evasins would severely attenuate the ability of the virus to replicate in normal tissue, which does not exhibit the local immunosuppression found in tumour microenvironments (Wang et al., 2003). The E4orf4 deletion in the ColoAd1 genome is thought to represent another potential way by which virus achieves tumour specificity. The E4orf4 protein is thought to re-direct cellular resources and pathways towards the synthesis of virus genomes by activating mTOR signalling (Miron et al., 2009). Deletion of E4orf4 attenuates virus replication in normal cells, but in transformed cells that have already directed pathways towards growth the function appears redundant (O'Shea et al., 2005). The ColoAd1 genome also possesses significant alterations to the E2B region, which is comprised of a mosaic of sequences from both Ad3 and Ad11p. The precise role of this chimera is still under investigation

but it is thought that it encodes a very efficient virus DNA polymerase and that this may increase replication rate and cytotoxicity.

One notable advantage of ColoAd1 is that the capsid is entirely derived from Ad11p for which the prevalence of neutralising antibodies in generally lower in humans relative to other serotypes and clinically relevant particle concentrations can infect tumour cells in whole human blood (Di et al., 2014).

As an adenovirus, ColoAd1 has many desirable features for a product candidate including the ability to produce consistent batches of high titre particles, a high fidelity double strand proof-reading polymerase and a robust non-enveloped protein capsid providing good stability under a range of conditions. Nevertheless, translating biological drug candidates from the laboratory to the clinic can be challenging, particularly how to identify the optimum starting dose for human trials.

Clinical experience with ColoAd1 has been encouraging thus far, showing live virus particles being recovered from the blood stream after systemic delivery (personal communication, PsiOxus Therapeutics). The main side effect is acute inflammation shortly after delivering particles. This is an expected toxicity for intravenous delivery and the effects are transient and can be manageable by dose and schedule. Most strikingly there is convincing histological data showing that, following intravenous delivery to patients with different types of epithelial cancer, ColoAd1 can access, infect and replicate in cells throughout the solid tumour mass, including expressing a high level of virus protein (which was used as the basis of the histological stain). This provides a very interesting option for encoding biologics within ColoAd1 for

intravenous delivery to patients with metastatic cancer, allowing targeted infection and transgene expression in disseminated tumour masses. Importantly, all pre-clinical data thus far confirms the selectivity of ColoAd1 for replication in tumours and early trial data supports these findings. This is central for the safety of "arming" the virus, particularly with pro-inflammatory cytokines such as IFN-γ or TNF-α which are exceptionally potent and could lead to systemic toxicity if expression were not restricted to the tumour microenvironment.

This possibility for targeted expression of therapeutic biologics selectively within tumours provides a platform for many new targeted therapeutic strategies, with the added advantage that the biologic is actually produced in the tumour – and does not pass through the bloodstream en route to the tumour. This should lead to high therapeutic indexes and may permit the use of potent biologics that are not normally useful for intravenous delivery because of systemic toxicities.

The central aim of this thesis is to use ColoAd1 to express a biologic that is capable of re-polarising TAMs to active their tumouricidal functions. The lead candidate agent to be developed is IFN-γ, formerly known as macrophage activating factor, and this will be the subject of the experimental chapters.

1.6 Thesis aims and hypothesis

1.6.1 Thesis aims

The overarching aim of this thesis is to use ColoAd1 armed with IFN-γ to re-educate tumour-associated macrophages, thereby attenuating their immunosuppressive functions and eliciting the tumouricidal properties of these cells. In the course of the thesis, a number of methodologies will be developed to examine the functions and phenotype of differentially polarised macrophages. Further, a number of models will be developed to create clinically relevant models of TAM polarisation and re-education.

1.6.2 Thesis hypothesis

1. The central hypothesis of this thesis is that macrophage plasticity can be harnessed therapeutically and could be utilised to locally activate the tumouricidal functions of tumour-associated macrophages.
2. The pro-inflammatory cytokine IFN-γ has the capacity to activate the tumouricidal functions of tumour-associated macrophages in the immunosuppressive microenvironment of a tumour.
3. ColoAd1-IFN-γ will circumvent the short-falls in the stability of IFN-γ to re-educate tumour-associated macrophages through the sustained production of IFN-γ and additionally through the effects of lysates generated by virus infection of tumour cells.

Chapter 2

Methods and methods

2 Materials and Methods

2.1 Cell lines

2.1.1 Cell line maintenance and sub-culturing

All cell lines (*Table 2.1*) were maintained in their respective DMEM or RPMI (Gibco™) base medias as detailed in the table below, and were supplemented with 10% Fetal Bovine Serum (Gibco™) and 1% Penicillin/Streptomycin (10mg/mL, Sigma™) in a humidified 37°C incubator (5% CO_2), unless otherwise specified. The majority of the murine macrophage work performed in cell lines, optimizing techniques and experimentation for characterising macrophage phenotypes and re-education using the IC-21 murine macrophage cell line, with results later validated using *in vivo* methodology. Similarly, with the scarcity of clinical samples and the significant level of optimisation required for the human macrophage experimentation from clinically-obtained samples, the THP-1 cell line was extensively used to optimize and develop experiments required to study polarisation and re-education, with clinical samples utilised later to validate results obtained *in vitro*.

With the exception of IC-21 and THP-1, cells were split before reaching confluency by enzymatic dissociation with Trypsin/EDTA (0.05%). In brief, culture media was aspirated and cells were washed twice with 15 mL of PBS. PBS was aspirated, and cells were dissociated using Trypsin/EDTA at 37°C for 2-5 minutes. Enzymes were neutralized by the additional of 10 volumes of culture media, from which cells were

subsequently re-seeded into new flasks. IC-21 cells experience toxicity associated with Trypsin and so were dissociated instead using Enzyme-free dissociation buffer (Sigma™).

THP-1 monocytes were maintained in suspension at concentrations between 0.3-1 x 10^6 cells/mL. For differentiation into macrophages, THP-1 cells were treated with 30 ng/mL PMA (Sigma™) for 24 hours, before media was replenished with new RPMI without PMA to avoid toxicities associated with pro-longed PMA exposure.

In the macrophage field, it is relatively common for researchers to switch their macrophage media to 0% FCS (serum starvation) 12-24 hours before beginning treatments. Such practices were not established in our laboratory when I began my research and as such, serum starvation has not been used in this thesis for macrophage experimentation.

Name	Information	Culturing Media	Source
A549	Human Lung adenocarcinoma	DMEM	ATCC
B16	Murine Melanoma	RPMI	ATCC
B16-OVA	Murine Melanoma, expressing Ovalbumin	RPMI	University of Oxford*[1]
IC-21	Murine peritoneal macrophage	RPMI	ATCC
DC-2.4	Murine dendritic cell line	RPMI	University of Oxford*[1]
IGROV-1	Human epithelial ovarian carcinoma	RPMI	ATCC
HEK 293A	Human embryonic kidney, adherent	DMEM	ATCC
SW480	Human colorectal adenocarcinoma	RPMI	University of Oxford*[2]
THP-1	Human Monocytic leukemia	RPMI	ATCC

Table 2.1. Cell lines

The cell lines used in this thesis along with their respective culturing media are detailed above. All cells were purchased from the American-type Cell Collection (ATCC), with the exception of B16-OVA and SW480. B16-OVA were provided as a kind gift from *[1] Dr. Gray Kueberuwa, Department of Oncology and SW480 were provided as a kind gift from*[2] Prof. Alison Banham, Nuffield Division of Clinical Laboratory Sciences

2.1.2 Mycoplasma testing

Mycoplasma testing was central to the work performed in this thesis. As much of the experimentation performed sought to induce inflammatory responses in macrophages, it was essential to know that cells were not exposed to mycoplasma as this could significantly skew results, masking positive results or inducing false-positives. Cell lines were routinely (every 2-3 months) tested for presence of mycoplasma using the MycoAlert™ kit (Lonza, UK) as per manufacturer's instructions. In short, supernatants from cell lines in culture where harvested when cells were between 50 and 80%

confluency, centrifuged (250 x g, 5 mins) to remove any cells, with the resulting supernatant collected and stored at -20°C until ready to analyse. Samples are thawed and reconstituted with the MycoAlert™ reagents and allowed to incubate for 15 minutes before 100 µL of the sample is analysed for luminescence.

The MycoAlert™ assay is principally a luciferase assay, where bacterially produced ATP reacts with luciferin to produce light in a luciferase-catalysed reaction, which can be detected using a Lumat LB 9507 luminometer (Berthold Technologies, UK):

ATP + luciferin + O_2 ➔ oxyluciferin + AMP + PPi + CO_2 + light

MycoAlert Substrate™ contains substrates for mycoplasmal enzymes, which catalyse the conversion of ADP to ATP. It is these increased levels of ATP which are utilised for in the luciferase-based MycoAlert™ kit which drive luminescence and indicate mycoplasma contamination of samples

2.2 In vivo experimentation

All animal experimentation was performed in accordance with Home Office Guidelines for animal welfare and was approved by animal ethics committee in the University of Oxford, working under the laboratory project license (PPL 30/2819, under Prof. L. Seymour) and my personal license (PIL 40/10545).

2.2.1 Housing conditions

Eight-week old BALB/c nude mice were purchased from Charles River™ and were housed at the John Radcliffe Biomedical sciences facility in individually vented cages, that were environmentally enriched and contained no more than six mice per cage. Mice were provided with formulated diets and given access to sterile water.

2.2.2 Intraperitoneal tumour injection and sample collection

Translation of *in vitro* virus infection experiments and resulting macrophage polarisation studies into an immunocompetent mouse model is limited by the human-tropic nature of adenovirus; ColoAd1 requires human cancer cells for replication that in turn will require a immune-compromised mouse for xenografting, which consequently limits the number of immune subsets available. Compounding these considerations, a number of ovarian cancer cell lines xenografted into the peritoneal cavity do not accurately re-capitulate ovarian ascites, often failing to grow in this environment, or instead forming solid omental tumours (Shaw et al., 2004) (personal communication, PsiOxus Therapeutics Ltd.). IGROV-1 cells were chosen for the murine ovarian ascites experiments as they have previously been demonstrated to recapitulate peritoneal ascites and are compatible with ColoAd1 infections (Shaw et al., 2004). Mice were injected under anaesthesia with 0.5 mL of PBS containing 2 x 10^6 IGROV-1 cells using a syringe with a 25-gauge needle. Mice were monitored daily over the course of peritoneal ascites development (up to 25 days) for changes in weight and behaviour. Ascites were harvested by peritoneal lavage. In short, mice were euthanised, then injected with 5 mL PBS containing 0.5 mM EDTA and were given a gentle peritoneal massage. A small incision was made through the abdomen and peritoneum into which a sterile Pasteur pipette was used to aspirate the ascitic fluid. Ascitic fluid was transported back to the main laboratory at 4°C in 15 mL polypropylene Falcon tubes (Corning™, USA), whereupon cells were pelleted by centrifugation (350 x *g*, 5 minutes). Residual red blood cells were lysed by resuspension of cells in 1ml red blood cell lysis buffer (Sigma™) and incubated for 5 minutes at 4°C, before 10 volumes of PBS were added and cells re-pelleted by centrifugation. Ascites cells were either stained for receptor

analysis by flow cytometry or were used in *ex vivo* culture as described below (*Section 2.2.4*).

2.2.3 *In vivo* treatment of ovarian ascites

After 25 days of ascites development (as described in Section 2.2.2), mice were given a single I.P. injection of 0.5 mL of PBS alone (control), or containing murine IFNγ (10ng/ml), ColoAd1 ($8x10^{10}$ VP/mL) or, ColoAd1- mIFNγ ($8x10^{10}$ VP/mL) for 7 days. To facilitate even distribution of the injected sample, a gentle peritoneal massage was applied. Mice were monitored for changes in behaviour and weight on a daily basis throughout the treatment. Ascites were collected for analysis on day 7 post-treatment (as described in Section 2.2.2).

2.2.4 *Ex vivo* treatment of murine ovarian ascites

Ascites were harvested after 25 days of development (as described in Section 2.2.2). Cells isolated from ascites were seeded into 48 well plates (Starlabs, UK) at a concentration of 2 $x10^5$ cells per well in complete RPMI medium. Cells were treated with 10 μL of either PBS (control), 10ng/ml murine IFNγ, ColoAd1-GFP ($8x10^{10}$ VP/mL) or, ColoAd1-mIFNγ ($8x10^{10}$ VP/mL) for 7 days. Cells were harvested using non-enzymatic methods for flow cytometry (Section 2.5.2.1), whilst supernatants were probed for levels of mIFNγ by ELISA (Section 2.5.3).

2.3 Patient samples

The limited availability of complex, immunocompetent models with which to study oncolytic adenovirus treatment of human cancers necessitates the development of models which better recapitulate the tumour microenvironment. As such, efforts were made in this thesis to utilise patient samples as an immunocompetent model for oncolytic adenovirus research. Ascites from patients with ovarian cancer represent an attractive model, as they contain a mixture of cancer cells and immune cells, are isolated by a minimally invasive procedure, and often provide a large numbers of cells for experimentation. Patients of the Churchill Hospital whom were diagnosed with advanced ovarian cancer and concurrent malignant ascites, were identified by Specialist Registrars on the ward when patients were scheduled for a drain of their ascites fluid on the ward (*Table 2.2*). Where possible, and in accordance with local NHS and University research ethics committees, patients were consented by a good clinical practice (GCP)-trained physician, and their collected ascites were obtained for research purposes. Samples included in this thesis are listed below with accompanying patient information where it was made possible.

Ascitic fluid from patient with advanced ovarian cancer	
Patient	**Previous treatment history**
1	Chemotherapy (un-specified)
2	Chemotherapy (un-specified)
3	R-CHOP*
5	No information available
6	No information available
7	Chemotherapy (un-specified)
8	No information available
9	Carboplatin
10	Cisplatin
35	Chemotherapy (un-specified) resistant; now treated with AKT inhibitor
36	Prior chemotherapy(un-specified); now treated with anti-estrogen therapy
37	Taxol

Table 2.2 Patient samples

A list of the patient samples utilised in this thesis and their previous treatment history is provided for reference purposes. * Patient 3 was originally treated for advanced ovarian cancer, presenting with ascites. The patient was treated with R-CHOP for the secondary acute leukemia that had developed

2.3.1 Collection and processing

Patient ascites were transferred to 500 mL centrifuge tubes (Corning) and the cells were pelleted by centrifugation (500 x *g*, 10 minutes, 37°C). Supernatants were removed and transferred into new centrifuge tubes and this process and spun again to ensure complete removal of cells. Cell-free supernatants were collected, aliquoted and stored at -20°C for future experimentation. Ascites cells had residual red blood cells lysed using red blood cell lysis buffer (Sigma™ , UK); 5ml of red blood cell lysis buffer was used to

resuspend cells, which were incubated for 5 minutes at 4°C before. 10 volumes of PBS were added to the mixture, and cells were re-pelleted by centrifugation.

2.3.2 *Ex vivo* culturing

Ascites cells were re-constituted in autologous ascitic fluid at a concentration of $2x10^6$ cells/mL, supplemented with HEPES buffer to a final concentration of 25 mM. Cells were re-suspended in 15 mL Falcon tubes (Corning) to a volume of 7 mL, then incubated on a rotating wheel, incubating cells at 37 °C

2.4 Production of IFN-γ-expressing ColoAd1

2.4.1 Molecular biology techniques for ColoAd-1 cloning

2.4.1.1 Bacterial transformation

To amplify recombinant DNA plasmids, transformation of bacterial *Escherichia coli* (*E. coli)* cells was utilised. For cloning of the ColoAd1 virus, XL-1 blue cells (Agilent) were thawed on ice before the addition of 5μL of DNA ligations (1-100 ng/mL DNA) for 30 minutes, with a 35 second heat shock at 42°C, before returning on ice for two minutes. 450 μL of SOC media was added, and the transformation mixture was streaked out on agar plates containing Kanamycin, and incubated overnight at 37°C.

Bacterial colonies were picked and grown as mini- or maxi- preps (5 mL or 120 mL Luria Broth (LB), respectively) under kanamycin or ampicillin selection. Preparations were incubated overnight at 37°C in an orbital shaker at 200 rpm (Sanyo Biomedical, USA)

2.4.1.2 Plasmid purification

Purification of bacterially amplified DNA plasmids was performed using the QIAprep MiniPrep kit (for use with mini-prepped 5 mL cultures, Qiagen) or the Qiagen MaxiPrep kit (for use with maxi-prepped 120 mL cultures, Qiagen). Purifications were carried out as per the manufacturer's instructions. Following production of fully cloned virus DNA, confirmatory DNA sequencing was performed (Source Bioscience).

2.4.1.3 DNA quantification

DNA was quantified by spectrophotometry using a Nanodrop (Thermo Scientific, UK). Before analysing the DNA content of samples, the machine was "blanked" using nuclease free water, before providing background readings by analysing a sample of the buffer in which the DNA was eluted, typically nuclease free water or elution buffer (Qiagen, UK). DNA concentration is calculated by recording the absorbance at 260nm, with the purity of the DNA sample determined by comparing the absorbance measured at 280nm (to indicate presence of protein or RNA contaminants).

2.4.1.4 DNA restriction digests

Restriction digests were used to prepare DNA fragments for subsequent ligation into appropriate vectors or were used to confirm successful ligations, digesting 7µg or 0.5µg of DNA respectively. Restriction digest reactions were performed in accordance with manufacturer's instructions (New England Biolabs, USA). In short, restriction digest reactions were usually performed at 37°C for 1 hour in a 20µL reaction comprising

DNA (to required concentration), 2μL of CutSmart™ Buffer, 1μL of each restriction enzyme required and nuclease-free water (to a final volume of 20μL).

2.4.1.5 DNA ligation

DNA fragments for insertion were generated by restriction digest, with correct fragments identified by gel electrophoresis and corresponding bands subsequently excised and purified using the QIAquick gel extraction kit, as per the manufacturer's instructions (Qiagen, UK). Recipient DNA vectors were prepared for ligation by restriction digest (as per the digestion performed for the insert) to generate compatible DNA overhangs, followed by de-phosphorylation of the vector (to reduce background colony formation from vector re-ligation) using 2μL of calf intestinal alkaline phosphatase at 37°C for 1 hour, as per manufacturer's instructions (Invitrogen, UK). Ligation reactions were performed as per manufacturer's protocols from New England BioLabs (NEB). In short, 2μL of T4 DNA ligase buffer, 1μL of T4 DNA ligase, insert and vector DNA (to a ratio of 3:1, insert: vector) were made up with nuclease-free water to a total reaction volume of 20μL, and incubated for 1 hour at room temperature. Ligation of the IFN-γ-containing mPSF shuttle plasmids into the ColoAd1 backbone has strict requirements for vector: insert ratios and for the temperature and duration of the ligation reaction; these are detailed below (*Table 2.3*).

Reaction componet	Reaction composition	Reaction conditions
10x T4 DNA Ligase Buffer	2µL	Incubated at 16°C for 12 hours
ColoAd1 backbone (vector)	60 ng	
mPSF shuttle (insert)	90 ng	
T4 DNA ligase	1µL	
Nuclease-free water	made up to 20µL final	

Table 2.3 DNA ligation reaction composition

DNA ligation was performed as per manufacturer's instructions (NEB). The composition of the reaction is detailed above – of particular note is the strict requirement for a 1:1.5 ratio of vector to insert for the ligation into the ColoAd1 backbone

2.4.1.6 Agarose gel electrophoresis

Digested DNA fragments were separated by gel electrophoresis to confirm successful ligations or to facilitate excision of DNA fragments for further manipulation. DNA was run on 1% w/v agarose gels (Invitrogen, UK), visualised by the addition of 0.5 µg / mL ethidium bromide. Gels were run in 0.5 x TAE buffer (0.3g EDTA, 1g Glacial acetic acid, 4.85g TRIS-base in 1L dH_20) for 40 minutes at 120V in electrophoresis gel tanks (BioRad, UK), with gels visualised under UV light using an Alpha Imager (Alpha Innotech, USA)

2.4.1.7 Addition of restriction endonuclease sites by PCR

To facilitate ligation of human and mouse IFN-γ sequences into the mPSF shuttle plasmids, NheI and NotI restriction sites were required to flank the IFN-γ sequences to be compatible with the multiple cloning site of the shuttle plasmid (*Table 2.4*). NheI and

NotI sequences were added to the IFN-γ sequences by PCR. PCR was performed using a PTC-225 DNA Engine Tetrad thermal cycler (MJ Research, USA), with the PCR reaction performed using Phusion DNA polymerase master mix (NEB), according to the manufacturer's instructions. In short, 1ng of template DNA was combined with 12.5µL of Phusion Master mix, 1.25µL of forward primer (10µM), 1.25µL of reverse primer (10µM) and made up to a total reaction volume of 25µL with nuclease free water. The primers and protocol for the PCR reaction are detailed below (*Table 2.5*).

Name	Sequence (5'➔3')
mPSF shuttle hIFNγ Forward	aaaagcggccgccacgccgccaaatatacaa
mPSF shuttle hIFNγ Reverse	ttttgctagcctgggatgctcttcgacctcga
mPSF shuttle mIFNγ Forward	aaaagcggccgccacgccgccaacgctacaca
mPSF shuttle mIFNγ Reverse	ttttgctagcgcagcgactccttttccgcttcctg

Table 2.4 Primers for addition of restriction endonuclease sites

Cyles	Step	Stage	Temp (°C)	Time (sec)
1	1	Primary denaturation	98	60
10	2	Denaturation	98	20
	3	Annealing	58	30
	4	Extension	72	60
25	5	Denaturation	98	20
	6	Annealing	65	30
	7	Extension	72	60
1	8	Final extension	74	360
	9	Holding	4	∞

Table 2.5 PCR Protocol

2.4.2 Cloning of human and murine IFN-γ into ColoAd1

Cloning of human and mouse IFNγ into the ColoAd1 virus was performed using an in house protocol optimised by PsiOxus Therapeutics Ltd. and is described in detail in Chapter 3. A schematic of the overall cloning strategy is provided in *Figure 2.1*. In short, human and mouse IFNγ sequences were ligated into the multiple cloning site of the shuttle plasmid following restriction digest of IFNγ plasmid and mPSF shuttle with NotI and NheI, to flank the IFNγ sequences with a CMV promoter and poly A tail. The ligation products were used to transform bacteria, which were grown on agar plates containing kanamycin. Colonies were picked and mini-prepped. Successful ligation into the shuttle plasmid made an expression cassette to enable CMV-driven transgene expression. The CMV-poly A cassette was further flanked by unique restriction sites (AsiSI and Sbf1) to facilitate digestion and ligation in the ColoAd1 backbone. The mPSF plasmid was digested with AsisI and SbfI to enable ligation into the ColoAd1 backbone. Ligation into ColoAd1 was performed overnight, with successful ligation confirmed by diagnostic restriction digests.

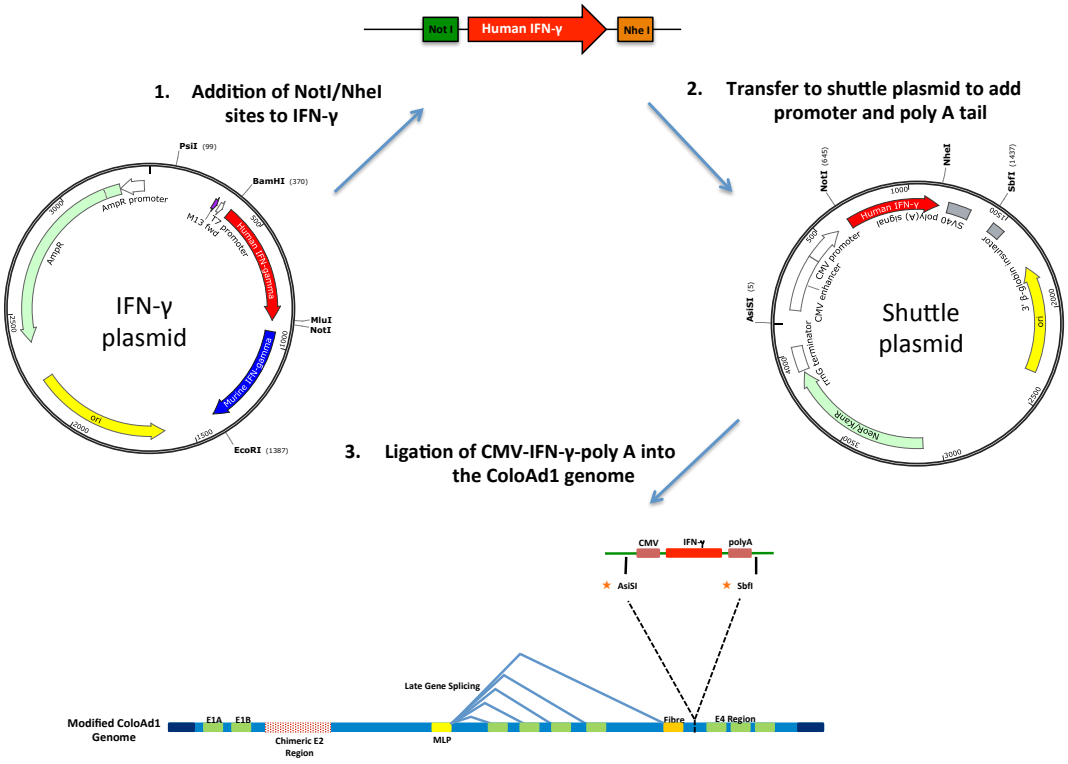


Figure 2.1 ColoAd1 cloning overview

The cloning strategy for arming ColoAd1 with IFN-γ is depicted in a simplified schematic. The full cloning process is described in Chapter 3

2.4.3 Growth and purification of ColoAd1-h IFN-γ and ColoAd1-m-IFN-γ

2.4.3.1 Virus Rescue

ColoAd1 genomes containing IFN-γ (10-15 µg of DNA) were first linearized using by restriction digest with AscI, following which, the DNA was cleaned up by MiniPrep (Qiagen). For transfection of virus genomes, T25 flasks (Corning) were seeded with 8 x 10^5 HEK 293A cells in complete DMEM media on the day prior to genome linearisation. Virus genomes were transfected into cells using a standard transfection procedure. In short, 20 µL of Lipofectamine 2000 and 30 µL of OptiMEM (Life

Technologies) were incubated together 5 minutes before being combined with an additional 50 µL OptiMEM containing linearised virus DNA, which was incubated together for 20 minutes at room temperature. This DNA:Lipofectamine complex was then combined with 4 mL of OptiMEM and added to the HEK 293A cells for 4 hours at 37°C. After this time, media was replaced with fresh DMEM (2% FBS). Cells were monitored for signs of cytopathic effect (CPE), at which point cells and supernatant were harvested using cell scrapers (BD, UK) and aliquoted at -80°C (*Figure 2.2*). 500 µL of this lysate was used to infect an 80% confluent T175 flask of HEK 293A cells, and the process of infection and waiting for CPE was repeated to generate a seed stock of virus.

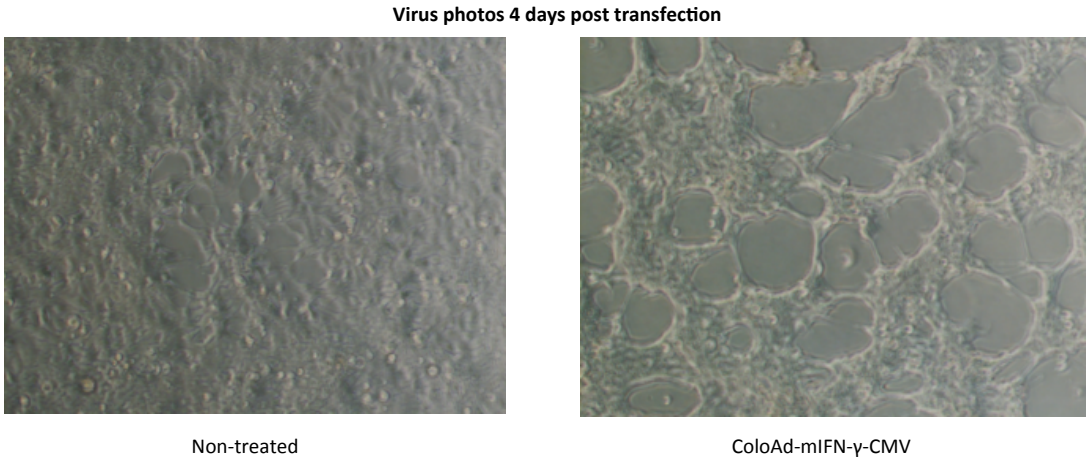


Figure 2.2 Rescue of ColoAd1 viruses expressing murine and human IFN-γ

Four days after transfection with virus genomes, HEK 293A demonstrate signs of cytopathic effect (CPE), **right panel**. Cells and supernatants were harvested at this point to generate a virus lysate.

2.4.3.2 Virus growth and banding

Per virus, two Hyperflasks™ (Corning) were seeded with 1 x 10^7 HEK293A cells each in 500 mL complete media (DMEM) per flask, which reached 80% confluency after 3

days. Each hyperflask was exchanged for fresh media for DMEM (2% FBS) containing 1 mL of virus seed stock generated previously. Virus infection was monitored over the course of the next four days to identify visible signs of infection, but before significant CPE. At this stage, cells were harvested from flasks by agitation and pelleted by centrifugation (500 x g, 5 minutes). Cell pellets were lysed by repeated freeze thaw cycles and were double-banded on caesium chloride gradients (Gradients p=1.45 (20.5g CsCl, 2.9ml 0.5M Tris pH 7.9, 25ml water) and p=1.32 (32.0g CsCl, 6.8ml 0.5M Tris pH7.9, 61.2ml water) in Beckman tubes (Beckman, UK), centrifuged at 25 000 x g at 4°C for 90 minutes using a Optima Ultra™ ultracentrifuge (Beckman Coulter, UK). Virus bands were extracted by a syringe, and excess caesium chloride dialysed out through the use of 10 000Mw cut off Slide-a-lyser dialysis cassettes (ThermoFisher) in Dialysis buffer (composition listed in *Table 2.6*). Virus banding was repeated to further purify virus stock, treated with Benzonase following the first dialysis to digest any contaminant extracellular DNA.

Reagents	Volume	Final Concentration
HEPES	50ml (1M pH8)	50mM
PBS	5 tablets	1x
$MgCl_2$ (hexahydrate)	20ml (10g/litre)	0.2 g/litre
$CaCl_2$	10ml (10g/litre)	0.1g/litre
Glycerol	100ml	10%

Table 2.6 Recipe for virus banding dialysis buffer

2.4.3.3 PicoGreen® Assay

Quantitation of virus particle number was performed using the Quant-iT™ PicoGreen® kit (Invitrogen) as per the manufacturer's instructions. In one modification to the

protocol, virus capsids were disrupted by treatment of TRIS/EDTA with 0.5% SDS at 56°C for 30 minutes. The assay relies on the ability of the fluorescent dye, PicoGreen®, binding to free double stranded DNA to increase the total fluorescence, which if compared against a range of double-stranded DNA standards, can be used to quantitate the number of virus particles relying on the calculation that 2.7×10^{10} virus particles equates to 1 μg/mL (Murakami, 1999). Performing serial dilution of known amounts of double-stranded DNA (e.g. bacteriophage lambda DNA), an accurate quantitation of unknown virus particles from viruses can be performed. The PicoGreen™ assay is essential for quantitation of virus particles, but is limited in that it cannot distinguish active particles from defective virus particles. The PicoGreen™ assay is therefore combined with the $TCID_{50}$ assay (described below) to quantitate what number of the total virus particles present are active and functional infectious units.

2.4.3.4 $TCID_{50}$ Assay

The tissue culture infective dose ($TCID_{50}$) quantifies the amount of virus required to produce a cytopathetic effect. The $TCID_{50}$ is similar to the plaque assay, in that it is a methodology by which the number of active particles in a virus stock preparation can be determined. An important advantage of this technique over a standard plaque assay however, is that it does not require an agar overlay onto cells, which can sometimes be toxic to some cancer cells used for adenovirus characterisation.

HEK 293A cells were chosen for the $TCID_{50}$ as they are used for the initial production of the virus, their infection kinetics are well documented in the laboratory and importantly, they provide very clear and distinctive cytopathetic effect, easily distinguished from aberrant plaques that can occur for other cell lines, yielding false

positives. HEK 293A cells (1 x 10^4) were seeded into wells of a 96 well flat-bottomed plate in 100 µL of complete DMEM prior to overnight incubation at 37°C, 5% CO_2. On the day of infection, media was aspirated and cells were washed once with PBS. Serial logarithmic dilutions from 10^{-5} to 10^{-12} virus particles of ColoAd1 (un-armed), ColoAd1-mIFN-γ or ColoAd1-hIFN-γ viruses were used to infect cells in 100 µL of DMEM (2% FCS) per well. Wells containing media alone were used as a control for reference. Plates were incubated for up to 7 days at 37°C, 5% CO_2 with an additional 100 µL of medium being added to wells on day 4. Development of cytopathic effect (CPE) was assessed by light microscopy.

To calculate the $TCID_{50}$, the cytopathic effects from each dilution of each virus and the ratio of CPE-positive to CPE-free wells are recorded, from which a $TCID_{50}$ can be calculated using the Reed-Muench method; as the virus titre recorded by $TCID_{50}$ yields a final titre that is 0.7 log higher than observed by plaque assay, the result can then be transformed to generate PFU/mL (Johnson et al., 2003.; LaBarre and Lowy, 2001).

2.4.4 Characterisation of IFN-γ-expressing ColoAd1

2.4.4.1 Kinetics of virus killing

To ensure that ColoAd1 encoding IFN-γ does not experience significant decrease the ability to lyse tumour cells, an MTS assay was performed and is described in detail in section 2.5.1

2.4.4.2 Virus production of IFN-γ

To confirm IFN-γ production by viruses, IGROV-1 cells were infected by ColoAd1 (un-armed), ColoAd1-mIFN-γ or ColoAd1-hIFN-γ viruses at a concentration of 100VPC, with supernatants harvested every 24 hours for a total of 72 hours infection. Description of the ELISA assay performed is provided in section 2.5.3.

2.5 Cellular Assays

2.5.1 MTS viability assay

Cell viability was determined by the MTS assay (Promega™), a colourimetric assay that measures metabolic activity. The MTS tetrazolium compound is metabolized by viable cells into a soluble Formazan product, which can be measured by absorption at 490nm. MTS reagent was added in a fixed ratio with media; 20 μL MTS reagent added per 100 μL of culture medium needed. For cell lines in a 96 well plate, media was aspirated, washed twice with PBS and 120 μL of MTS-containing media added per well, and samples incubated at 37°C for 1 hour before measuring absorbance with a Wallac 1420 Victor^2 multi-label counter (PerkinElmer Life and Analytical Sciences, UK). MTS assay was utilised to examine whether encoding IFN-γ within ColoAd1 would significantly affect the oncolytic ability of the virus. Here, IGROV-1 cells were seeded overnight in flat bottom 96 well plates (Corning) in 100 μL of complete media at a density of 12 x 10^3 cells per well. For infection with virus, media was aspirated and

virus dilutions were added to cells in 100 μL of RPMI (2% FBS). Cells were topped up with 20 μL of RPMI (2% FBS) after 3 days of infection. At each time point, supernatants were aspirated and cells washed twice with PBS before the addition of MTS-containing media (as described above). The MTS assay was also utilised to assess the viability of tumour samples using a 24 well plate format; media was again aspirated and washed with PBS before the addition of 600 μL of MTS-containing culture media added per well and incubated for 90 minutes before measuring absorbance.

2.5.2 Flow cytometry

2.5.2.1 Cell surface receptor analysis

Adherent cells were harvested from culturing plates by non-enzymatic means as to reduce non-specific tryptic digestion of cell surface receptors. In brief, culture media was aspirated and cells were washed twice with 15 mL of PBS. PBS was aspirated, and cells were dissociated using 2-4 mL of enzyme-free dissociation buffer (Sigma™) at 37°C for 5-10 minutes. Cells were pelleted by centrifugation (350 x *g*) for 5 minutes then washed with 5 mL MACS™ buffer (PBS, 2mM EDTA and 0.5% BSA) to reduce clumping and provide receptor stability. To exclude dead cells from flow cytometric analysis, cells were stained using the live/ dead stains, Zombie Dye-Green™ or Zombie Dye-NIR™ (Biolegend), at a 1:100 dilution in PBS for 30 minutes at 37 °C in the dark (see representative figure below, *Figure 2.3*). To prevent non-specific receptor binding, macrophages were treated with an anti-human or anti-mouse FcR block (BD Bioscience, 1μL per $1x10^6$ cells) in 100 μL of MACS™ Buffer for 10 minutes at 4 °C. Unless otherwise stated, cells were stained with pre-conjugated fluorescent antibodies in a final volume of 100 μL of MACS buffer containing antibody (for a full list see *Table 2.7*), at a concentration of 2 x 10^5 cells per sample for 30 minutes, at 4°C in the dark, in

V-bottom 96 well plates (Corning™). Cells were washed with 200 µL of MACS buffer and pelleted by centrifugation (350 x *g*) for 5 minutes, re-suspended with 200 µL of MACS buffer and re-pelleted. Cells were re-suspended with a further 200 µL of MACS buffer and re-pelleted again for a total of three washing steps.For flow cytometric analysis, cells were resuspended in 200 µL of MACS™ buffer and were analysed using a FACS Calibur™ (Becton Dickenson, UK). Where samples were co-stained using multiple fluorescent antibodies, appropriate compensation was performed using OneComp eBeads (eBioscience, UK). Analysis of flow cytometer data was performed using FlowJo (TreeStar Inc., USA). In this thesis, results of surface receptor staining are (largely) presented as the mean fluorescence intensity (MFI) of the receptors, rather than the percentage of cell positivity. This choice largely reflects the nature of macrophage receptor expression between different macrophage subtypes. Specifically, many subtypes of macrophages express the same selection of surface receptors, with the phenotypic differences in these subtypes occurring at the level of relative expression of these receptors on the cell surface (i.e. low or high receptor expression, as apposed to a binary absent or present receptor). As such, presentation of the data as MFI is useful because it allows quantitative assessment of the level of a given receptor on a cell surface.

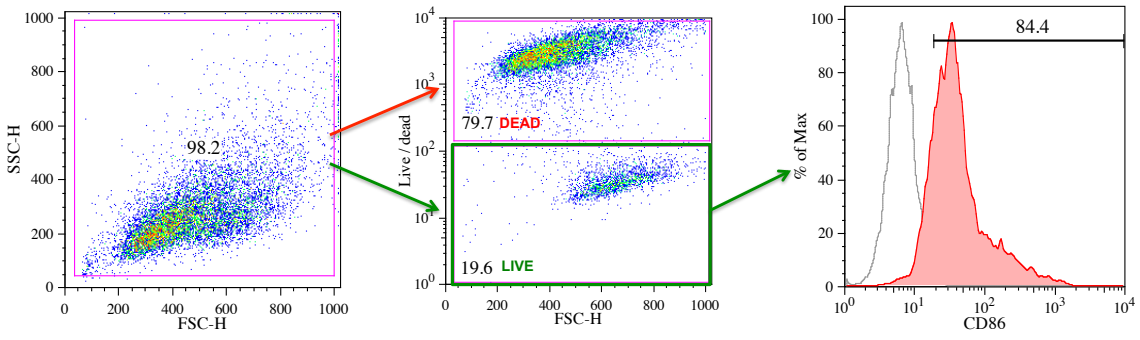


Figure 2.3 Removing dead cells from flow cytometric analysis

THP cells were incubated at 60°C for 10 minutes, then combined with un-treated THP-1 cells to generate a mixed live and dead population. These cells were stained with Zombie Dye-green, and further stained for CD86. **Left panel**: Total cells can be gated by Forward and side scatter. **Central panel**: live cells can be distinguished from dead cells by Zombie Dye fluorescence in the green channel. **Right panel**: Live cells can be gated on, and their receptor staining analysed

2.5.2.2 Intracellular cytokine staining

Flow cytometry was also utilised to measure cytokine production from cells by intracellular cytokine staining, as an alternative to the ELISA methodology. Intracellular cytokine staining is particularly useful at is allows both receptor expression and cytokine production to be measured on the same cells simultaneously. However, intracellular cytokine staining requires co-incubation with a protein transport inhibitor to trap nascent cytokines within cells for detection. For longer incubation times (>24 hours) this becomes toxic to cells; given that most macrophage re-education experiments in this thesis extend in excess of 24 hours, this technique was incompatible with many studies. In this thesis, intracellular cytokine staining was used to measure murine TNF-α production in IC-21 cells to confirm an M1 phenotype. IC-21 cells were seeded in 24 well plates at a density of 5 $x10^5$ cells per well in 0.5mL of complete RMPI, and left to adhere overnight. The following day media was exchanged for fresh M1 -(LPS 1 ng/mL) and mIFN-γ (10 ng/mL), or M2- media (IL-4, 10 ng/mL) in RPMI containing the protein transport inhibitor brefeldin A ("GolgiPlug™", 1nM final concentration) and were allowed to incubate for 24 hours at 37°C. Cells were harvested by non-enzymatic means as described previously. In short, cells were washed twice with 1.5 mL of PBS, then dissociated using 0.5 mL of enzyme-free dissociation buffer

(Sigma™) at 37°C for 5-10 minutes. Cells were pelleted by centrifugation (350 x *g*) for 5 minutes then washed with 5 mL MACS™ buffer (PBS, 2mM EDTA and 0.5% BSA) to reduce clumping and provide receptor stability. Samples were permeabilised by incubating cells in 200µL of fixation/permeabilisation solution (BD Biosciences) for 20 minutes at 4°C. Cells were subsequently stained for TNF-α production using a PE-conjugated, anti-mouse TNF-α antibody using a modified version of the staining protocol as described for surface receptor staining; where MACS buffer was used to re-suspend antibodies and perform washing steps for surface receptor staining, intracellular cytokine staining instead requires perm/wash solution (BD Biosciences), a solution that maintains the permeability of the cells for staining and washing steps.

Anti-mouse Target	**Fluorophore**	**Clone**	**Anti-human Target**	**Fluorophore**	**Clone**
CD4	FITC	GK1.5	CD4	FITC	OKT4
CD8	PE	53-6.7	CD8	PE	HIT8a
CD14	PE-Cy7	Sa14-2	CD14	PE Cy5	63D3
CD11b	APC	M1/70	CD11b	PE Cy5	ICRF44
CD40	FITC	3/23	CD40	FITC	1C10
CD64	PerCP Cy5.5	X54-5/7.1	CD64	FITC	10.1

F4/80	FITC	BM8	CD68	FITC	Y1/82A
F4/80	APC	BM8	CD68	APC	Y1/82A
CD80	PE	16-10A1	CD80	PE	2D10
CD86	APC	Gl-1	CD86	APC	IT2.12
CD169	PerCP Cy5.5	3D6.112	CD169	APC	7239
B7-H2	PE	HK5.3	B7-H2	APC	2D3
B7-H4	APC	HMH4-5G1	B7-H4	PeCy7	MIH 43
I-A/I-E	PE Cy5	M5/114.15.2	HLA-A, -B, -C	FITC	W6/32
HK-2b	FITC	AF6-88.5	HLA-DR	PE/Cy5	L243
MHCI :SIINFEKL (HK-2b: SIINFEKL)	PE	25-D1.16	SIRP-1α	PE	B4B6
Cd11c	PeCy5	N418	EpCAM	PeCy7	9C4
NK1.1	APC	PK 136	CD46	-N/A-	TRA-2-10
TNF-α	PE	MP6-XT22	EGFR	APC	AY13

Table 2.7 List of antibodies used for flow cytometry

All antibodies were purchased from Biolegend and were purchased with respective isotypes. For studying expression of human MHC I, the HLA-A, -B, -C antibody was chosen as this recognises the three major types of human MHC I α subunit. For the detection of human MHC II, the HLA-DR antibody was chosen, as it is more abundant than the HLA-DP and HLA-DQ variants

2.5.2.3 Measurement of NO production

NO was measured using DAF-FM di-acetate (4-amino-5-methylamino- 2′,7′-difluorofluorescein diacetate) (Life Technologies™). In brief, DAF-FM di-acetate passively accumulates in cells, becoming de-acetylated by intracellular esterases to DAF-FM. Upon interaction with NO, DAF-FM fluorescence increases >150-fold as it forms a highly fluorescent benzotriazole product which can be detectable by

fluorescence microscopy at 515 nm wavelength by flow cytometry or fluorescence microscopy.

Adherent cells in 24 or 48 well plates had media aspirated, and washed three times 0.5 mL PBS. Cells were incubated with 5μM DAF-FM in 0.5 mL of RPMI for 1 hour at 37°C in the dark, washed 3 times with PBS, and incubated with 1 mL RPMI for an additional 15 minutes to allow complete de-esterification by intracellular esterases.

For flow cytometric analysis, cells were harvested by non-enzymatic methods cells and were resuspended in 200 μL of MACS™ buffer, then analysed using a FACS Calibur™ (Becton Dickenson).

2.5.2.4 Fluorescent ligand uptake

The FITC-labeled ligands zymosan (Life Technologies™), dextran (20, 000 molecular weight, Sigma™) and OVA (Sigma™) were re-constituted in DMSO, and aliquoted for freezing in 5-10μL volumes (equivalent to a single usage for an experiment) to reduce freeze thawing. Murine IC-21 or human THP-1 macrophages were seeded at a density of 5 $x10^5$ cells per well in 24 well plates and cultured for 24 hours in 0.5 mL of RPMI (10% FBS) supplemented with LPS (1 ng/mL) and IFN-γ (10 ng/mL) ("M1"), or with IL-4 (10 ng/mL) ("M2") before treatments with fluorescent ligands.

For uptake assays, macrophage media was aspirated, washed twice with PBS and replaced with 100 μL of fresh media containing fluorescent ligands at a concentration ranges of 1-1000 μg/mL, where they were incubated for 1 hour at 37°C in the dark. Cells were washed three times with PBS then harvested using non-enzymatic dissociation buffer. Cells were pelleted by centrifugation (350 x *g*) for 5 minutes and re-suspended with 200 μL Trypan Blue (0.4% w/v) to quench the fluorescence of non-

specifically adsorbed particles on the surface of the macrophages. Samples were washed once with 1 mL MACS ™ buffer and were pelleted again, then resuspended in 200 μL MACS buffer for analysis using a BD FACS Calibur™ to determine the mean fluorescence intensity.

2.5.2.5 Cellular phagocytosis assay

Macrophages were seeded at a density of 2.5 $x10^5$ cells per well in 48 well plates for 24 hours, after which time media was aspirated, washed twice with PBS and fresh media containing 2.5 $x10^5$ CFSE-stained tumour cells was added. Macrophages and tumour cells were incubated for 6 hours, were then harvested using non-enzymatic dissociation methods (previously described). Cells were stained for surface receptors (CD11b for human macrophages and F4/80 for mouse macrophages) to identify the macrophage populations. Cells were analysed by flow cytometry, identifying phagocytosed tumour cells as those double-stained for a macrophage marker and CFSE (upper right quadrant of flow cytometry plots, *Figure 2.4*).

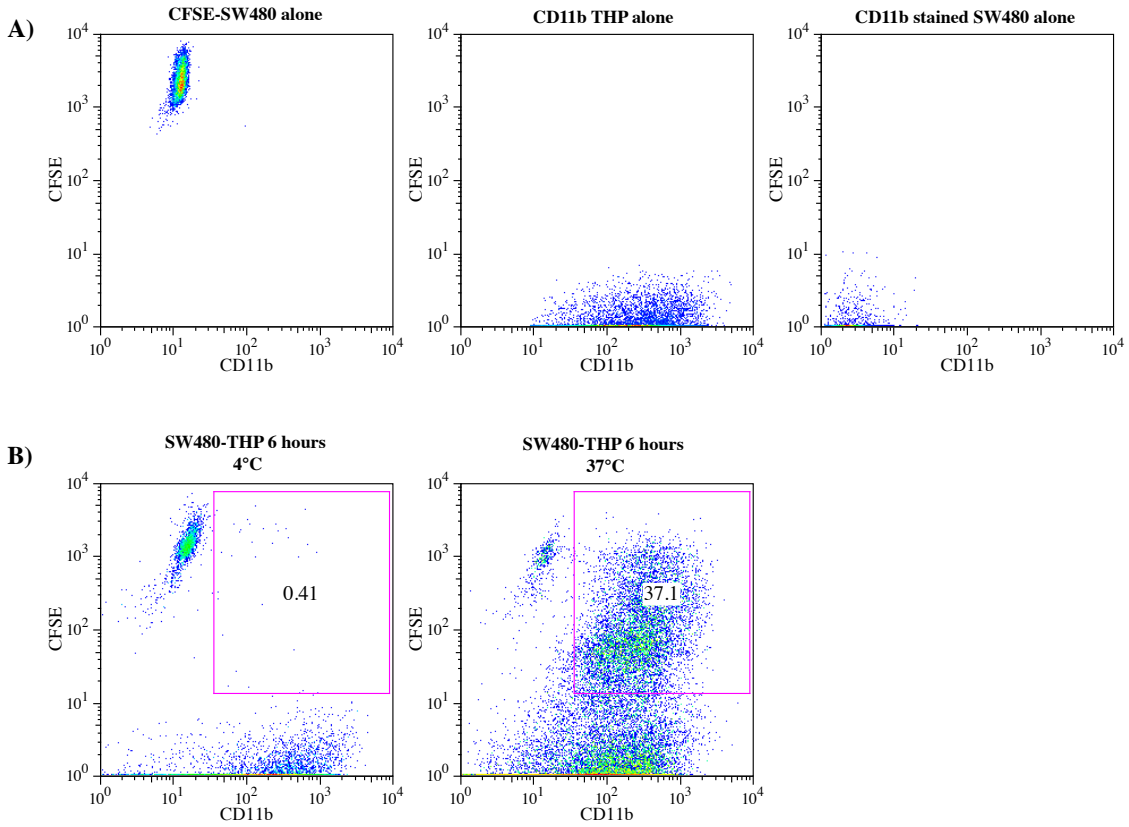


Figure 2.4 Studying cellular phagocytosis by flow cytometry

A) Tumour and macrophage staining is specific. Tumour staining (**left panel**) does not bleed into CD11b staining, and CD11b specifically stains THP-1 cells without bleed through into the CFSE channel (**central and right panels) B)** Phagocytosis gate is defined by utilising a control sample of tumour and macrophages that were incubated at 4°C, which inhibits cellular phagocytosis (**left panel**). This enables accurate determination of phagocytosed tumour cells (**right panel**)

2.5.2.6 Cross-presentation assays

Macrophages have been suggested to stimulate anti-tumour immune responses through their ability to phagocytose, and subsequently present tumour-antigen derived from cancer cells. To assess the ability of macrophages to present antigen, cross-presentation assays were performed *in vitro*. Classical antigen presentation assays have co-cultured antigen presenting cells (largely dendritic cells) with T cells in the presence of peptide antigen, with the induction of T cell proliferation or T cell cytokine secretion used as

the principal measure of effective cross presentation. However, a small number of antibodies are now available that are able to recognise an antigen bound in the MHC I cleft on an antigen presenting cells. As such, cross-presentation of a few antigens can now be directly measured by flow cytometry, staining antigen presenting cells for MHC I with antigen bound in its cleft. In short, the methodology consisted of "pulsing" human and murine macrophages with peptide for 6 hours an staining for presence of the MHC I-bound peptide on the cell surface in the same manner as described for cell surface receptor staining (section 2.5.2.1). For murine studies using SIINFEKL, anti-MHC I: SIINFEKL was used at a dilution of 1:400. For human studies using p53, anti-MHC I: p53 was used at a dilution of 1:100.

Murine models of antigen presentation have been dominated by the study of the model antigen, ovalbumin (OVA). An antibody has been raised against the immunodominant epitope of the OVA antigen, SIINFEKL, bound in the cleft of MHC I and provides a tool for studying cross-presentation of OVA protein and SIINFEKL peptide. To validate the technique, experiments with SIINFEKL cross-presentation were first optimised using the murine dendritic cell, DC 2.4 (*Figure 2.5*). DC 2.4 were seeded at a density of 5 x10^5 cells per well in 24 well plates allowed to adhere overnight, before being pulsed with 1-, 10-, or 100- ng/mL of SIINFEKL peptide for 6 hours to determine that a range of peptide concentrations can be cross-presented (*Figure 2.5A*). To show that this cross presentation could be influenced by the polarisation state of the dendritic cell, the same experiment was repeated but included pre-polarisation of the DC 2.4 cells towards M1(LPS and mIFN-γ) or M2 (IL-4) phenotypes, before a 6-hour pulse of SIINFEKL (1 ng/mL) (*Figure 2.5A*). This initial optimisation showed that the SIINFEKL cross-

presentation method is a useful functional technique and can be utilised for phenotypic studies.

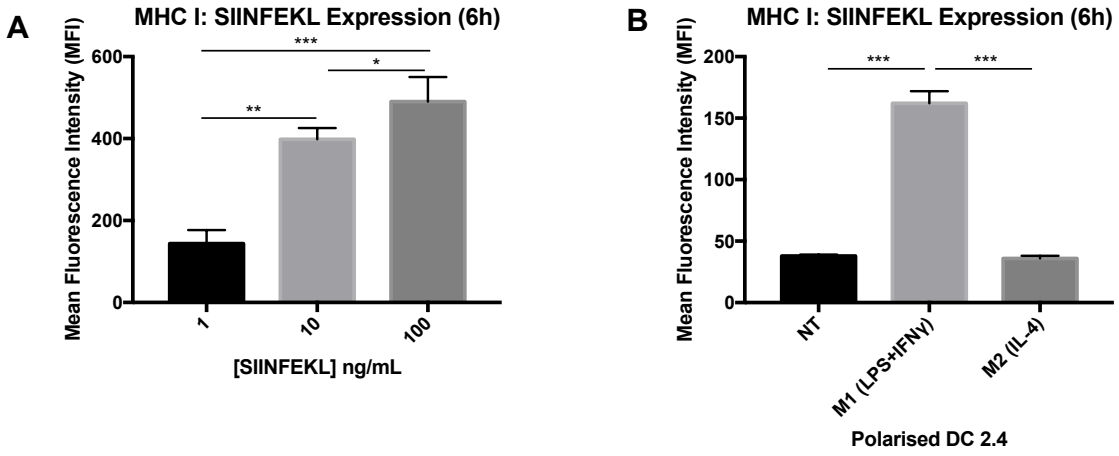


Figure 2.5 Optimisation of SIINFEKL cross-presentation using murine dendritic cells

A) DC2.4 cells were seeded at a density of 5 x10^5 cells per well in 24 well plates and left to adhere overnight in 0.5 mL of RPMI (10% FBS). Media was aspirated and exchanged for RPMI containing SIINFEKL peptide to a final concentration of 1-, 10-, or 100- ng/mL. Dendritic cells were incubated with peptide for 6 hours, after which time cells were harvested for staining. **B)** Dendritic cells were seeded at a density of 5 x10^5 cells per well in 24 well plates and cultured for 24 hours in 0.5 mL of RPMI (10% FBS) supplemented with LPS (1 ng/mL) and mIFN-γ (10 ng/mL) ("M1"), or with IL-4 (10 ng/mL) ("M2"), or RPMI alone ("NT"). Media was aspirated and exchanged for RPMI containing SIINFEKL peptide to a final concentration of 1 ng/mL, and incubated for 6 hours, after which time cells were harvested. Cells were harvested using non-enzymatic dissociation buffer and stained with anti-MHCI:SIINFEKL (1:400 dilution). Samples were analysed for fluorescence using a BD FACS Calibur™ to determine the mean fluorescence intensity, displayed as bar charts. Results represent n=3, with errors bars indicating SD. Statistical analysis of significance was performed by one-way ANOVA, with a Tukey post-test. $P<0.05$ (*), $P<0.01$ (**), or $P<0.001$ (***)

The SIINFEKL cross-presentation method was extended into murine macrophages using both peritoneally-lavaged macrophages and the murine macrophage cell line IC-21. Peritoneal macrophages were harvested from 12 week old C57/B6 mice by a peritoneal lavage with 5 mL of PBS (2mM EDTA/ 0.5% BSA). Red blood cells removed by red blood cell lysis buffer (Sigma), followed by plastic adherence in 24

well plates for 1.5 hours at 37 °C, with cells remaining in suspension removed by PBS washing. IC-21 cells were obtained from ATCC. Cells were seeded at a density of 5 x10^5 cells per well in 24 well plates allowed to adhere overnight, before being pulsed with varying concentrations of SIINFEKL peptide for 6 hours. No-peptide controls were added to confirm specificity of the antibody during staining. Cross-presentation was also performed using the full length OVA protein. Cells were seeded as described, with either DC 2.4 cells or IC-21 cells incubated with 10-, 100- or 1000-μg of full length OVA for 6, 12 or 24 hours; cross presentation of SIINFEKL peptide from full length OVA was performed as described previously for SINFEKL peptide. To extend this work further into a more realistic context, where tumour antigen may be obtained from phagocytosed cancer cells, a B16 cells overexpressing the OVA antigen were utilised. To generate a B16-OVA lysate, these cells were non-enzymatically harvested from a T175 when ~80% confluency was reached (corresponding to ~1 x10^7 cells). Cells were washed with PBS and pelleted by centrifugation (250 x g, 5 mins), then re-suspended in 0.5 mL of PBS and subjected to five rounds of freeze thawing to ensure lysis of the cells. Lysate was re-constituted in RPMI to appropriate concentrations and incubated with antigen presenting cells, with presentation of SIINFEKL on MHC I assessed as described previously.

For the study of human cross presentation by the human macrophage cell line THP-1, a similar methodology was employed. Here, p53 peptide (obtained from Prof. Alison Banham) was utilised as a model antigen, with detection of cross presentation by the monoclonal antibody T1-116C which recognises HLA-A2 complexed with the p53 peptide RMPEAAPPV derived from wild type human p53 protein. This antibody was generated by immunising mice with a HLA-A2-p53RMP peptide tetramer. Cells were

seeded and pulsed with peptide in the same method as described previously for murine macrophages. Lysates of SW480 cells were generated by a very similar method as for murine macrophages, with the exception of virus infection; two T175 flasks of SW480 were allowed to reach 60% confluency before media was exchanged for fresh RPMI (2% FCS) alone or containing ColoAd1 (1000 VPC). After 72 hours, cells were harvested by non-enzymatic means and lysates generated by free thawing as described for murine B16-OVA cells; cells were washed with PBS and pelleted by centrifugation (250 x g, 5 mins), then re-suspended in 0.5 mL of PBS and subjected to five rounds of free thawing to ensure lysis of the cells. For detection of cross presentation, cells were stained with the anti-MHC I:p53 antibody (T1-116c, 1:100 antibody dilution) but also for EGFR (1:100) such as to remove any tumour-associated MHC I: p53 expression from the analysis (*Figure 2.6*).

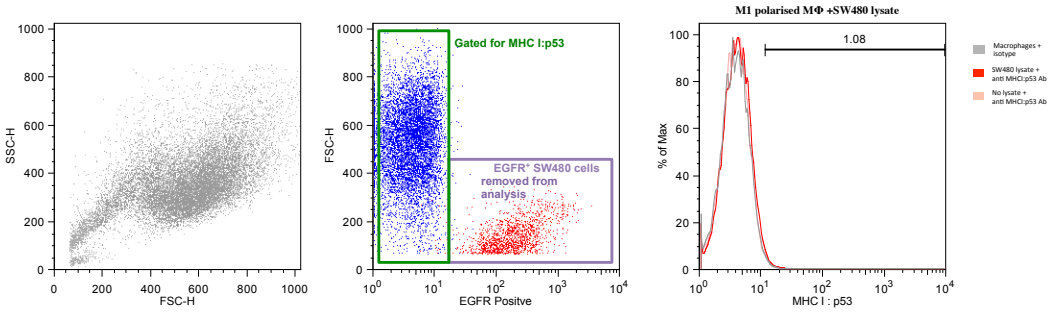


Figure 2.6 Gating strategy for cross-presentation of SW480 lysate

Samples containing both THP-1 cells and SW480 lysates (left panel) were stained for EGFR and MHC I-p53 complexes. To remove any potential staining of SW480 lysates with the MHC I-p53 antibody, SW480 lysates were identified by their EGFR expression and removed from further analysis (center panel). The resulting macrophage-specific staining can be analysed for MHC I-p53 – a representative example is displayed here from M1 macrophages pulsed with SW480 lysates (right panel)

2.5.3 Enzyme-linked immunosorbent assay (ELISA)

ELISAs were used to detected levels of cytokines present in supernatants. For studies

of macrophage polarisation, the levels of IL-12 (p40), IL-10 and TNF-α were frequently measured as markers of different macrophage phenotype by standard ELISA development kits (Peprotec, UK). Species-specific ELISA kits were purchased from Peprotech to detect murine and human levels of these cytokines. Similarly, for measurement of murine and human IFN-γ produced by armed ColoAd1, anti-murine- and anti-human-IFNγ kits were used respectively.

In brief, capture antibodies for the respective cytokines were incubated in Micro-Immuno 96 well plates (Nunc) over night at room temperature. Un-bound capture antibody was removed by wash buffer (4 x 300μL washes with PBS-Tween (0.05%)). Plates were blocked for non-specific binding using 300μL per well of PBS (1% BSA) for 1 hour at room temperature. Plates were again washed, and then incubated with samples or known standard concentrations of the cytokine of interest, serially diluted 1:2 to generate a standard curve. Un-bound antigen was removed through washing with a wash buffer with PBS-Tween (0.05%). Bound samples were incubated with a detection antibody against the cytokine of interest for 2 hours at room temperature. Samples were washed again, then incubated with an avidin- horseradish peroxidase conjugate for 30 minutes which catalyses the oxidation of TMB (3,3',5,5'-Tetramethylbenzidine, ThermoFisher ™), added at 50 μL per well for 5 minutes following the removal of avidin-HRP by washing. Oxidation of TMB, in combination with the addition of an acidic Stop solution (Alpha, UK) enables quantitation of bound cytokines by reading absorbance at 450 nm with a Wallac 1420 Victor 2 multi-label counter (PerkinElmer Life and Analytical Sciences).

To assess changes in macrophage phenotype, levels of IL-12 (p40), IL-10 and TNF-α were measured by ELISA. For human macrophage studies, THP-1 macrophages were

seeded in in 48 well plates at a density 2 x 10^5 cells per well 0.5 mL of RPMI containing M1 media, M2 media, media containing IFN-γ or media along. Cells were polarised for 24-48 hours and often re-polarised towards alternative states for an additional 24-48 hours (unless otherwise stated). After appropriate polarisation, cell supernatants were collected and centrifuged (250 x g, 5 mins) to pellet any cells. Supernatants were subsequently stored at -20°C until analysis by ELISA by anti-human IL-10, IL-12 and TNF-α kits. Murine macrophage cytokine production was assessed using IC-21 cells, with macrophages cultured and polarised as with human macrophages, with samples harvested and stored in the same manner, but using anti-murine IL-10, IL-12 and TNF-α kits for cytokine detection.

The ELISA was also used assess IFN-γ production by human or mouse IFN-γ-armed ColoAd1 viruses. Here, IGROV-1 cells were seeded overnight in flat bottom 48 well plates (Corning) in 100 μL of complete media at a density of 5 x 10^4 cells per well. For infection with ColoAd1 (un-armed), ColoAd1-mIFN-γ or ColoAd1-hIFN-γ virus, media was aspirated and respective viruses were added at a concentration of 100VPC in a volume of 200 μL of RPMI (2% FBS) per well. Cells were topped up with 20 μL of RPMI (2% FBS) after 3 days of infection. Supernatants were harvested, pelleted by centrifugation to remove any residual dead tumour cells, then probed for levels of murine IFN-γ or human IFN-γ by anti-murine IFN-γ or anti-human IFN-γ ELISA kits respectively.

2.6 Data processing and statistical analysis

Initial processing of data was performed using Microsoft Office Excel 2010 for Mac (Microsoft) and GraphPad Prism 6 (GraphPad Inc.). Where applicable, statistical analysis of data was performed with GraphPad Prism 6; normality of data was assessed using the D'Agostino-Pearson test, with the details of statistical tests performed identified in the figure legends for respective data.

Chapter 3

Production of ColoAd1 viruses “armed” with human and murine IFN-γ

3 Production of ColoAd1 viruses "armed" with human and murine IFN-γ

3.1 Introduction

The potent immunostimulatory properties of IFN-γ make it an attractive candidate to target immunosuppression in the tumour microenvironment. Of the many immunostimulatory functions associated with IFN-γ, its reported ability to activate macrophages is of particular interest to this thesis. IFN-γ has previously been suggested to demonstrate limited therapeutic potential, owing to its short-half life. Taken together, these factors make IFN-γ an attractive transgene to encode within an oncolytic virus; a tumour-targeted oncolytic virus would provide a means to deliver IFN-γ locally to the tumour microenvironment, whilst continuous virus-mediated IFN-γ production would also circumvent the issue of short half-life.

In this chapter, human and mouse forms of IFN-γ were encoded into a promising oncolytic adenovirus currently in clinical trial, ColoAd1 (Kuhn et al., 2008). The creation and use of these IFN-γ "armed" viruses produced forms the basis for the rest of the thesis.

3.1.1 Chapter aims

1. Produce two armed ColoAd1 viruses, encoding mouse and human IFN-γ respectively
2. Examine the performance of these viruses and confirm production of transgene

3.2 Results

3.2.1 Production of ColoAd1 viruses armed with human or murine IFN-γ virus

A shuttle plasmid-based system was developed in-house at PsiOxus Therapeutics to simplify manipulations of the ColoAd1 genome and streamline insert of candidate therapeutic transgenes into the virus. Traditional virus cloning strategies have tended to rely on homologous recombination; however, owing to large regions of homology within virus genomes (such as with inverted terminal repeats/ long terminal repeats) the efficiency of such approaches is often sub-optimal and laborious (Chartier et al., 1996). Instead, PsiOxus Therapeutics uses a single shuttle plasmid system to facilitate the insertion of DNA into the ColoAd1 genome, which comprises a promoter and poly A tail to flank target DNA. The company now possesses two shuttle plasmid systems, containing CMV and splice acceptor promoters, to drive gene expression by CMV or the adenovirus major late promoters respectively. Such shuttle systems facilitate easier gene transfer into the ColoAd1 genome and allow for comparison of transgene production from CMV driven promoters or those linked to late gene expression (strictly associated with virus replication) and thus, a more tumour-specific expression of transgene. Unfortunately, at the time of virus production during my thesis, the splice acceptor virus shuttle system was still in development, and so CMV was used as the choice of promoter for the production of IFN-γ.

3.2.1.1 Sub-cloning of IFN-γ into the ColoAd1 backbone

The DNA sequences of human and murine IFN-γ were obtained from the PubMed nucleotide databases (http://www.ncbi.nlm.nih.gov/genbank/, accession numbers NM_000619.2 and NM_008337 respectively), and were synthesised into a single DNA plasmid externally by Life Technologies™ . The human and murine IFN-γ sequences were each flanked by a pair of unique restriction sites (BamHI/MluI sites flanking human IFN-γ, and EcoRI/NotI sites flanking murine IFN-γ) to enable manipulation of the human or murine IFN-γ sequences specifically (*Figure 3.1A*). The choice of these restriction sites was originally designed for compatibility for cloning into the multiple cloning site of a lentivirus construct within the laboratory. However, cloning into the PsiOxus shuttle vector required flanking of the human and murine IFN-γ sequences with NotI and NheI restriction sites so as to be compatible with the PsiOxus shuttle plasmid. NotI and NheI restriction sites were therefore added to the 5' and 3' ends of the IFN-γ sequences respectively, by PCR.

With correct restriction sites added, the IFN-γ sequences were ligated into the multiple cloning site of the shuttle plasmid following restriction digest with NotI and NheI (*Figure 3.1B*). This results in IFN-γ transgenes with a CMV promoter and poly A tail, in a cassette flanked by a further set of unique restriction sites that would facilitate ligation into the ColoAd1 back bone (*Figure 3.1C*).

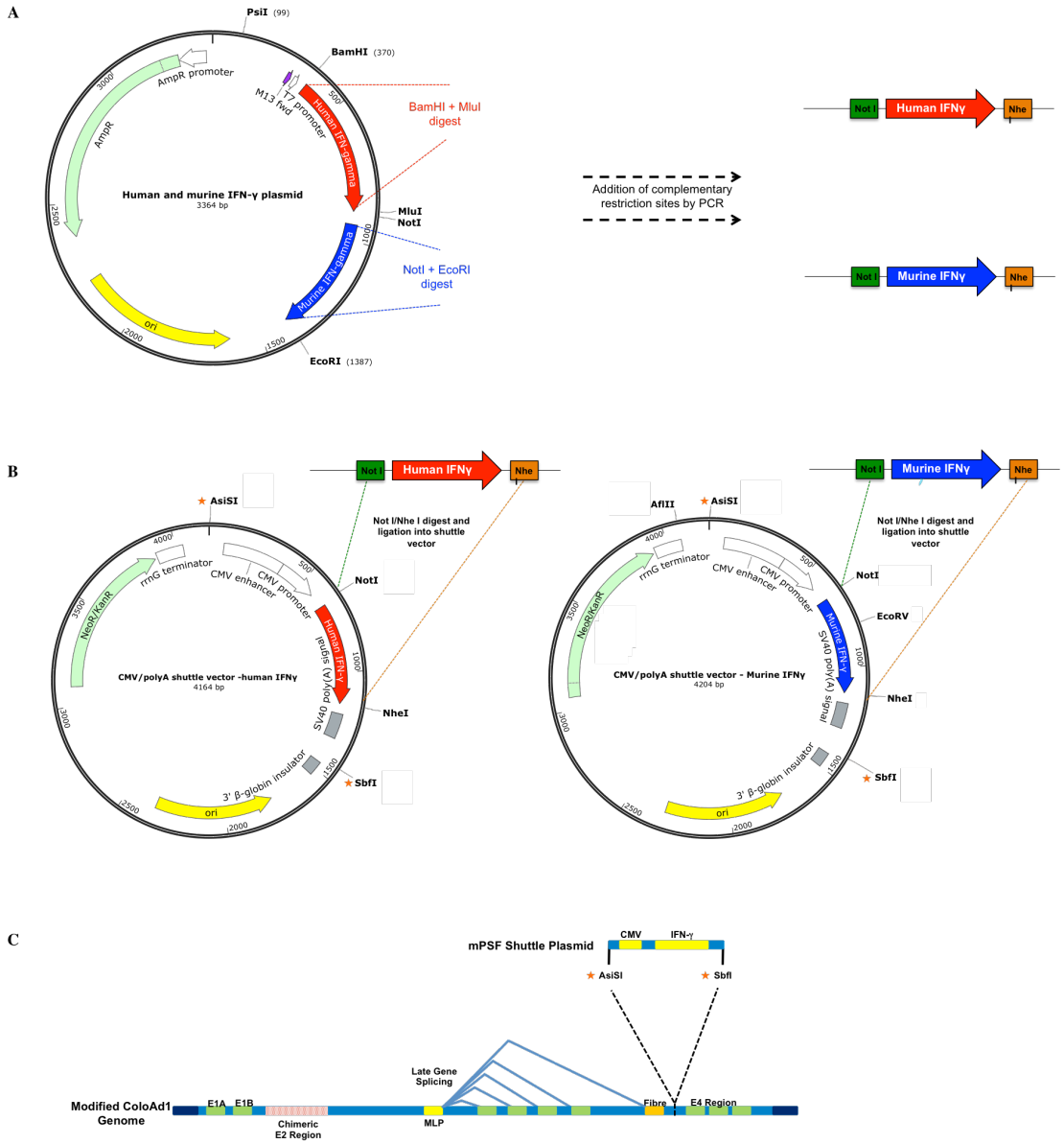
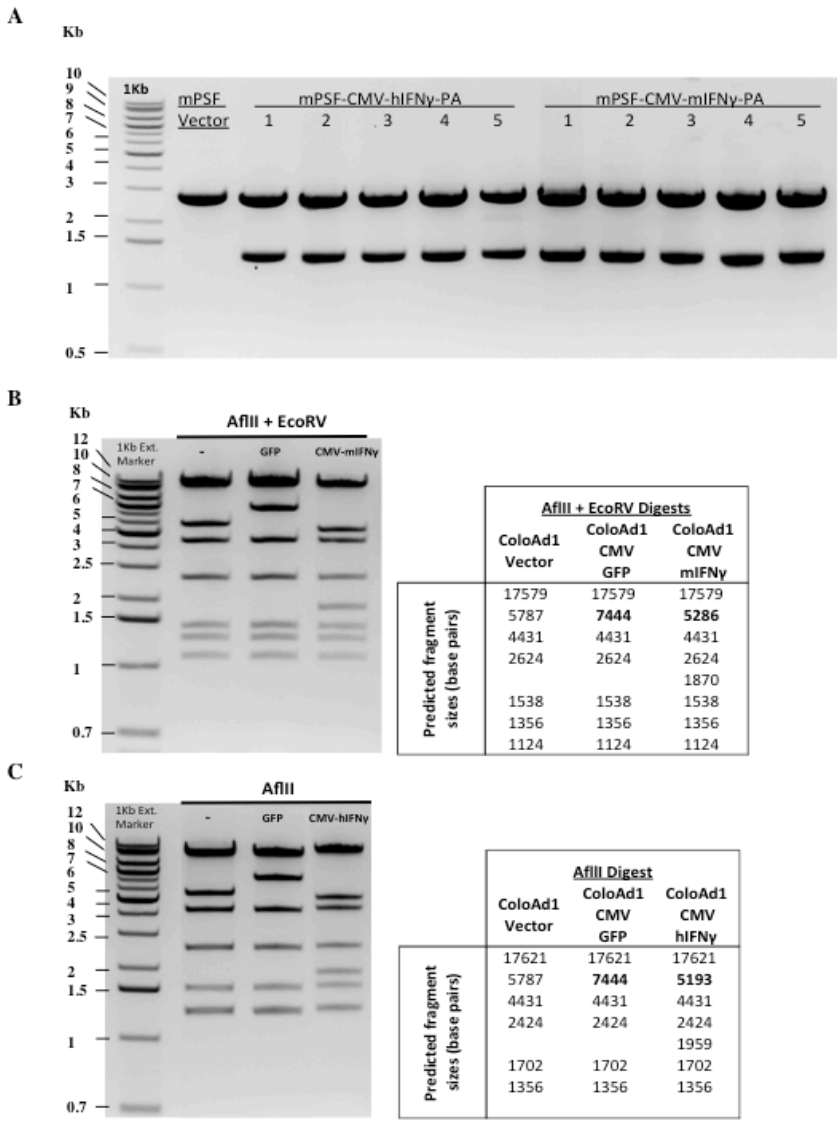


Figure 3.1 Cloning strategy for inserting IFN-γ into ColoAd1

A) Human and murine IFNγ sequences were synthesised into a plasmid by Life Technologies™ . Human and murine IFN-γ sequences were generated by restriction digest with BamHI + Mlul or NotI + EcoRI respectively, and isolated by gel extraction. To facilitate ligation into the CMV shuttle plasmid, (compatible) NotI and NheI restriction sites were added by PCR to the 5' and 3' ends of the IFN-γ sequences respectively. **B)** To flank IFN-γ sequences with a CMV promoter and poly A tail, and to facilitate insertion into the ColoAd1 genome, IFN-γ sequences were added into the CMV shuttle plasmid. Both shuttle plasmids and IFN-γ sequences were digested with NotI and NheI, followed by ligation of IFN-γ into the plasmid internally to the CMV and poly A elements **C)** Insertion of the CMV-IFNγ-polyA cassette into the ColoAd1 was achieved by restriction digest of the shuttle plasmid (external to the cassette) and ColoAd1 genome using the unique restriction sites AsiSI and Sbf1 (indicated by stars), followed by an overnight ligation

Test digests of the IFN-γ –containing shuttle vectors were performed to confirm successful ligation; Digests with NheI (site flanking the 3' end of the IFN-γ fragment and within the multiple cloning site of the shuttle) and AsiSI (shuttle plasmid-specific site) were used to confirm that the IFN-γ had ligated correctly into the CMV shuttle vector. Here, the upper bands represent digested shuttle vectors, with the lowers bands of 1.120 Kb and 1.153 Kb corresponding to the murine and human fragments, respectively, which have been cut from the shuttle plasmid (*Figure 3.2A*).

Having confirmed successful ligation into the shuttle plasmid, the IFN-γ sequences now form an expression "cassette", with a CMV promoter upstream and a poly A tail downstream of the IFN-γ DNA. This IFN-γ transgene was subsequently ligated into the ColoAd1 backbone, following restriction digestion with enzymes flanking this "cassette" (Sgf1 and Sbf1). Test digests were again performed to confirm successful ligation of the IFN-γ DNA into the ColoAd1 backbone (*Figure 3.2B+C*). For the ColoAd1-murine IFN-γ construct, plasmids were digested with AflII and EcoRV (*Figure 3.2B*); the presence of murine IFN-γ adds an EcoRV site into the construct whilst disrupting one of the AflII sites in the multiple cloning site of the ColoAd1 backbone, providing a unique band of 1.87 Kb when digested with EcoRV. This same EcoRV in the ColoAd1-murine IFN-γ site causes the smaller band at 5.28 Kb, relative to the 5.7 Kb in the ColoAd1 un-modified genome and the 7.4 Kb fragment for the GFP-containing ColoAd1. A similar pattern is observed for the ColoAd1-human IFN-γ construct (*Figure 3.2C*); the presence of human IFN-γ yields a smaller band at 5.19 Kb, relative to the 5.7 Kb in the ColoAd1 un-modified genome and the 7.4 Kb fragment for the GFP-containing ColoAd1.



AflII + EcoRV Digests

Predicted fragment sizes (base pairs)	ColoAd1 Vector	ColoAd1 CMV GFP	ColoAd1 CMV mIFNγ
	17579	17579	17579
	5787	**7444**	**5286**
	4431	4431	4431
	2624	2624	2624
			1870
	1538	1538	1538
	1356	1356	1356
	1124	1124	1124

AflII Digest

Predicted fragment sizes (base pairs)	ColoAd1 Vector	ColoAd1 CMV GFP	ColoAd1 CMV hIFNγ
	17621	17621	17621
	5787	**7444**	**5193**
	4431	4431	4431
	2424	2424	2424
			1959
	1702	1702	1702
	1356	1356	1356

Figure 3.2 Sub-cloning of murine and human IFN-γ into the ColoAd1 backbone

A) Ligation of human and mouse IFN-γ into the shuttle plasmids, "mPSF-CMV-hIFNγ-PA" and "mPSF-CMV-mIFNγ-PA" respectively, was confirmed by digesting five clones from each ligation with NheI and AsiSI. As a control, the shuttle plasmid containing no insert ("mPSF vector") was also digested. **B)** Insertion of the CMV-mIFNγ-PA construct in the ColoAd1 backbone ("CMV-mIFNγ") was confirmed by restriction digest with AflII and EcoRV, using the ColoAd1 backbone ("-") or ColoAd1 backbone modified by a CMV-GFP-PA construct ("GFP") as controls. **C)** Similarly, insertion of the CMV-hIFNγ-PA construct in the ColoAd1 backbone ("CMV-hIFNγ") was confirmed by restriction digest with AflII. All gel electrophoresis was performed using 1% agarose gels, resolved at 110V for one hour. Molecular weights were visualised using the 1Kb ladder (**A**) or 1Kb extension ladder (**B**+**C**) from New England Biolabs

3.2.2 *In vitro* characterisation of virus

The human and murine IFN-γ-encoding viruses were produced and purified by transfection of virus DNA into 293A cells, subsequent recovery of virus particles and caesium chloride banding, described in more detail previously in this thesis (*section 2.4*). To confirm that the IFN-γ-modified viruses maintained their oncolytic activity and could successfully produce transgene, a number of *in vitro* assays were performed.

3.2.2.1 Virus quantitation

Following purification of virus by caesium chloride gradient banding, quantitation of virus particles was performed by a number of methods. The PicoGreen™ assay was utilised (*Materials and methods, 2.4.3.3)* to determine the total number of virus particles present in the purified virus preparation. Whilst providing quantitation of total virus present in the samples, the PicoGreen™ assay does not discriminate between functional, infectious virus and non-functional virus. To resolve this, a tissue culture infective dose ($TCID_{50}$) assay was performed (*Materials and methods, 2.4.3.4)*, infecting HEK 293A cells with serial logarithmic dilutions of ColoAd1 (un-armed), ColoAd1-mIFN-γ or ColoAd1-hIFN-γ viruses for 7 days, then recording the CPE observed for each dilution of virus to calculate the particle forming units (PFU). The results of the total virus particle quantitation, particle forming units and the corresponding particle to infectivity ratios for each virus are detailed in *Table 3.1*. The results demonstrate that all viruses were banded to high titers and exhibit good infectivity. For both engineered viruses, the particle to infectivity ratios are very similar and are both less infectious than parental virus, however the differences are not dramatic.

	Total virus particles (Vp /mL)	Infectious units (PFU / mL)	Particle: Infectivity ratio ((Vp/mL) / (PFU/mL))
ColoAd1	9.4×10^{11}	8.94×10^{9}	105.2
ColoAd1-CMV-mIFNγ	6.5×10^{12}	4.39×10^{10}	148.7
ColoAd1-CMV-hIFNγ	1.2×10^{12}	9.08×10^{9}	132.1

Table 3.1 Concentrations of engineered ColoAd1 viruses

3.2.2.2 Kinetics of virus killing

To ensure that ColoAd1 encoding IFN-γ does not cause a significant decrease in infectivity, replication or lytic ability of the virus, a cell-killing assay was performed to see if any significant differences in the kinetics of virus killing could be identified. In keeping with the focus of this thesis, an ovarian cancer cell line was used to demonstrate the oncolytic activity of the IFN-γ-modified virus. IGROV-1 cells were chosen as a representative model for virotherapy in ovarian cancer, as a number of other ovarian cancer cells within the laboratory are either very sensitive or resistant to virus-mediated lysis (such as OVCAR and SKOV cells, respectively).

To define a suitable concentration of virus with which to observe differences in virus killing, IGROV cells were infected with a range of ColoAd1 concentrations (*Figure 3.3A*). At the highest concentration of virus (1000 VPC) >70% of cells were lysed by 24 hours, whilst for the lowest concentration (10 VPC) 50% cell death was only achieved by 96 hours, representing two extremes of virus killing kinetics. To enable detection of any subtle changes in virus killing, a concentration of 100 VPC was therefore used to infect IGROVs with ColoAd1, ColoAd1-mIFNγ or ColoAd1-hIFNγ (*Figure 3.3B*).

Comparison between the times for cell killing between the modified and un-modified viruses showed considerable differences at the 48- and 72-hour time differences, however, these differences were largely resolved by 96 hours and the viruses were indistinguishable by 120 hours. These results suggest that the different viruses demonstrate differences in kinetics, as dramatic differences were observed between the viruses for time taken to achieve 50% cell killing, with IFN-γ-modified exhibiting slower kill. However the results also demonstrate that these early kinetic differences do not alter the overall oncolytic ability of the viruses, with negligible differences in cell death observed between the viruses at the 96- and 120-hour time points.

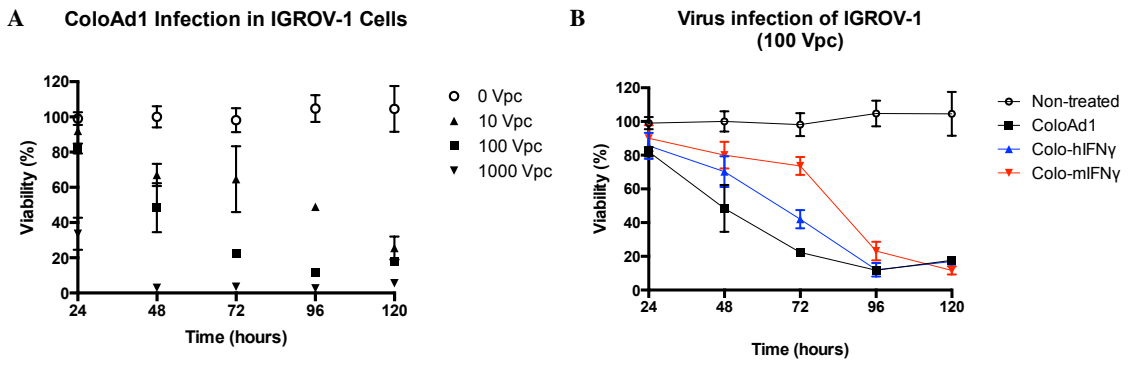


Figure 3.3 Oncolysis of IGROV-1 cells by ColoAd1-IFN-γ

A) IGROV-1 cells were plated at 10 000 cells per well in 96 well plate format and infected with 0, 10, 100 or 1000 virus particles per cell (VPC) of ColoAd1 virus. Cell viability was measured using the MTS assay across a 5-day period with intervals every 24 hours. **B)** IGROV-1 cells were infected with 100 VPC of ColoAd1, ColoAd1-mIFNγ and ColoAd1-hIFNγ for five days, with cell viability measured using the MTS assay across a five day period with intervals every 24 hours. Cells were infected in a volume of 100µL of RPMI, with an additional 20µL of fresh RPMI added on day three. Results represent n=3. Error bars depict standard deviation

3.2.2.3 Virus production of IFN-γ

To assess the ability of the engineered ColoAd-1 viruses to produced IFN-γ, IGROV-1 cells were infected with IFN-γ-modified viruses to a final virus concentration of 100VPC, with the supernatants harvested every 24 hours for a total of three days (*Figure 3.4*). Earlier time points for IFN-γ production (24-72 hours) were favoured over later time points (96-120 hours) for harvesting supernatants as these allow measurement of IFN-γ from (largely) intact cells before significant lysis occurs; later time points would not give an accurate measurement of virus-mediated IFN-γ production and secretion from cells. The results demonstrate that the engineered viruses are capable of functional IFN-γ production, with increases in IFN-γ production over time most likely reflecting an increase in virus replication. Importantly, the levels of IFN-γ produced are within the range of 1-200 ng/mL which has previously been demonstrated to modulate the phenotype of macrophages (Duluc et al., 2009).

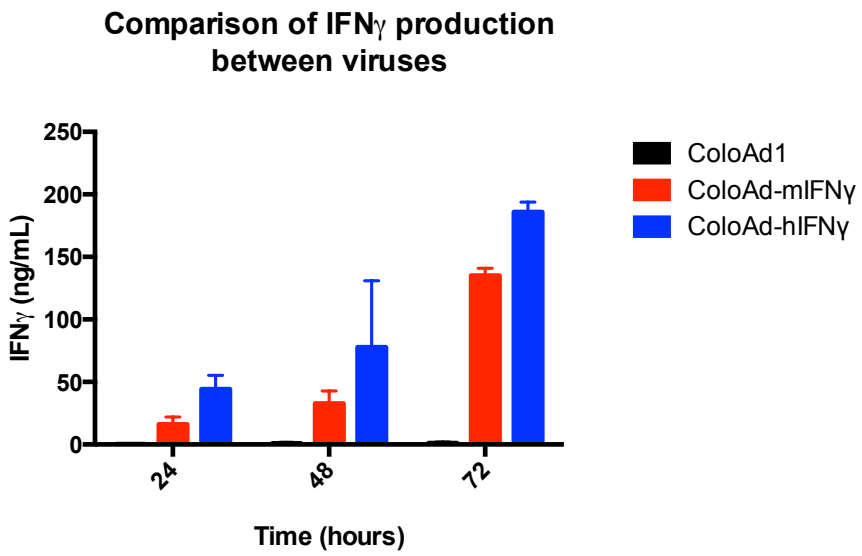


Figure 3.4 Production of IFN-γ by ColoAd1 armed with murine or human IFN-γ

IGROV-1 cells were plated at a concentration of 50 000 cells per well in 48 well plates. Cells were infected with 100 VPC of ColoAd1, ColoAd1-mIFNγ or ColoAd1-hIFNγ in 200μL of complete RPMI and incubated for three days. Supernatants were harvested at 24 hour intervals, frozen and were later probed for levels of mIFNγ and hIFNγ using anti-murine IFNγ and anti-human IFNγ ELISA kits (Peprotec™) respectively. Results represent n=3. Error bars depict standard deviation

3.2.2.4 Virus replication does not occur in macrophages

A disadvantage of using the CMV promoter to drive expression of IFN-γ, is that its production of transgene is not as restricted to tumour cells as would be for viruses using the splice-acceptor promoter. As this project aims to therapeutically modulate macrophage phenotype through IFN-γ production by virus-infected tumour cells, it is important to establish whether ColoAd1-IFN-γ is capable of infecting, replicating and

producing transgene under the CMV promoter in macrophages as this may significantly influence the polarisation of macrophages.

To address these questions, I utilised the GFP reporter ColoAd1 viruses in macrophage infection experiments. Un-polarised human macrophages (THP-1 cells) or murine macrophages (IC-21) were treated with increasing concentrations of ColoAd1, with GFP expression under the control of either the CMV or SA promoter (*Figure 3.5*). As positive controls, 293A cells were also infected with virus. Cells were incubated with virus for three days, to allow for any potential infection and subsequent replication in macrophages to occur, assessed by GFP positivity. As expected, infection of 293A cells demonstrated dose-dependent increases in GFP for both CMV- and SA- GFP viruses, with the total percentage of cells positive for GFP further increasing between the 24-and 72-hour time point. Infection of IC-21 with either virus demonstrated no evidence of GFP positivity for any concentration of virus at either of the time points. Absence of any GFP positivity was also observed in THP-1 cells infected with ColoAd1-SA-GFP virus. For the ColoAd1-CMV-GFP virus however, some GFP positivity was observed. At 24 hours, approximately 2% of cells infected with 100- and 1000-VPC of ColoAd1-CMV-GFP showed positivity for GFP which increased to 5% of cells by 72 hours. The results demonstrate some very low level, non-specific infection of human macrophages by ColoAd1-CMV-GFP at the highest concentration; the absence of any considerable increases in GFP between the 24- and 72-hour time points confirms a lack of replication. No GFP infection is observed for the infection of murine cells. Even at the highest concentration of ColoAd1-SA-GFP, there was negligible production of GFP observed in macrophages, demonstrating that the virus-specific promoter restricts virus replication and transgene production to tumour cells alone.

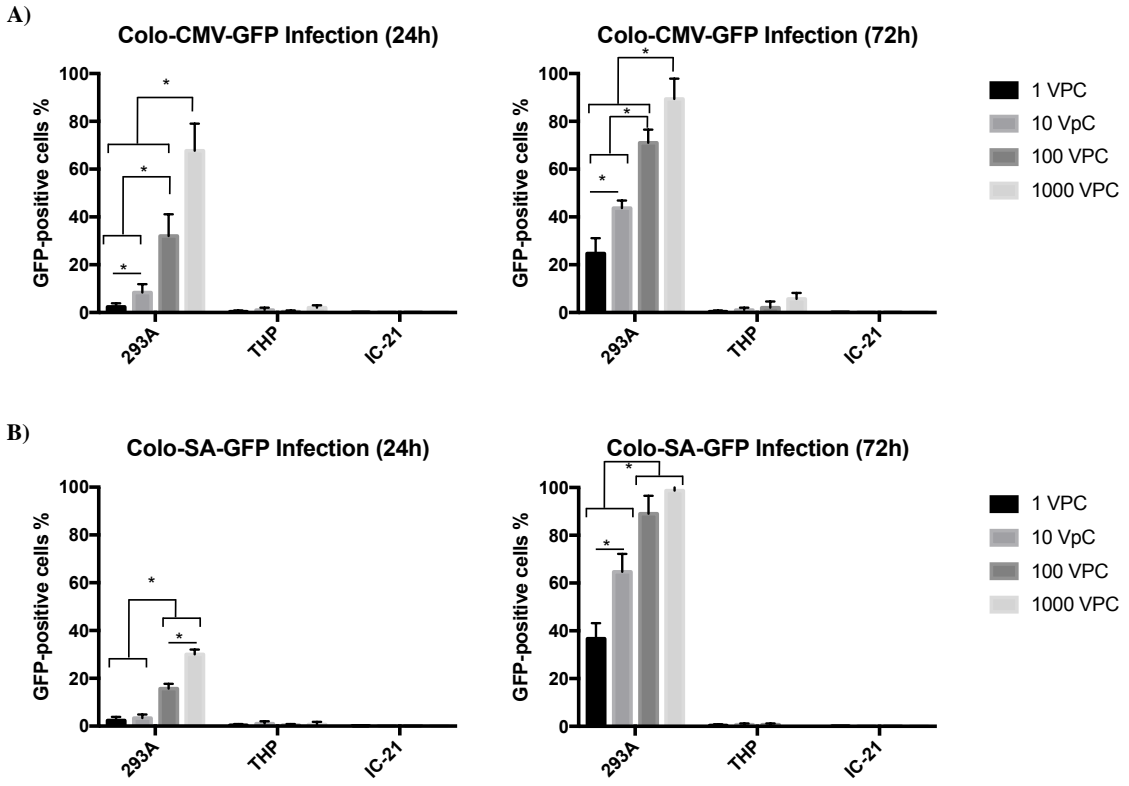


Figure 3.5 Infecting human and murine macrophages with ColoAd1

THP-1 macrophages, IC-21 macrophages and 293A cells were seeded in 48 well plates at a density 2 x 10^5 cells per well in 0.5 mL RPMI. Cells were infected with 1, 10, 100 or 1000 VPC of either ColoAd1-CMV-GFP (**A**) or either ColoAd1-SA-GFP (**B**), with GFP expression assessed by flow cytometry at 24 (**left panels**) or 72 hours (**right panels**). The values from non-treated controls typically gave negligible background GFP positivity of less than 1% for each cell type. These values were subtracted from the treated samples as to normalise the data and to remove background. Results represent n=3. Error bars depict standard deviation. Statistical analysis of significance was performed by one-way ANOVA, with a Tukey post-test. $P<0.05$ (*)

The GFP positivity observed ColoAd1-CMV-GFP infection of human macrophages seemed non-specific and negligible. However, such findings could suggest that the ColoAd1-CMV-IFN-γ virus would be able to produce transgene from macrophages. Independent of any infection, it is also possible that virus particles alone might have the potential to effect macrophage phenotype. For either of these possibilities, it is important to address whether viruses would be able to significantly alter macrophage phenotype, as this could complicate later experimentation aiming to separate the re-polarising properties of IFN-γ from the presence of virus.

To address whether ColoAd1-CMV-IFN-γ viruses are able to produce transgene in macrophages, ColoAd1-CMV-hIFN-γ and ColoAd1-CMV-mIFN-γ were used to infect THP-1 and IC-21 cells respectively (*Figure 3.6*) at the same virus concentration range used previously. As a control that the infections were successful and that human and murine IFN-γ could be detected, 293A cells were also infected with ColoAd1-CMV-hIFN-γ and ColoAd1-CMV-mIFN-γ viruses (*Figure 3.6B*). As additional controls, murine and human macrophages were polarised towards M1 and M2 phenotypes to induce (positive control) and suppress (negative control) IFN-γ production, respectively (*Figure 3.6A*). In both human and murine macrophages, infection with virus did not result in any significant induction of IFN-γ production relative to non-treated or M2 controls.

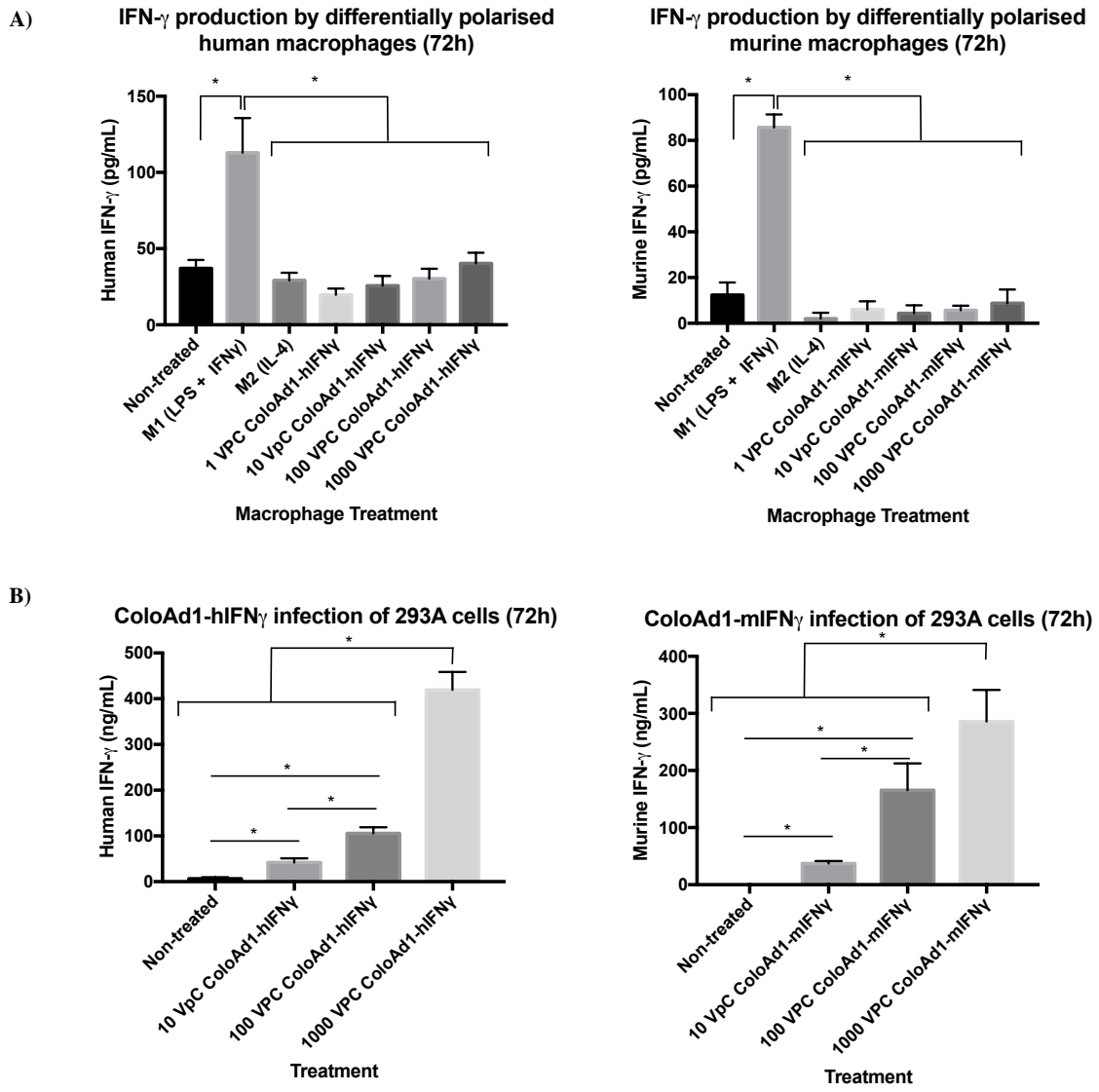


Figure 3.6 Assessing production of IFN-γ following virus infection

THP-1 macrophages, IC-21 macrophages and 293A cells were seeded in 48 well plates at a density 2 x 10^5 cells per well in 0.5 mL RPMI. **A)** THP-1 macrophages and IC-21 macrophages were infected with 1, 10, 100 or 1000 VPC of ColoAd1-hIFN-γ and ColoAd1-mIFN-γ, respectively. As controls, macrophages were also treated with M1 (LPS 1 ng/mL) and IFN-γ (10 ng/mL) and M2 (IL-4, 10 ng/mL) polarising conditions or with media alone (non-treated). **B)** As positive controls for infection, 293A cells were also infected not treated, or infected with 10, 100 or 1000 VPC of ColoAd1-hIFN-γ (**left**) and ColoAd1-mIFN-γ (**right**). Supernatants were harvested after 72 hours, centrifuged to remove any dead cells (300 x g, 5 mins) frozen and were later probed for levels of mIFNγ and hIFNγ using anti-murine IFNγ (right panels) and anti-human IFNγ (left panels) ELISA kits (Peprotec™) respectively. Results represent n=3. Error bars depict standard deviation. Statistical analysis of significance was performed by one-way ANOVA, with a Tukey post-test. $P<0.05$ (*)

3.3 Discussion of results

In this chapter I demonstrated the successful cloning of IFN-γ into the ColoAd1 virus. The choice of CMV promoter to drive IFN-γ production is in many ways advantageous as a proof-of-principle. However, the promiscuous nature of CMV-driven transgene expression could prove problematic when wanting to ensure tumour-specific virus replication and transgene production. This is of particular importance for a project such as this that aims to modulate the phenotype of macrophages, as it becomes important to delineate the effects of virus produced interferon from cancer cells, from any off-target effects of virus infection macrophages and potentially producing interferon. As discussed, it was unfortunate that more virus-specific promoters could not be utilised at the time, but future work will aim to clone IFN-γ into a splice-acceptor driven cassette and murine and human ColoAd1-SA- IFN-γ viruses produced.

The results of the virus infections of macrophages with the splice-acceptor containing virus demonstrate that the ColoAd1 virus does not replicate in human or murine macrophages. Similarly, infection of murine macrophages with the CMV-driven GFP virus show that ColoAd1 is not infecting, nor replicating within murine macrophages. In contrast, slight GFP positivity was observed for the ColoAd1-CMV-GFP infections of human macrophages, albeit at very low levels (< 5%). That there was no dramatic increase in GFP positivity from the 24- to 72-hour time points indicates that any low level infection did not result in virus replication.

Low level infection of macrophages would represent an off-target infection for IFN-γ armed virus and could therefore be considered a problem for organs such as the liver if delivered intravenously, as a virus capable of producing IFN-γ within the kupfer cells in the liver may cause toxicity issues (Tao et al., 2001). As stated previously however, the usage of CMV driven expression was chosen on the basis of being able to provide a proof-of-principle, with the aim to use the virus-specific promoters later in development. Having shown that SA-driven GFP expression was attenuated in human and murine macrophages, this suggests that non-specific infection of macrophage will not prove an issue when IFN-γ is placed under the virus-specific SA promoter.

It was important to know whether the small GFP positivity observed in human macrophages would correlate with an ability to induce IFN-γ expression. As this project aimed to stimulate macrophages by expressing IFN-γ from tumour cells infected with virus, having a virus also capable of infecting and producing IFN-γ within macrophages could significantly complicate establishing the relative contributions of virus and tumour cell-secreted IFN-γ in the final phenotype of macrophages. The results of the IFN-γ production experiments in macrophages showed that infection with armed ColoAd1 viruses did not result in IFN- γ production. As such, these results demonstrate that the changes in macrophage phenotype observed later in this thesis were a result of virus infection of tumour cells, and subsequent IFN-γ produced from these infected tumour cells.

In this chapter, it was demonstrated that the IFN-γ encoding viruses are functionally active, retaining the ability to lyse cancer cells and are able to produce functional IFN-γ to levels that have previously been reported to modulate of immune cells (Aki et al., 1994; Dickensheets et al., 1999; Duluc et al., 2009). Whilst there were no significant differences in the ability to kill cancer cells observed between the un-modified and IFN-γ-encoding viruses at the 96- and 120-hour time points, the un-modified virus demonstrates considerably greater cell death at the 72-hour time point. This could be a reflection in delayed genome replication owing to a larger genome size for IFN-γ-encoding viruses. However, that the large differences in the killing kinetics seen at 72 hours are largely resolved by 96 hours, would suggest that the consequences of this 24-hour delay are not dramatic to the overall ability to lyse cancer cells. Confirmation that infective virus units (as a function of the total virus particles) were being produced was corroborated during the virus manufacture process, as assessed by the TC_{ID}-50 assay. Thus, there are no significant differences between the modified and un-modified viruses ability to infect cells. It would be interesting to perform some mechanistic studies to investigate whether the encoding of IFN-γ results in reduced number of virus particles released per cell relative to un-modified (using virus burst assays), or whether it affects how far virus may spread (using modified plaque assays), however these were not of principal focus to the thesis.

Indeed, a central mechanism proposed by this project is that subsequent infection by progeny virus would amplify the levels of IFN-γ produced and that the presence of lysed tumour cells would contribute to the induction of an anti-immune response, perhaps by providing a source of tumour antigen for IFN-γ-polarised macrophages to cross present to CD8 T cells. However, I subscribe to the widely held opinion within the oncolytic virotherapy field that the efficacy of this therapeutic modality lies in the initial lysis and production of transgene by oncolytic viruses; it is the partial lysis, rather than complete virus-mediated tumour de-bulking, which "lights a fire" within a tumour to instigate a chain reaction of events that collectively shift the balance of the tumour microenvironment toward pro-inflammatory, anti-tumour mediated immune responses (Melcher et al., 2011; Seymour and Fisher, 2016). As such, for the context of this project, the primary goals were to ensure that the insertion of the IFN-γ gene results in functional production of IFN-γ by the virus, and ensure that this doesn't significantly hinder the ability of the virus to lyse tumour cells.

Chapter 4

Use of cell phenotype to assess macrophage polarisation and plasticity

4 Use of cell phenotype to assess macrophage polarisation and plasticity

4.1 Introduction

This chapter seeks to identify a selection of macrophage markers that can be used to distinguish macrophages in different polarisation states, enabling assessment of their phenotypic plasticity. Importantly this will permit evaluation of whether macrophage polarisation is truly reversible and whether "re-education" is a plausible strategy in the context of cancer therapy.

As discussed previously, the M1 and M2 nomenclature is largely an extension of the Th1/Th2 paradigm for CD4 T cells (Biswas and Mantovani, 2010). With increased research into macrophage subsets, it has become apparent that the sheer spectrum of diversity in macrophage polarisation cannot be encapsulated by designation of cells as either M1 or M2. However, whilst over-simplistic, this nomenclature can still provide a useful conceptual framework to distinguish broadly inflammatory versus broadly suppressive macrophages. This chapter is focused on identifying a set of markers to distinguish between inflammatory or suppressive macrophages, as a simple means to assess changes in macrophage phenotype that could have implications for therapy.

Since the discovery of "alternatively" polarised macrophages (Stein et al., 1992), the identification of these cells and their further sub-division into distinct phenotypic

groups has been a central focus for the field. Initially, characterisation of the "alternatively activated" M2 macrophage was based on the finding of mannose receptor (CD206) up-regulation in studies of mice treated with IL-4 and IL-13 (Gordon, 2003; Stein et al., 1992). Since these early findings, the list of receptors putatively up- or down-regulated depending on polarisation state far exceeds a single marker and it is widely accepted that both M1 and M2 subtypes can be further divided (Martinez et al., 2006).

Macrophages isolated from tumours have been described as being highly immunosuppressive, inhibiting T cell function and antigen presentation, along with more generalised suppressive mechanisms; production of suppressive cytokines such as IL-10 and recruitment of suppressive cell types such as Treg cells (Biswas and Mantovani, 2010). To begin defining receptors that may discriminate between the classical M1 and M2 phenotypes, a list of candidate surface receptors was derived from the literature. Given the association of TAM with immunosuppression however, this search was refined for receptors that have been identified previously on tumour-associated macrophages and have recognised immune-regulatory functions (*Table 4.1*). Candidate receptors of TAMs include those typically associated with M1 phenotypes; in such cases, the down-regulation of M1-type receptors is as much a marker of TAMs as is the up-regulation of immunosuppressive, M2-type receptors.

	Receptor	Function	Significance in tumours
Conventional "M1" polarisation marker	CD64	High affinity IgG receptor	CD64 expression on macrophages is considered an "M1" marker owing to its up-regulation by IFN-γ (Hristodorov et al., 2015). As a high affinity IgG receptor, CD64 is central to the mechanism of action for many antibody-based cancer therapies. For example, CD64 expression has been shown to mediate antibody-dependent cellular phagocytosis of melanoma cells (Mancardi et al., 2013) and can mediate the antibody-dependent cellular cytotoxicity of rituximab (Kakinoki et al., 2004).
	CD40	Co-stimulatory molecules	CD80 and CD86 expression on antigen presenting cells provide co-stimulation for T cells by engaging with CD28. CD80 and CD86 expression has been shown to be down-regulated in tumours (Tirapu et al., 2006), correlating with increased levels of inhibitory co-receptors such as CTLA-4 (Zheng et al., 2004). CD40-CD40L is of therapeutic interest as CD40 is down-regulated in tumours. Therapeutic stimulation of CD40 re-establishes co-stimulation of T cells, resulting in strong anti-tumour CD8 T cell responses (Honeychurch et al., 2003). Downregulation of CD40, CD80 and CD86 receptors is observed from macrophages isolated from tumours and thus, represents potential markers of TAMs (Sica and Mantovani, 2012).
	B7-1 (CD80)		
	B7-2 (CD86)		
	MHC I	Antigen presentation	Loss or down-regulation of MHC I is a common immunoediting mechanism by which tumours can reduce tumour immunosurveillance (Angell et al., 2014; Korkolopoulou et al., 1996). Levels of both MHC I and II have been shown to be reduced in tumours and on the surrounding stromal cells. Low MHC levels on myeloid cells represent one of the underlying causes of reduced presentation of tumour antigens, and consequently low MHC II represents a marker of suppressive, or tumour-associated macrophages (Movahedi et al., 2010).
	MHC II		
Conventional "M2" polarisation marker	B7-DC (PD-L2)	Regulation of T cell activation	The PD1-PDL1 interaction has received great interest for tumour immunotherapy, as this interaction is integral in the induction tumour tolerance, suppressing effector T cell function (Karwacz et al., 2011). PD-L2 is of interest as its expression is restricted to antigen presenting cells, and may be a critical regulator of CD8 T cell activity (Latchman et al., 2001).
	B7-H4 (PD-L4/VTCN)		
	SIRP-1α	Regulator of phagocytosis	CD47 is a prominent "don't eat me" signal, which is found overexpressed on a number of tumours including bladder cancer, leukaemia and non-Hodgkin's lymphoma (M. P. Chao et al., 2010; Jaiswal et al., 2009; Kamba and McDonald, 2007; Zhao et al., 2011). Increased expression of CD47 provides a means to evade phagocytosis as binding of CD47 to its partner, SIRP-1α, on the surface of macrophages causes the downstream activation SHP-1 phosphatase to down-regulate macrophage phagocytosis (Kant et al., 2002; Veillette et al., 1998). Antagonism of the CD47:SIRP interaction is currently in clinical trial, using an anti-CD47 antibody (Liu et al., 2015).
	CD169 (Sialadhesin)	Member of the sialic acid-binding family	CD169 is a sialic acid-binding lectin, present on inflammatory populations macrophages (Asano et al., 2011). CD169+ macrophages have recently been shown to be responsible for the phagocytosis and cross-presentation of dead tumour cell antigens, with a wider antigen repertoire cross-presentated than by dendritic cells, correlating with strong anti-tumour CD8 responses. The expression of CD169 on antigen presenting cells correlates with effective cross-presentation of tumour antigens (Asano et al., 2011; Bernhard et al., 2015).

Table 4.1 Major immunomodulatory receptors of macrophages

An extensive literature review was performed to identify surface receptor markers present on tumour-associated macrophages that have reported roles underpinning their immunomodulatory functions. M1 and M2 markers can be identified on TAMs, with decreased levels of M1 markers and increased levels of M2 markers driving the immunosuppressive phenotype. Literature searches were performed using PubMed's search function (http://www.ncbi.nlm.nih.gov/pubmed) using with combinations of search terms such as "TAM", "immunoregulation", "immune suppression", "T cell suppression" and "antigen presentation"

A central hypothesis of this thesis is that tumour-associated macrophages can be "re-educated", harnessing the plasticity of this cell type for therapy (Duluc et al., 2009; Ruffell et al., 2012a). A selection of the more prevalent immune-modulatory macrophage receptors were therefore explored in this chapter to try and generate a morphological profile that can be used to distinguish different macrophage subsets. Importantly, this should enable identification of macrophages responding to different polarisation stimuli and enable assessment of the feasibility of therapeutic "re-education" of macrophages, particularly from the TAM-like M2 state to the more pro-inflammatory M1 state.

4.1.1 Chapter aims

1. Identify cellular markers to define M1- and M2 –type macrophages in mouse and human models of polarisation
2. Use these markers to address the plasticity of polarised macrophages, examining to what degree inter-conversion between phenotypes is possible
3. Explore whether therapeutic "re-education" of macrophages is a plausible hypothesis and evaluate whether IFN-γ can mediate such "re-education"

4.2 Results

4.2.1 Studying murine macrophage polarisation

Some of the earliest data on alternatively polarised macrophages was derived using mouse macrophages (Stein et al., 1992). As such, mouse macrophages have been relatively well characterised and were thought to provide an ideal starting point with which to explore re-education. To ensure an unlimited supply of macrophages for polarisation studies, initial experimentation was performed using the mouse macrophage cell line IC-21.

4.2.1.1 Receptor expression on polarised murine macrophages

IC-21 cells were polarised towards classically activated M1 macrophages (conditioned with M1 medium, consisting of lipopolysaccharide (LPS) + murine IFN-γ (mIFN-γ), alternatively activated macrophages (conditioned with M2 medium, containing IL-4) or polarised with IFN-γ for 24 hours, before harvesting cells and staining for a CD40, CD64, CD80, CD86, MHC I, MHC II, SIRP-1α, B7-H2 and B7-H4 (*Figure 4.1*).

The results demonstrated varied receptor expression among the differently polarised macrophages. As a general trend, the receptor profiles of M1- and IFN-γ polarised macrophages were very similar (e.g. for CD80, MHC I), and demonstrated significantly increased levels of all receptors examined compared to M2 macrophages, with the exceptions of SIRP-1α, B7-H2 and B7-H4. SIRP-1α is particularly interesting as it shows significantly higher expression in M2-polarised macrophages than the more pro-inflammatory M1- and IFN-γ polarised macrophages.

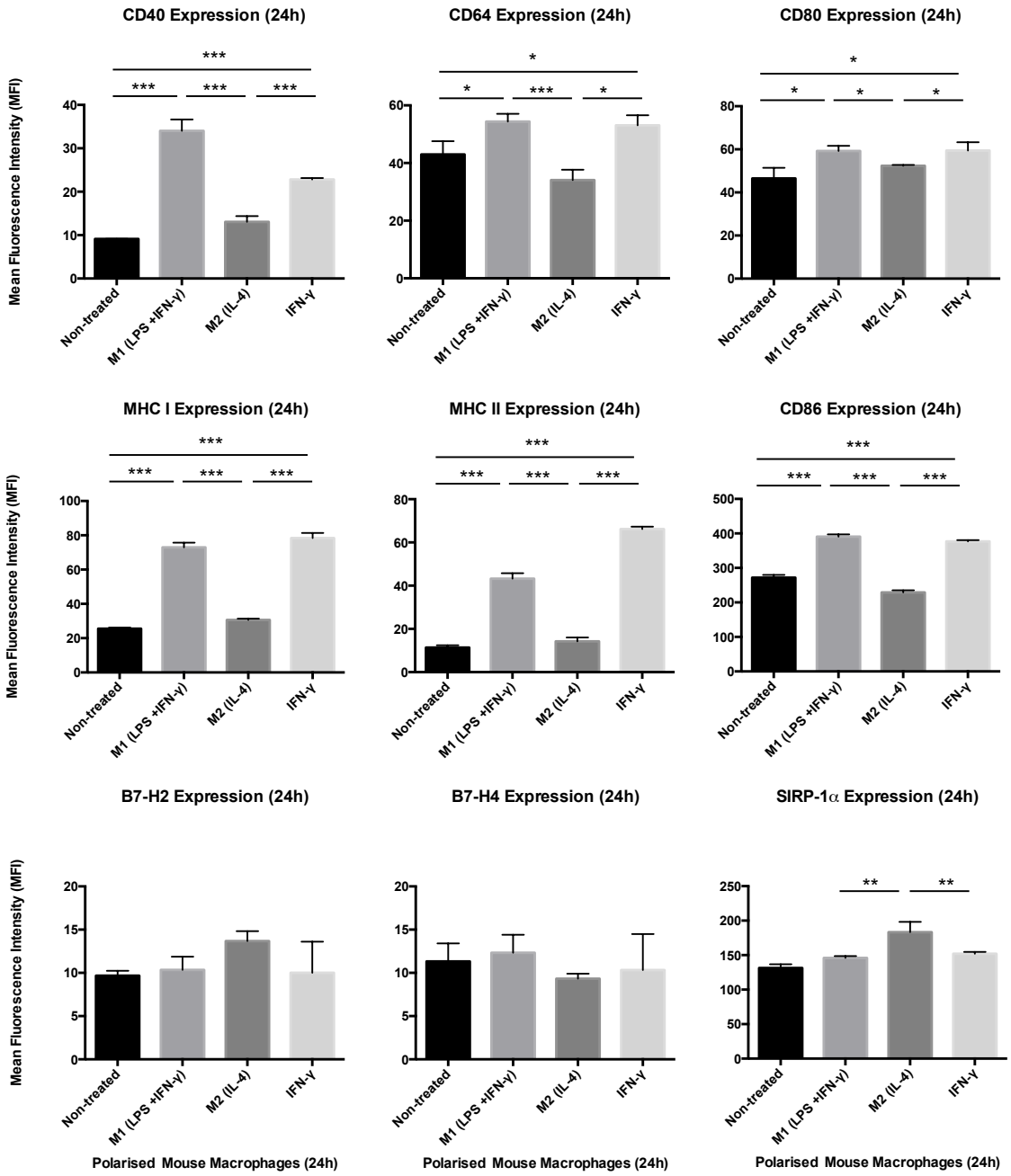


Figure 4.1 Differentially polarised murine macrophages display varied receptor expression

IC-21 macrophages were seeded in 48 well plates at a density 2 x 10^5 cells per well in 0.5 mL of M1 media (LPS 1 ng/mL) and mIFN-γ (10 ng/mL), mIFN-γ alone media (10 ng/mL) with or M2 media (IL-4, 10 ng/mL) in RPMI (10% FBS) for 24 hours. Cells were harvested using non-enzymatic dissociation buffer, incubated with an Fc block, and stained for surface receptors whose expression was analysed using a BD FACS Calibur™. Receptor expression of given receptors is expressed as mean fluorescence intensity (MFI) in bar charts. Results represent n=3, with errors bars indicating SD. Statistical analysis of significance was performed by one-way ANOVA, with a Tukey post-test. P<0.05 (*), P<0.01 (**) P<0.001 (***)

These results indicate that there were no significant differences in expression between M1- and mIFN-γ – polarised macrophages for a number of receptors, including CD64, CD80, CD86 and MHC I, suggesting that IFN-γ alone has the ability to up-regulate many pro-inflammatory receptors to levels equivalent to those observed when it is combined with TLR4 stimulation by LPS.

4.2.1.2 *In vitro* re-education of M2 murine macrophages; receptor analysis

A central aim of this chapter is to evaluate the plastic, reversible nature of macrophages in a therapeutic context. Re-polarising TAMs would constitute a change from an M2-suppressive-like population of cells toward a more pro-inflammatory M1 phenotype. To model this *in vitro*, murine macrophages were polarised toward an M2 phenotype for 24 hours, before media was exchanged for M1- or mIFN-γ –containing media for an additional 24 hours, with potential changes in phenotype assessed by flow cytometric staining of CD40, CD80, MHC I and MHC II (*Figure 4.2)*.

The results demonstrate that a significant change in phenotype is observed for M2 macrophages "re-educated" in this manner. Re-education by both M1 medium and mIFN-γ alone were able to significantly increase the levels of CD40, CD80 and MHC I relative to M2 controls. A different pattern was observed for MHC II expression however, as intriguingly only treatment with mIFN-γ alone was able to induce significant up-regulation of MHC II.

Whilst CD80 illustrated significant re-education of M2 macrophages, it was interesting to note that significant differences were not observed between M1- and M2-macrophages for CD80 expression. Significant differences were observed between these macrophages for CD80 expression in earlier in this thesis (*Figure* 4.1), but this was after 24 hours polarisation, whilst *Figure* 4.2 presents 48-hour data. Together these data show that CD80 can be used as a marker to describe re-education and polarisation, as even at 48 hours the levels of CD80 observed are higher in the M1 macrophages relative to M2 are higher; however, over time it would suggest that the separation between M1 and M2 CD80 expression decreases.

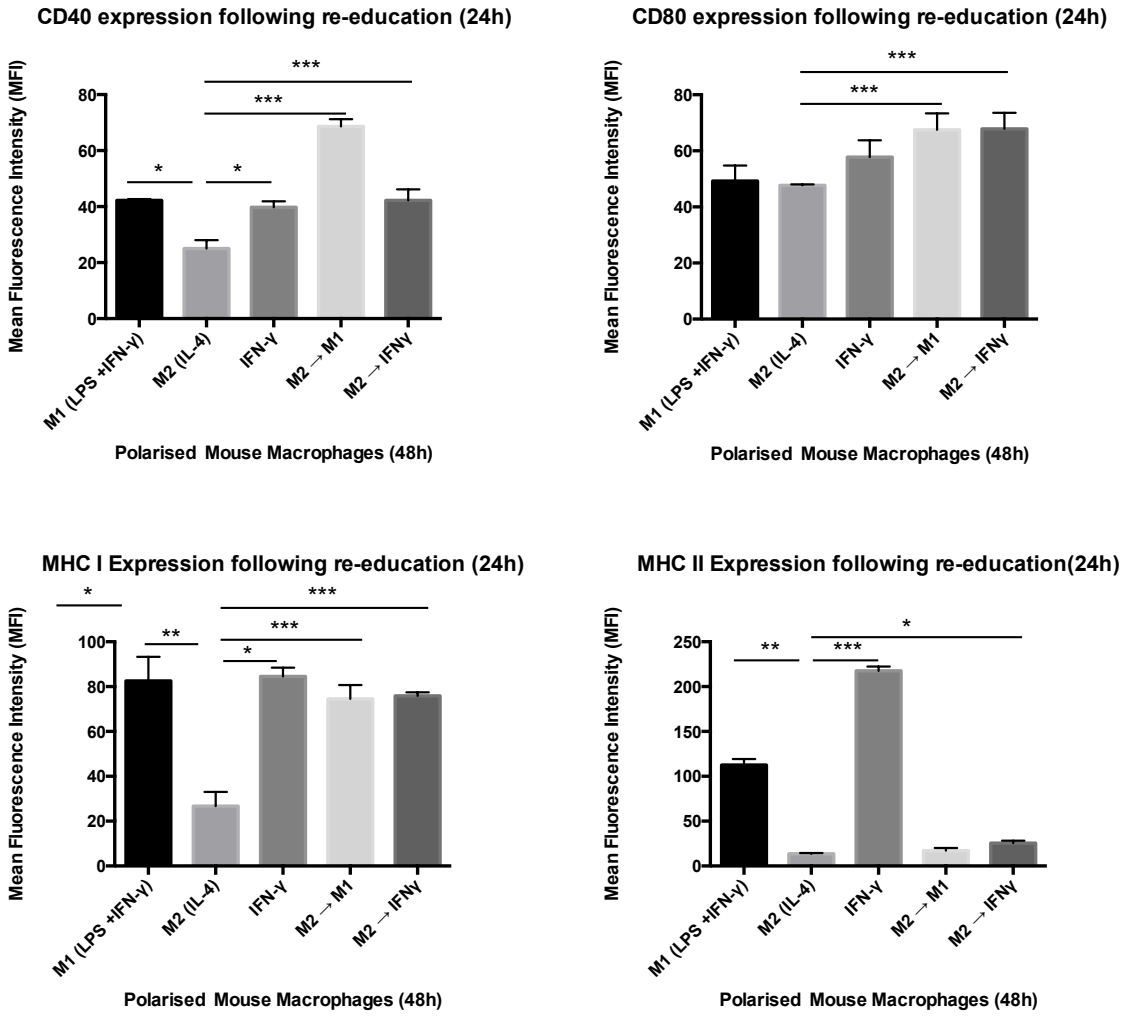


Figure 4.2 M2 murine macrophages can be re-educated using IFN-γ *in vitro*

IC-21 macrophages were seeded in 48 well plates at a density 2 x 10^5 cells per well in 0.5 mL of M1 media (LPS 1 ng/mL) and mIFN-γ (10 ng/mL), mIFN-γ alone media (10 ng/mL) with or M2 media (IL-4, 10 ng/mL) in RPMI (10% FBS) for 24 hours. After 24 hours media was replaced for fresh media containing respective cytokines. In parallel, M2 macrophages had their media exchanged for M1 media (LPS 1 ng/mL) and mIFN-γ (10 ng/mL) or mIFN-γ alone media (10 ng/mL). In each case, cells were incubated for an additional 24 hours before beings were harvested using non-enzymatic dissociation buffer, incubated with an Fc block, and stained for surface receptors whose expression was analysed using a BD FACS Calibur™. Receptor expression of given receptors is expressed as mean fluorescence intensity (MFI) in bar charts. Results represent n=3, with errors bars indicating SD. Statistical analysis of significance was performed by one-way ANOVA, with a Tukey post-test. P<0.05 (*), P<0.01 (**) P<0.001 (***)

4.2.1.3 *In vitro* re-education of M2 murine macrophages; cytokine analysis

M1 macrophages are characterised by a TNF-α^{high}, IL-12^{high}, IL-10^{low} cytokine profile, with the converse pattern exhibited by M2 macrophages. To confirm that re-education of macrophages at the level of receptor expression were also correlating with a change in cytokine secretion, TNF-α from the supernatants of these samples was measured (*Figure 4.3)*. After 24 hours M1 and mIFN-γ polarised macrophages produced significantly increased levels of TNF-α compared to M2 macrophages, as would be expected. Following re-education of M2 macrophages for a further 24 hours, both M1- and mIFN-γ-containing media were able to significantly increase TNF-α levels above M2 control. Such preliminary results prompted the expansion of these experiments into a human cell line system.

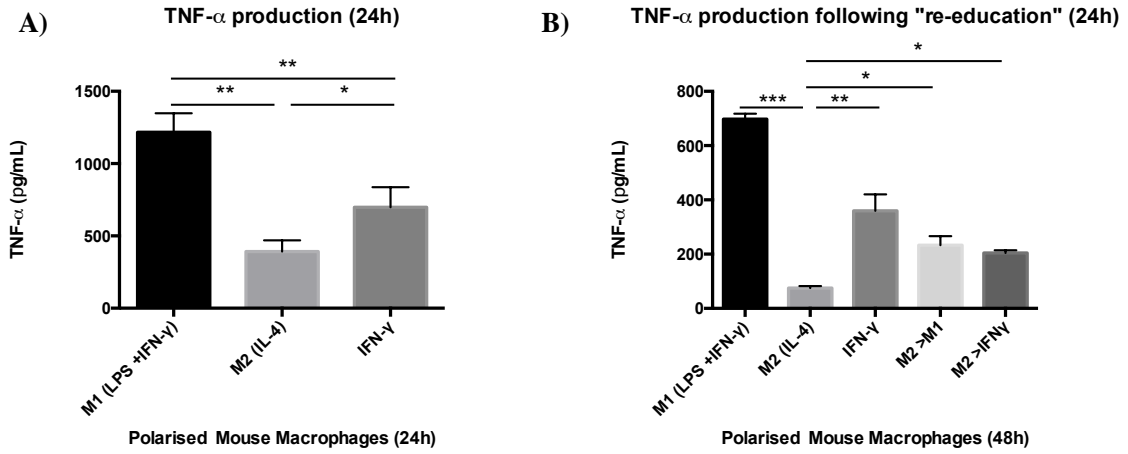


Figure 4.3 Re-educated murine macrophages exhibit changes in TNF-α production

IC-21 macrophages were seeded in 48 well plates at a density 2 x 10^5 cells per well in 0.5 mL of M1 media (LPS 1 ng/mL) and mIFN-γ (10 ng/mL), mIFN-γ alone media (10 ng/mL) with or M2 media (IL-4, 10 ng/mL) in RPMI (10% FBS) for 24 hours. After 24 hours media was replaced for fresh media containing respective cytokines. In parallel, M2 macrophages had their media exchanged for M1 media (LPS 1 ng/mL) and mIFN-γ (10 ng/mL) or mIFN-γ alone media (10 ng/mL). In each case, cells were incubated for an additional 24 hours before supernatants were harvested and probed for levels of TNF-α by ELISA. Results represent n=3, with errors bars indicating SD. Statistical analysis of significance was performed by one-way ANOVA, with a Tukey post-test. P<0.05 (*), P<0.01 (**) P<0.001 (***)

4.2.2 Studying human macrophage polarisation

Initial characterisation of human macrophages was performed using monocyte-derived macrophages obtained from either peripheral blood (from healthy laboratory donors) or leukocyte cones (NHS Blood Service). However, given the number of studies and the subsequent optimisation required for these studies, the quantity and availability of human macrophages quickly became a limiting factor for experimentation. An alternative source of macrophages, not requiring isolation from donors, would be very useful for these studies. For that reason we explored the THP-1 model of human macrophages derived using PMA (phorbol 12-myristate 13-acetate)-stimulated THP 1-monocyte cell line. The findings with these cells were then validated with studies in macrophages obtained from clinical samples.

4.2.2.1 Generation of macrophages by PMA differentiation of THP-1 cells

Treatment of human monocytes with phorbol esters such as PMA can induce terminal differentiation of these cells to form macrophages. Differentiation using PMA has been previously observed in the human monocytic cell line THP-1, with many research groups using such methodologies in macrophage research. Initial studies aimed to optimise treatment conditions for generating macrophages from the THP-1 cell line using PMA stimulation. Monocytes were treated with either 0, 3, 30 or 300 ng/mL of PMA for 24 hours, with differentiation to macrophages evaluated changes in morphology, adherence and receptor expression.

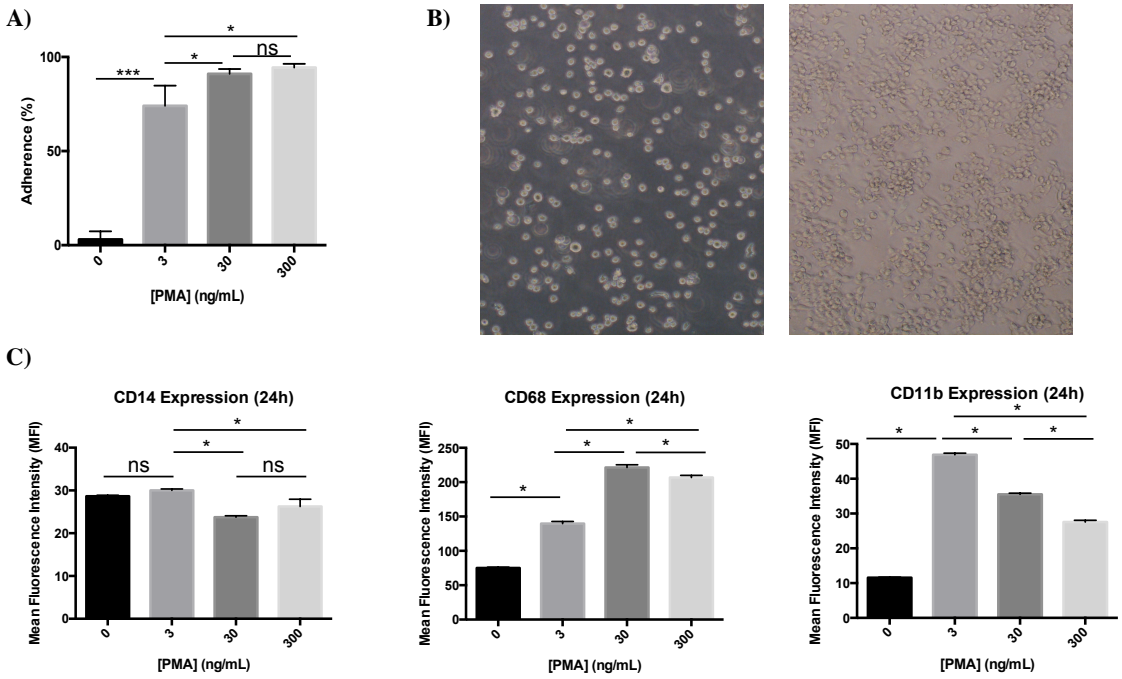


Figure 4.4 PMA differentiation of THP-1 monocytes into macrophages

THP-1 monocytes were seeded in 48 well plates at a density 2 x 10^5 cells per well 0.5 mL of RPMI (10% FBS) supplemented with 0-,3-, 30- or 300-ng/mL of PMA. Cells were incubated in their respective concentrations of PMA for 24 hours. **A)** Cells in suspension vs. adherence were counted manually using a haemocytometer to determine the total number of cells adhered. **B)** Morphological changes associated with suspension (left panel) and adhered cells (right panel) were assessed by light microscopy. **C)** Cells were harvested using non-enzymatic dissociation buffer, stained on the surface for CD14 and CD11b and intracellularly stained for CD68, then analysed using a BD FACS Calibur™ . Results represent n=3, with errors bars indicating SD. Statistical analysis of significance was performed by one-way ANOVA, with a Bonferroni post-test. $P<0.05$ (*), $P<0.001$ (***) or non-significant (ns)

Differentiation of THP-monocytes into a macrophage phenotype is correlated with a change from suspension- to adherent- cell characteristics and a more macrophage-like morphology. All concentrations of PMA used induced significant increases in adherence above the non-treated controls which were all in suspension; 3ng /mL PMA induced approximately 70% of cells to adhere, whilst concentrations of PMA ≥ 30ng/ mL, caused greater than 90% of cell to adhere. (*Figure 4.4A*). Whilst there was a clear change in the number of adherent cells between the lower and higher PMA concentrations, the morphology of the adherent macrophages did not appear to exhibit drastic differences (*Figure 4.4B*). Based on these results, the optimal concentration of PMA for future studies that would yield maximal adherence would be in the 30-300 ng/ mL range. Differentiation of THP-1 cells was characterised by receptor expression using CD68, CD11b and CD14 (*Figure 4.4C*).

CD68 is a heavily glycosylated protein involved in lysosomal trafficking and is highly expressed on macrophages. CD14 was one of the first pattern recognition receptors (PRR) identified, acting as a co-receptor along with TLR-4 in the binding of LPS. Expression of CD14 is principally expressed on monocytes and its expression is considered a marker of the monocytic cell line. CD11b is considered a marker of the myeloid lineage of cells, where it acts as a complement receptor.

After 24 hours, increasing PMA concentrations correlated with decreasing CD14 expression, with significant reductions in CD14 observed between the lowest (3 ng/mL) and highest (300 ng/mL) PMA concentrations. CD14 levels inversely correlated with CD68, as increasing PMA concentrations elevated CD68 expression, as would be expected. Interestingly, levels of CD11b increased dramatically at the lowest PMA

concentration compared to controls, although this enhancing effect was less strong at higher levels of PMA. Taken together, these results indicate a shift away from the monocytic lineage, shift toward the macrophage lineage, as evidenced by increased expression of CD68 and CD11b. This analysis of adherence and receptor expression confirms other findings that PMA treatment can generate human macrophage cell lines, herein referred to as "THP-1 macrophages", and validates their usage as a model for human macrophages. The optimum rise in CD11b was observed at 3 ng/ml, while the greatest increases in CD68 and adherence were seen at 30 ng/ml and above. In view of these findings, combined with literature reports that prolonged incubation with higher concentrations of PMA is deleterious to macrophage function and viability, a concentration of 30 ng/mL was selected for further studies.

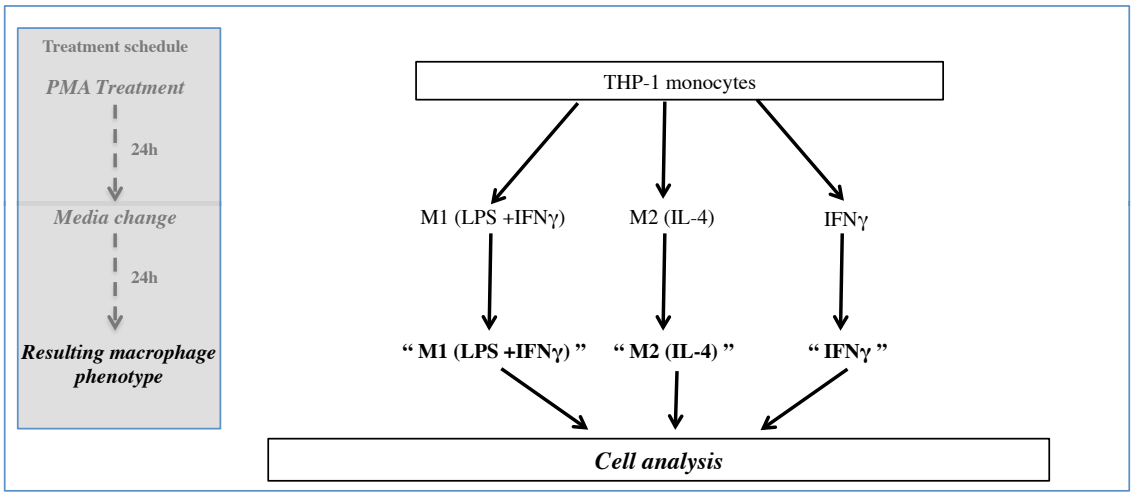


Figure 4.5 **Experimental strategy for creation of differentially polarised THP-1 macrophages over a 24-hour exposure**

4.2.2.2 Receptor and cytokine expression on polarised THP-1 macrophages

To examine whether these THP-1 macrophages are amenable to differential polarisation, human macrophages were polarised towards classical M1 activation (LPS + human IFN-γ (hIFN-γ), alternatively activated macrophages (IL-4) or polarised with hIFN-γ alone for 24 hours (*Figure 4.5*), before harvesting cells and staining for a CD40, CD64, CD80, CD86, MHC I and MHC II (*Figure 4.6A*). Consistent with the murine macrophage results obtained earlier, the pattern of receptor activation between M1- and hIFN-γ-polarised macrophages was significantly higher than the M2-polaried macrophages in all receptors studied. The difference in cell phenotype was further confirmed by ELISA data for TNF-α production, which showed significant increases for the M1- and hIFN-γ-polarised macrophages (*Figure 4.6B*). IL-12 was significantly higher in M1 macrophages relative to all other polarisations, however, its expression appeared to be almost absent in M2 macrophages. The difference in IL-12 production here between M1- and hIFNγ, appears to suggest a requirement for TLR signalling for IL-12 production.

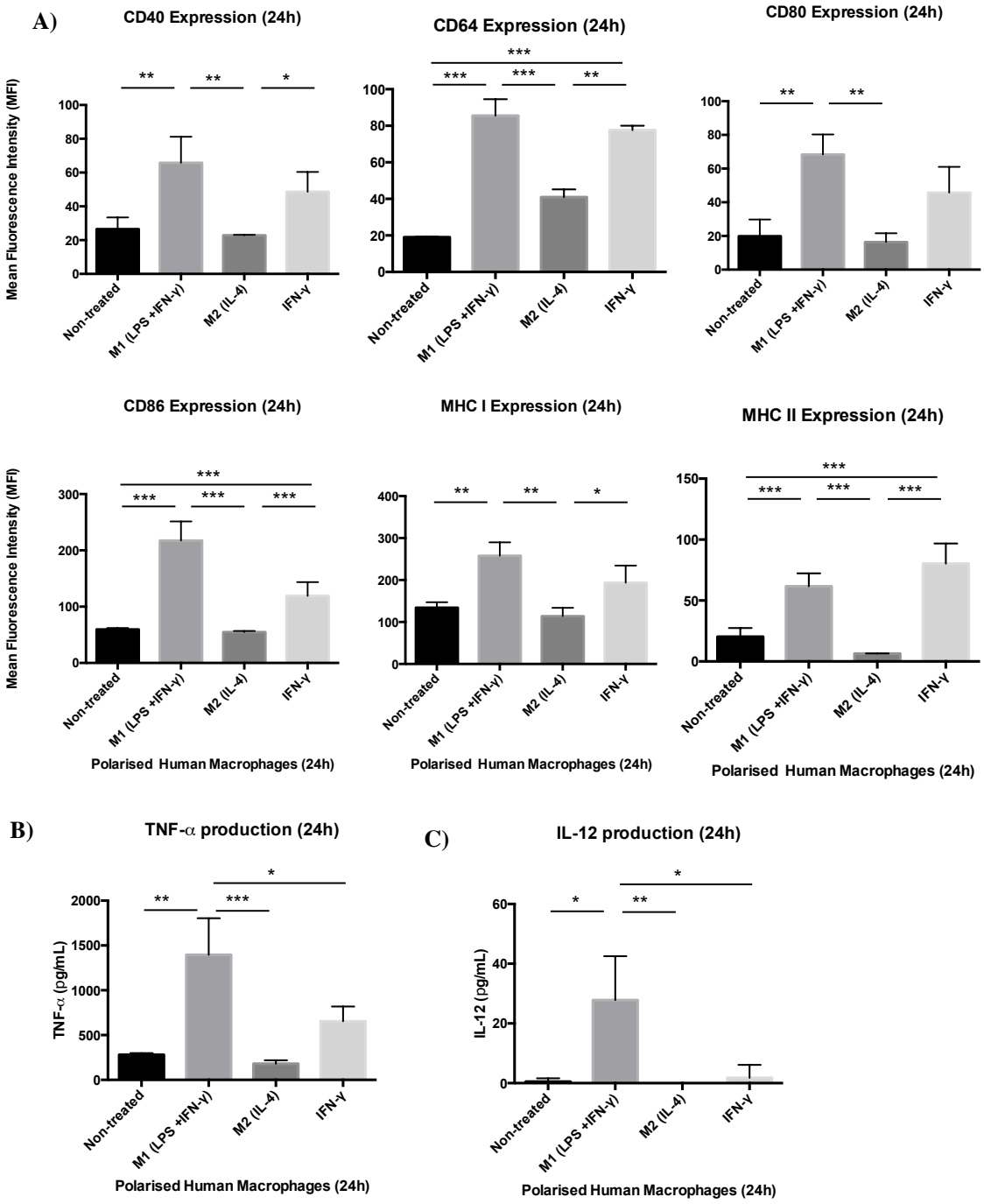


Figure 4.6 **Differentially polarised THP-1 macrophages display varied receptor expression and cytokine production after 24 hours**

THP-1 macrophages were seeded in M1 media (LPS 1 ng/mL) and hIFN-γ (10 ng/mL), hIFN-γ alone media (10 ng/mL) with or M2 media (IL-4, 10 ng/mL) in RPMI (10% FBS) for 24 hours. **A)** Cells were harvested using non-enzymatic dissociation buffer, incubated with an Fc block, and stained for surface receptors whose expression was analysed using a BD FACS Calibur™. Receptor expression of given receptors is expressed as mean fluorescence intensity (MFI) in bar charts. **B + C)** Supernatants of treated macrophages were harvested and probed for levels of TNF-α and IL-12 by ELISA. Results represent n=3, with errors bars indicating SD. Statistical analysis of significance was performed by one-way ANOVA, with a Tukey post-test. P<0.05 (*), P<0.01 (**) P<0.001 (***)

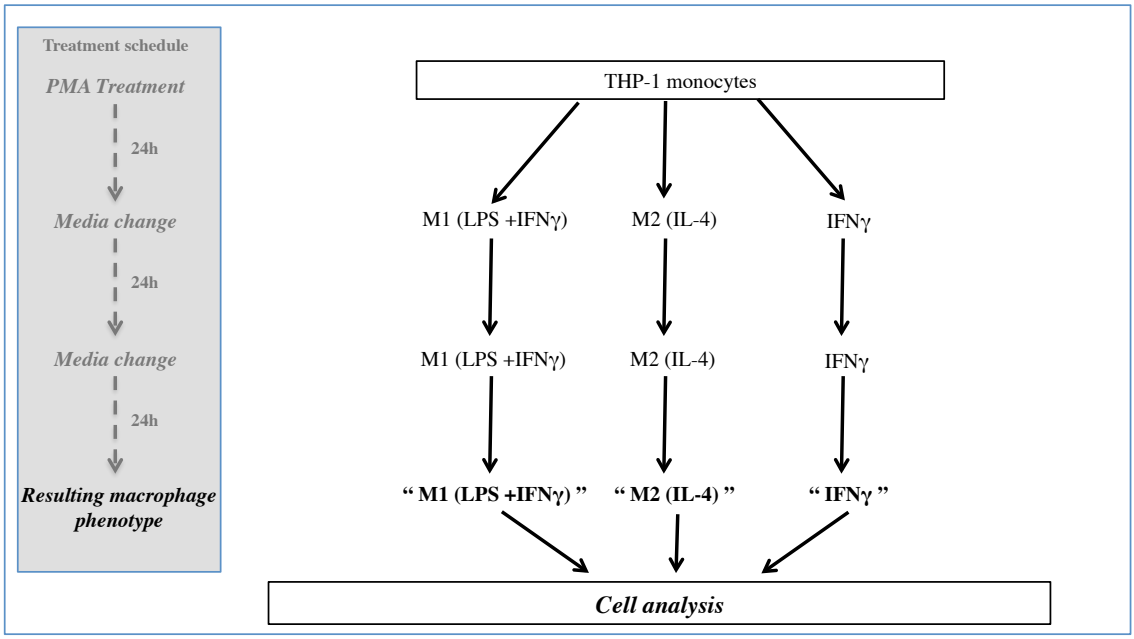


Figure 4.7 **Experimental strategy for creation of differentially polarised THP-1 macrophages over 48 hours using two consecutive 24-hour exposures**

Practical studies of macrophage re-education requires a 48 hour duration, where the initial 24 hours is used to establish the initial differentiation status and the second 24 hours is used for re-education. To establish a framework for this, control studies were performed using a simple 48 protocol, where THP-1 macrophages were stimulated with M1, M2 or hIFN-γ for 24 hours, after which time media were replaced with fresh M1, M2 or hIFN-γ –containing media respectively and cultured for an additional 24 hours (*Figure 4.7*).

As expected, studying receptor expression at 48 hours post-polarisation showed pronounced differences in CD40, CD80 and MHC II between both the M1 and hIFN-γ treated macrophages and their M2 counterparts (*Figure 4.8*). Although positivity of MHC I is near identical between groups (*Figure 4.8B*), the difference in MHC I expression is clear when studying the mean fluorescence intensity (MFI), where it becomes apparent that M2 polarised cells have lower levels of MHC1 (per cell) than

M1 or IFN-γ treated macrophages (*Figure 4.8C*). The use of MFI is useful because it allows quantitative assessment of receptors that fluctuate under different treatments, without disappearing entirely; accordingly MFI is used as the preferred descriptor of receptor staining for CD40, CD80 and MHC II as well as MHC I throughout these studies.

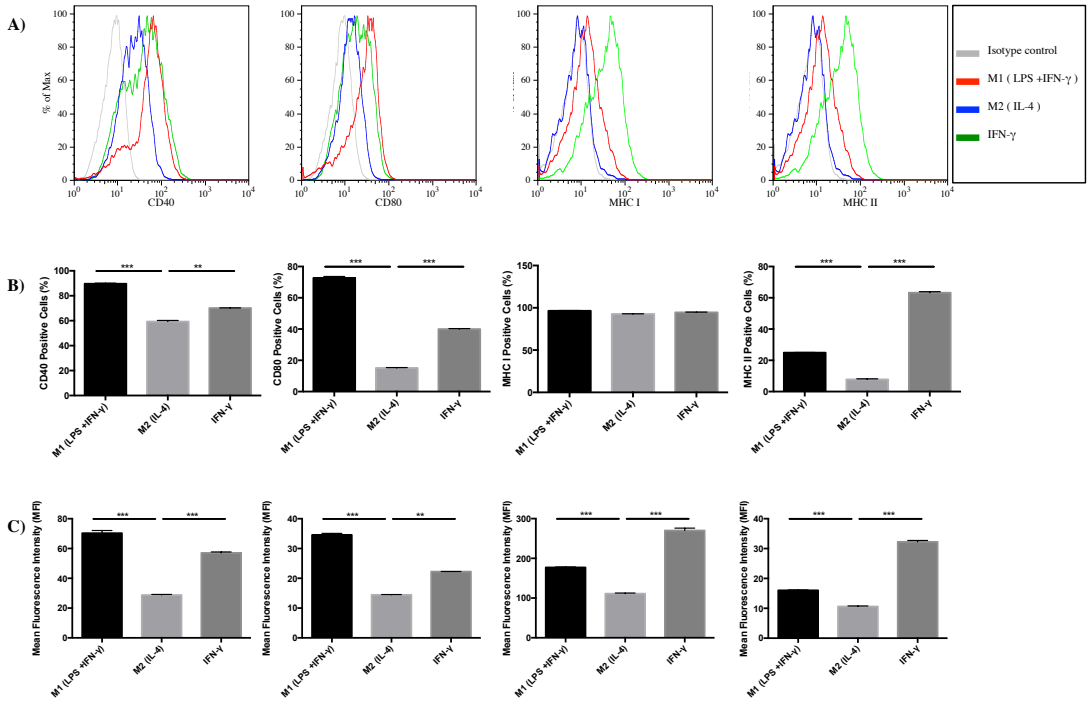


Figure 4.8 Receptor expression by macrophages differentially polarised using the 48 hour exposure protocol

THP-1 monocytes were seeded in 48 well plates at a density 2 x 10^5 cells per well in 0.5 mL of RPMI (10% FBS) supplemented with 30-ng/mL of PMA for 24 hours. Media was exchanged for M1 media (LPS 1 ng/mL) and hIFN-γ (10 ng/mL), hIFN-γ alone media (10 ng/mL) with or M2 media (IL-4, 10 ng/mL) for 24 hours, then replenished with new media for an additional 24 hours. Cells were harvested using non-enzymatic dissociation buffer, stained for CD40, CD80, MHC I and MHC II then analysed using a BD FACS Calibur™ . **A)** Flow cytometry histogram traces show expression of to M1, M2 or IFN-γ media after 48 hours of polarisation. **B)** Positivity for expression of given receptors on the THP-1 macrophages are displayed in bar charts, in contrast to **C)** showing mean fluorescence intensity for each of the markers. Results represent n=3, with errors bars indicating SD. Statistical analysis of significance was performed by one-way ANOVA, with a Bonferroni post-test. P<0.01 (**) P<0.001 (***)

4.2.2.3 Re-education of M2 polarised THP-1 macrophages

The above studies demonstrated clear differences in receptor expression between macrophages exposed to differential polarisation over 48 hours. This provided an opportunity to explore whether previously M2-polarised cells could be re-polarised toward a more M1-like phenotype (*Figure 4.9*). Extending the previous experiment, THP macrophages were polarised with M2 media for 24 hours at which point their media was changed into either M1-or hIFN-γ-containing media for a further 24 hours (denoted as "M2 ➔M1" and "M2 ➔hIFN-γ" respectively) (*Figure 4.10*).

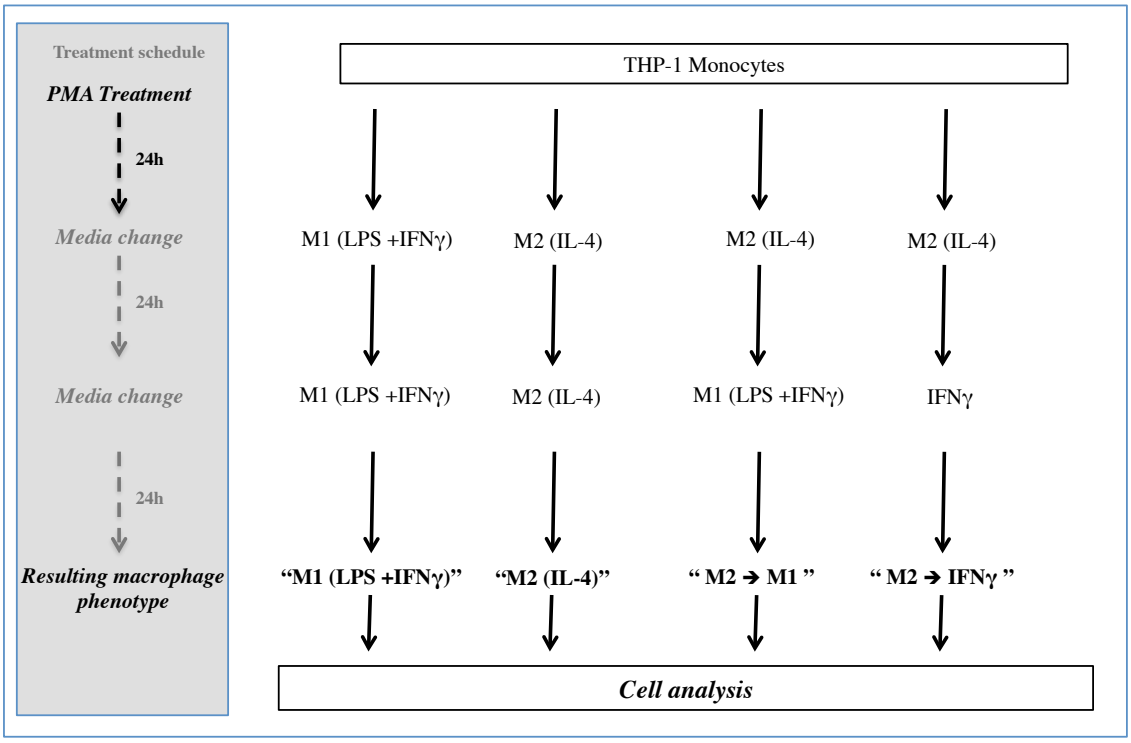


Figure 4.9 Experimental strategy for creation of differentially polarised macrophages over 48 hours using two consecutive 24 hour exposures

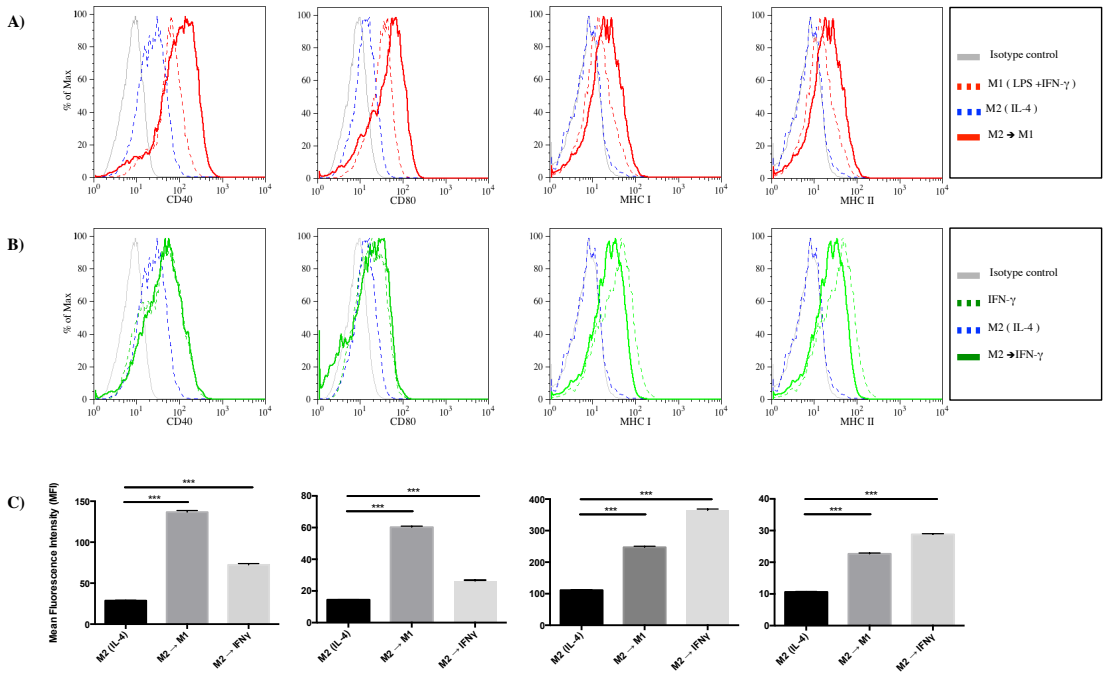


Figure 4.10 Receptor expression by macrophages differentially polarised using the 48 hours exposure protocol

THP-1 monocytes were seeded in 48 well plates at a density 2 x 10^5 cells per well in 0.5 mL of RPMI (10% FBS) supplemented with 30 ng/mL of PMA for 24 hours. Media was exchanged for M1 media (LPS 1 ng/mL) and hIFN-γ (10 ng/mL), hIFN-γ alone media (10 ng/mL) with or M2 media (IL-4, 10 ng/mL) for 24 hours, then re-stimulated with their respective conditions by supplementing media with new cytokines for an additional 24 hours, to the same final concentrations as with the initial stimulation. Cells were harvested using non-enzymatic dissociation buffer, stained for CD40, CD80, MHC I and MHC II then analysed using a BD FACS Calibur™. **A)** Flow cytometry histogram traces show expression of to M1, M2 or IFN-γ media after 48 hours of polarisation. **B)** Positivity for expression of given receptors on the THP-1 macrophages are displayed in bar charts, in contrast to **C)** showing mean fluorescence intensity for each of the markers. Results represent n=3, with errors bars indicating SD. Statistical analysis of significance was performed by one-way ANOVA, with a Bonferroni post-test. P<0.01 (**) P<0.001 (***)

Both M1 and hIFN-γ containing media were able to re-polarise M2 macrophages toward a profile of markers that resemble M1-type macrophages. Treatment with hIFN-γ yielded highest expression of MHC I and MHC II, although M1 media also gave higher levels than M2 media. Similarly both M1 media and hIFN-γ were able to increase expression of CD40 and CD80, and in this case the M1 media generated the highest the levels of both receptors.

4.2.2.4 Re-education of M2 polarised THP-1 macrophages in the presence of M2 media

In the context of a TAM (or another alternatively polarised macrophage), any therapeutic "re-education" would take place in microenvironments rich in signals driving the alternative polarisation. As such, re-polarisation stimuli would need to be able to overcome existing suppressive signalling to mediate their effects. To test this, the previous experiment was extended to include treatment groups where M1 or IFN-γ media was added to M2 media already containing the cells (*Figure 4.11*).

Results from this study show that re-polarisation is still able to occur even in the presence of suppressive media and further, that the same pattern of receptor change was observed - M1 treatments yielded the highest levels of CD40 and CD80, and IFN-γ, the higher levels of MHC expression (*Figure 4.12*).

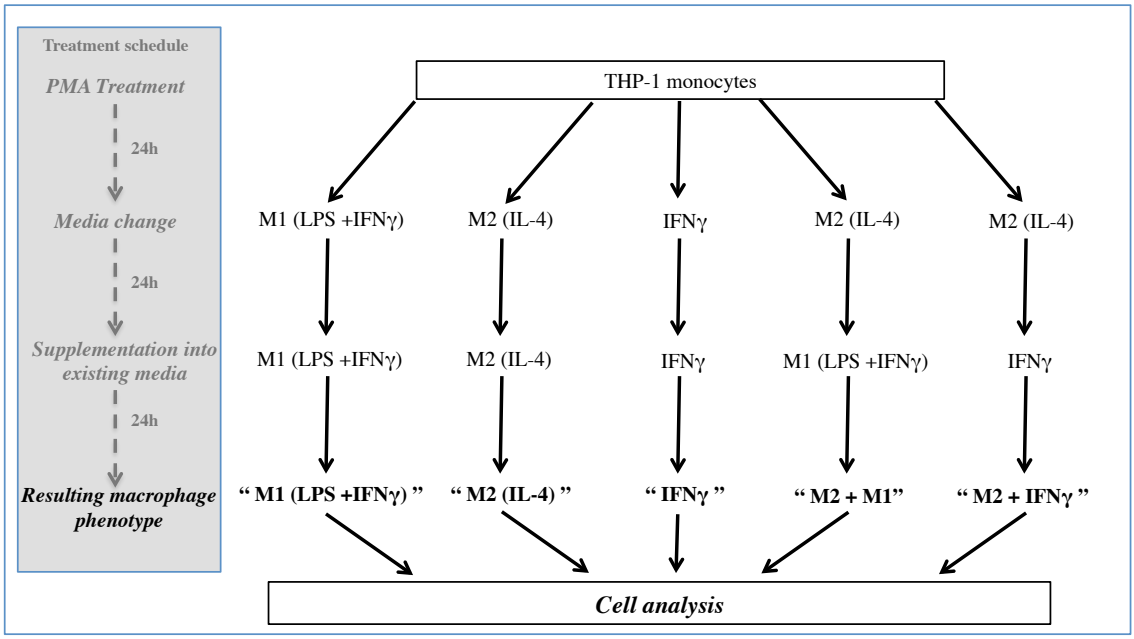


Figure 4.11 Schematic of *in vitro* re-education of M2-polarised macrophages

Comparing the data for re-education in the presence or absence of suppressive media yields some interesting observations (*Figure 4.13*). First, all treatment groups were able to induce a shift away from the M2 polarisation state to resemble a more M1-like macrophage. Second, the pattern of change for receptors after M1 or IFN-γ treatments was consistent irrespective of the presence of suppressive medium. Third, with the exception of MHC II with IFN-γ, treatments in the presence of M2 media yielded lower levels of re-education than without the M2 media. Dramatic examples of this include CD40 and CD80 expression following re-education with M1 media, where the presence of M2 media almost halved the level of receptor expression. The ability re-education with IFN-γ alone to mediate high levels of MHC II expression even in the presence of M2 media was surprising and warrants further investigation. Overall, these data support the hypothesis that macrophages previously polarised toward an M2-phenotype can be converted back toward an M1 phenotype by either a combination of LPS and IFN-γ or using IFN-γ alone.

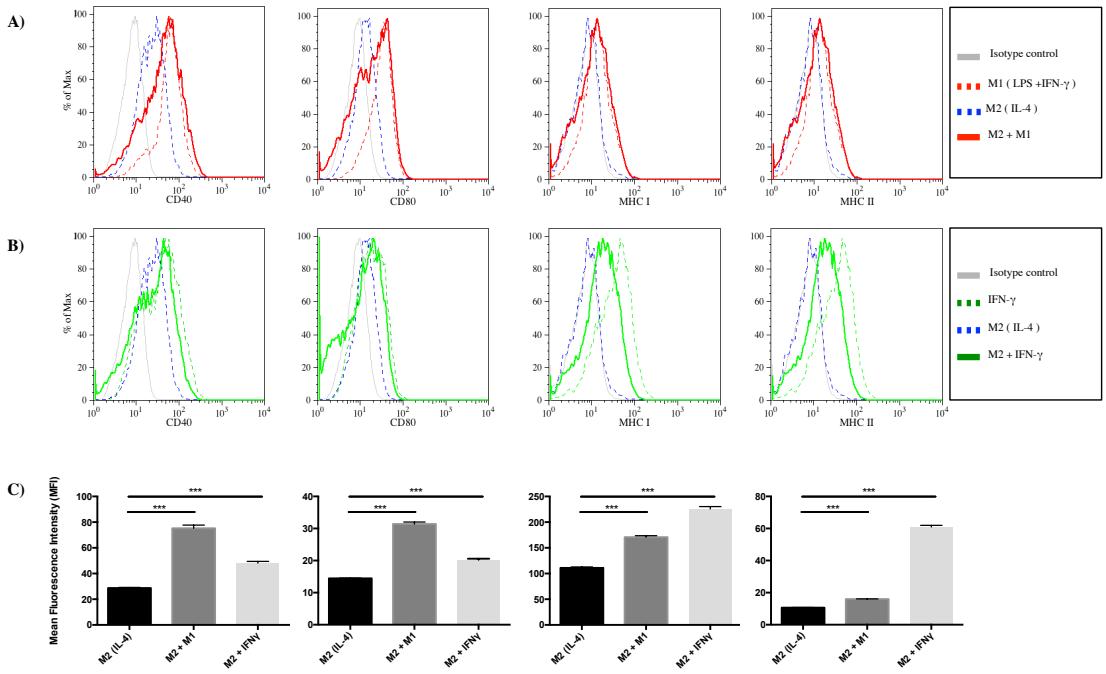


Figure 4.12 ***In vitro*** **re-education of M2-polarised macrophages**

THP-1 monocytes were seeded in 48 well plates at a density 2 x 10^5 cells per well in 0.5 mL of RPMI (10% FBS) supplemented with 30-ng/mL of PMA for 24 hours. Media was exchanged for M1 media (LPS 1 ng/mL) and hIFN-γ (10 ng/mL), hIFN-γ alone media (10 ng/mL) or with M2 media (IL-4, 10 ng/mL) for 24 hours. After 24 hours media was supplemented with new M1, M2 or hIFN-γ respectively (to the same final concentration of cytokine as with the initial stimulation) for an additional 24 hours,. In parallel, M2-treated cells were supplemented with M1 or hIFN-γ. Cells were harvested using non-enzymatic dissociation buffer, stained for CD40, CD80, MHC I and MHC II then analysed using a BD FACS Calibur™ . **A)** Flow cytometry histogram traces show the addition of M1 into M2 after 24 hours "M2 + M1" compared to M1- or M2- alone **B)** Histogram traces show the addition of hIFN-γ into M2 media after 24 hours "M2 + IFN-γ" compared to M1- or M2- alone **C)** This panel shows mean fluorescence intensities from the corresponding samples in **A)** and **B)**. Results represent n=3, with errors bars indicating SD. Statistical analysis of significance was performed by one-way ANOVA, with a Bonferroni post-test. P<0.001 (***)

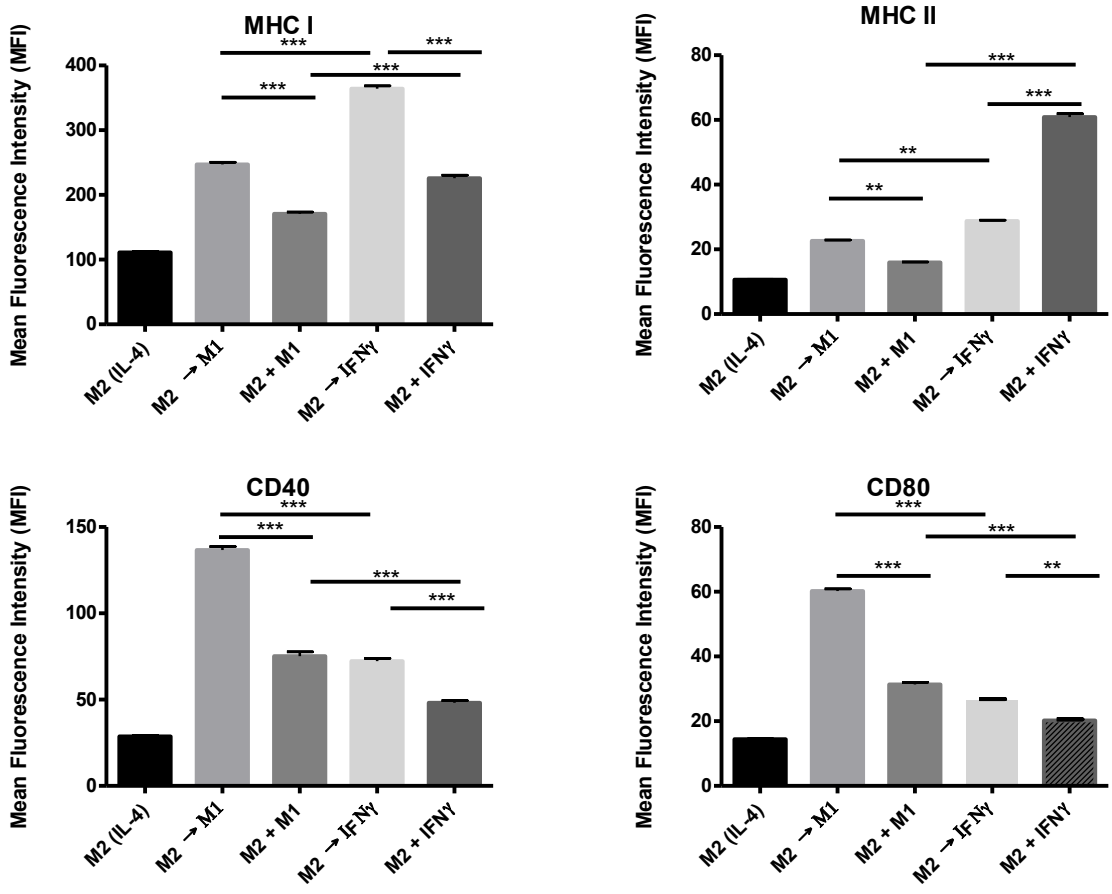


Figure 4.13 Comparison of "re-education" in the presence or absence of M2 media

This figure shows a comparison of the mean fluorescence intensities from re-educated macrophages corresponding to Figures 4.10 and 4.12. Columns show the change from M2 to M1 media after 24 hours "M2 ➔ M1", the change from M2 to hIFN-γ media after 24 hours "M2 ➔ IFN-γ", the addition of M1 into M2 after 24 hours "M2 + M1" and the addition of hIFN-γ into M2 media after 24 hours "M2 + IFN-γ" compared to M1- or M2- alone. Results represent n=3, with errors bars indicating SD. Statistical analysis of significance was performed by one-way ANOVA, with a Bonferroni post-test. P<0.01 (**), P<0.001 (***)

4.2.2.5 Re-education of M2 polarised THP-1 macrophages; cytokine analysis

M1 and M2 macrophages can be characterised by TNF-α^{high}, IL12^{high}, IL-10^{low} and TNF-α ^{low}, IL12 ^{low}, IL-10^{high} profiles respectively. To assess whether receptor data from the re-education experiments correlates with a more global change in polarisation state of the macrophages, supernatants were harvested and analysed by ELISA for TNF-α profiles (*Figure 4.14*). For both M1 medium and hIFN-γ alone, re-polarisation showed increased TNF-α production relative to the M2 macrophages although significance was only observed for M1 re-educated macrophages. Such findings strengthen the polarisation data achieved by receptor analysis and provide a level of functional information suggestive of a behavioural change in the macrophages undergoing re-education

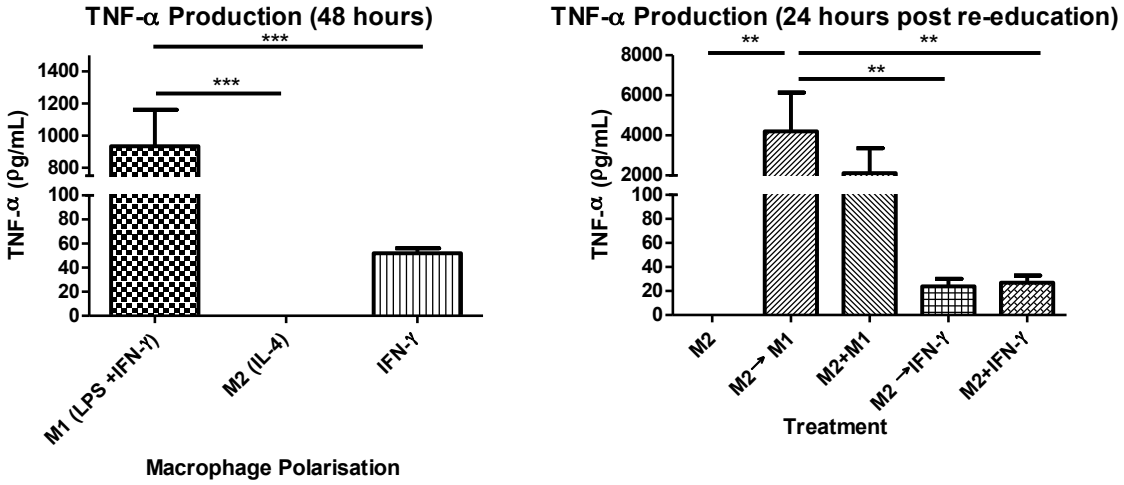


Figure 4.14 Comparison of TNF-α expression in "re-educated" macrophages

TNF-α levels in the supernatants of M1, M2 or hIFN-γ polarised macrophages for 48h were assessed by ELISA (left panel). Columns show the change from M2 to M1 media after 24 hours "M2 ➔ M1", the change from M2 to hIFN-γ media after 24 hours "M2 ➔ IFN-γ", the addition of M1 into M2 after 24 hours "M2 + M1" and the addition of hIFN-γ into M2 media after 24 hours "M2 + IFN-γ" compared to M1- or M2- alone (right panel). Results represent n=3, with errors bars indicating SD. Statistical analysis of significance was performed by one-way ANOVA, with a Bonferroni post-test. P<0.01 (**), P<0.001 (***)

4.2.3 Polarising THP-1 macrophages using tumour cell lines

Combinations of IL-4, IL-13 and IL-10 have largely defined alternative polarisation of macrophages. However, in the context of solid tumours the prevalence of such cytokines is questionable, raising questions as to the validity of assuming a TAM-type profile for M2-type polarised macrophages (Martinez and Gordon, 2014). In an attempt to reconstitute the plethora of soluble tumour-derived factors, experiments were performed using the supernatants of tumour cell lines as a source of relevant cytokines for macrophage polarisation.

4.2.3.1 Supernatants from tumour cell lines polarise macrophages toward an M2-type profile

For these experiments, supernatants from three different tumour cell lines were used. As a large amount of this thesis has been focused on advanced ovarian cancer, two ovarian cancer cell lines were chosen as they have been described in clinical models of peritoneal metastasis. The colorectal cell line SW480 was chosen because of its compatibility with future functional studies of antigen presentation (*See Chapter 5*). Such tumour cell line supernatants were used as culture medium for THP-1 macrophages, polarising macrophages for 48 hours before receptor analysis (*Figure 4.15*)

Studying these results indicate that the receptor profiles appear quite similar between M2 and tumour cell line polarised macrophages. In the case of CD80 and MHC II, expression of receptor by MFI suggests that both M2 media and tumour supernatants induce a near-identical expression profile, whilst CD64 expression is slightly more

down-regulated with tumour supernatant co-culture, relative to M2 biasing media alone. The lower expression of CD64 in tumour supernatant cultured macrophages relative to M2 counterparts might be suggestive of other immune-suppressive cytokines or factors present within the tumour supernatants.

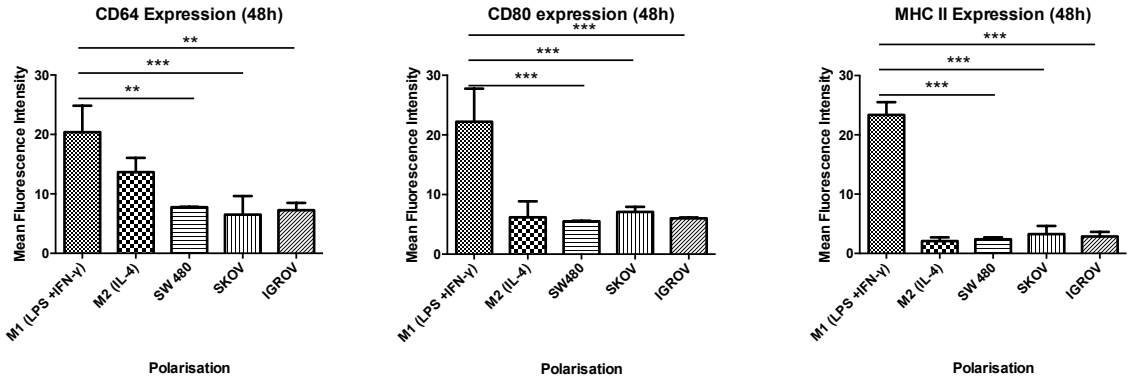


Figure 4.15 Polarisation of human macrophages by supernatants

THP-1 monocytes were seeded in 48 well plates at a density 2 x 10^5 cells per well 0.5 mL of RPMI (10% FBS) supplemented with 30ng/mL of PMA for 24 hours to generate THP-1 macrophages. Three tumour cell lines (SW480, SKOV and IGROV) were seeded into T175 flasks with 50% confluency and allowed to grow for 48 hours (to approximately 90% confluency). Supernatants from these flasks were harvested and spun down to remove any cells in suspension. THP-1 macrophages were incubated with M1 media (LPS 1 ng/mL) and hIFN-γ (10 ng/mL), M2 media (IL-4, 10 ng/mL) or tumour cell line supernatants for 48 hours. Cells were harvested and stained for CD64, CD80 and MHC II, with mean fluorescence intensities obtained by flow cytometry. Results represent n=3, with errors bars indicating SD. Statistical analysis of significance was performed by one-way ANOVA, with a Tukey post-test. P<0.01 (**), P<0.001 (***)

4.2.3.2 Re-education of macrophages polarised by tumour cell line supernatants

Having demonstrated that a similar profile to M2-polarised macrophages is observed for macrophages treated with tumour supernatants, I examined whether these macrophages are amenable to "re-education" in a comparable manner to that observed previously (*Figure 4.16*). THP-1 macrophages were therefore cultured with tumour cell supernatants for 24 hours before having media replaced with either M1 or IFN-γ containing media for an additional 24 hours. In all treatment groups studied, the results show that the receptors of 're-educated' macrophages all shift towards a more M1-type phenotype (*Figure 4.17*). Treatment with M1 and IFN-γ alone yield higher expression of CD80 relative to the non-treated control with no significant differences in CD80 expression between these two treatments. In contrast, IFN-γ alone yields higher expression of MHC II than observed for the M1 treatments. Similarly for CD64 expression, IFN-γ alone increases CD64 levels to higher than that observed for M1 treatments. These results support the hypothesis that polarisation of tumour-associated macrophages may be dynamic and reversible.

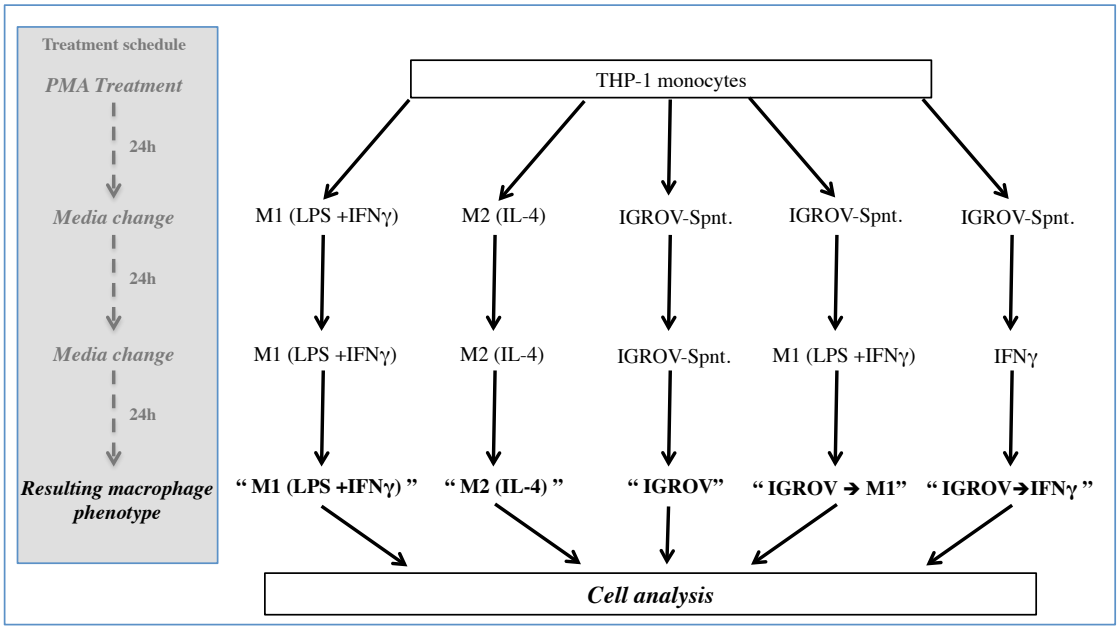


Figure 4.16 Schematic for re-education of tumour supernatant polarised macrophages

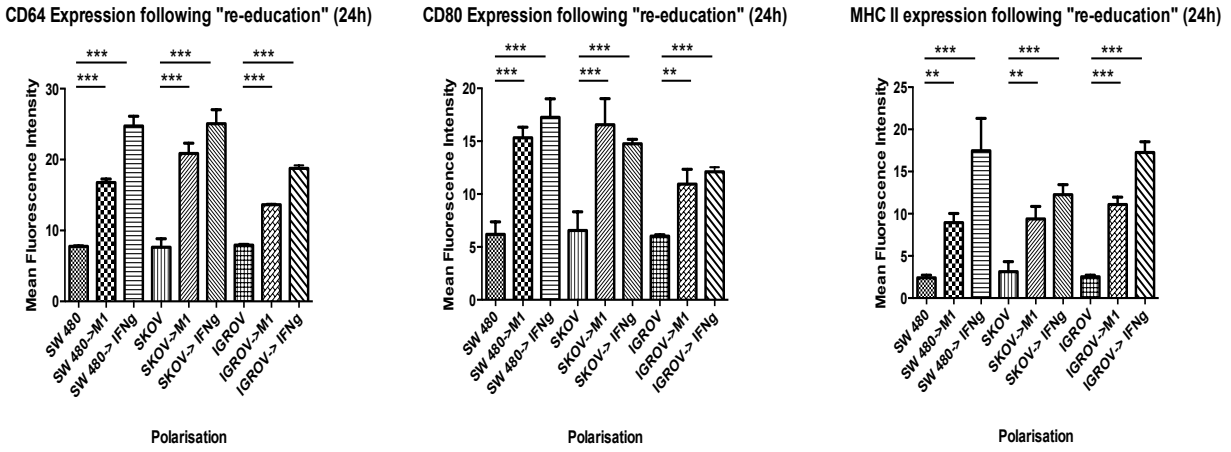


Figure 4.17 Re-education of tumour supernatant polarised macrophages

THP-1 macrophages were polarised for 24 hours with either M1-, M2- or tumour-supernatant media. After 24 hours, media was removed, washed 2x PBS, and media was replaced for respective conditions. In parallel, macrophages treated with tumour supernatants for 24 hours, had their media changed for M1 (LPS 1 ng/mL) and hIFN-γ (10 ng/mL) or hIFN-γ alone (10 ng/mL) media, and were cultured for an additional 24 hours. THP-1 macrophages polarised by three tumour cell line supernatants for 24 hours before "re-education" with M1- or IFN-γ media for an additional 24 hours. Cells were harvested and stained for CD64, CD80 and MHC II, with mean fluorescence intensities obtained by flow cytometry. Results represent n=3, with errors bars indicating SD. Statistical analysis of significance was performed by one-way ANOVA, with a Tukey post-test. P<0.01 (**), P<0.001 (***)

4.2.3.3 Re-education of macrophages polarised by from tumour cell line supernatants; cytokine analysis

Further, evidence that IFN-γ alone is able to revert expression to levels akin to M1 macrophages strengthens the argument for using IFN-γ as an agent for therapeutic re-education of macrophages. Again, to confirm that macrophage re-polarising is occurring at more than just the receptor level, supernatants from these re-education experiments were probed for levels of TNF-α, IL-12 and IL-10 (*Figure 4.18)*

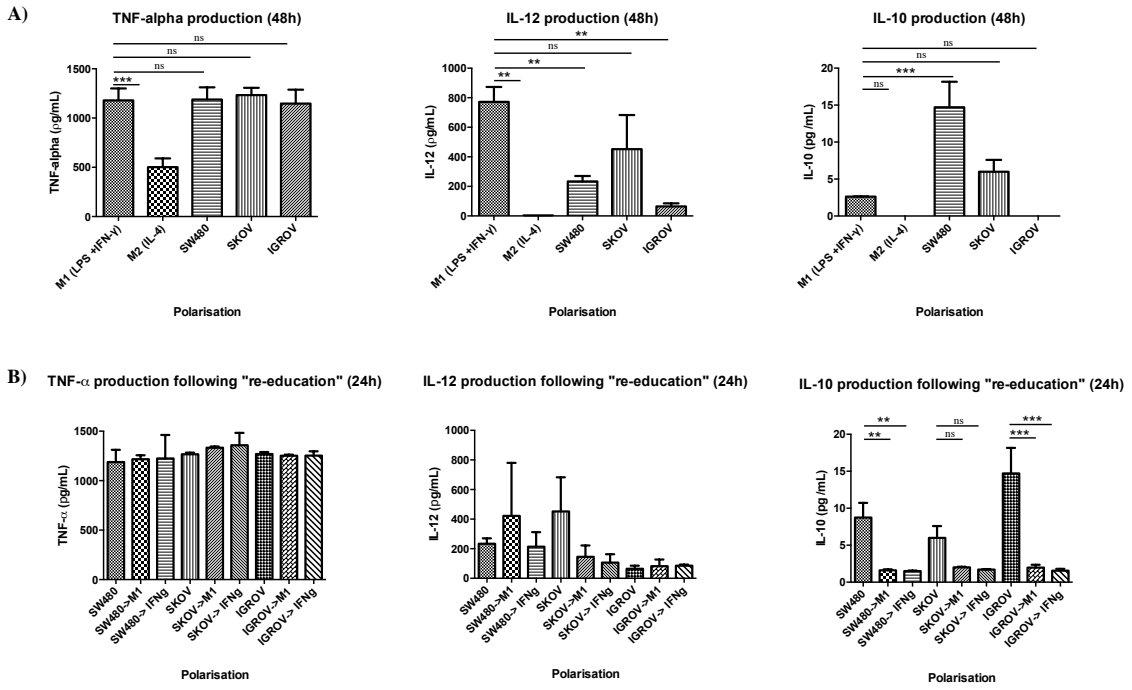


Figure 4.18 Re-education of tumour supernatant polarised macrophages; TNF-α readout

THP-1 macrophages were polarized using tumour cell line supernatants for 48 hours, or after 24 hours were "re-educated" with M1- or hIFN-γ media for an additional 24 hours as per the schematic (***Figure 4.16***). Supernatants were harvested from these samples and cytokine levels of TNF-α, IL-12 and IL-10 were probed for using an ELISA for the tumour-supernatant polarised (**A**) and subsequently "re-educated" (**B**) macrophages. To account for existing cytokine levels within the tumour supernatants, background levels of cytokines present within the untreated tumour supernatants were subtracted from the results of the treated groups, such that any change observed in the media represents a change in macrophage secretion of cytokines. Results represent n=3, with errors bars indicating SD. Statistical analysis of significance was performed by one-way ANOVA, with a Tukey post-test. P<0.01 (**), P<0.001 (***) or non-significant (ns)

Measuring cytokines produced by macrophages grown in tumour-conditioned supernatants is challenging, as background levels of some cytokines is high. TNF-α has previously been a strong marker for induction of an M1-type response, however, background levels of TNF-α present in tumour cells' supernatants appear as high found in the supernatants of M1-polarised macrophages. Similarly, IL-12 levels are higher than might be expected in certain tumour cell lines – particularly for SKOV-3 cells that display a level of IL-12 that is not significantly different from M1- treated cells alone (*Figure 4.18*). This complicates the usage of these markers as metrics of re-education, as it may be difficult to see changes in cytokine expression above baseline levels. As expected, the originally high levels of TNF-α and IL12 for the cell line-polarised macrophages prohibited seeing any macrophage-mediated changes in IL-10 proved more helpful as treatments in all cell lines reduced the levels of IL-10, which may be indicative of shift toward a more pro-inflammatory phenotype (*Figure 4.18*).

4.2.4 Developing a co-culture model for more realistic studies of macrophage polarisation and re-education

Having shown that macrophages polarised with tumour cell supernatants are still susceptible to re-education, a tumour/macrophage co-culture system was developed. One advantage of using a co-culture setting is that any additional contact-dependent interactions between macrophages and tumour cells that may contribute to macrophage polarisation can be incorporated. The major driving force behind developing a co-culture model is that it provides the opportunity to infect tumour cells with oncolytic adenovirus, enabling examination of how virus infection might affect macrophage polarisation over time.

4.2.4.1 Co-culture of THP-1 and IGROV-1 generates an M2-like profile

Initial characterisation of co-cultures was performed using the IGROV-1 human ovarian carcinoma cell line. To examine whether co-cultures of tumour cells and macrophages would result in M2-polarised macrophages, THP-1 macrophages and IGROV-1 cells were co-cultured in 2:1. 1:1, and 1:2 ratios of IGROV-1 cells to macrophages for 48 hours with the levels of polarisation assessed by MHC II and CD80 levels (*Figure 4.19*).

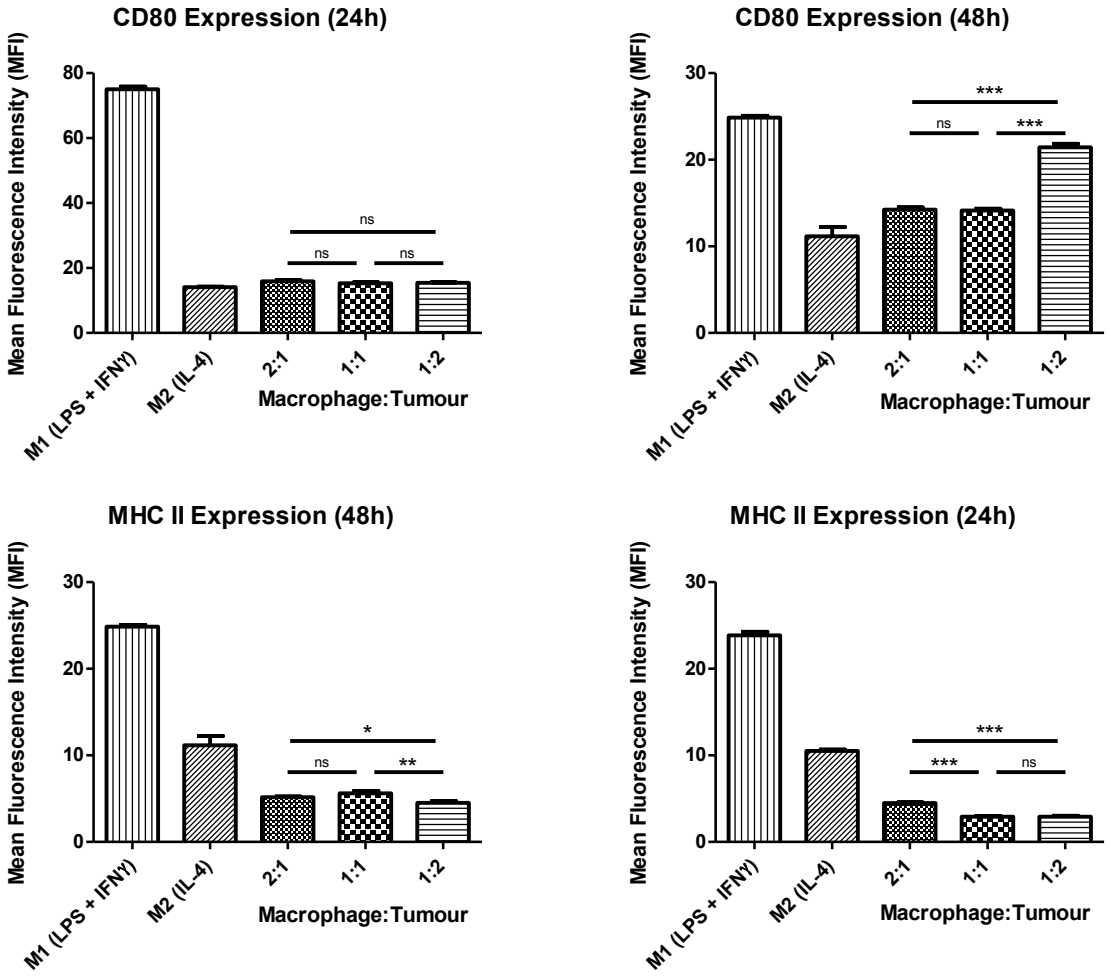


Figure 4.19 Development of a IGROV :macrophage co-culture model

THP-1 macrophages were seeded in 6 well plates at a density 1 x 10^5 cells per well in 0.5 mL of RPMI (10% FBS) supplemented M1 media (LPS 1 ng/mL) and hIFN-γ (10 ng/mL) or M2 media (IL-4, 10 ng/mL) for 24 or 48 hours. In addition, THP-1 macrophages (1 x 10^5 cells) were seeded in co-culture with either 0.5 x 10^5, 1 x 10^5 cells or 2 x 10^5 IGROV-1 cells for 24 or 48 hours to make 2:1, 1:1 or 1:2 ratios of macrophages to tumours. Cells were harvested using non-enzymatic dissociation buffer, stained on the surface for MHC II and CD80 then analysed using a BD FACS Calibur™ to determine the mean fluorescence intensity. Cells were additionally stained for EpCAM as a tumour marker, to enable exclusion of cancer cells from the analysis. Results represent n=3, with errors bars indicating SD. Statistical analysis of significance was performed by one-way ANOVA, with a Tukey post-test. $P<0.05$ (*), $P<0.01$ (**), $P<0.001$ (***) or non-significant (ns)

These results demonstrate that macrophages co-cultured in this way exhibit a phenotype close to the M2- or IGROV supernatant-polarised macrophages. Independent of time cultured, or ratio of macrophage: tumour cells, all co-cultured macrophages show significantly reduced levels of MHC II and CD80.

Having demonstrated that IGROV-THP co-culture can generate M2-polarised macrophages, this experiment was extended to use as a model for re-education. The 1:1 ratio of IGROV-1 and THP macrophages was used as it was found to be significantly suppressed relative to M1- controls. IGROV-1 and THP-macrophages were co-cultured for 24 hours, prior to any treatment for re-education by oncolytic viruses. As illustrated in *Figure 4.20*, hIFN-γ (10 ng/mL), ColoAd1 (100VPC) or ColoAd1-hIFN-γ (100VPC) was added into the co-cultures to examine their ability to re-educate these macrophages. CD80 expression was largely un-altered by treatment with ColoAd1 or ColoAd1-hIFN-γ, although this might reflect a lack of significant tumour cell lysis after 3 days of infection. Similarly, hIFN-γ had no significant effect on CD80 expression. Conversely, hIFN-γ induced significant changes to the MHC II levels throughout the experiment indicating that it can overcome the inherent suppressive media. ColoAd1 induced small increases in MHC II levels however this was not significant. In contrast, ColoAd1-hIFN-γ significantly increased MHC II expression at both 24 and 72 hours, suggesting that the hIFN-γ production was mediating the increases in MHC II levels.

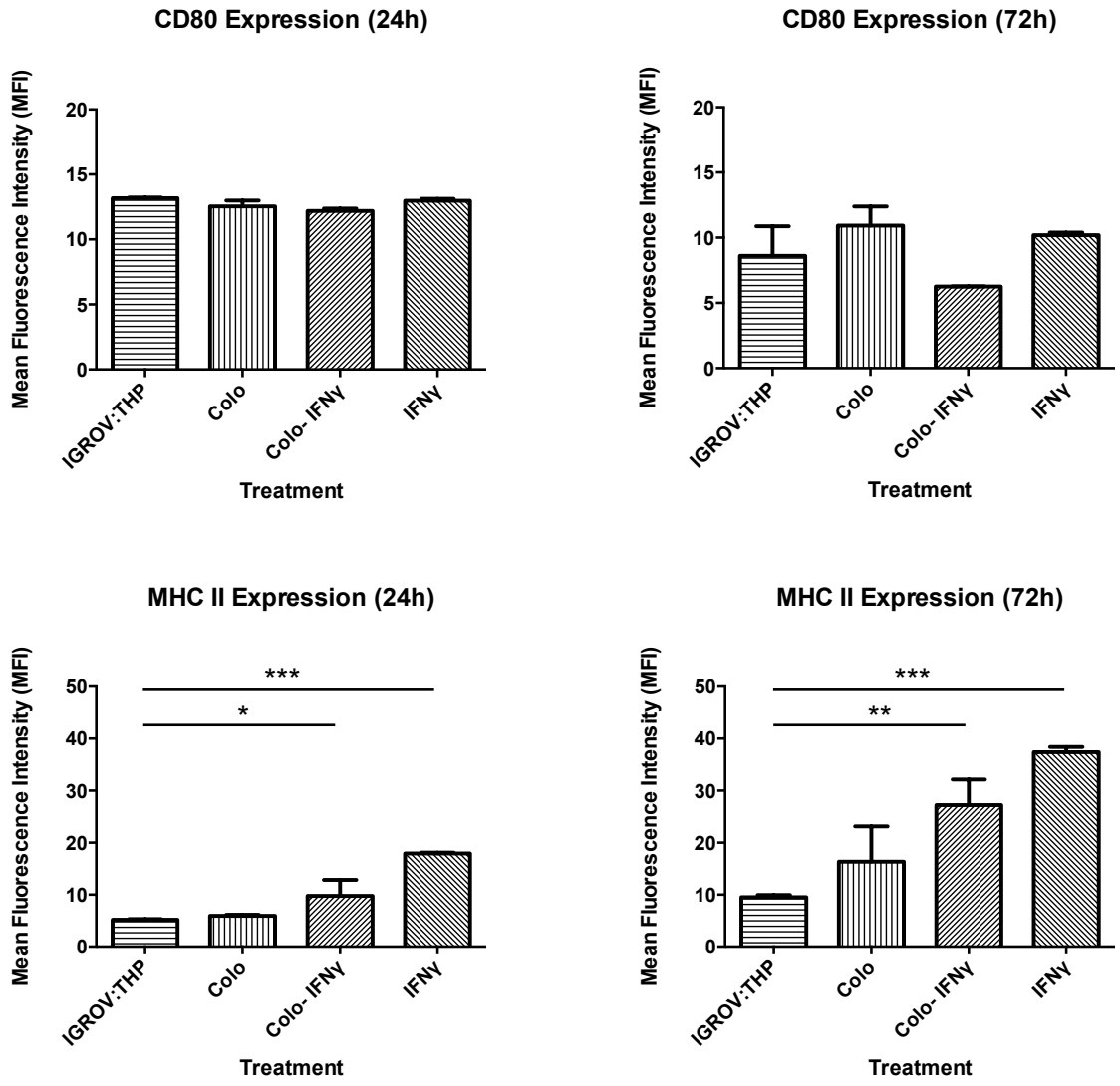


Figure 4.20 Re-polarising THP-macrophages in co-culture with tumour cells using ColoAd1 , ColoAd1-hIFNγ or hIFNγ

THP-1 macrophages (1 x 10^5 cells) were seeded in co-culture with 1 x 10^5 cells IGROV-1 to make 1:1 ratios of macrophages to tumour cells. After 24 hours, 10 μL of media ("IGROV:THP"), ColoAd1 virus (100 virus particles per cell, "Colo"), ColoAd1- hIFN-γ virus (100 virus particles per cell, "Colo-IFN-γ") or hIFN-γ (10 ng/mL, "IFN-γ") was added to the co-culture. Cells were harvested at 24 hour and 72 hour time point post treatment using non-enzymatic dissociation buffer, stained on the surface for CD80 (upper panels) and MHC II (lower panels) then analysed using a BD FACS Calibur™ to determine the mean fluorescence intensity. Cells were additionally stained for EpCAM as a tumour marker, to enable exclusion of cancer cells from the analysis. Results represent n=3, with errors bars indicating SD. Statistical analysis of significance was performed by one-way ANOVA, with a Tukey post-test. $P<0.05$ (*), $P<0.01$ (**), $P<0.001$ (***)

4.2.4.2 Co-culture of THP-1 and SW 480 generates an M2-like profile

The same co-culture and re-education experiments were performed using the SW480 colorectal adenocarcinoma cell line. The choice of this cell line in particular is due its p53 status, which will be discussed and utilised in detail in chapter 5 for antigen presentation assays. Under co-culture conditions with THP-1 macrophages, SW480 cells were able to induce a similar profile of receptor on the macrophages as was observed in IGROV-1 co-culture; CD80 and MHC II expression was significantly down-regulated relative to both M1 and IFN-γ macrophages (*Figure 4.21)*. Having established that the same pattern of macrophage suppression was established as in the IGROV-1 co-cultures, the SW480 co-cultures were treated with IFN-γ (10 ng/mL), ColoAd1 (100VPC) or ColoAd1-hIFN-γ (100VPC) (*Figure 4.22)*.

CD80 expression at 24 hours was increased significantly for all treatment groups, with no significant differences observed between the ColoAd1-hIFN-γ and hIFN-γ groups. By 72 hours, the increases observed in CD80 expression was diminished in all treatments groups with the exception for the ColoAd1-hIFN-γ treated group which maintained a significant elevation of CD80. The pattern of MHC II expression following treatment was very similar to that observed with the IGROV co-culture, with both ColoAd1-IFN-γ and IFN-γ inducing significant increase in MHC II after 72 hours. In contrast to the IGROV co-culture model, only IFN-γ treatment was able to induce significant elevation of MHC II after 24 hours.

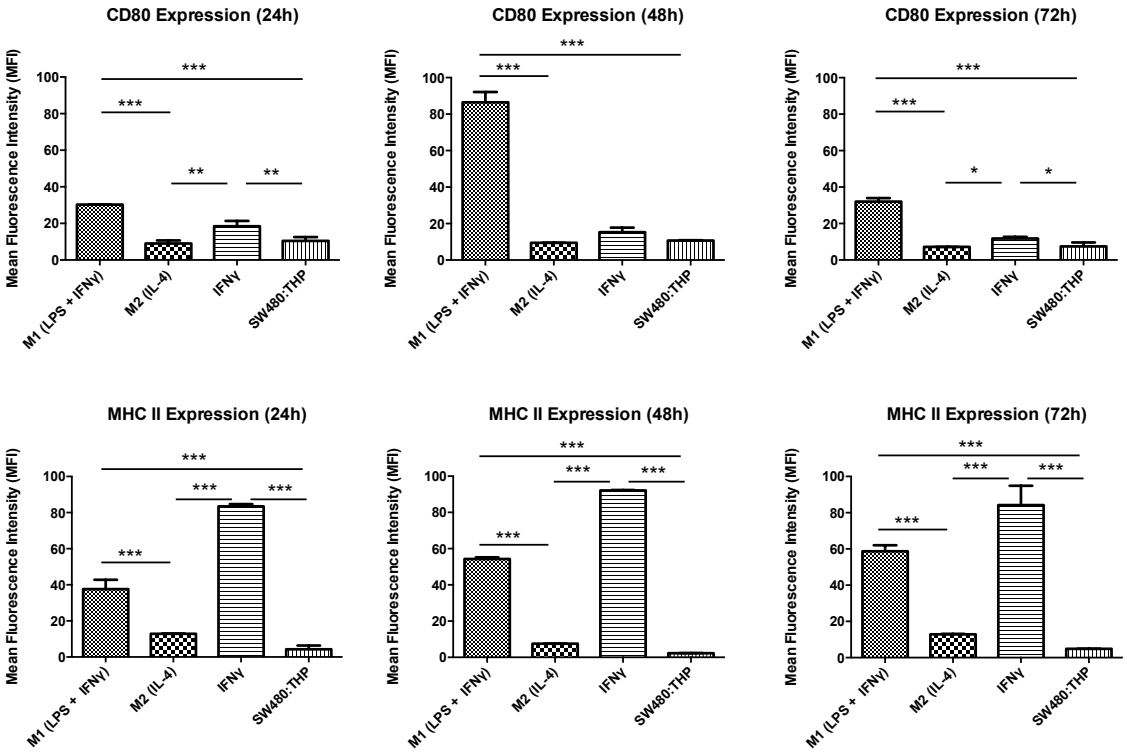


Figure 4.21 Co-culture of SW80 and THP-1 polarises toward an M2 type macrophage

THP-1 macrophages were seeded in 6 well plates at a density 1 x 10^5 cells per well in 0.5 mL of RPMI (10% FBS) supplemented M1 media (LPS 1 ng/mL) and hIFN-γ (10 ng/mL), hIFN-γ alone (10 ng/mL) or M2 media (IL-4, 10 ng/mL). In addition, THP-1 macrophages (1 x 10^5 cells) were seeded in co-culture with 1 x 10^5 cells SW480 to make 1:1 ratios of macrophages to tumour cells. After 24 hours, 10 µL of media ("Non-treated"), ColoAd1 virus (100 virus particles per cell, "Colo"), ColoAd1-hIFN-γ virus (100 virus particles per cell, "Colo- IFN-γ") or hIFN-γ (10 ng/mL, "IFN-γ") was added to the co-culture. Cells were harvested at 24 hour and 72 hour time point post treatment using non-enzymatic dissociation buffer, stained on the surface for CD80 (upper panels) and MHC II (lower panels) then analysed using a BD FACS Calibur™ to determine the mean fluorescence intensity. Cells were additionally stained for EpCAM as a tumour marker, to enable exclusion of cancer cells from the analysis. Results represent n=3, with errors bars indicating SD. Statistical analysis of significance was performed by one-way ANOVA, with a Tukey post-test. P<0.05 (*), P<0.01 (**), P<0.001 (***)

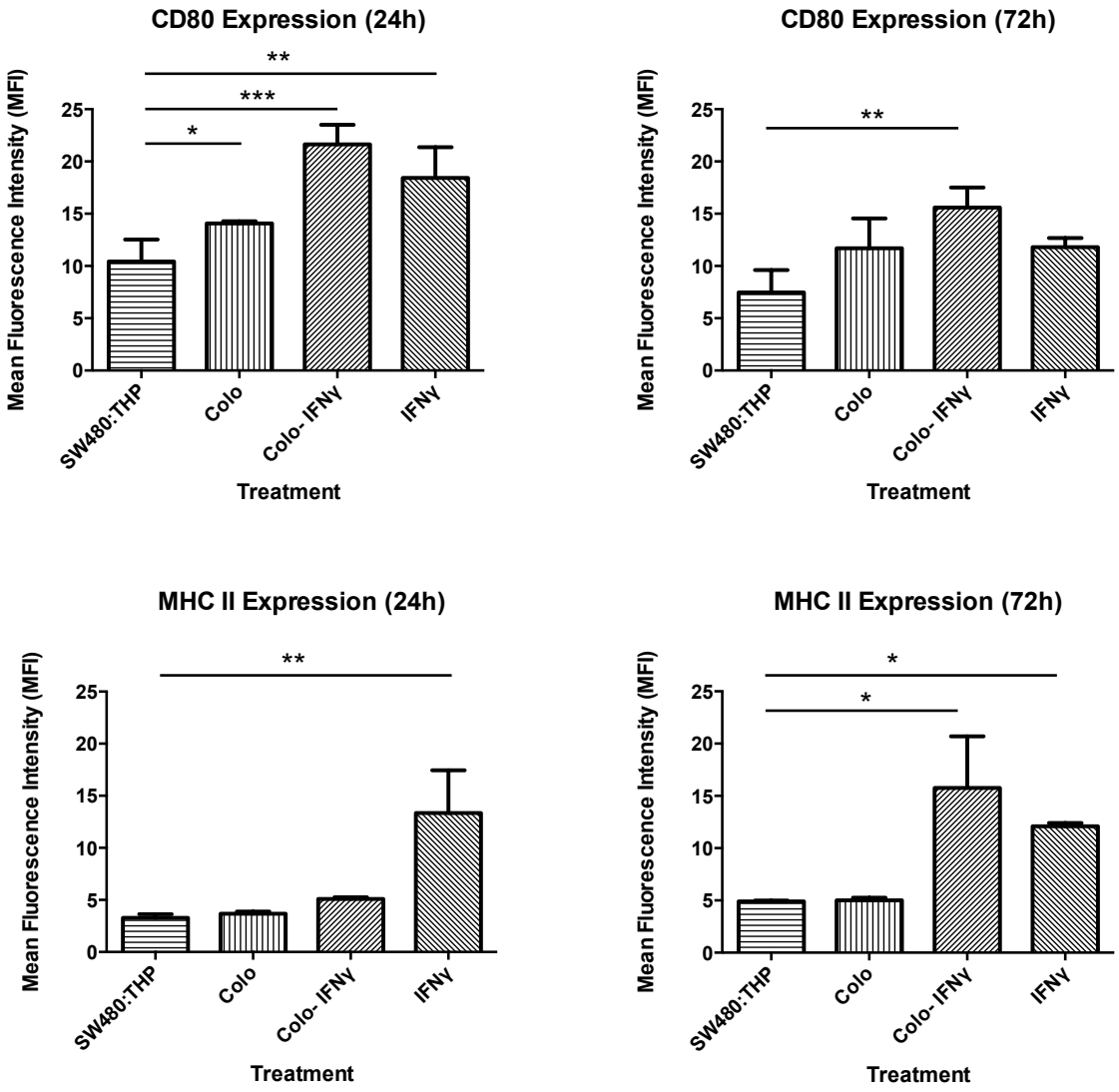


Figure 4.22 Re-polarising THP-macrophages in co-culture with SW480 cells using ColoAd1 , ColoAd1-hIFNγ or hIFNγ

THP-1 macrophages (1 x 10^5 cells) were seeded in co-culture with 1 x 10^5 cells SW480 to make 1:1 ratios of macrophages to tumour cells. After 24 hours, 10 μL of media ("SW480:THP"), ColoAd1 virus (100 virus particles per cell, "Colo"), ColoAd1-hIFN-γ virus (100 virus particles per cell, "Colo- IFN-γ") or hIFN-γ (10 ng/mL, "IFN-γ") was added to the co-culture. Cells were harvested at 24 hour and 72 hour time point post treatment using non-enzymatic dissociation buffer, stained on the surface for CD80 (upper panels) and MHC II (lower panels) then analysed using a BD FACS Calibur™ to determine the mean fluorescence intensity. Cells were additionally stained for EpCAM as a tumour marker, to enable exclusion of cancer cells from the analysis. Results represent n=3, with errors bars indicating SD. Statistical analysis of significance was performed by one-way ANOVA, with a Tukey post-test. $P<0.05$ (*), $P<0.01$ (**), $P<0.001$ (***)

4.3 Discussion of results

Plasticity is a central facet of macrophages and one that could be exploited therapeutically. The malleable nature of these cells is reflected in their marker expression: Rarely do macrophage receptors exhibit a binary on/off profile; they are distinguished instead by differential levels of expression. Whilst biologically such features most likely account for the diversity of macrophage function, experimentally, this can complicate definitive identification of different macrophage subsets. As such, it was a priority to identify a selection of markers that might be able to tease apart different subsets of macrophages, providing a framework under which therapeutic re-education of macrophages could be assessed.

The choice of optimal markers was based on those that had the greatest difference in expression – either by total expression or intensity of expression- between the classical M1 and M2 states. Overall, the biggest differences could be observed by studying the mean fluorescence intensity for each of the receptors rather than percentage positivity of the cells. This is intuitive given that many markers show positivity of expression of macrophages but it is their intensity that is most relevant for function. Consequently the majority of studies reported here focused on the MHC I and II receptors in combination with CD40, CD80 or CD64. When studying cytokine levels in this chapter, experimentation has largely focused on changes in TNF-α, IL-12 and IL-10. The choice of these markers is largely informed by the literature, where a IL-12^{high}/TNF-α^{high}/IL-10^{low} phenotype describes an M1 macrophage (Solinas et al., 2009). Further, early studies I performed in the lab studied changes in cytokine production from tumour-associated macrophages isolated from patients with colorectal cancer. Using qPCR, I found that

changes in these three cytokines were most prevalent and dynamic. As such, studying the change in cytokines during macrophage re-education is largely centered on varying levels of TNF-α, IL-12 and IL-10 in this thesis.

Re-polarising macrophages that have been suppressed by the tumour microenvironment represents an attractive therapeutic strategy. An advantage of this approach is that unlike other TAM-centric therapeutic strategies, re-education utilises existing cells present within the tumour microenvironment. A number of publications have demonstrated that resident macrophages within the tumour have the capacity to be tumouricidal and induce anti-tumour immune responses, supporting the argument that existing- not just newly recruited -macrophages can be tumouricidal (Josephs et al., 2015).

The concept of TAM re-education as is a novel idea, which has only tentatively been explored by other research groups. Indeed, many reports of "re-education", refer to the inhibition of the formation of suppressive-type, tumour-associated macrophages as opposed to a reversal in phenotype of a tumour-polarised macrophage. There are few examples of macrophages that have been actively suppressed, prior to a re-polarising event. One successful example includes a mouse model of breast cancer which showed that TAMs exhibited increased STAT-3 levels along with a cytokine expression profile of IL-12^{low}, IL-10^{high} and TGF-β^{high} that could be reversed upon treatment with an analogue of curcumin, hydrazinocurcumin (Zhang et al., 2013). In contrast to other examples of macrophage polarisations which have only sought to inhibit the generation of tumour-associated macrophages (Hagemann et al., 2008; Watkins et al., 2007), this

chapter attempted to specifically address the question of re-polarising (to M1-like) those macrophages that have previously been polarized (to M2-like).

The importance of studying stimulation in pre-suppressed macrophages is that this might provide the most stringent and realistic test of macrophage re-polarisation within a tumour environment. Additionally, there is the possibility that macrophages that are made inflammatory after being initially suppressed may exhibit higher levels of activation than those made inflammatory without prior suppression. It has been previously reported that co-treatment of macrophages with LPS and IL-4 reduces levels of pro-inflammatory cytokine production such as TNF-α and IL-6, whilst pre-treatment with IL-4 followed by LPS stimulation increased TNF-α and IL-6 secretion to levels above that of macrophages treated with LPS alone (Stout et al., 2009).

Initial re-education experiments focused on evaluating pre-polarising macrophages toward an M2-phenotype, then assessing their ability to be re-polarised toward a more M1-like state. Studying receptors, CD40, CD80, MHC I and MHC II were all significantly up-regulated above the M2 alone cells, indicating a change in phenotype of the cells both for cells treated with M1 media or hIFN-γ alone. Most importantly, this was achieved both when media was changed completely from M2 and also when M2 media was simply supplemented with M1 or hIFN-γ (*Figure 4.10* and *Figure 4.12*). Re-polarising cells with M1 media consistently induced higher levels of CD40 and CD80 than hIFN-γ alone, potentially suggesting a requirement for TLR signalling to induce maximal expression (*Figure 4.13)*. There are suggestions that increased levels of hIFN-γ can compensate for the lack of TLR signalling, as signalling through TLR-4 and CD40 acts to lower the threshold of activation for IFN-γ mediated signalling. It would

therefore be useful to repeat the re-education experiments with increasing doses of hIFN-γ to see whether the levels of CD40 and CD80 expressed can match the levels achieved using M1 media. For MHC I and II however, re-education with hIFN-γ consistently induced significantly higher levels of expression than those achieved with M1 media. Combined, these results indicate that re-education appears to be a plausible hypothesis and that macrophage phenotypes can be modulated sequentially in response to different stimuli, which follows the view of a number of groups (Stout et al., 2005).

Cytokine analysis of the same data corroborated the findings that a change in phenotype was occurring (*Figure 4.14)*. Most intriguing was the finding that TNF-α levels were significantly higher for the macrophages re-educated with M1 media than the cells treated with M1 media alone. Such results suggest that re-polarising macrophages might result in a more inflammatory cell type than naïve macrophages stimulated with M1 conditions. In the context of a tumour this lays credence to the approach of targeting existing TAMs rather than recruiting new ones into the tumour microenvironment.

This work was then extended to look into whether the same effects could be observed in macrophages pre-polarised by more tumour-like conditions. Macrophage polarisation in the tumour is by no means understood. A range of polarising stimuli have been identified, and can be shown *in vitro* to generate subsets of macrophages with defined phenotypes; for example combinations of IL-4 and IL-13 induce programs of tissue repair and Th2 activity, immune complexes and IL-10 or glucocorticoids induce programs of immunoregulation (Mantovani and Sica, 2010). As to defining what specific cytokines or factors are the predominant regulators of suppressor macrophages within tumours is still unresolved. To circumvent this issue, macrophages were

polarised with tumour cell line supernatants, which should in theory, incorporate any factors released by tumours cells.

Repeating re-education experiments using tumour cell line supernatants to polarise the macrophages showed positive results. Expression of CD64, CD80 and MHC II for the tumour-polarised macrophages was consistent with levels experienced for M2 polarised macrophages (*Figure 4.18*). Re-education by M1 media or IFN- γ induced significant up-regulation of all receptors stained, indicating a change in phenotype of the macrophages. Cytokine analysis was complicated by high background levels of TNF-α and IL-12, which although background levels could be subtracted, prevented measuring any significant changes in expression of these cytokines induced by M1 or hIFN-γ (*Figure 4.18*). Background levels of IL-10 were almost undetectable for SW480 and SKOV in the tumour supernatants. Following polarisation, IL-10 levels however showed significant reduction from that of tumour-polarised macrophages when re-educated, using either M1 media or IFN- γ for the re-polarisation. Whilst many of these data were promising, some further experimentation could be performed to demonstrate that it was the presence of tumour cell-specific factors that are driving changes of these macrophages towards an M2/TAM phenotype. Future studies should incorporate media from "normal" (non-cancerous) cell lines to ensure that the effects observed are not related to other factors such as reduced nutrient availability following culturing with other cells previously.

The initial results of the co-culture were very promising, identifying that macrophages in these co-cultures display a phenotype more akin to M2-type cells, with low CD80 and MHC II expression for both IGROV and SW480 co-cultures. Similarly, re-

education profiles –as assessed by MHC II- appeared to suggest that macrophages were amenable to therapeutic re-education by hIFN-γ alone or virus produced hIFN-γ, with significant increases in MHC II observed for these two treatments groups. It was intriguing then that the patterns of re-education were so different for CD80 between the two co-culture models. In the IGROV model, no significant differences were induced in any treatment group or at any time point, whilst in contrast, all treatment groups were able to induce significant changes in receptor expression at 24 hours for the SW480 co-culture. This could be reflected in the different cytokine profile of the tumour cells, with IGROV having previously been shown to produce high quantities of IL-10 and GM-CSF, which may create a more suppressive environment for therapeutics intervention (Hagemann et al., 2006). It would be interesting to expand these studies to include tumour cells with known immunosuppressive properties, or known pro-inflammatory properties, and compare the ability to induce TAM polarisation and their amenability to therapeutic intervention.

Chapter 5

Functional outcomes of macrophages polarisation

5 Functional outcomes of macrophage polarisation

5.1 Introduction

Chapter 3 sought to establish morphological markers to best characterise macrophages of different polarisation states. It was found that macrophages treated for 24h with M1 media showed a receptor expression profile quite distinct from those treated for 24h with M2 media. From here on these will be referred to as M1 and M2 cells, respectively. This chapter seeks to examine whether there are functional consequences of differentially polarised M1 and M2 macrophages and if such functional differences correlate with the markers identified.

First, some of the archetypal functions of macrophages in the body are examined with respect to how they are affected by the polarisation states induced using M1 and M2 media. Although several macrophage properties are examined, particular attention is paid to production of NO and the ability of macrophages to phagocytose different substrates.

Historically, the induction of iNOS leading to the production of NO by tumour-infiltrating macrophages was thought to represent the major tumoricidal effector mechanism of these macrophages, with NO and its peroxynitrite radical derivatives inducing DNA damage and subsequent death in a range of tumour cell lines (Garbán et al., 1999). Accordingly production of NO is taken as a marker of 'M1' polarised, tumouricidal macrophages.

In the context of macrophages within tumours, two emerging areas of interest are how macrophages phagocytose tumour cells and whether macrophages play an important role as presenters of tumour antigens. The former question has been largely stimulated by research studying the role of the phagocytosis-evasion, CD47 (Zhao et al., 2011). It has been shown that the macrophages can be highly effective anti-tumour immune cells as they can ingest tumour cells directly. But in analogy to other prominent tumouricidal immune effectors, tumours have evolved mechanisms to evade such anti-tumour immunity. CD47 has been shown to be a prominent "don't eat me" signal, and its expression has found to be up-regulated in a number of tumour cell types (Theocharides et al., 2012). CD47 interacts with its partner on macrophages, SIRP-1, to induce negative regulation of cellular phagocytosis mechanisms. The level of SIRP-1 expression on different macrophage subsets is not yet clear, but it is intriguing to propose that 'M2' type macrophages (TAMs) may have elevated SIRP-1 levels. Such findings have already prompted the development of a therapeutic antibody targeting CD47, which has been shown to antagonise the anti-phagocytic signalling and significantly enhance phagocytosis of tumour cells by macrophages. This has lead to the initiation of a clinical trial to examine its therapeutic potential. It is feasible that SIRP-1 may provide an equally valid target for intervention, and antagonizing both receptors simultaneously might show at least additive effects.

All macrophage subtypes are associated with a level of phagocytosis, although for M2 macrophages this is generally associated with scavenging and tissue remodeling, whereas for M1 it is usually associated with cytocidal activities (Mantovani et al.,

2012). In characterising the activities of cells polarised with M1 and M2 media, it therefore is useful to compare a range of different substrates for phagocytosis.

Second, whilst the role of macrophages in antigen presentation is incompletely understood – particularly in the context of the presentation of tumour antigens - a seminal paper by Asano et al. demonstrated that macrophages may be crucial in the induction of anti-tumour immune responses (Asano et al., 2011). Those authors showed that macrophages serve as the principal antigen presenting cell to cross-present dead cell antigens. This could be of particular importance in the context of oncolytic virus infection – Macrophages have been shown to be a major infiltrating cell type following successful oncolytic virus infection for a number of viruses, and this has been associated with increased T cell infiltration and induction of anti-tumour immune response (Jakeman et al., 2015a). Given that macrophages cross-present tumour cells killed by conventional methods, it could be proposed that cells killed in the context of virus infection with enhanced danger-associated molecular pattern (DAMP) and pathogen-associated molecular pattern (PAMP) release, might exhibit enhanced cross presentation associated with macrophage activation.

These observations suggest that macrophages have the potential to engulf live or dead tumour cells and cross present their associated tumour antigens to generate effective anti-tumour CD8 T cells. That tumours appear to have selectively evolved mechanisms to try and down-regulate their phagocytosis through CD47, suggests the importance of this feature of macrophages as a potent tumoricidal mechanism. What is unclear however, is how the polarisation states of macrophages may influence all of these cellular properties.

5.1.1 Chapter aims

1. Assess whether macrophages polarised with M1 and M2 media show different functional behaviour
2. Assess whether "re-education" of macrophages is observed in these functional assays, similar to the receptor studies reported in Chapter 4.
3. Examine the phagocytic and cross-presenting abilities of macrophages in a tumour context, and see how these are affected by differential polarisation
4. Examine the phagocytic and cross-presenting capacity of macrophages in the context of oncolytic virus infection.

5.2 Results

Initial experiments set out to confirm that the production of NO can act as a functional marker of M1-polarised macrophages using the experimental systems developed in this thesis. Notably, it was important to determine whether NO could be used as a functional marker in both mouse and human macrophage settings and whether the production of NO is a reversible process when cells are subject to re-education.

5.2.1 Nitric Oxide production

The majority of studies measuring NO production have utilised the Greiss Reagent, which measures nitrite radicals in the supernatants of NO-producing macrophages. DAF-FM di-acetate (4-amino-5-methylamino-2′,7′-difluorofluorescein diacetate) represents a newer, flow cytometry-based methodology that boasts increased sensitivity of detection with the advantage of being able to identify and study the individual NO-producing macrophages during flow analysis. In brief, the di-acetate passively accumulates in cells whereupon interaction with NO forms a highly fluorescent product that is detectable by fluorescence microscopy or flow cytometry.

5.2.1.1 NO is an effective functional marker of macrophage polarisation in human and murine macrophages

Murine macrophages (IC-21) were polarised for 24 hours using M1 and M2 media. DAF-FM-containing media was then added to the macrophages for an hour, and the

resulting NO production was analysed by flow cytometry (*Figure 5.1*). The results show that this methodology is extremely sensitive and has a high dynamic range, with detection of NO visible by fluorescence microscopy and flow cytometry (*Figure 5.1A and B*). After 24 hours, there is clear up-regulation of NO production by the M1 macrophages which is significantly higher than that produced by either non-treated or M2-treated macrophages (*Figure 5.1C*).

The assay was repeated to include polarised THP-1 human macrophages, using the same methodology. The same pattern of NO production was observed for the human macrophages as for the murine cell line, with M1 macrophages exhibiting significantly higher levels of NO production than either non-treated or M2 macrophages (*Figure 5.2*). MFI readings of NO were far higher in the human samples across all polarisation states, with a considerable difference in M1 NO production observed between species. For example, an MFI of 1400 was observed for human M1 macrophages compared to a value of only 150 for murine M1 macrophages. Whilst, the MFI values observed in the human macrophages were higher, the fold change between polarisation states was not as pronounced. Human M1 macrophages experienced a 2-fold increase in the level of NO produced relative to M2 polarised macrophages. In contrast, M1 murine macrophages experienced a 3-fold increase in NO relative to M2 cells. Importantly the pattern of NO production was consistent between human and mouse macrophages, with M1-polarised macrophage clearly distinguishable from non-treated and M2 macrophages by their levels of NO production.

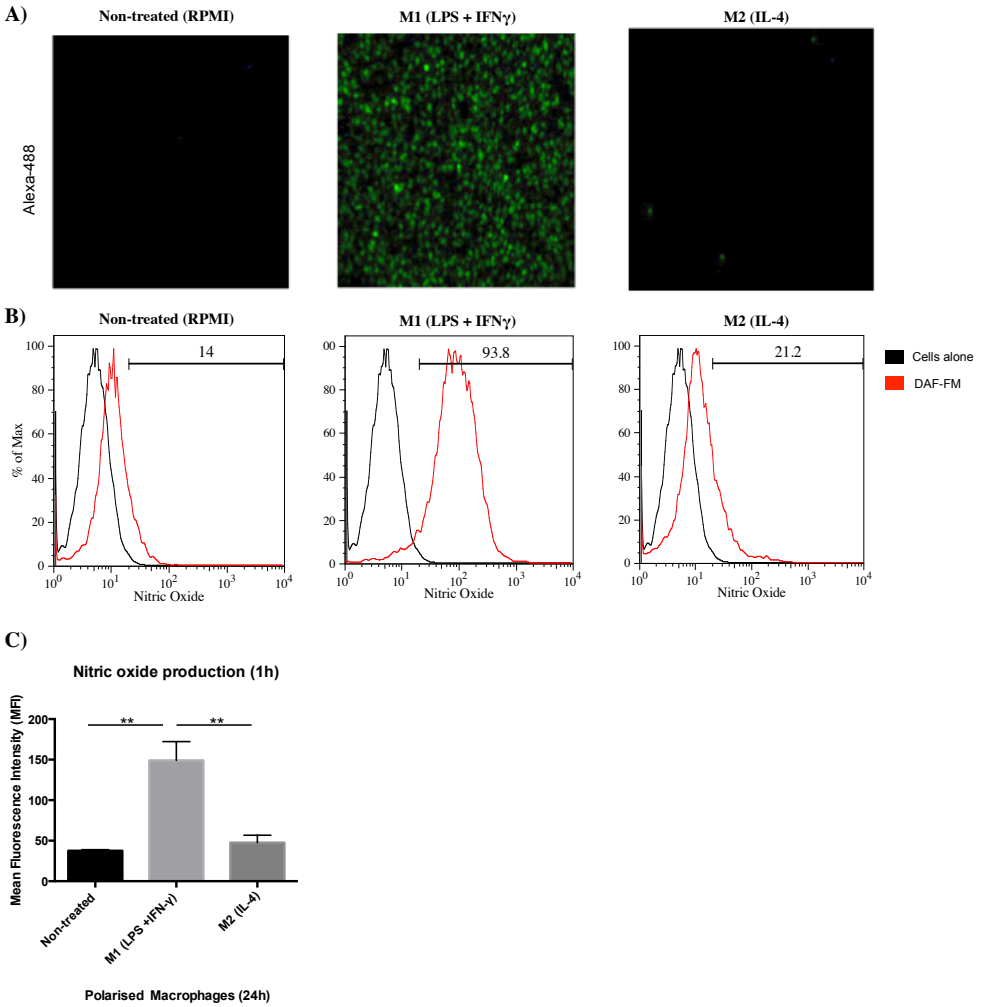


Figure 5.1 NO production by differentially polarised macrophages

IC-21 cells were plated out at 2 x 10^5 cells per well in 12 well plates in 0.5 mL of RPMI (10% FBS) alone, M1 media (LPS 1 ng/mL) and murine IFN-γ (10 ng/mL) or M2 media (IL-4, 10 ng/mL) for 24 hours. NO was measured using DAF-FM Diacetate (Life Technologies™), with cells incubated at 5μM DAF-FM in 0.5 mL of RPMI for 1 hour at 37°C, washed 3 times with PBS, and incubated with 1 mL RPMI for an additional 15 minutes to allow complete de-esterification of intracellular esterases. Cells were harvested using non-enzymatic dissociation buffer analysed for fluorescence using a FACS Calibur™ to determine positivity or mean fluorescence intensity. **A)** Fluorescence microscopy demonstrates high levels of NO, evidenced by green fluorescent macrophages in the M1 polarised cells (central panel). **B)** Flow cytometry histograms represent gated positive cells percentage for NO production. **C)** Extent of NO production is demonstrated by mean fluorescence intensity. Results represent n=3, with errors bars indicating SD. Statistical analysis of significance was performed by one-way ANOVA, with a Tukey post-test. P<0.01 (**)

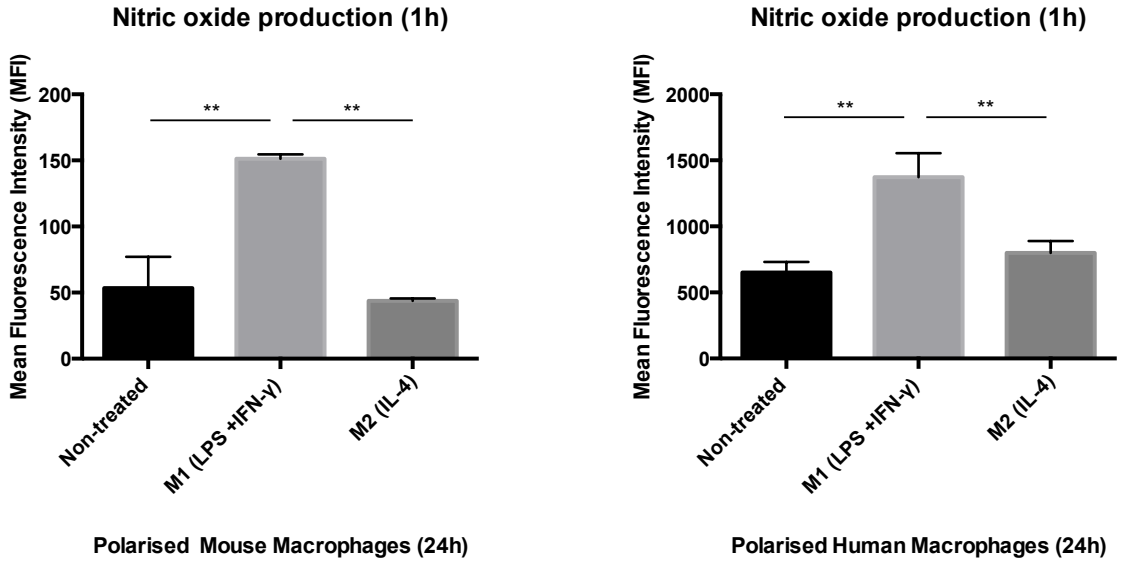


Figure 5.2 NO production by differentially polarised human and mouse macrophages

IC-21 cells (Left panel) or THP-1 macrophages (right panel) were plated out at 2 x 10^5 cells per well in 12 well plates in 0.5 mL of RPMI (10% FBS) alone, M1 media (LPS 1 ng/mL) and murine or human IFN-γ (10 ng/mL) or M2 media (IL-4, 10 ng/mL) for 24 hours. NO was measured using DAF-FM Diacetate (Life Technologies™), with cells incubated at 5μM DAF-FM in 0.5 mL of RPMI for 1 hour at 37°C, washed 3 times with PBS, and incubated with 1 mL RPMI for an additional 15 minutes to allow complete de-esterification of intracellular esterases. Cells were harvested using non-enzymatic dissociation buffer and analysed for fluorescence using a FACS Calibur™ to determine positivity of NO producing macrophages. The extent of NO production is demonstrated by mean fluorescence intensity. Results represent n=3, with errors bars indicating SD. Statistical analysis of significance was performed by one-way ANOVA, with a Tukey post-test. $P<0.01$ (**)

It was shown earlier in this thesis that macrophages can exhibit sequential changes in phenotype, re-educated from M2 toward M1-like polarisation in response to IFN-γ alone or in combination with LPS. Demonstration of re-education has only been shown so far by changes in receptor expression or cytokine secretion. As a more stringent test to assess whether these changes in receptor expression are indicative in a change of behaviour by these macrophages, re-education experiments were performed using NO production as a read-out for change in functionality of the cell.

5.2.1.2 NO can demonstrate re-education of murine macrophages

As per previous re-education experiments, murine cells were first polarised for 24 hours with IL-4. These M2 macrophages were then either treated with M1 media or murine IFN-γ (mIFN-γ), with these cytokines supplemented into the existing M2 media. Alternatively, M2 media was removed and replaced for fresh media containing M1 cytokines or mIFN-γ alone (*Figure 5.3*). Importantly, the final concentrations of cytokines added were equivalent for both methods of re-education. As controls, NO levels were measured in an additional group of macrophages that were polarised for 48 hours with media alone "non-treated", M1 media (LPS + mIFN-γ) or M2 (IL-4) media. For the control macrophages, the pattern of NO production after 24 hours corroborates previous data, with the significant decrease in NO production relative to M1 cells indicating that there is a significant functional change between these cells (*Figure 5.4A*). After 48 hours the levels of NO production observed for M1 cells were considerably decreased, in keeping-with literature reports that NO is well regulated to ensure only transient production of such toxic radicals. Intriguingly, the levels of NO production in M2-treated macrophages increased to levels that were not-significantly different to the M1 cells. Non-treated macrophages displayed similar background levels throughout the 48-hour period.

As previously observed, 24 hours of re-education by switching media from M2 to M1 or IFN-γ alone induced significant increases in NO production relative to M2 media alone, with no significant differences observed between the M1 and IFN-γ alone treatments (*Figure 5.4B, left panel*). After 48 hours incubation, NO levels had also risen with the M2 treatment. Intriguingly, when the M2 media was left *in situ* (after 24 hours), supplementation with M1 or IFN-γ induced a similar pattern as when the M2 media was removed, with both treatments increasing NO production above the levels observed for M2 macrophages (*Figure 5.4B, right panel*).

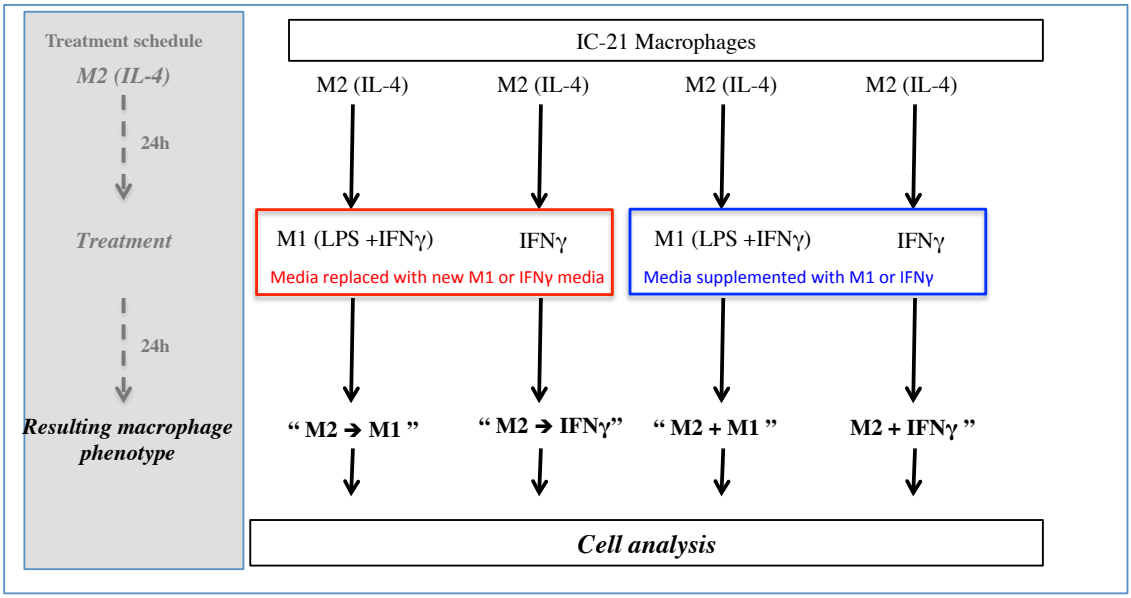


Figure 5.3 Schematic for re-education of M2 polarised murine macrophages using NO as a readout

In short, IC-21 macrophages were polarised for 24 hours with IL-4 to make an M2 phenotype, after which time they were re-educated with either M1 media or IFN-γ alone for a further 24 hours. For re-education, the existing M2 media in which the macrophages had been polarised was either exchanged for fresh M1 media or IFN-γ media (illustrated by the red box) or was supplemented with M1 media or IFN-γ media (illustrated by the blue box), such that the final concentration of M1 and IFN-γ medias are equivalent between treatment groups

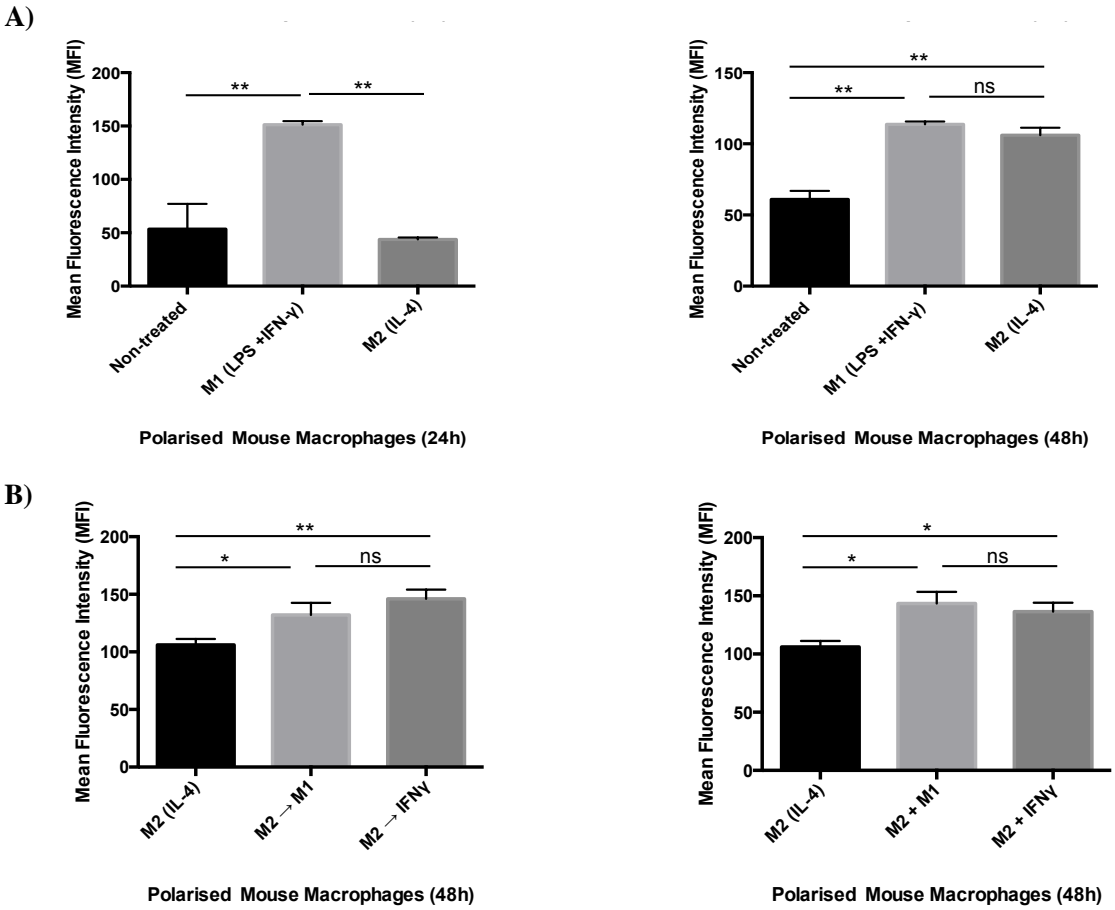


Figure 5.4 NO can demonstrate re-education of M2 polarised murine macrophages

A (left panel) IC-21 cells were plated out at 2 x 10^5 cells per well in 12 well plates in 0.5 mL of RPMI (10% FBS) alone, M1 media (LPS 1 ng/mL) and mIFN-γ (10 ng/mL) or M2 media (IL-4, 10 ng/mL) for 24 hours. **A (right panel)** After 24 hours media was replenished with new M1 or M2 media respectively and incubated for an additional 24 hours. **B (left panel)** M2 macrophages were treated by replacing media for fresh media containing. M1 or IFN-γ cytokines ("M2 ➔M1" or "M2 ➔ IFN-γ", respectively). **B (right panel)** Alternatively, M2 macrophages were treated by the supplementation of M1 or IFN-γ cytokines into the existing M2 media containing ("M2 + M1" or "M2 + IFN-γ", respectively). In both treatment groups, cytokines were added to equivalent final concentrations.NO was measured using DAF-FM Diacetate (Life Technologies™), with cells incubated at 5μM DAF-FM in 0.5 mL of RPMI for 1 hour at 37°C, washed 3 times with PBS, and incubated with 1 mL RPMI for an additional 15 minutes to allow complete de-esterification of intracellular esterases. Cells were harvested using non-enzymatic dissociation buffer analysed for fluorescence using a FACS Calibur™ to determine positivity. Extent of NO production is demonstrated by mean fluorescence intensity. Results represent n=3, with errors bars indicating SD. Statistical analysis of significance was performed by one-way ANOVA, with a Tukey post-test. $P<0.05$ (*), $P<0.01$ (**), $P<0.001$ (***), non-significant (ns)

Such data suggests that "re-education" of macrophages by inflammatory stimuli such as the combination of LPS with mIFN-γ can induce a functional change in behaviour of previously M2-polarised macrophages. Impressively, IFN-γ alone is able to induce the same phenotypic changes as with M1-media, indicating that this cytokine can act alone and does not require TLR stimulation to induce up-regulation of NO. It is interesting to observe that the levels of NO increase for the M2 polarised macrophages from 24- to 48-hours such that there is no significant difference observed between M1 and M2 macrophages at 48-hours. On their own, these data might suggest that NO is of limited utility as functional marker of polarisation. However, the results of the re-education suggest that NO may still act as a good functional marker for re-education, as both M1 and IFN-γ treatments, in both media replacement and supplementation, were able to induce a significant increase in NO production compared to M2 alone.

5.2.1.3 NO can demonstrate re-education of human macrophages

The same re-education experiment was performed using human THP-1 macrophages with the results appearing almost identical to the murine studies, with a few exceptions. For example at 48 hours, there were significant differences in the levels of NO between M1 and M2 macrophages, whereas in the murine studies there were no differences observed between M1 and M2 macrophages at this time. In this human re-education experiment, 24 hour polarisation samples were not recorded as for the murine study but should be included in future experiments for proper comparison between the models. For re-education, the human study showed a similar pattern to the murine system in the samples re-educated by media replacement. In contrast to the murine system however, re-education by supplementation did not show significant changes using human macrophages.

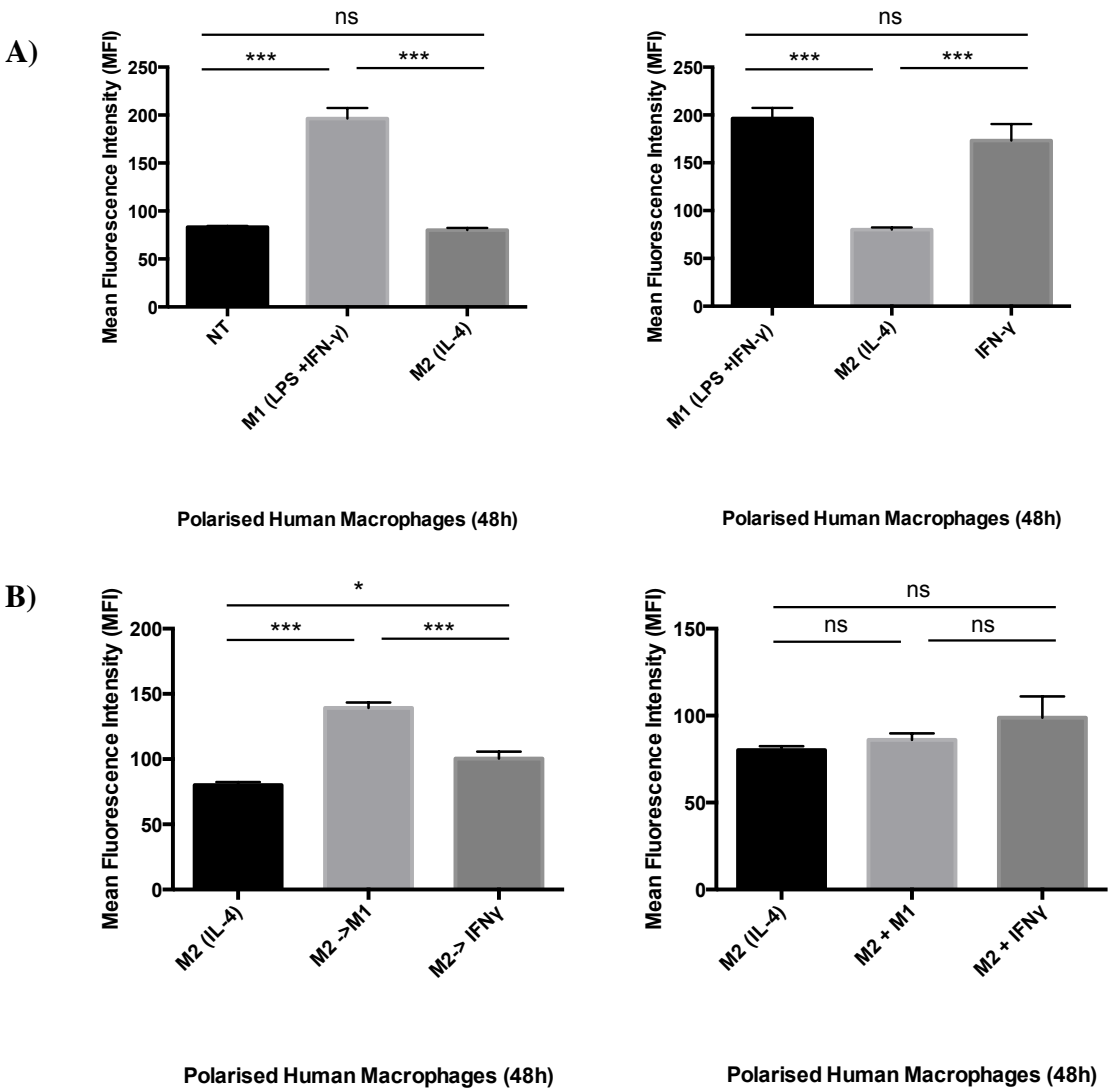


Figure 5.5 NO can demonstrate re-education of human macrophages

A) THP-1 macrophages cells were plated out at 2 x 10^5 cells per well in 12 well plates in 0.5 mL of RPMI (10% FBS) alone, M1 media (LPS 1 ng/mL) and IFN-γ (10 ng/mL), M2 media (IL-4, 10 ng/mL) or IFN-γ (10 ng/mL), alone for 48 hours. After 48 hours incubation, the NO levels were measured **B (left panel)** M2 macrophages were treated by replacing media for fresh media containing. M1 or IFN-γ cytokines ("M2 ➔M1" or "M2 ➔ IFN-γ", respectively). **B (right panel)** Alternatively, M2 macrophages were treated by the supplementation of M1 or IFN-γ cytokines into the existing M2 media containing ("M2 + M1" or "M2 + IFN-γ", respectively). In both treatment groups, cytokines were added to equivalent final concentrations. NO was measured using DAF-FM Diacetate (Life Technologies™). Cells were harvested using non-enzymatic dissociation buffer analysed for fluorescence using a FACS Calibur™ to determine positivity. NO production is demonstrated by mean fluorescence intensity. Results represent n=3, with errors bars indicating SD. Statistical analysis of significance was performed by one-way ANOVA, with Tukey post-test. P<0.05 (*), P<0.01 (**), P<0.001 (***), non-significant (ns)

5.2.1.4 ColoAd1 can stimulate NO production in human macrophages

The overall aim of this thesis is to assess whether it is possible to re-educate macrophages with oncolytic adenovirus expressing IFN-γ, therefore the effect of exposing non-polarised macrophages directly to ColoAd1 particles was assessed by measuring NO production. There are indications in the literature that certain viruses may activate macrophage NO production via ligation of CD46 (Paludan et al., 2000), accordingly human macrophages were incubated with wild-type adenovirus serotype 5 (Ad5, which does not directly stimulate CD46), ColoAd1 and ColoAd1-hIFN-γ (both of which infect cells predominantly via CD46) or with a CD46-agonising antibody. In addition, supernatants from DLD-1 human colorectal carcinoma cells infected with ColoAd1 or ColoAd1-IFN-γ were added to examine the effect of any soluble mediators released during virus infection on NO production by macrophages.

Differential polarisation of human macrophages after 24 hours (*Figure 5.6A*) recapitulated the pattern of NO oxide production observed previously in this chapter, with M1 and IFN-γ macrophages exhibiting significantly higher levels NO production relative to non-treated and M2 macrophages. In parallel, engagement of the CD46 receptor by monoclonal antibody similarly induced significantly higher levels of NO production relative to non-treated and M2 macrophages (*Figure 5.6B*). Compared to M1 macrophages, engagement of CD46 by the antibody appeared to increase the levels of NO produced; however these results were not significant. In a similar pattern to the CD46 antibody, addition of all the free viruses increased NO production relative to non-treated and M2 macrophages. Addition of Ad5 and ColoAd1 virus particles yielded comparable levels of NO production to M1 macrophages, with no significant differences observed between these three groups. Treatment with free ColoAd1-IFNγ

virus stimulated significantly higher NO production than all other groups. These results indicate that these free viruses and the CD46 antibody are all able to stimulate NO production in macrophage (relative to non-treated and M2 macrophages), but with the exception of ColoAd1-IFNγ, none are able to stimulate NO production levels above classical M1 stimulation. In parallel to these experiments, the ability of free virus and supernatants from virus-infected cells to stimulate NO production was compared (*Figure 5.6C*). No significant differences were observed in the abilities of ColoAd1 free virus and ColoAd1 supernatant to induce NO production (relative to non-treated macrophages), despite the levels of ColoAd-1 supernatant appearing lower than free virus. Both ColoAd1-IFNγ free virus and ColoAd1-IFNγ supernatant induced significantly higher NO production than all other treatment groups. Perhaps surprisingly, ColoAd1-IFNγ supernatant experienced significantly lower NO production than the free virus. That ColoAd1-IFNγ virus induced higher NO than ColoAd1 virus, and that both ColoAd1-IFNγ virus and supernatant increased NO production relative to IFNγ alone may suggest that these are concentration-based effects of IFNγ.

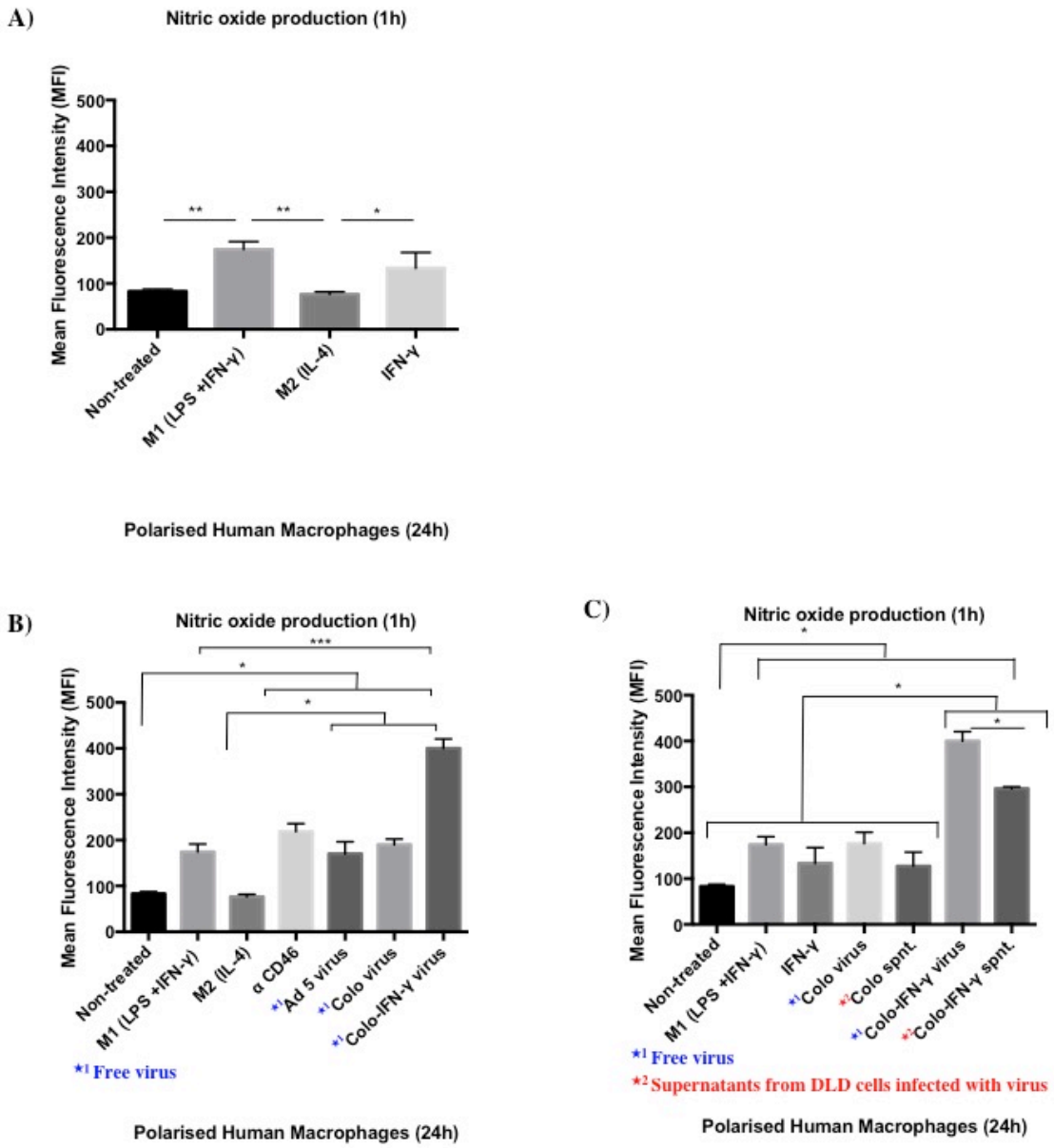


Figure 5.6 ColoAd1 can induce NO production in human macrophages

A) Non-treated (media alone), M1-, M2- or IFN-γ polarised THP-1 macrophages cultured for 24h were assessed for their ability to produce NO. In parallel, un-polarised macrophages were treated with fresh media containing free virus (**denoted by $^{\star 1}$**) or supernatants from virus-infected cells (**denoted by $^{\star 2}$**), and their ability to induce NO production assessed **(B+C). B)** Macrophages were treated with an anti-human CD46 monoclonal antibody (Biolegend, 1µg/mL) or 1000 virus particles per cell of Adenovirus serotype 5, ColoAd1 or ColoIFNγ for 24 hours. **C)** DLD-1 cells were infected with ColoAd1 or ColoIFNγ for 72 hours, at which stage samples were harvested and spun down (500 x *g*, 5 mins.) to generate a cell-free supernatant, "spnt.". Virus supernatant of either ColoAd1 or ColoIFNγ was added to macrophages for 24 hours. For ease of comparison, the values of NO induced by free virus are included on this graph. Level of NO production is demonstrated by mean fluorescence intensity. Results represent n=3, with errors bars indicating SD. Statistical analysis of significance was performed by one-way ANOVA, with a Tukey post-test. $P<0.05$ (*), $P<0.01$ (**), $P<0.001$ (***)

5.2.1.5 ColoAd1 mediated re-education of macrophages is associated with changes in NO production

Extending previous re-education experiments, the ability of ColoAd1 or ColoAd1-IFN-γ to re-educate M2-polarised cells was examined (*Figure 5.7*). Differential polarisation of macrophages, confirmed that different levels of NO production are still observed after 48 hours (*Figure 5.7A*). All treatment groups for M2 macrophages significantly increased the production of NO oxide relative to un-treated M2 macrophages (*Figure 5.7B*). For both viruses, supernatants from virus-infected cells induced higher levels of NO than free viruses alone – significantly so, in the case of ColoAd1-IFN-γ. Such a pattern suggests that soluble mediators released during infection may drive activation of NO in macrophages. Alternatively, this may purely be an effect of increased virus particle stimulation of macrophages –infection for 72 hours should exponentially increase the number of virus particles present in the supernatant, which would be expected to increase the levels of NO.

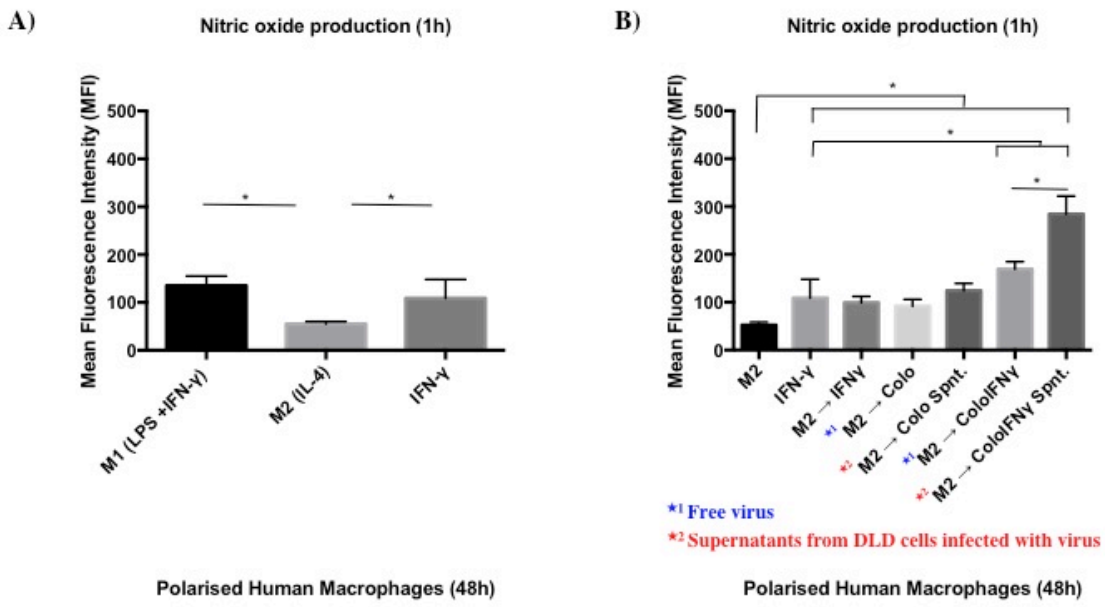


Figure 5.7 ColoAd1 treated macrophages show increased NO production

A) Non-treated (media alone), M1- and M2- polarised THP-1 macrophages cultured for 48h were assessed for their ability to produce NO. **B)** In parallel, after 24 hours an additional set of M2-polarised macrophages had their media replaced with mediated containing IFN-γ, media containing free ColoAd1 or ColoAd1-IFNγ viruses (**denoted by $^{\star 1}$**), or supernatants from DLD-1 cells infected (1000VPC for 72)with either ColoAd1 or ColoAd1-IFNγ viruses (**denoted by $^{\star 2}$**). These treatments were incubated for 24 hours after which time their ability to induce NO production was assessed. NO was measured using DAF-FM Diacetate (Life Technologies™), as previously described in this chapter. Level of NO production is demonstrated by mean fluorescence intensity. Results represent n=3, with errors bars indicating SD. Statistical analysis of significance was performed by one-way ANOVA, with a Tukey post-test. P<0.05 (*), P<0.01 (**), P<0.001 (***)

5.2.2 Phagocytosis is an effective functional marker of macrophage polarisation

Macrophages are highly phagocytic cells, and their activities can be characterised using a range of fluorescently conjugated ligands. Three such ligands were explored as a means to evaluate different aspects of phagocytosis, to determine whether changes in the polarisation of macrophages correlates with a functional change in particle scavenging.

5.2.2.1 Differential uptake of zymosan can distinguish murine M2 macrophages

The first of these ligands was zymosan from *Saccharomyces cerevisiae*, a ß-glucan found on the cell surface of yeast. This agent was used as a surrogate marker of general phagocytosis of pathogen particles. zymosan bio-particles were labeled with Alexa-488 and can be easily visualised by flow cytometry. The murine cell line IC-21 was pre-polarised to either M1 or M2 phenotypes for 24 hours, then incubated with a range of concentrations of zymosan for 1 hour, with the amount of phagocytosed zymosan assessed by flow cytometry (*Figure 5.8*).

The results indicate that there are differential levels of zymosan taken up by these murine macrophages, with M2-polarised macrophages containing more zymosan at 40- and 400- particles per cell. This agrees with previously reported data that M2a-type macrophages express high levels of dectin-1, a lectin-like immune receptor that binds ß-

glucan associated with many pathogen surfaces (Lefèvre et al., 2010). However, at the higher concentration of zymosan (4000 particles per cell), the difference in uptake between M1- and M2- polarised macrophages is not significant. These data suggest that M2 macrophages are more efficient in phagocytosing lower amounts of zymosan – which may reflect increased scavenger receptor expression- but that in conditions where zymosan is in excess, the functional difference observed at the lower zymosan concentrations between the M1 and M2 macrophages is lost. Despite repeated attempts, this assay could not be replicated using human macrophages. After considerable assay optimization, uptake of zymosan by human macrophages was still severely limited, unable to show significant uptake of these fluorescent particles let alone show any differences between the M1- and M2- polarised cells. This result was somewhat surprising given that Dectin-1 expression has previously been reported on THP-1 cells (Rogers et al., 2013), suggesting that the cells possess the surface receptor required for uptake. For the purposes of this thesis, absence of zymosan phagocytosis by the human macrophages used here precluded further utilisation of this ligand for future study.

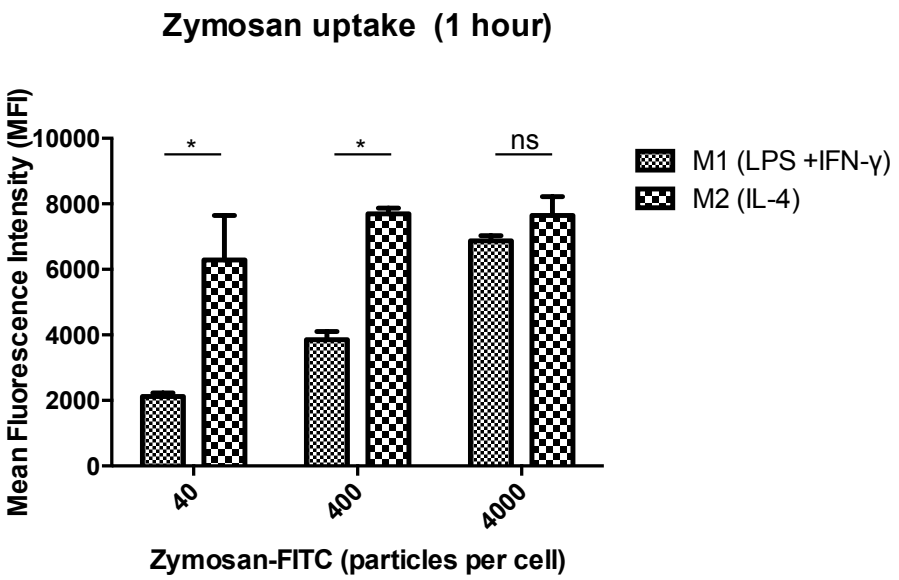


Figure 5.8 Uptake of zymosan by differentially polarised murine macrophages

Murine IC-21 macrophages were seeded at a density of 5 x10^5 cells per well in 24 well plates and cultured for 24 hours in 0.5 mL of RPMI (10% FBS) supplemented with LPS (1 ng/mL) and mIFN-γ (10 ng/mL) ("M1"), or with IL-4 (10 ng/mL) ("M2"). Macrophages were incubated with 40-, 400-, or 4000 particles per macrophage of FITC-labeled zymosan bioparticles for 1 hour in fresh media containing corresponding polarisation media conditions. Cells were harvested using non-enzymatic dissociation buffer and washed 2x with Trypan Blue (0.4% w/v) to quench the fluorescence of non-specifically adsorbed particles on the surface of the macrophages. Samples were analysed for fluorescence using a BD FACS Calibur™ to determine the mean fluorescence intensity, displayed as bar charts. Results represent n=3, with errors bars indicating SD. Statistical analysis of significance was performed by a T-test, with a Sidak-Bonferroni post-test. $P<0.05$ (*), or non-significant (ns)

5.2.2.2 Dextran can be utilised as a functional marker for murine and human polarised macrophages

Dextran is a complex, branched polysaccharide consisting of repeating α1-6 linked units of glucose, a structure not generally associated with microbial pathogens. Its uptake by macrophages has been reported in studies of macropinocytosis and by receptor mediated uptake, implicating the involvement of many C-Type lectin receptors such as DC-SIGN, the macrophage mannose receptor and other scavenger receptors whose expression is typically up-regulated on alternatively-activated macrophages.

Again, M1- and M2- polarised human and murine macrophages were incubated with varying concentrations of FITC-labeled dextran, and its uptake was measured after one hour. As a general pattern, M2- polarised macrophages exhibit higher levels of dextran uptake than their M1 counter parts with a few exceptions. For the mouse macrophages, the greatest difference in dextran-uptake is observed for the lower concentrations of dextran (100 μg/ mL) with a plateau observed for the highest concentration (1000 μg/ mL), perhaps demonstrating saturation of the scavenging receptors. For the human macrophages, M2-type macrophages still predominate in dextran uptake, however the effect of concentration is the opposite as for murine macrophages, with increasing concentrations showing increased differential between the M1 and M2 macrophages.
These results indicate that uptake of dextran could be a useful functional marker to distinguish between M1- and M2-type macrophages in both human and mouse cells, and will be used later in this thesis as an indicator of M1- or M2- type cells.

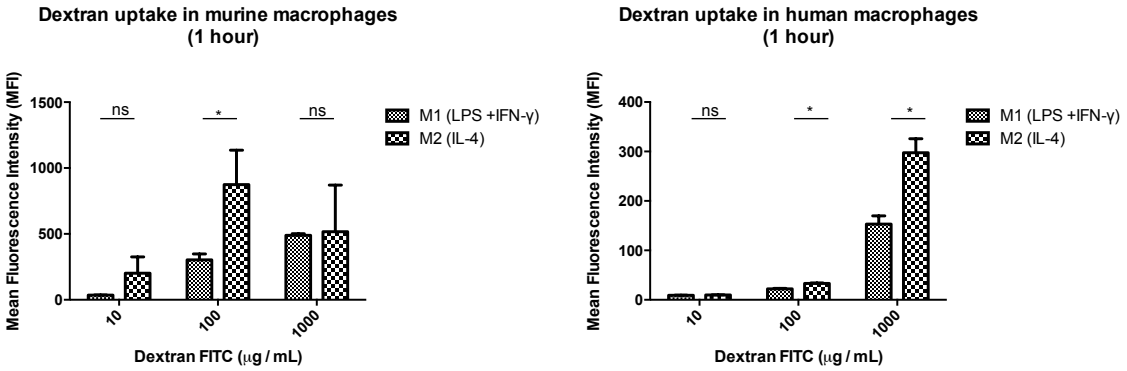


Figure 5.9 Uptake of dextran by differentially polarised macrophages of murine and human origin

Murine IC-21 (left panel) or human THP-1 (right panel) macrophages were seeded at a density of 5 x10^5 cells per well in 24 well plates and cultured for 24 hours in 0.5 mL of RPMI (10% FBS) supplemented with LPS (1 ng/mL) and IFN-γ (10 ng/mL) ("M1"), or with IL-4 (10 ng/mL) ("M2"). Macrophages were incubated with 10-, 100-, or 1000 μg/mL of FITC-labeled dextran for one hour in fresh media containing corresponding polarisation media conditions. Cells were harvested using non-enzymatic dissociation buffer and washed 2x with Trypan Blue (0.4% w/v) to quench the fluorescence of non-specifically adsorbed particles on the surface of the macrophages. Samples were analysed for fluorescence using a BD FACS Calibur™ to determine the mean fluorescence intensity, displayed as bar charts. Results represent n=3, with errors bars indicating SD. Statistical analysis of significance was performed by a T-test, with a Sidak-Bonferroni post-test. $P<0.05$ (*), or non-significant (ns)

5.2.2.3 Uptake of fluorescently labeled Ovalbumin protein (OVA) does not discriminate between murine and human polarised macrophages

The final fluorescently labeled substrate for phagocytosis was the glycoprotein Ovalbumin, OVA, a major constituent of chicken egg whites. This protein is extensively used in immunology and vaccinology as a model antigen system. OVA protein is known to be heavily mannosylated, making it a target for the macrophage mannose receptor. Human and mouse M1 and M2 macrophages were incubated with FITC-labeled OVA at a range of concentrations for an hour, and the level of uptake was assessed by flow cytometry. The levels of OVA were significantly higher in murine M2 type macrophages than M1 at all concentrations studied, with approximately 10-fold differences in uptake observed between the 10 and 100 μg/ mL concentrations of OVA. The same pattern was however not observed for the human macrophages, with no significant differences observed for M1- or M2- uptake at any of the given concentrations. Up-regulation of the mannose-receptor has been well documented in M2-polarised macrophages and most probably explains the differences in uptake of the OVA protein in murine cells, although the lack of differential uptake in human cell subtypes is hard to explain.

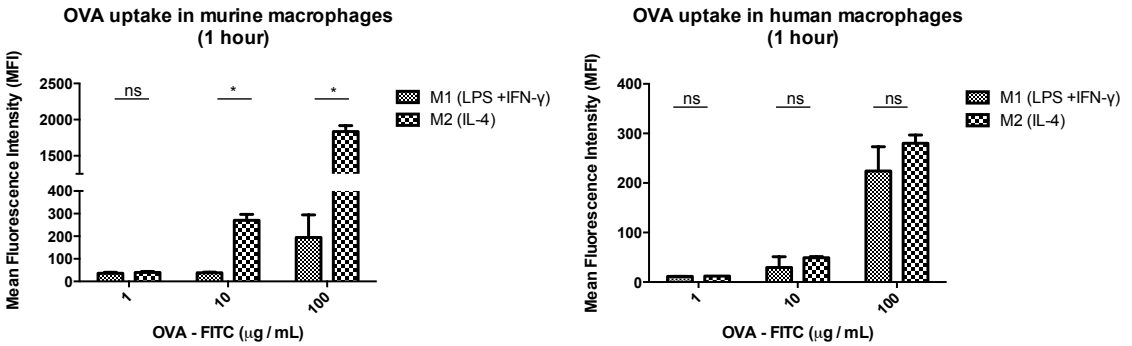


Figure 5.10 Uptake of OVA by mouse and human macrophages

Murine IC-21 (left panel) or human THP-1 (right panel) macrophages were seeded at a density of 5 x10^5 cells per well in 24 well plates and cultured for 24 hours in 0.5 mL of RPMI (10% FBS) supplemented with LPS (1 ng/mL) and IFN-γ (10 ng/mL) ("M1"), or with IL-4 (10 ng/mL) ("M2"). Macrophages were incubated with with 1-,10-, or 100 μg/mL of OVA-FITC for 1 hour in fresh media containing corresponding polarisation media conditions .

Cells were harvested using non-enzymatic dissociation buffer and washed 2x with Trypan Blue (0.4% w/v) to quench the fluorescence of non-specifically adsorbed particles on the surface of the macrophages. Samples were analysed for fluorescence using a BD FACS Calibur™ to determine the mean fluorescence intensity, displayed as bar charts. Results represent n=3, with errors bars indicating SD. Statistical analysis of significance was performed by a T-test, with a Sidak-Bonferroni post-test. $P<0.05$ (*), or non-significant (ns)

This result counter-indicates the use of OVA uptake as a functional assay for distinguishing between M1 and M2 macrophages in human settings, although it provides a good model for murine cells. Murine macrophages therefore provide a useful opportunity to utilise the antigen-presentation methodology associated with OVA to investigate the other main scope of this chapter: how polarisation states affect antigen presentation and the relevance of this in the tumour setting.

5.2.3 Cross presentation of antigen by differentially polarised macrophages

5.2.3.1 Assessing the abilities of differentially polarised murine macrophages to cross-present OVA (257-264) and full-length OVA antigens

Many conventional studies of antigen presentation involve *in vivo* studies, vaccinating mice with known antigens to examine the antigen specific antibody responses by ELISA or measuring antigen-specific T cells by ELISPOT. One model antigen, the chicken egg protein OVA, has formed a significant part of vaccination research in mice and is well established in the field. The octapeptide SIINFEKL represents an eight amino acid sequence from the full length OVA protein ($OVA_{257-264}$), and is naturally processed from OVA to be bound and presented on MHC I molecules as an immunodominant epitope. The generation of an antibody that recognises the SIINFEKL peptide bound to H-2Kb has enabled the direct examination of SIINFEKL cross-presentation by antigen presenting cells using flow cytometry.

5.2.3.2 Peritoneal macrophages are able to cross-present SIINFEKL peptide

Having optimised the SIINFEKL antigen presentation system in dendritic cells and demonstrated that polarisation can influence cross presentation (see Materials and methods, *Section 2.3.2.6*), the same experiment was repeated in mouse macrophages. Due to the nature of the anti-SIINFEKL: MHC I antibody being restricted to H-$2K^b$,

mouse macrophages were harvested by peritoneal lavage of C57/B6 mice (mice from the same genetic background as DC 2.4 cells).

To see whether this methodology would work with *ex vivo* macrophages, freshly isolated peritoneal macrophages were cultured for 6 hours with 100 ng/mL of SIINFEKL peptide (*Figure 5.11A*). The results show that macrophages are able to cross-present peptide and that this can be detected by flow cytometry. Following this result, the study was expanded to perform a pilot investigation into whether polarisation status may play a role. Peritoneal macrophages were isolated and cultured in media alone, M1 media or M2 media for 24 hours prior to pulsing with SIINFEKL peptide (*Figure 5.11B*). When analysed by flow cytometry, M1 macrophages showed higher MFI values for the SIINFEKL:MHC complex Whilst preliminary, these results suggest that there may be differences in cross presentation of SIINFEKL in macrophages when cells are in different inflammatory conditions. The expression of CD64 and CD80 shows the expected patterns for M1 and M2 macrophages indicating that the polarisation was successful, and this may help validate the antigen presentation data despite the lack of biological replicates in this pilot study. Further experimentation was therefore warranted.

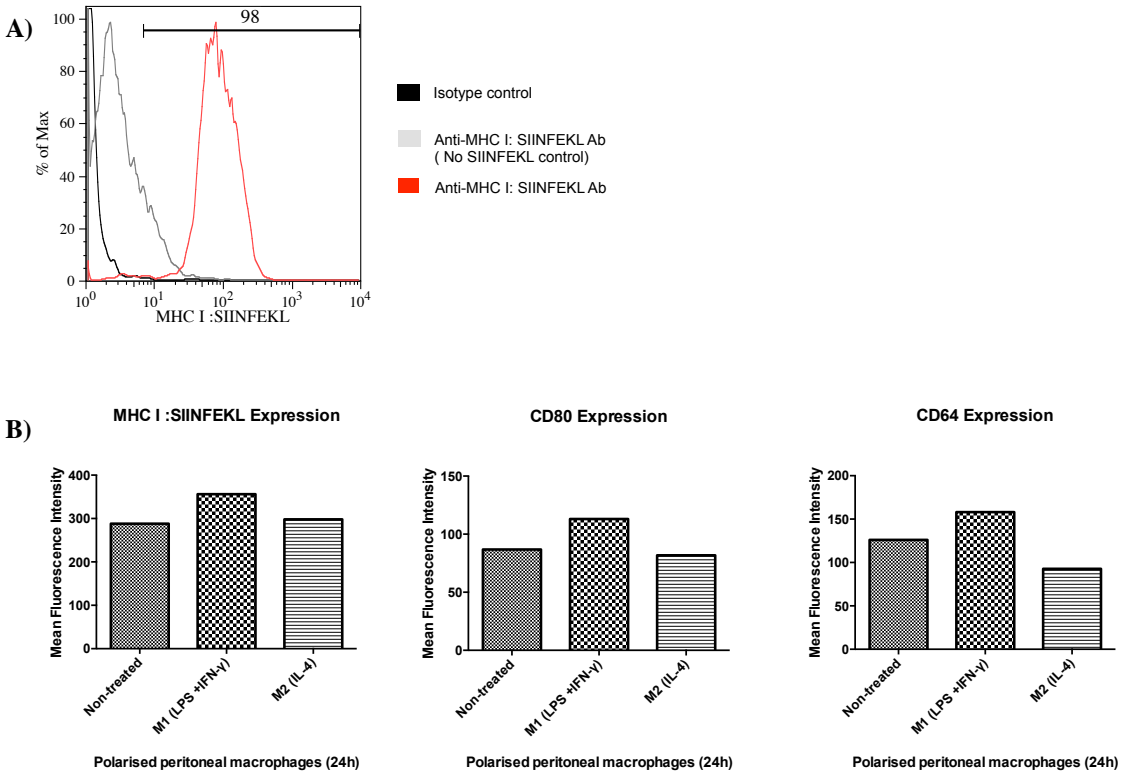


Figure 5.11 Cross-presentation of SIINFEKL by peritoneal-derived mouse macrophages

.**A)** Peritoneal-derived macrophages were pulsed with 10 ng/mL SIINFEKL for 6 hours in fresh RPMI (10% FBS), and stained on the surface for MHC I: SIINFEKL. Flow cytometry histogram represents gated positive cells percentage **B)** Peritoneal-derived macrophages were cultured for 24 hours in RPMI (10% FBS) alone ("Non-treated"), supplemented with LPS (1 ng/mL) and IFN-γ (10 ng/mL) ("M1"), or with IL-4 (10 ng/mL) ("M2"). Macrophages were pulsed with 10 ng/mL SIINFEKL for 6 hours in fresh RPMI (10% FBS) and stained on the surface for MHC I: SIINFEKL, CD80 and CD64. Samples were analysed using a BD FACS Calibur™ to determine the mean fluorescence intensity, displayed as bar charts. Results represent n=1

These preliminary data supported further research into the macrophage antigen presentation question. Replicates were not performed as I was limited both biologically (there were a limited number of mice available for this study) and technically, as there were low numbers of macrophage isolated. As these studies were preliminary and were used to support proof-of-principle that macrophages can cross-present SIINFEKL, these experiments were not replicated. Peritoneal derived macrophages represent a good model for mouse macrophages, however, yield of macrophages are low (<1 $x10^6$ cells per mouse) without prior elicitation. Whilst elicitation might solve the issue of low cell numbers, various methods of elicitation have been shown to stimulate macrophages towards a pro-inflammatory phenotype which would conflict with attempts at polarisation. To circumvent this issue, subsequent studies were performed using the mouse cell line IC-21 to provide an adequate source of macrophages for antigen presentation studies. Importantly, this cell line is derived from the same genetic background as DC2.4 cells (the C57/B6 mouse strain) and is therefore compatible with the SIINFEKL detection system by flow cytometry.

5.2.3.3 Increased SIINFEKL peptide cross-presentation by M1 macrophages

To extend the findings from the peritoneal macrophage studies, IC-21 macrophages were polarised with M1 and M2 media for 24 hours before being treated with 10 ng/mL of SIINFEKL peptide for a 6-hour incubation. Studying receptor positivity, the results demonstrate that for the non-polarised and M2-polarised macrophages, cross

presentation of SIINFEKL is negligible (*Figure 5.12A*). M1 macrophages on the other hand are able to cross present antigen effectively. Presentation of SIINFEKL is best demonstrated by studying the percentage of cells that are positive for the SIINFEKL: MHC I receptor, as differences in MFI were found to be non-significant (*Figure 5.12B*). Most likely, the lack of significance in MFI is a result of relatively small shifts in the fluorescence peak of positive cells – whilst, this doesn't effect the ability to clearly distinguished positively and negatively stained cells, it does mean that the resulting differences in MFI values are not dramatic.

To confirm that the changes in polarisation status were effective, IC-21 macrophages were also compared for expression of the M1 markers TNF-α and CD80 *(Figure 5.12C*). Increased levels of TNF-α and CD80 were observed by MFI for M1 polarised macrophages relative to their M2 counterparts, indicating that the macrophages had been successfully polarised and validating that the differences in antigen presentation were indeed a result of their altered polarisation states.

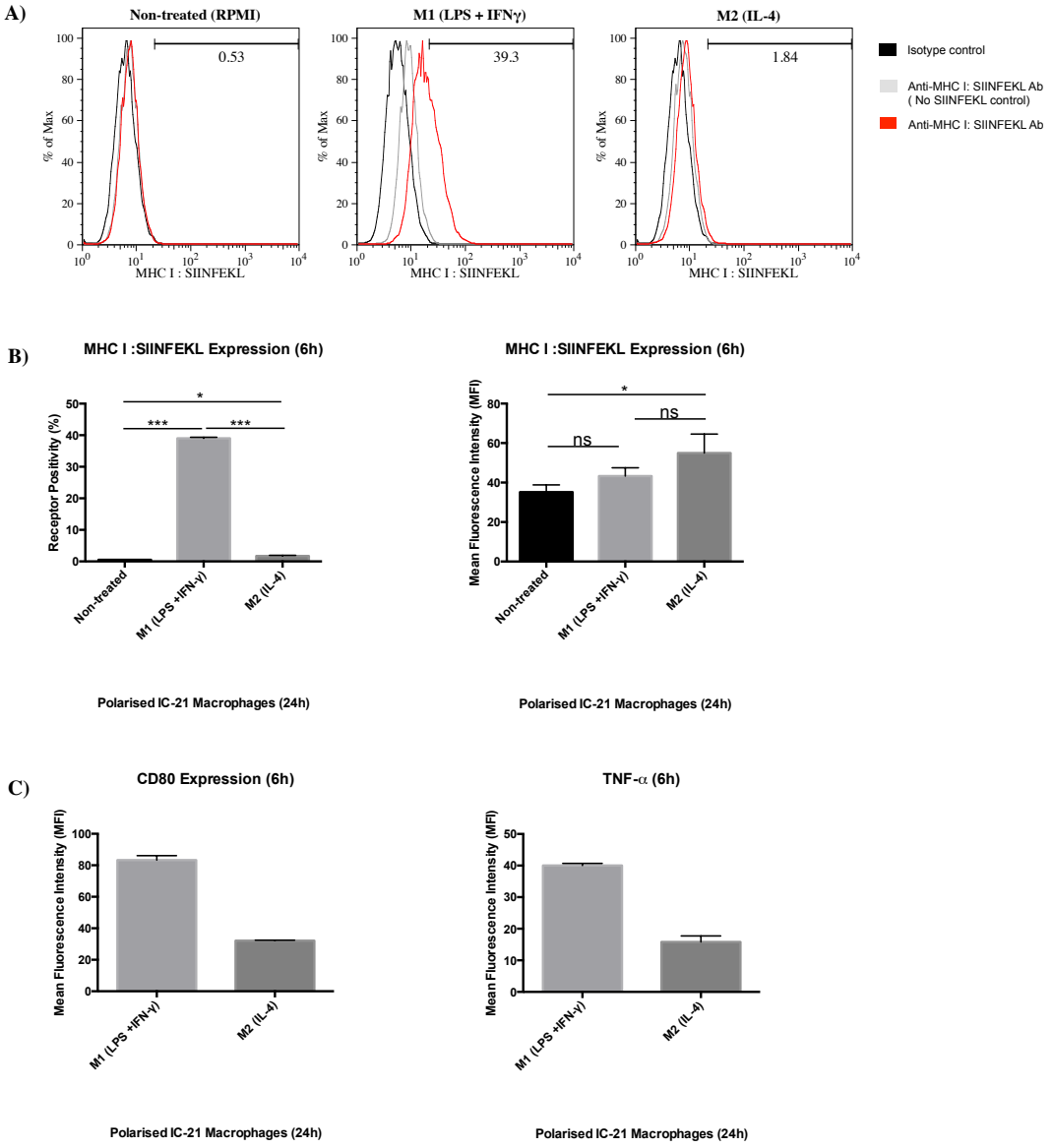


Figure 5.12 Antigen presentation of SIINFEKL by IC-21 murine macrophages

IC-21 macrophages were seeded at a density of 5 x10^5 cells per well in 24 well plates and cultured for 24 hours in 0.5 mL of RPMI (10% FBS) alone ("Non-treated"), supplemented with LPS (1 ng/mL) and mIFN-γ (10 ng/mL) ("M1"), or with IL-4 (10 ng/mL) ("M2"). Macrophages were pulsed with 10 ng/mL SIINFEKL for 6 hours in fresh media containing corresponding polarisation media conditions (10% FBS), harvested using non-enzymatic dissociation buffer and stained on the surface for MHC I: SIINFEKL (1: 400 dilution). **A)** Flow cytometry histogram represents gated positive cells percentage. **B)** Antigen presentation data is presented as a percentage of MHC I: SIINFEKL -positive cells (left panel) or as MFI of the receptor staining (right panel). **C)** To confirm that polarisation towards M1 or M2 phenotype was successful, macrophages were also co-stained for CD80 or intracellularly for TNF-α production. Samples were analysed using a BD FACS Calibur™ to determine the mean fluorescence intensity, displayed as bar charts. Results represent n=3, with errors bars indicating SD. Statistical analysis of significance was performed by one-way ANOVA, with a Tukey post-test. P<0.05 (*), P<0.01 (**), P<0.001 (***) or non-significant (ns)

5.2.3.4 Comparing the antigen processing capacity of OVA between differentially polarised macrophages

OVA-DQ™ , a modified form of the OVA protein, was used to explore cellular routing of internalized antigens in macrophage subsets. OVA-DQ contains a labile group that quenches fluorescence of endocytosed OVA protein until it reaches the acidified environment of lysosomes where proteolytic activity takes place, thereby enabling fluorescent detection of processed OVA. Evaluating cellular processing of OVA-DQ can therefore act as a surrogate for increased antigen processing.

IC-21 macrophages were polarised to M1- or M2- phenotypes and incubated with OVA-DQ for six hours, the same duration of time as for the normal antigen presentation experiments. In parallel, M1 and M2 macrophages were incubated for six hours with FITC-labeled OVA (utilised earlier in this chapter). This enable measurement of both OVA uptake (using OVA-FITC) and subsequent its processing in acidified compartments (using OVA-DQ).

M2 macrophages showed up to approximately 20-fold greater uptake of OVA-FITC relative to M1 cells (*Figure 5.13A*). Studying the processing of OVA-DQ by mean fluorescence intensity indicated higher levels of antigen acidification for the M2-polarised macrophages (*Figure 5.13B*). Given the OVA uptake data, it is un-surprising that there are higher levels of processing activity in the M2 macrophages at each concentration of OVA studied; higher uptake of OVA will increase the availability of

this substrate for processing. To resolve this, the DQ acidified processing values were standardised against the amount of OVA being phagocytosed (*Figure 5.13C*).

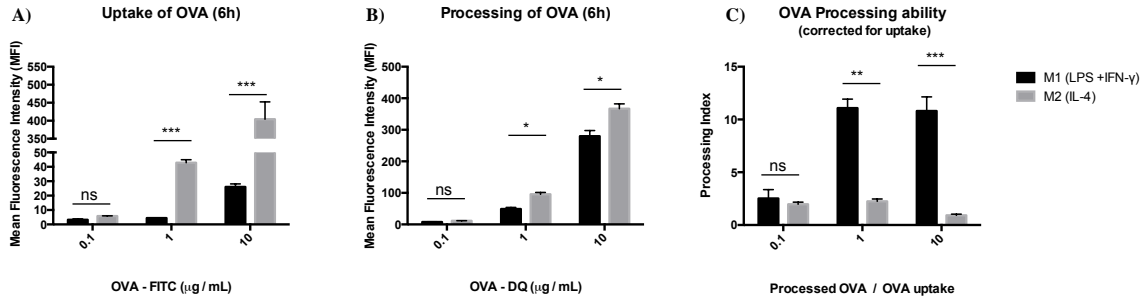


Figure 5.13 Processing of OVA antigen by murine macrophages

IC-21 macrophages were seeded at a density of 5 x10^5 cells per well in 24 well plates and cultured for 24 hours in 0.5 mL of RPMI (10% FBS) supplemented with LPS (1 ng/mL) and mIFN-γ (10 ng/mL) ("M1"), or with IL-4 (10 ng/mL) ("M2"). Macrophages were pulsed with 0.1-,1-, or 10 μg/mL of either OVA-FITC (**A**) or OVA-DQ (**B**) for 6 hours in fresh media containing corresponding polarisation media conditions .Cells were harvested using non-enzymatic dissociation buffer and washed 2x with Trypan Blue (0.4% w/v) to quench the fluorescence of non-specifically adsorbed OVA-FITC or OVA-DQ particles on the surface of the macrophages. Samples were analysed for fluorescence using a BD FACS Calibur™ to determine the mean fluorescence intensity, displayed as bar charts. Results represent n=3, with errors bars indicating SD. Statistical analysis of significance was performed by one-way ANOVA, with a Tukey post-test. P<0.05 (*), P<0.01 (**), P<0.001 (***) or non-significant (ns)

Normalising the cellular processing data shows that antigens internalized into M1-macrophages undergo much more extensive processing in acidified compartments than antigens entering the equivalent M2 cells. Such differences correlate with the enhanced cross-presentation of SIINFEKL peptide observed for M1 macrophages, although SIINFEKL does not require significant antigenic processing to be cross-presented. In contrast full length OVA does require intracellular processing to allow cross

presentation on MHC I, and it seems feasible that M1-type macrophages would achieve this more efficiently. This possibility is evaluated in the following sections.

5.2.3.5 Cross presentation of full –length OVA by dendritic cells

As a positive control for the antibody-detection of SIINFEKL presentation on MHC I, DC2.4 dendritic cells were pre-polarised with M1-media and incubated with 10 ng of SIINFEKL peptide (*Figure 5.14*). The pattern of SIINFEKL expression is consistent with previous data and displays a decrease in positivity for receptor expression with increasing incubation time, as would be expected over this 24-hour period. Disappointingly, however, no presentation of the SIINFEKL epitope was detectable under any conditions when the cells were incubated with full length OVA. These data indicate that full length OVA is not measurably cross-presented by DC 2.4 cells.

This result was surprising given that equivalent OVA concentrations have been used successfully in other reported *in vitro* assays to stimulate OVA-specific T cell proliferation, however no groups have reported presentation of full length OVA on dendritic cells utilising this flow cytometric method. This may indicate that biological readouts are more sensitive than flow cytometry or could represent technical issues with the assay.

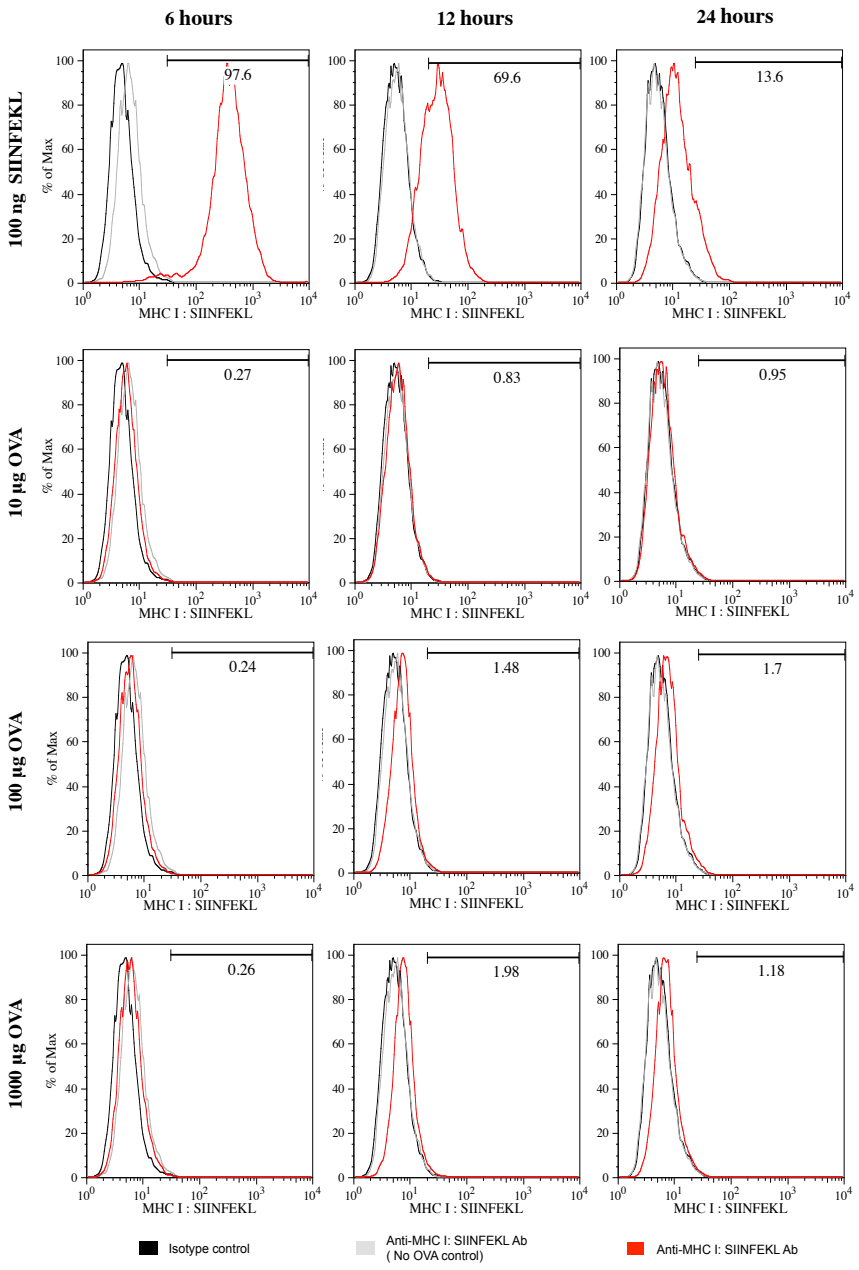


Figure 5.14 Cross-presentation of full-length OVA by murine dendritic cells

DC 2.4 cells were seeded at a density of 5 x10^5 cells per well in 24 well plates and cultured for 6-, 12-, or 24- hours in 0.5 mL of RPMI (10% FBS) alone containing either 10-, 100- or 1000-µg of full length OVA (Sigma). As a positive control, dendritic cells were pre-polarised with M1 media, then pulsed with 10ng of SIINFEKL peptide (**Top panels**). Dendritic cells were harvested using non-enzymatic dissociation buffer and stained on the surface for MHC I: SIINFEKL (1: 400 dilution). Dendritic cells were harvested using non-enzymatic dissociation buffer and stained on the surface for MHC I: SIINFEKL (1: 400 dilution). Flow cytometry histogram represents gated positive cells percentage. Results represent n=3

5.2.3.6 Cross presentation of full –length OVA by macrophages

To assess whether the absence of detection of cross presentation of full length OVA was limited to dendritic cells and to explore whether macrophages may be more effective, the assay was extended to include IC-21 macrophages. There are many reports in the literature that macrophages have a higher capacity for phagocytosis and processing relative to their dendritic cell counterparts. However, our studies showed that while the cross-presentation of SIINFEKL octapeptide was greater in M1 relative to M2 treated cells (*Figure 5.15, left panels*). As before, no presentation of full length OVA could be detected by either cell type. It seems that full length OVA at this concentration is not effectively cross presented by macrophages *in vitro*, and that this is not affected by polarisation state (*Figure 5.15, right panels*).

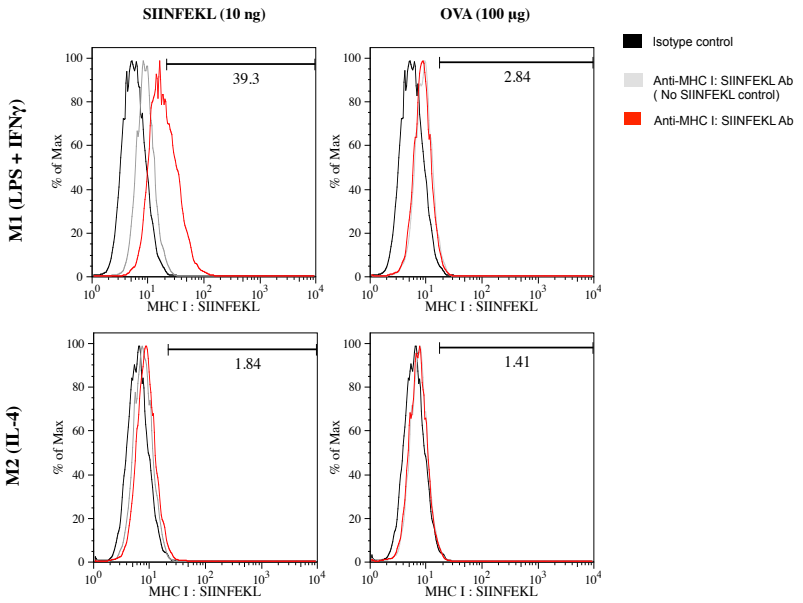


Figure 5.15 IC-21 macrophages do not cross-present full length OVA

IC-21 macrophages were seeded at a density of 5 x10^5 cells per well in 24 well plates and cultured for 24 hours in 0.5 mL of RPMI (10% FBS) supplemented with LPS (1 ng/mL) and mIFN-γ (10 ng/mL) ("M1", upper panels), or with IL-4 (10 ng/mL) ("M2", lower panels). Macrophages were pulsed with 10 ng/mL SIINFEKL for six hours as a positive control for SIINFEKL presentation (**left panels**). Alternatively, macrophages were pulsed with 100µg of OVA protein (**right panels**) Macrophages were harvested using non-enzymatic dissociation buffer and stained on the surface for MHC I: SIINFEKL (1: 400 dilution). Flow cytometry histogram represents gated positive cells percentage. Results represent n=3

Antigen presentation of full length OVA might perhaps be rescued by increased cellular uptake via prior opsonisation, using anti-OVA antibodies to promote cellular scavenging of OVA via Fc receptors. Blood samples were therefore obtained from CD57BL/6 mice vaccinated against the OVA protein (kindly provided by Dr. Thomas Hills) and isolated the serum. Such serum should contain polyclonal antibodies raised against the OVA protein, and this was demonstrated using serially diluted serum to stain B16-OVA mouse melanoma cells that express the OVA protein on the cell surface by flow cytometry (Figure 5.16).

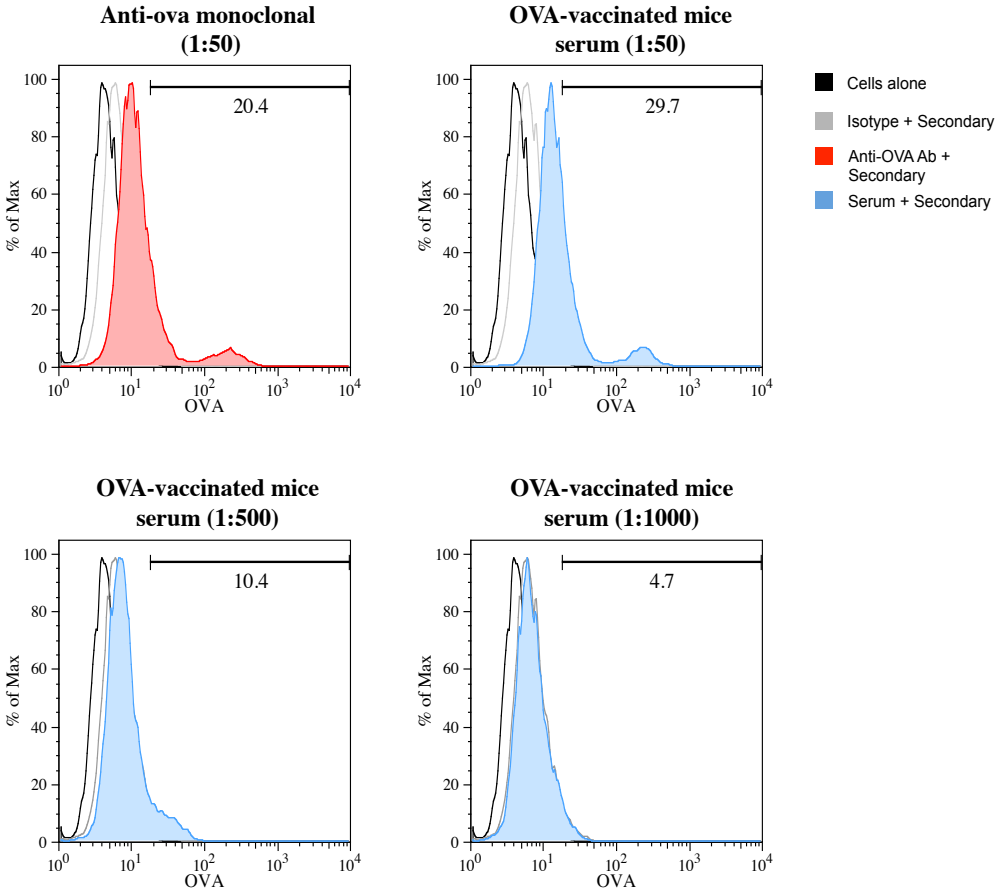


Figure 5.16 Generation of polyclonal anti-OVA serum

Anti-OVA serum was obtained from OVA-vaccination studies performed by Dr. Tom Hills. B16 cells were engineered to express full-length OVA on their surface and these "B16 OVA" cells, were provided as a kind gift from Dr. Kueberuwa. To assess the ability of the anti-OVA serum to bind OVA protein, $1x10^6$ of these B16 OVA cells were stained at 1:50, 1:500 and 1:1000 dilutions, then stained with secondary antibody and analysed for fluorescence by flow cytometry to confirm specific binding

To assess whether the Fc receptor-mediated increased uptake of OVA into M1 cells (*Figure 5.17A , right panels*) would lead to enhanced presentation on MHC I, the OVA uptake experiments were repeated following pre-incubation of OVA with a polyclonal anti-OVA antibody. The results demonstrated that pre-incubation increases the ability of M1 macrophage to phagocytose OVA such that there are no significant differences observed between M1 and M2 cells at 10-100 μg/mL OVA. Such increases in OVA uptake for M1 macrophages could be explained by the increased Fc-receptors found on these macrophages, such as in the case of the high affinity IgG receptor, CD64 (*Figure 5.17B*). To see if the increases in OVA uptake mediated by opsonisation would correlate with increased antigen presentation, the OVA antigen presentation assay was repeated. The results however show that pre-opsonising OVA does not increase the levels of cross-presentation, confirming again that full length OVA is not detectably cross-presented by these macrophages *in vitro* (*Figure* 5.18).

Whilst the antigen presentation data for full-length OVA was disappointing, its failure may represent technical limitations with the assay or with insufficient solubility of the OVA protein itself. No groups have reported presentation of full length OVA by either dendritic cells or macrophages *in vitro* using this flow cytometric method. To extend the SIINFEKL cross-presentation question, it might be useful to synthesise a version of the octapeptide that is flanked by a number of amino acids from the full OVA sequence on N- and C terminals on the SIINFEKL peptide to model the need for at least low levels of antigen processing.

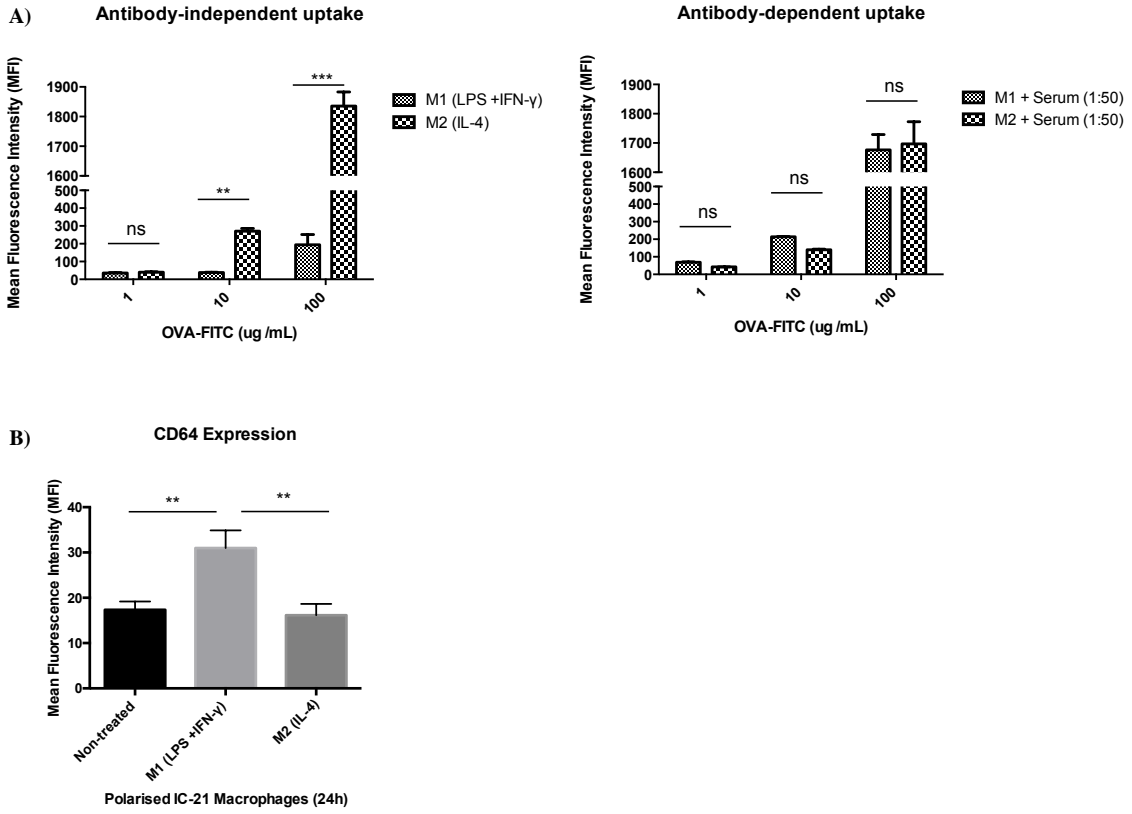


Figure 5.17 Uptake of OVA by mouse and human macrophages

Murine IC-21 macrophages were seeded at a density of 5 x10^5 cells per well in 24 well plates and cultured for 24 hours in 0.5 mL of RPMI (10% FBS) supplemented with LPS (1 ng/mL) and IFN-γ (10 ng/mL) ("M1"), or with IL-4 (10 ng/mL) ("M2"). Macrophages were incubated with with 1-,10-, or 100 μg/mL of OVA-FITC without (**A - left panel)** or with **(A - right panel**) an hours pre-incubation of anti-OVA serum, before incubating for an for 1 hour in fresh media containing corresponding polarisation media conditions .Cells were harvested using non-enzymatic dissociation buffer and washed 2x with Trypan Blue (0.4% w/v) to quench the fluorescence of non-specifically adsorbed particles on the surface of the macrophages. **B)** Additonally, M1 and M2 macrophages were stained for CD64. Samples were analysed for fluorescence using a BD FACS Calibur™ to determine the mean fluorescence intensity, displayed as bar charts. Results represent n=3, with errors bars indicating SD. Statistical analysis of significance was performed by a T-test, with a Sidak-Bonferroni post-test. P<0.05 (*), P<0.01 (**), P<0.001 (***) or non-significant (ns)

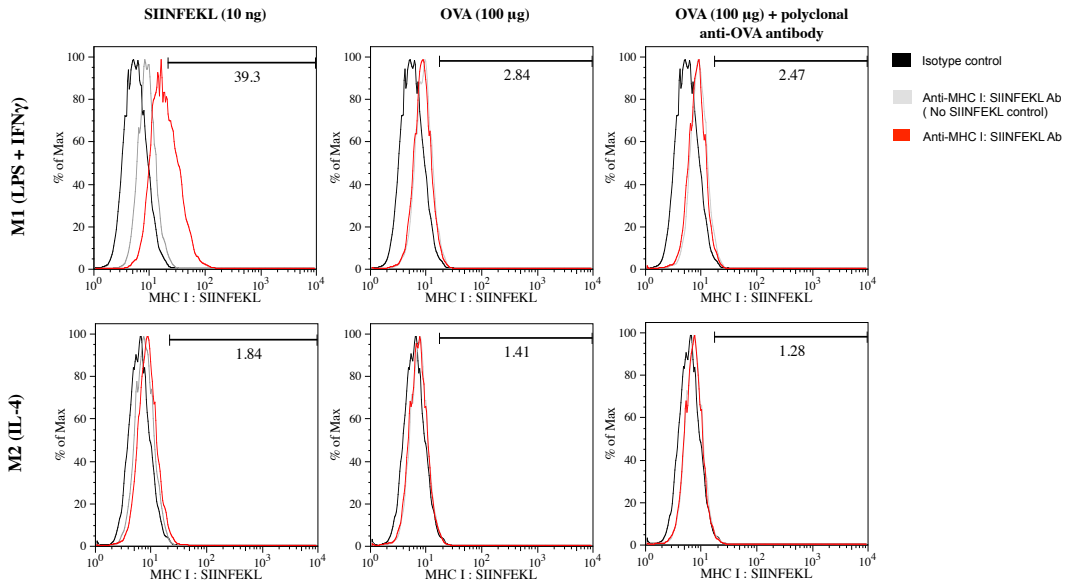


Figure 5.18 IC21 cannot cross present full length OVA, even when opsonised

IC-21 macrophages were seeded at a density of 5 x10^5 cells per well in 24 well plates and cultured for 24 hours in 0.5 mL of RPMI (10% FBS) supplemented with LPS (1 ng/mL) and mIFN-γ (10 ng/mL) ("M1", upper panels), or with IL-4 (10 ng/mL) ("M2", lower panels). Macrophages were pulsed with 10 ng/mL SIINFEKL for 6 hours as a positive control for SIINFEKL presentation (**left panels**). Alternatively, macrophages were pulsed with 100ug of OVA protein either not-incubated (**central panels**) -or given 1 hours pre-incubation with anti-OVA polyclonal antibody (**right panels**)- for 6 hours. Cells were stained on the surface for MHC I: SIINFEKL (1: 400 dilution). Flow cytometry histogram represents gated positive cells percentage. Results represent n=3

5.2.3.7 Cross-presentation of tumour cell-associated antigens

The central motivation for studying antigen presentation by macrophages in this thesis has been to test the hypothesis that M1-type macrophages would pre-dominate the cross-presentation of tumour antigen from dead or dying tumour cells and that this would be particularly important in the context of oncolytic virus infection. Whilst it has been demonstrated (particularly using the isolated SIINFEKL epitope) that M1 macrophages may be important in this cross presentation process, processing and presentation of full length antigens by macrophages has not been shown. The OVA-expressing murine melanoma cell line B16-OVA provides a useful model to explore the possibility that macrophages may cross-present antigens more efficiently from tumour cells than from purified protein, using the flow cytometric method optimised above.

B16-OVA cells were grown to confluency in a large flask and were harvested by non-enzymatic means to generate a concentrated pellet of cells. The presence of the OVA antigen on these cells was confirmed by flow cytometry, and a cell lysate was subsequently generated by multiple freeze-thaw cycles. M1- and M2-polarised IC-21 macrophages were incubated with 100 μg/mL of B16-OVA cell lysate for six hours before measuring presentation of the MHC I : SIINFEKL epitope by flow cytometry. The results demonstrated small, but significant, expression of MHC I: SIINFEKL on the surface of M1-polarised macrophages. In contrast, expression of the SIINFEKL peptide of M2 cells is almost negligible, suggesting that M1 cells are might be more proficient in processing cell-associated antigen relative to M2 cells. Whilst the increase in SIINFEKL presentation may be significant relative to M2 cells, it is questionable whether this represents a genuine increase in cross-presentation, as the values are so

low. This may well represent a technical limitation of the antibody, and further experimentation utilising a more reliable and published methodology (such as T cell proliferation) should be used to validate whether these increases in SIINFEKL presentation constitute genuine increases in cross-presentation.

5.2.3.8 Comparing the ability of macrophages to phagocytose tumour cells

These data indicate that M1-type macrophages may be able to cross-present antigens generated by tumour cell lysis, but does not provide any insight into the mechanism. The OVA-DQ studies (*Figure 5.17)* suggest the difference could be related to a higher acidification or proteolytic activity within the M1 cells and there may be also be differences between the levels of lysed B16-OVA cells taken up by M1- and M2-macrophages. To try and resolve this, a cellular phagocytosis assay was developed to compare phagocytosis of tumour cells by macrophages of different polarisation.

B16-OVA cells were stained with CFSE dye then either incubated at 37°C or at 56°C for 30 minutes to generate fluorescent populations of live or necrotic cells respectively. These tumour cells were then incubated in a 1:1 ratio with M1 or M2 macrophages for 6 hours to study the levels of phagocytosis (*Figure 5.20*).

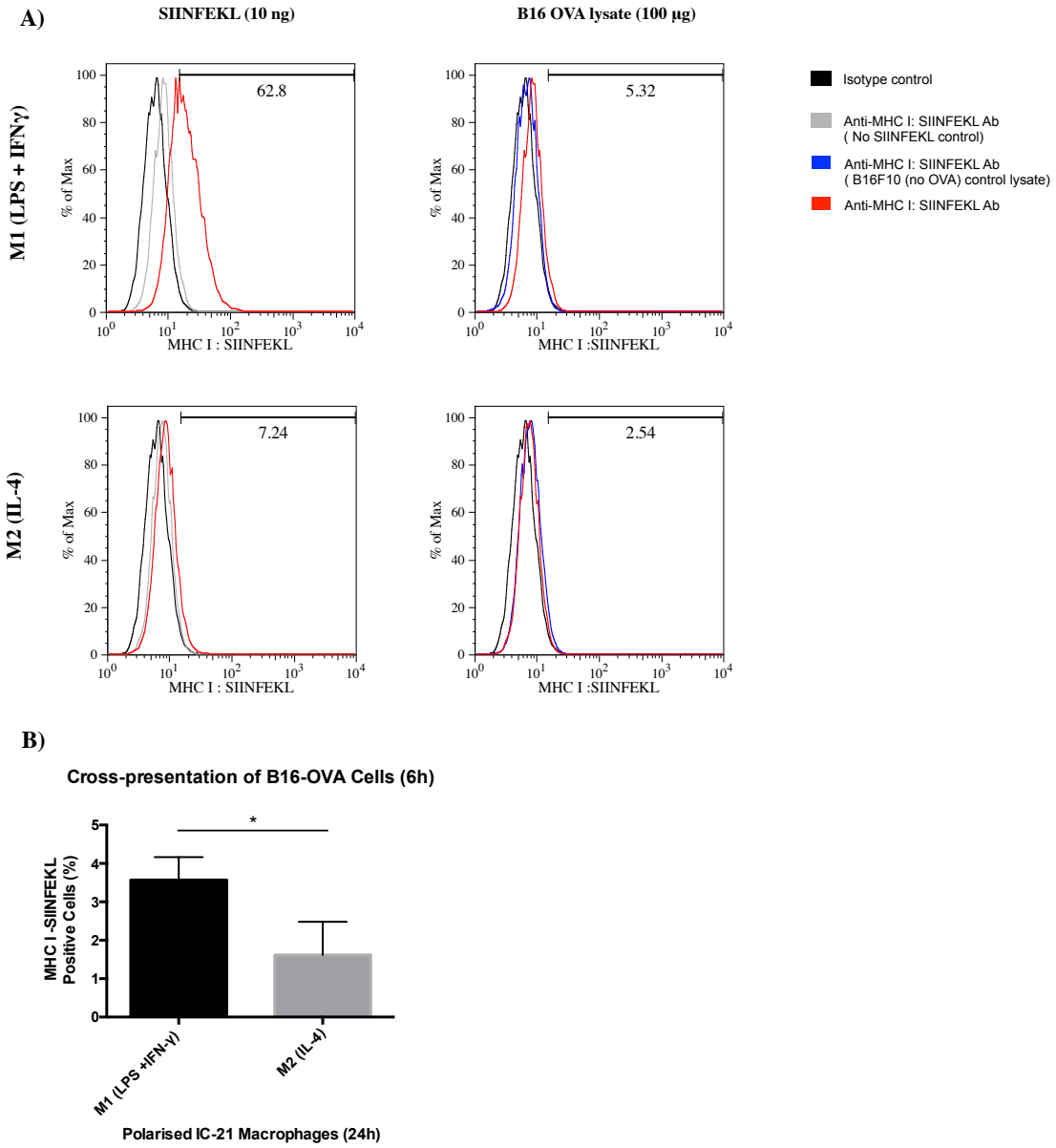


Figure 5.19 M1-polarised macrophages can cross-present B16OVA tumour antigen

IC-21 macrophages were seeded at a density of 5 x10^5 cells per well in 24 well plates and cultured for 24 hours in 0.5 mL of RPMI (10% FBS) supplemented with LPS (1 ng/mL) and IFN-γ (10 ng/mL) ("M1",), or with IL-4 (10 ng/mL) ("M2", lower panels). **A)** M1 or M2 Macrophages were pulsed with 10 ng/mL SIINFEKL for 6 hours as a positive control for SIINFEKL presentation (**left panels**). Alternatively, macrophages were pulsed with 1000ug /mL of B16-OVA cell lysate (**right panels**) for 6 hours. Macrophages were harvested using non-enzymatic dissociation buffer and stained on the surface for MHC I: SIINFEKL (1: 400 dilution). Flow cytometry histogram represents gated positive cells percentage. **B)** Comparison of positivity for the MHC I:SIINFEKL complex between M1 and M2 macrophages was corrected for background non-specific binding and analysed for statistical significant by a T-test. Results represent n=3

The results show little background phagocytosis of live B16-OVA cells by macrophages, however phagocytosis of these cells by M1 macrophages is still significantly lower than both the non-treated and M2-polarised macrophages. There are increased levels of phagocytosis for the necrotic B16-OVA cells for all macrophages, however the same pattern is observed with M2 –polarised macrophages showing the highest levels of B16-OVA phagocytosis. These results may reflect the role of M2 macrophages in tissue damage and repair, scavenging dead or dying cells as a means to regulate homeostasis.

The small background levels of phagocytosis might be a consequence of CD47 expression on B16 cells, which are known to express this receptor to evade phagocytosis (Zhao et al., 2011). Whilst CD47 expression might decrease phagocytosis, its expression reflects the complexity of inducing phagocytosis as a therapeutic strategy and adds to the stringency of this assay; future experimentation may wish to include CD47 antagonism to see how this modulates macrophage phagocytosis.

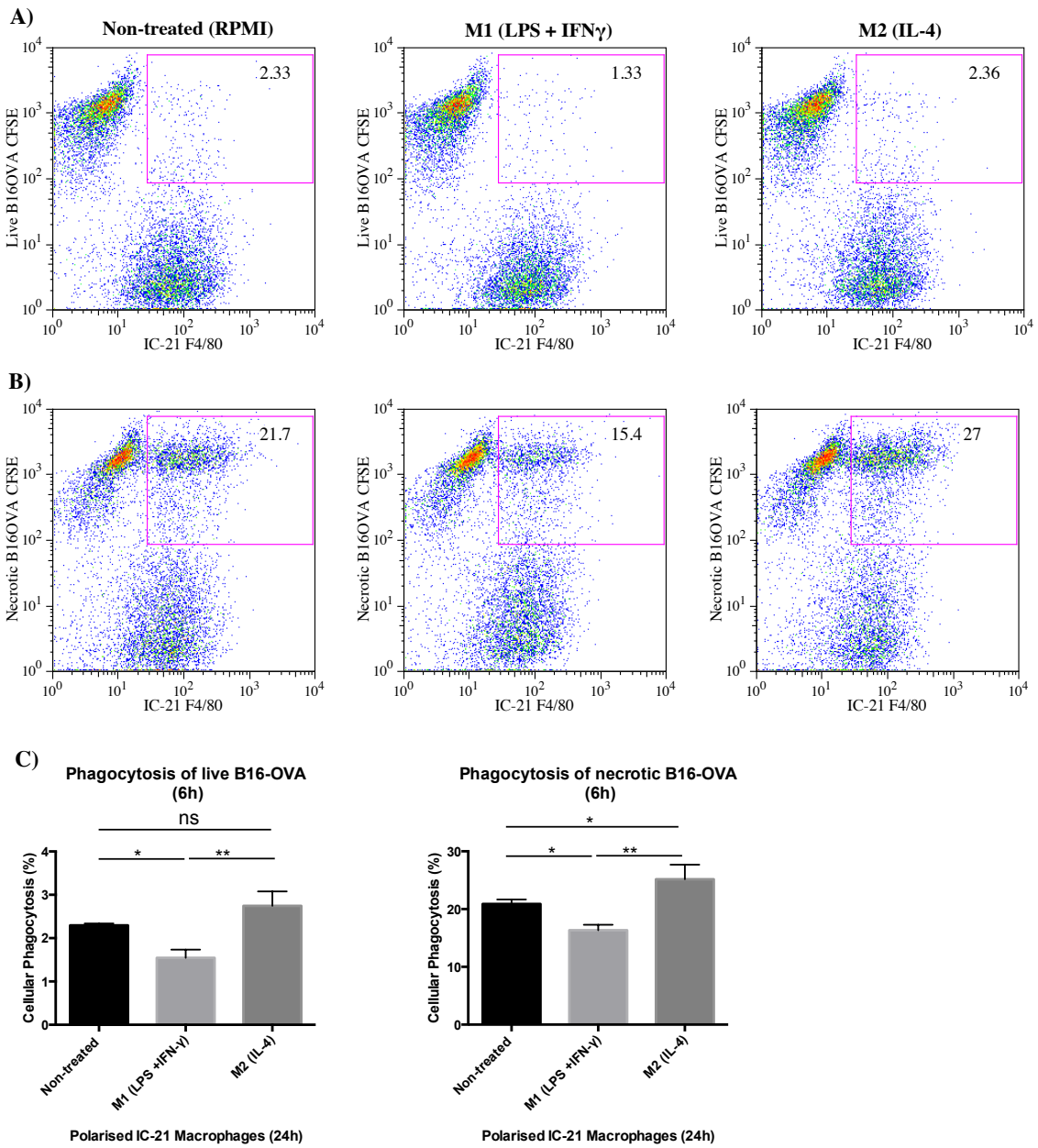


Figure 5.20 Polarisation of IC-21 macrophages determines the ability to phagocytose B16-OVA cells

IC-21 macrophages were seeded at a density of 2.5 x10^5 cells per well in 48 well plates and cultured for 24 hours in 0.5 mL of RPMI (10% FBS) supplemented with LPS (1 ng/mL) and mIFN-γ (10 ng/mL) ("M1"), or with IL-4 (10 ng/mL) ("M2"). Macrophages were then incubated for 6 hours with 2.5 x10^5 CFSE-stained B16-OVA cells that had been previously incubated at 37 °C ("Live", **A**) or at 56 °C ("Necrotic", **B**). Macrophages and B16-OVA cells were harvested using non-enzymatic dissociation buffer and stained on the surface for F4/80 to identify the macrophage populations. Phagocytosed B16-OVA cells were identified as those double-stained for F4/80 and CFSE (Upper right hand quadrant, **A** and **B**). Percentages of phagocytosed cells are summarised in bar charts (**C**). Results represent n=3. Statistical analysis of significance was performed by one-way ANOVA, with a Tukey post-test. P<0.05 (*), P<0.01 (**), P<0.001 (***) or non-significant (ns)

Having explored the role of macrophage polarisation on phagocytosis and cross-presentation of tumour cells and their associated antigens, it was logical to assess what would happen in the context of an oncolytic virus infection: in particular to determine whether virally-infected cells are phagocytosed by M1 and M2 to the same levels as with necrotic cells and whether the pattern of antigen presentation is the same. However our work uses adenovirus as the oncolytic agent, and it is human specific and does not replicate in murine cells. Accordingly it was necessary to develop an assay for antigen presentation by human macrophages.

5.2.3.9 Human macrophages efficiently phagocytose virally lysed SW480, but fail to cross present p53

To study cross-presentation in a human macrophage model, a p53-based system was employed (as a kind gift from Prof. A. Banham). p53 peptide RMPEAAPPV derived from wild type human p53 protein was provided along with a monoclonal antibody that detects this peptide complexed with HLA-A2, giving a methodology by which cross-presentation of a human antigen (relevant to cancer) can be studied in the HLA-A2-positive THP-1 macrophage cell line. To examine whether differentially polarised macrophages can cross-present p53 from tumour cells, lysates from the SW480 colorectal cancer cell line were generated by multiple freeze-thawing, or by virus infection with ColoAd1.

The abilities of the macrophages to accumulate cancer cell antigens were measured using a cellular phagocytosis as described earlier (*Figure 5.21*, top panel). The results show that there is minimal phagocytosis of live SW480 cells, with no discernable differences in the baseline levels of cellular phagocytosis between the different polarisation states (*Figure 5.21*, top panel). In contrast, macrophages of all polarisation states studied were able to phagocytose virally lysed SW480. Whilst, there was a slight increase in the number of virally lysed cells by M2-polarised macrophages, this effect was not significant.

Following the phagocytosis of virally-lysed cells, macrophages were analysed for evidence of cross-presentation of the p53 antigen (*Figure 5.22*). In parallel with the SW480 experiment, M1 and M2 macrophages were pulsed with p53 peptide or with a concentrated lysate of un-treated or virus-infected SW480 cells, generated by multiple freeze-thaw cycles. To exclude detection of any MHC I: p53 complexes present on SW480 cells (which would yield a false-positive signal for cross presentation), samples containing mixtures of SW480 and THP-1 cells were stained with EGFR to identify, and subsequently exclude, any cancer cells when analysing expression of MHC I:p53. Incubation of the p53 peptide alone illustrated differences between M1 and M2 macrophages in their ability to cross-present antigen, with M1 macrophage demonstrating significantly higher levels of MHC I: p53 (*Figure 5.22A*). For the incubation of macrophages with lysates of SW480 cells, the results demonstrate that there was no detectable cross presentation of p53 from either the SW480 freeze-thawed lysate or virus lysate by any macrophages (*Figure 5.22B*).

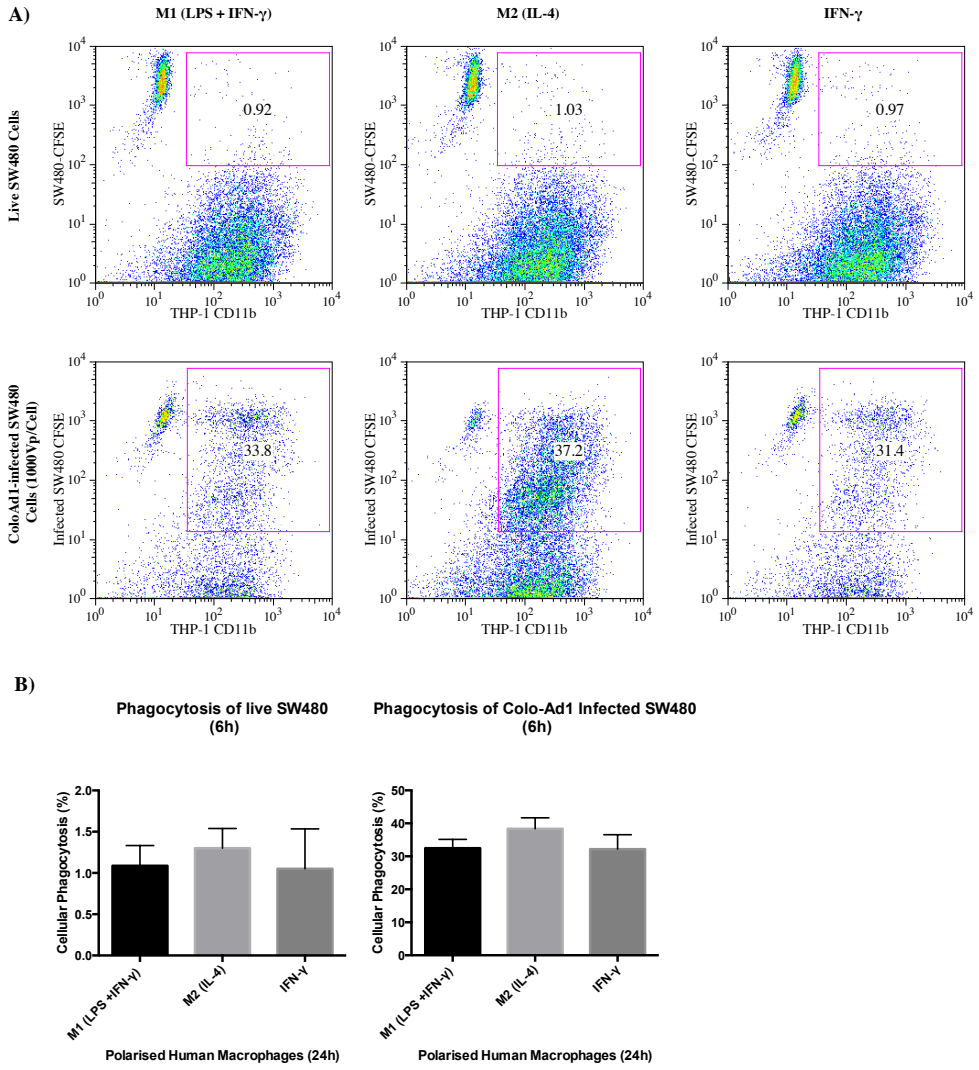


Figure 5.21 Phagocytosis of virus-infected p53-positive tumour cells

M1, M2 and IFN-g polarised macrophages were generated as previously described, seeded in 48 well plates at a density of 2.5 x10^5 cells/ well. SW480 cells were stained with 5μM CFSE (Life Technologies™ and were either non-treated or infected with ColoAd1 (1000vp) for 72h. **A)** Macrophages were incubated for 6 hours with 2.5 x10^5 non-treated SW480 cells (**upper panels**) or with 2.5 x10^5 ColoAd1-infected SW480 cells (**lower panels**). Macrophages and SW480 cells were harvested using non-enzymatic dissociation buffer and stained on the surface for CD11b to identify the macrophage populations. Phagocytosed SW480 cells were identified as those double-stained for CD11b and CFSE (**A,** Upper right hand quadrants). Gates were determined by 4°C control samples, to identify genuine phagocytosis. **B**) Percentages of phagocytosed cells are summarised in bar charts (**C**) Macrophages were pulsed for 6 hours with 10μg/mL of wild-type p53 peptide, 1000 ug/mL of SW480 freeze thawed lysate or the virus lysate of 2.5 x10^5 SW480 cells. Macrophages harvested using non-enzymatic dissociation buffer and stained on the surface for MHC I: p53 and EGFR (to gate out any SW480 expression of MHC I: p53). Results represent receptor positivity, determined by flow cytometry using a BD FACS Calibur™ . Results represent n=3, with errors bars indicating SD

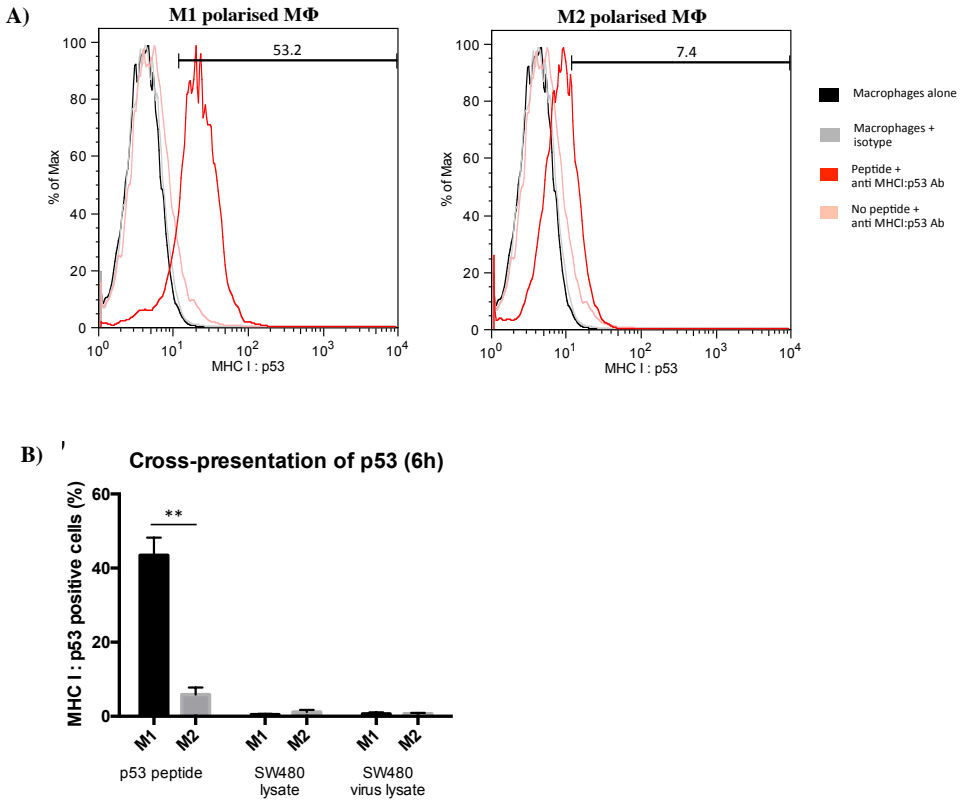


Figure 5.22 Cross presentation of virus-infected p53-positive tumour cells

M1 and M2 polarised macrophages were generated as previously described, seeded in 48 well plates at a density of 2.5 x10^5 cells/ well. **A)** Macrophages were pulsed for 6 hours with 10µg/mL of wild-type p53 peptide or with an equivalent volume of media (no peptide control), after which time they were stained for MHC I:p53 complexes on the surface. **B)** Additionally, M1 and M2 macrophages were pulsed with lysates from 2.5 x10^5 un-treated or virus infected (1000VPC, 72 hours) SW480 cells for 6 hours and the levels of MHC I:p53 complexes on the surface of macrophages assessed by flow cytometry. To ensure MHC I:p53 levels were specific to macrophages, samples were co-stained with EGFR to identify SW480 cells, which were then removed from the analysis. Percentages of macrophage p53 cross presentation cells are summarised in a bar chart. Results represent receptor positivity, determined by flow cytometry using a BD FACS Calibur™ . Results represent n=3, with errors bars indicating SD. Statistical analysis of significance was performed by one-way ANOVA, with a Tukey post-test. P<0.01 (**)

5.3 Discussion of results

A central objective of this chapter was to identify functional assays that might discriminate between macrophages of different polarisations. NO was chosen as a key assay to investigate as the enhanced production of NO is one of the better-described attributes of a pro-inflammatory macrophages (MacMicking et al., 1997). The ability for such macrophages to produce NO has been well described as a major effector mechanism to control bacterial infections. As a potential marker of a macrophage population that could be of therapeutic benefit in the tumour, NO is of particular importance. Indeed, NO producing macrophages have been previously identified as a tumouricidal population of cells that can contribute to tumour cell apoptosis and the induction of an anti-tumour immune response (Keller et al., 1990; Miguel et al., 2010).

With the potential toxicity associated with NO radical formation, production of NO is a well-regulated process. Under inflammatory conditions requiring NO production, IFN-γ can signal through STAT-1 to increase binding of the interferon-response element, IRF-1, to the iNOS promoter. Under anti-inflammatory conditions however, such as in environments rich in IL-4, -10, or -13, signalling through STAT-6 increases IRF-2 production which can antagonise and outcompete IRF-1, thereby suppressing NO production (Mosser and Edwards, 2008). Consistent with this, the results of alternatively polarised macrophages showed that there are distinct patterns of NO production between M1- and M2-polarised cells.

The large separation in NO production between M1 and M2 macrophages made this assay appealing for re-education experiments, as this might provide an opportunity to see clear re-polarisation of cells. The results of the re-education experiments were

extremely positive, as both human and mouse macrophages previously polarised by IL-4 were able to be re-educated towards an M1-type phenotype. Such data supports the hypothesis that macrophages can be re-polarised and identify NO production as a marker with which to detect such polarisation. It is interesting to note that that other Th2 cytokines have been studied in a similar manner to examine their ability to inhibit NO production in macrophages. When the highly immunosuppressive cytokine IL-10 was added to activated murine macrophages, it was demonstrated that there was no inhibition NO production; treatment of IFN-γ-polarised macrophages with IL-10 actually augmented NO production (van Den Broek et al., 2000).

The only example where the increases in NO following re-education were not significant was in the case of human macrophages re-educated in the presence of existing M2 media. It would be interesting to explore whether such results could be improved by increasing the concentrations of LPS and/or IFN-γ, or increasing the time length of re-education by 12-24 hours.

It has been shown previously that both herpes simplex (HSV) and measles viruses (MV) are able to stimulate NO production in macrophages, albeit by different mechanisms of action. Infection with herpes has been shown to increase NO through simulating TNF-α, which can then act in an autocrine manner to stimulate macrophages. Importantly, HSV infection has been shown to overcome inhibition to IL-4 to increase NO production (Paludan et al., 2000). Similarly, previous work has identified that CD46 ligation by measles virus might engage NO and IL-12 production in macrophages, by a mechanism involving recruitment of SHP-1 phosphatase (Parker et al., 2000). In these studies, measles virus was identified for its ability to up-regulate NO production

however this was only identified in macrophages with co-treatment of IFN-gamma (Paludan et al., 2000). Such findings may be of particular relevance for ColoAd1. Unlike other adenoviruses that infect cells via CAR, group B adenoviruses utilise CD46 for entry; an interaction which on immune cells has been demonstrated to induce suppressive signalling, even when immune cells are pre-stimulated with inflammatory cytokines. The data presented here indicate that ColoAd1 can potently activate NO production, at similar levels to those obtained using CD46 ligation by an agonising antibody. To confirm that this is truly an effect mediated by ligation of the CD46 by virus however, it would useful to repeat these experiments in the presence of a blocking CD46 antibody or to use an additional ColoAd1 virus genetically engineered such that it no longer binds CD46 (one such virus is currently under construction in the laboratory. The implication that CD46 ligation by virus in the presence of IFN-γ would induce enhance pro-inflammatory NO production in macrophages, seems to be proven correct in these studies the ColoAd1-IFN-γ virus induced significantly higher levels of NO production in all applications studied. It is interesting to note that ColoAd1- IFN-γ virus alone increased NO levels above ColoAd1 alone. Such results may indicate "contamination" by free IFN-γ in the preparations of ColoAd1-IFN-γ particles, or may indicate expression of IFN-γ following infection of macrophages. Importantly, all treatments with virus were able to mediate re-education. It was interesting however, that supernatants from virus-infected tumour cells were more potent mediators of re-education than virus particles alone. Such data suggest that factors released from dying cells following infection might be providing additional stimulation.

Whilst NO appeared to be an ideal candidate for distinguishing differentially polarised macrophages, phagocytosis assays were also evaluated as a means to identify polarised

macrophages. Despite multiple attempts, use of zymosan was not conducive to efficient experimentation as it showed poor solubility and the resulting poly-dispersity of the particles appeared to yield variable results. Importantly, zymosan phagocytosis could not be achieved in the human macrophages during my studies. A number of receptors have been reported to be of central function to phagocytosis of zymosan including Dectin-1, CD14, TLR-2 and TLR-6 (Gantner et al., 2003; Rogers et al., 2013). It was surprising then that zymosan phagocytosis was absent in human macrophage as THP-1 cells have previously been reported to express all the required receptor for effective zymosan up-take (Gantner et al., 2003; Parker et al., 2004; Rogers et al., 2013). The limited usage of zymosan as a functional assay in murine macrophage studies alone precluded its usage in further murine and human macrophage re-education studies. Dextran proved more useful, showing significant differences between M1 and M2 macrophages for both mouse and human cells, albeit in a very concentration-specific manner. Whilst the results of the dextran were promising, it was not pursued further as it was felt that phagocytosis of this ligand would be too heavily dependent on up-regulation of specific glycan binding receptors. Whilst expression of these receptors has been documented in classic models of alternative polarisation, their expression in tumours has not been definitively characterised. As future studies intend to use these functional assays in more complex tumour models, future examination of the receptors underpinning dextran uptake in these contexts would need to be performed before this assay could be utilised.

It has previously been identified that professional phagocytes can engulf OVA by pinocytosis or receptor-mediated endocytosis by utilising scavenger receptors. One such scavenger receptor, the mannose receptor, has been largely attributed with the receptor-

mediated phagocytosis of OVA protein. Importantly, mannose receptor up-regulation was one of the first markers describing alternative activation of macrophages by polarisation with IL-4 alone or in combination with IL-13 (Gordon, 2003). Given that OVA uptake in IL-4 treated murine macrophages was significantly enhanced relative to M1-polarised cells, increased mannose receptor expression present on M2-polarised murine macrophages provides a very plausible explanation for these results. This could be confirmed by blocking antibodies to the macrophage mannose receptor, or pre-treatment with mannan to show that the effect is a specific result of the mannose receptor and not general up-regulation of other scavenger receptors, such as those with mannose-type carbohydrate recognition domains (e.g. DC-SIGN). Such data may explain the results observed for the murine macrophages, however the reason for the lack of any significant differences in OVA uptake using human macrophages remains unclear. Mannose receptor has been identified in both human and mouse macrophages, induced in the same manner through IL-4 polarisation at concentrations equivalent to those used in studies in this thesis. Indeed, differential mannose receptor expression would have easily resolved the differences between human and murine macrophages studies and would have been a simple experiment. Despite significant optimisation of antibody however, human mannose receptor expression could not be identified by flow cytometry and so, a comparison between murine and human macrophage mannose receptor was not possible. A number of experiments could be performed to try and resolve the discrepancy between OVA uptake in human and murine macrophages including further optimisation of mannose receptor staining (using multiple clones of anti-human mannose receptor antibody) and increasing concentration ranges of OVA, but this was not a significant focus of the thesis. Instead, research was focused onto the antigen presentation of OVA in the mouse model.

Whilst increased uptake of OVA by M2-type macrophages provided a good functional marker to distinguish M1- and M2- polarised cells, it was concerning that this factor might prohibit further studies examining presentation of OVA on MHC I. OVA was chosen as a model system for antigen presentation in order to define the differential effect of macrophage polarisation on the ability to cross-present antigen; a readout that would be presumably skewed, if there was such preferential uptake of OVA by M2 macrophages.

It was intriguing to note then that the level of antigenic processing was significantly higher for M1-type macrophages. Is has been shown previously that cytokines such as IFN-γ can increase the processing capacity of antigen presenting cells through a number of factors including subunit switching of the proteosome (Schroder et al., 2003). The significant differences in antigenic processing obtained here may well suggest that whilst M1-type endocytose less OVA, they are better able to process and present the antigen that they have endocytosed. Clearly a fine balance of proteasome activation is required, as excessive proteolytic activity could be deleterious to the quality of peptides being generated. In the context of this assay however, increased DQ-OVA activity has been shown to correlate with increased antigen presentation and T cell stimulation in a number of studies (Ichihashi et al., 2013). In the context of cross-presentation, the increased processing of OVA-DQ observed by M1 macrophages cannot be directly correlated to the results of SIINFEKL cross-presentation. However, such results do suggest that M1 macrophage may possess a increased propensity for antigen processing relative to M2 cells. From these data it is clear that M2 macrophages are significantly

more effective at phagocytosis of full length protein (OVA), but that M1 macrophages are better at cross presentation of peptide (SIINFEKL).

A central aim for this chapter was to assess the cross-presenting capacity for macrophages of different polarisation. Initial work focused on the OVA-derived octapeptide, SIINFEKL, for which flow cytometric analysis of cross-presentation has been well-established. The results demonstrated that macrophages cultured in LPS and IFN-γ are significantly better at cross-presenting SIINFEKL peptide than their M2-polarised counterparts. Such results confirm the original hypothesis that IFN-γ would facilitate cross-presentation of antigen and that macrophages of an M1-type polarisation would consequently be more efficient at cross-presentation.

IFN-γ has been shown to facilitate processing of antigen by inducing the switch from the constitutively active proteasome, to the immunoproteasome by induction of new subunits such as LMP-2, LMP-7, MECL and PA28 (Niewerth et al., 2014; Schroder et al., 2003) Further, IFN-γ has been shown to facilitate peptide transport and loading, inducing the ER transporter TAP, the chaperone protein Tapasin and increasing levels of MHC I (Schroder et al., 2003).

The results of the cross-presentation of SIINFEKL were promising, however, SIINFEKL requires no processing before presentation on MHC I and perhaps does not create the most realistic of tumour models. As such, the ability of full-length OVA to be presented was investigated further. The implication that the increased uptake of OVA is mediated through mannose-receptor-mediated endocytosis is of particular importance as it has been shown that the route by which OVA (and other extracellular antigen)

enters a cell has significance for antigen presentation (Burgdorf et al., 2008; Klotz et al., 2009). Using the OVA model in murine dendritic cells, receptor-mediated uptake of OVA by the mannose receptor exclusively directs uptake and cellular processing towards cross-presentation on MHC-I (Burgdorf et al., 2007). Alternatively, uptake by alternative means (such as pinocytosis) largely resulted in presentation toward MHC-II, and cross presentation to MHC I to a lesser extent. Whether the same pattern exists for macrophages had not been fully explored.

Despite significant optimisation of the assay, cross-presentation of full length OVA could not be observed by either M1- or M2-polarised macrophages. Whilst concentrations within the range used here have previously been shown to induce cross presentation of OVA, the readouts have almost exclusively been at the level of T cell proliferation and have not been demonstrated using the flow cytometry staining of the MHC I:SIINFEKL complex. That the majority of researchers utilise T cell proliferation as a read-out for OVA cross-presentation, may suggest technical limitations in the ability of the antibody to detect of cross-presented OVA and certainly highlight that T cell proliferation is the more established technique. Future work should therefore look to repeat much of this experimentation using T cell proliferation assays, pulsing macrophages with OVA in the presence of T cells isolated from OTII mice, whose T cells have a transgenic T cell receptor that endows specificity for SIINFEKL (Robertson et al., 2000). Utilising T cell proliferation would also advantageous as it provides a more accurate readout of cross presentation; whilst detection of the MHC I-SIINFEKL complexes demonstrates that the antigen can be processed and presented on the cell surface, it doesn't necessarily mean that this would correlate with effective cross-presentation to T cells to induce activation. T cell activation is determined by the

stimulatory or inhibitory cytokines and surface receptors present on the antigen-presenting cell. Of particular relevance to the tumour microenvironment, antigen presented by PD-L1-expressing dendritic cells induce T cell tolerance and down-regulation of the T cell receptor (Karwacz et al., 2011). As such, studying cross presentation by T cell proliferation would provide a more comprehensive assay.

It has been shown that opsonised soluble antigen can be presented to both MHC I and II. It particular, this can be utilised as a means to circumvent reduced antigen uptake. One such example is in the case of plasmacytoid dendritic cells, which in mice, have been shown to have an impaired ability to phagocytose extracellular antigen. Here, opsonisation of antigen is able to overcome the reduced antigen uptake and facilitate antigen presentation to both MHC I and II. Importantly, it has been demonstrated that IgG-opsonised antigen can be routed for cross presentation when receptor mediated uptake proceeds through stimulatory Fc receptors such as CD64 (Platzer et al., 2014).
IFN-γ has been to shown to up-regulate a number of stimulatory Fc receptors on macrophages and dendritic cells, including CD64 and CD32a, whilst down-regulating suppressive Fc receptors such as CD32b (Boruchov et al., 2005; Nimmerjahn and Ravetch, 2008; Tridandapani et al., 2002). In the experiments performed in this chapter and previously in this thesis, treatment of macrophages with IFN-γ alone or in combination with LPS has induced CD64 up-regulation.

Opsonising OVA with polyclonal serum generated from OVA vaccinated mice was able to rescue the deficit in OVA uptake observed between M1- and M2- polarised macrophages. Taken together with the CD64 staining, such data imply that opsonised OVA can be endocytosed via the increased expression of activatory Fc receptors present

on IFN-γ-polarised macrophages; blocking experiments using antagonistic antibodies against CD64 and CD32A would be required to confirm that this is the mechanism by which OVA uptake is being restored. With previously published data suggesting that endocytosis of opsonised antigen can facilitate presentation of antigen in cells with impaired phagocytosis, opsonised OVA was added to macrophages to see if this may restore the absence of cross-presentation, however this was not successful.

The most relevant context for cross-presentation studies of tumour antigen, would be antigen associated with tumour cells. To this end, B16F10 melanoma cells transduced with OVA protein were lysed for usage as an OVA substrate. Previous reports have demonstrated that the localisation of antigen can make a significant impact on its presentation, with indications that cell-associated antigen may be presented in a far more efficient capacity than free protein (Gutiérrez-Martínez et al., 2015; Wolkers et al., 2004). In the case of OVA it has been demonstrated that cell-associated OVA can be cross-presented and induce T cell stimulation to a far higher extent than cytosolic or free OVA protein (Shen et al., 2004). Here it was thought that in the cellular-association of OVA on B16 cells combined with the addition of additional signals such as DAMPs from the cell lysis combined might increase cross presentation on macrophages. Cross presentation of antigen cell associated OVA was tentatively observed, but only for the M1-polarised cells and should be subject to further experimentation to validate its authenticity; as it stands, it would be hard to conclusively conclude that either full length or cell-associated OVA is cross presented in the studies performed in this thesis. As discussed at some length previously in this chapter, T cell studies would provide a logical extension of the OVA cross-presentation experimentation. A major concern with the cross-presentation data from B16-OVA lysate was the low levels of SIINFEKL-

MHC I complex identified by flow cytometry. With no data (that I have been able to find to date) that supports detection of cross-presented full length OVA by flow cytometry, it hard to compare these levels of detection with other reports; this result warrants further investigation. Such a result would be in contrast with the supporting cellular phagocytosis data, that indicated M2-type macrophages had ingested more dead tumour cells expressing OVA. Such results are perhaps quite concordant with the earlier processing data with DQ-OVA, suggesting that IFN-γ-polarised macrophages are better equipped for processing antigen for cross presentation than IL-4 polarised cells. That M2-macrophages ingest more necrotic tumour cells is quite an interesting result on its own, although is perhaps not unexpected. Much data attributes M2 macrophages with increased scavenger activity and regulation of tissue repair (Sica and Mantovani, 2012). Certainly, it has been shown that increased phagocytosis of apoptotic and necrotic cells can drive macrophage polarisation toward an M2 phenotype (Ferracini et al., 2013).

Extending this work into a human model, the opportunity to study cross-presentation of tumour-associated antigen at the level of the antigen-presenting cell is limited, however collaboration enabled the study of antigen presentation of the tumour-associated p53 peptide. Here, we found that results of the human macrophages confirmed those in the mouse models, showing that M1 macrophages are able to cross-present wild-type p53 peptide far more than M2-polarised cells.

The advantage of a human cellular system for these studies is that the ColoAd1 can be utilised to study the effect of viral-lysed cells on cross presentation of tumour-associated antigen. A series of experiments were performed to lyse the SW 480 cell line

using ColoAd1, a colorectal line with the mutant p53, which could then be used to pulse macrophages and assess cross-presentation. Whilst subject to two point mutations, the transcription factor p53 in the SW480 cell line is by no means over-expressed. For future studies, it may be advisable to increase expression of p53 somehow. Induction of cell stress by UV irradiation been shown to enhance accumulation of p53 in a range of cell types and certain adenoviruses have been shown to exert similar effects (O'Hagan and Ljungman, 2004; Querido et al., 1997). It was hoped that in addition to facilitating cell lysis and release of additional DAMPs and PAMPs, virus infection might also act to increase p53 levels. It has been previously shown that for certain adenovirus serotypes (such as Ad1-3, -7 and -11) infection is associated with accumulation of p53 in a process mediated by the adenovirus E1B-55K protein (Lomonosova et al., 2005; Zhang et al., 2005). Given the interest of p53-orientated vaccination strategies and antigen presentation studies in ovarian cancer, combined with the potential p53 accumulation induced by virus, this could have been a fortuitous opportunity to study the impact of virus infection on antigen presentation of a tumour antigen within a human setting. Whilst there was no cross-presentation observed for the SW480 lysates, it would have been advisable to add a HLA-A2 mismatched tumour cell line as an additional control. This becomes of particular importance in assays such as these, where two different cell types are left in high concentrations for long incubations as this could enhance transfer of MHC I complexes between cells; transfer of pre-formed peptide-MHC I complexes to antigen-presenting cells has been described in a term coined "cross-dressing" (Wakim and Bevan, 2011). Such work will require further optimisation of cross-presentation of cellular p53 before it can be utilised in this manner.

Chapter 6

Studies of macrophage polarisation and re-education using translational models

6 Studies of macrophage polarisation and re-education using translational models

6.1 Introduction

This chapter seeks to build upon the *in vitro* findings from chapters 3 and 4 by looking at macrophage re-education in more advanced pre-clinical models. Cell culture has its value in helping to identify important receptors and pathways but it is the tumour microenvironment that can really influence macrophage behavior. After cell culture, mouse models are typically used as the next stage along a research pathway, but for the subjects of this thesis (viruses and cytokines and macrophages) species-specific events can limit the utility of animal models (Eggerding and Pierce, 1986; Hay, 2003; Jakeman et al., 2015b). In the case of ColoAd1, murine cells are not permissive to replication and only xenograft models can be used, and this raises issues both of the immune-incompetence of the host animal and the species mismatch between the tumour cells and macrophages which are the focus of these studies. Working with relevant model systems is important because failing to develop or interpret model systems correctly is often cited amongst the reasons for poor outcomes in clinical trials (Jakeman et al., 2015b).

The imperative to develop more representative pre-clinical models is best illustrated by the low success rates of drugs developed using conventional pre-clinical models (Hoelder et al., 2012). Of the lead candidates identified using classical *in vitro* and *in*

vivo experimentation, less than 10% of these will ever reach the final stages of a clinical trial, the majority failing not because of unacceptable toxicity, rather because they show insufficient therapeutic efficacy (Jakeman et al., 2015b). This indicates a problem with the models themselves giving deceptively positive results (rather than toxicity-sensitive tissues that are not included in the model), most likely because the reductionist approach removes many of the factors that confound drug activity in the clinical setting.

With this in mind, it can be useful to supplement murine studies with work using primary human cells and biopsies. *Ex-vivo* biopsy culture of human tumours is a useful approach that can provide the correct context for cells including appropriate multicellular interactions and extracellular fluid components. Human ovarian ascites offers a particular interesting *ex-vivo* model with relatively easily available biopsy material containing macrophages, lymphocytes cancer cells and fibroblasts. A number of cellular studies have been performed using this model and several important features of cellular interactions and immune suppression have been identified. However, unlike work in mice *ex-vivo* models are closed systems and generally only useable for a relatively short period of time. Biopsies are also variable between subjects or even between drains in the same subject as disease or treatments progress. No single model system appears to perfectly recapitulate every aspect of the clinical disease, it is therefore important to use more than one model while recognizing the strengths and weaknesses of each.

In this chapter, murine and human models have been developed to study ovarian cancer using peritoneal ascites from xenografted IGROV-1 cells in murine hosts and also ascites drains taken from patients with ovarian cancer. In advanced ovarian cancer, the

development of ascites is thought to involve the disruption of tumour capsules within the ovaries, disseminating into the peritoneal space in the form of free tumour cells or spheroid cells (Ahmed and Stenvers, 2013). This is often accompanied by excessive fluid transfer into the peritoneal space. From here, tumour cells are able to migrate to distant organs, promoting metastases to multiple sites. The discomfort of such fluid results in patients attending the ward frequently to have their fluid drained, in a non-invasive, outpatient-based procedure, providing an opportunity to collect these samples for research (Kipps et al., 2013).

Previously in this thesis, supernatants from tumour cell lines have been used to generate a phenotype which more closely resembles a TAM than macrophages polarised with IL-4 alone. This work is extended here to examine what effects tumour ascites might have on macrophage polarisation. Macrophages isolated from solid tumours of patients with ovarian cancer have been identified as suppressive cells, but not as much is known about macrophages in the context of ascites (Hagemann et al., 2006). Ascitic fluid is known to contain tumour and stromal cells along with a range of soluble factors that may contribute to an immune suppressive environment, which may all impact on macrophage polarisation and the efficacy of immunomodulatory oncolytic virotherapy (Kipps et al., 2013).

6.1.1 Chapter aims

1. To evaluate macrophage phenotype and potential for "re-education" in a murine xenograft model of ovarian cancer.
2. To develop a methodology maintaining malignant peritoneal ascites *ex vivo*, for sufficient time to conduct virus infection and macrophage re-education studies in clinical biopsy samples
3. To explore whether therapeutic "re-education" of ascites macrophages is a plausible therapeutic strategy and evaluate whether IFN-γ can mediate such "re-education"

6.2 Results

6.2.1 Developing a murine xenograft model of ovarian peritoneal ascites

6.2.1.1 IGROV IP Pilot study: time for ascites development

An early objective in developing this experimental system was to see whether human tumour cells could polarise murine macrophages towards a suppressive TAM phenotype. If so, this would provide an *in vivo* model in which to test the ability of oncolytic virus expressing murine IFN-γ (mIFN-γ) to re-educate TAMs.

In pilot studies using an intraperitoneal IGROV-1 xenograft model, an important cellular read-out was to demonstrate the presence of both tumour cells and macrophages, to ensure the sufficient presence of a host cell for virus infection and a target cell for secondary activation, respectively. Tumour cell numbers appeared very low for the first 15 days following I.P. injection of tumour cells (< 5% of total peritoneal cells), increasing by the final time point to constitute approximately 20% of the total cellular mass within the ascitic fluid (*Figure 6.1*). Macrophage numbers were far more consistent, constituting greater than 50% of the total cells within the ascitic fluid throughout.

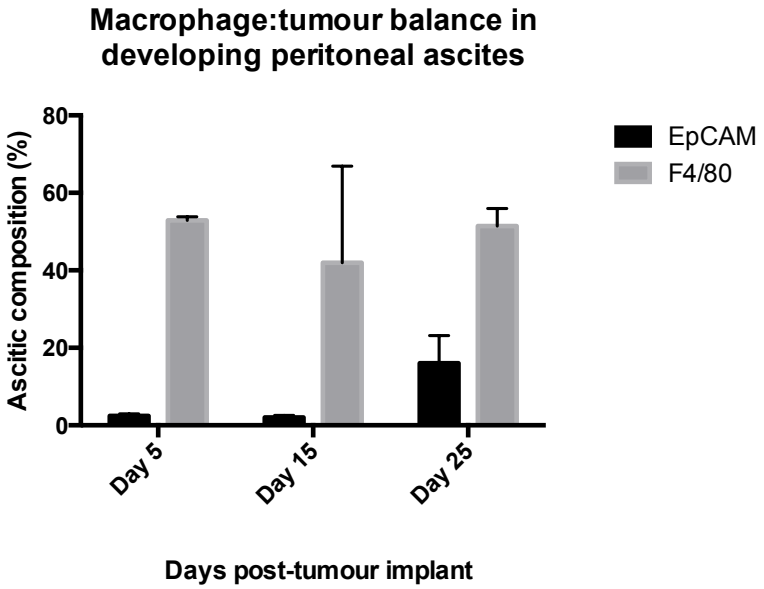


Figure 6.1 Development of a peritoneal IGROV-1 xenograft model

12 Balb/c Nude mice were injected I.P. with 2 x 10^6 IGROV-1 human tumour cells. Peritoneal fluid was harvested at days 5, 15 and 25 by peritoneal lavage, with the peritoneal cavity washed with an additional 5mL of PBS (0.5mM EDTA) to ensure collection of all cells. Cells were treated with an Fc block and live/dead stain, then stained for human EpCAM (epithelial cellular adhesion molecule, EpCAM, is a glycosylated membrane protein responsible for signalling and adhesion events. Whilst present on normal epithelial cells, its expression is significantly up-regulated in a number of tumour types including ovarian and colorectal cancers (Munz et al., 2009) and F4/80 (a transmembrane protein expressed on a number of murine macrophage subsets) and analysed for receptor positivity using a FACS Calibur™. Results represent n=4 (where n corresponds to the number of animals per group/time point), with errors bars indicating SD. Statistical analysis of significance was performed by one-way ANOVA, with a Tukey post-test

6.2.1.2 IGROV IP Pilot study: phenotype of peritoneal macrophages

The phenotype of the macrophages was monitored across the course of the experiment to determine if human tumour cells are able to polarise murine macrophages towards a TAM phenotype. The results of the receptor staining were quite variable, with the macrophage expression of CD64 and CD86 resembling an M2-type macrophage, whilst expression of MHC II and CD80 was far more similar to an M1-type profile (*Figure 6.2*). It might be expected that changes in receptors may emerge as tumours progress, however no dramatic patterns of changes in receptor expression on these macrophages were observed over time; there were slight increases in CD64 expression and slight decreases in CD80 expression, however these were not statistically significant.

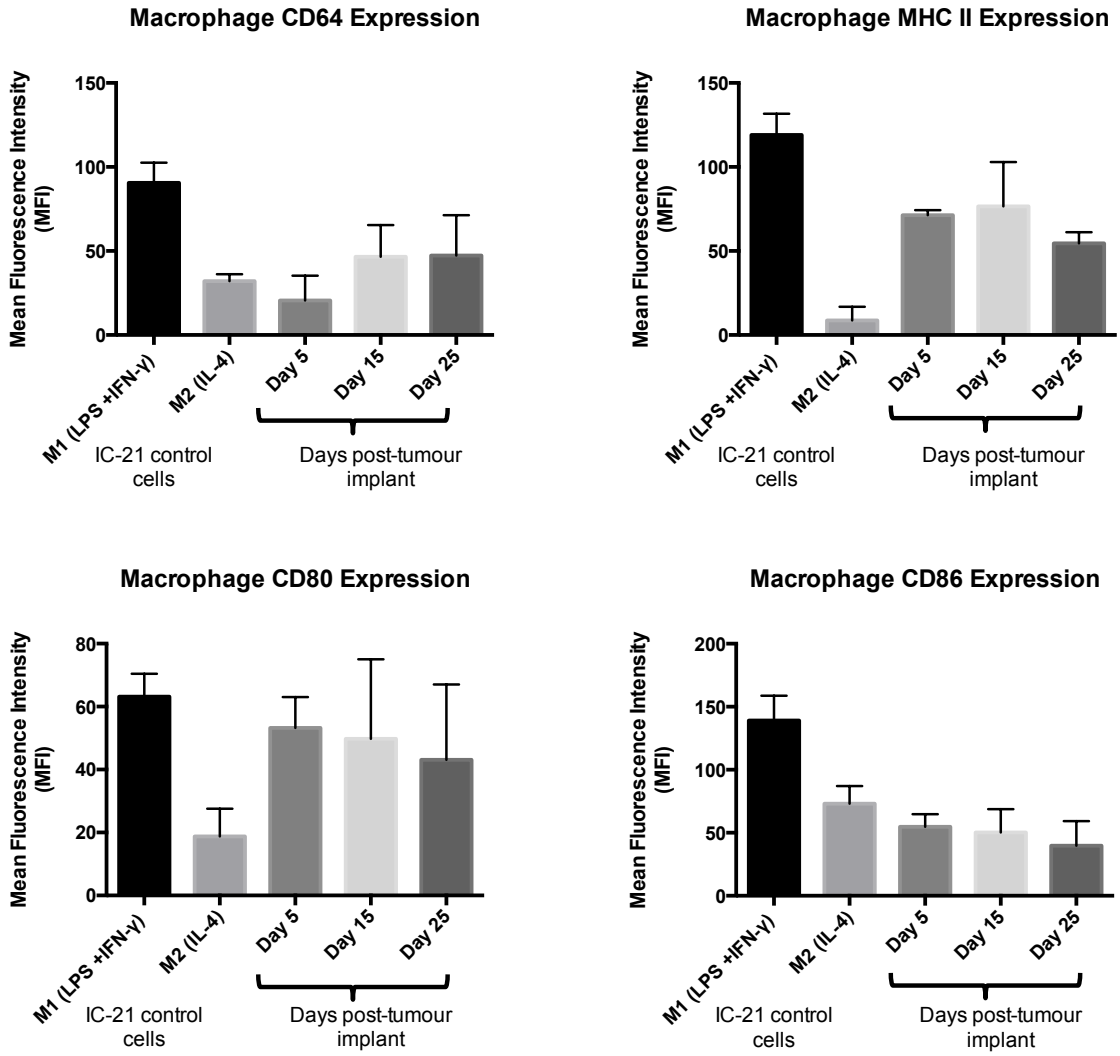


Figure 6.2 Phenotype of peritoneal macrophages during ascites formation

12 Balb/c Nude mice were injected I.P. with 2 x 10^6 IGROV-1 human tumour cells. Peritoneal fluid was harvested at days 5, 15 and 25 by peritoneal lavage, with the peritoneal cavity washed with an additional 5mL of PBS (0.5mM EDTA) to ensure collection of all cells. As controls for differential receptor expression, IC-21 murine macrophages were polarised for 24 hours toward M1 or M2 phenotypes (as previously described). Cells were stained for F4/80, then co-stained for MHC II, CD64, CD80 or CD86 and analysed for their mean fluorescence intensity using a FACS Calibur™. Results represent n=4, (where n corresponds to the number of animals per group/time point; except in the case of IC-21 cells, for which n equals biological replicates). Errors bars indicating SD. Statistical analysis of significance was performed by one-way ANOVA, with a Tukey post-test

6.2.1.3 IGROV IP Pilot study: characterising immune cell in ascites

From these results, it was clear that the 25 day post- tumour implant would be the optimal time for therapeutic intervention as there was sufficient tumour cells and macrophages present, even if the phenotype of these resident macrophages were not conventionally TAM-like. To determine which other immune cells are present in ascites at this stage, samples were also stained for markers of dendritic cells and NK cells, as polarisation of macrophages and indeed response to oncolytic virotherapy, can be influenced by the other resident immune cells (*Figure 6.3*). High CD11b presence corroborates F4/80 staining, indicating that myeloid cells form the predominant infiltrate in this model of ascites, for which some may also exhibit CD11c positivity. The expression of CD11c is likely indicative of dendritic cells within these samples. Quite a large range of positivity was observed for NK1.1, ranging from 7-30%, which perhaps indicates that NK cell infiltration is somewhat more variable than with other myeloid cell types studied.

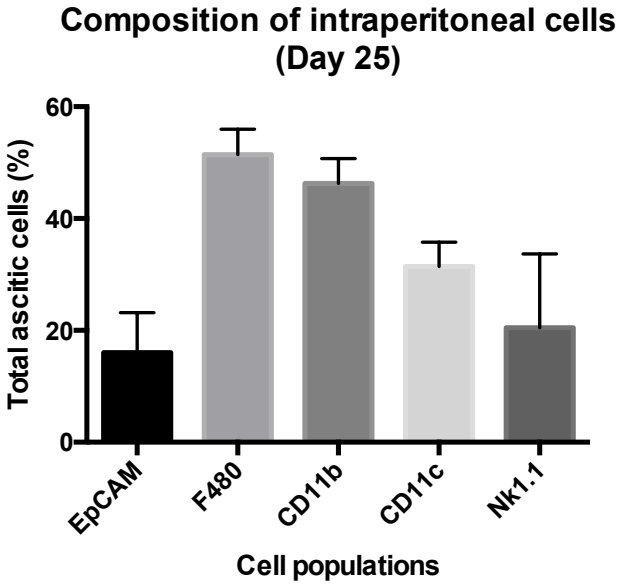


Figure 6.3 Cellular composition of murine peritoneal ascites

Balb/c Nude mice were injected I.P. with 2 x 10^6 IGROV-1 human tumour cells. Peritoneal fluid was harvested at day 25 by peritoneal lavage. Cells were stained for EpCAM, F4/80, CD11b, CD11c and NK1.1, with receptor positivity assessed using a FACS Calibur™. Results represent n=4 (where n corresponds to the number of animals per group/time point)

6.2.1.4 IGROV IP Pilot study: *ex vivo* re-education of macrophages from ascites

Whilst the results of the phenotyping data could not conclusively show that the peritoneal macrophages in this model were following a TAM profile, it was of interest to determine whether these macrophages were still amenable to therapeutic changes in polarisation. As a surrogate for *in vivo* treatment of ascites samples, total cells collected from the 25 day time point were cultured *ex vivo*, and treated for one week with ColoAd1, ColoAd1-mIFNγ or mIFNγ alone to look for any indications of immune modulation assessed by flow cytometry), virus infection (assessed by GFP fluorescence) and production of transgene in the IFN-γ armed virus (assessed by ELISA) (*Figure 6.4*). Given the limited cell numbers available, the GFP-expressing ColoAd1 virus was utilised to assess virus infection (*Figure 6.4A*). Flow cytometry revealed that all samples were infected with virus, although the levels varied from 10-40% GFP-positivity which could reflect the varying tumour numbers present in the ascites samples. Infection with the ColoAd1-mIFNγ virus was also successful, with all treated samples producing mIFNγ in the range of 20-90 pg/mL (*Figure 6.4B*). mIFNγ was undetectable in all other samples and importantly was absent from the mIFNγ-treated sample. Such results highlight the short half-life of this cytokine, validating the virus-mediated delivery approach described in this thesis.

High MHC II expression has consistently proved one of the most effective markers of M1 macrophage polarisation in this thesis and was used here to examine any changes in macrophage phenotype (*Figure 6.4C*). Both ColoAd1 and ColoAd1-mIFNγ treatments led to increased MHC II levels in macrophages above PBS control and mIFN-γ, however significant increases were only observed for ColoAd1 treatments compared to

PBS alone. The lack of increase in MHC II in response to mIFN-γ seems surprising, although this might reflect the absence of mIFN-γ observed in the ELISA.

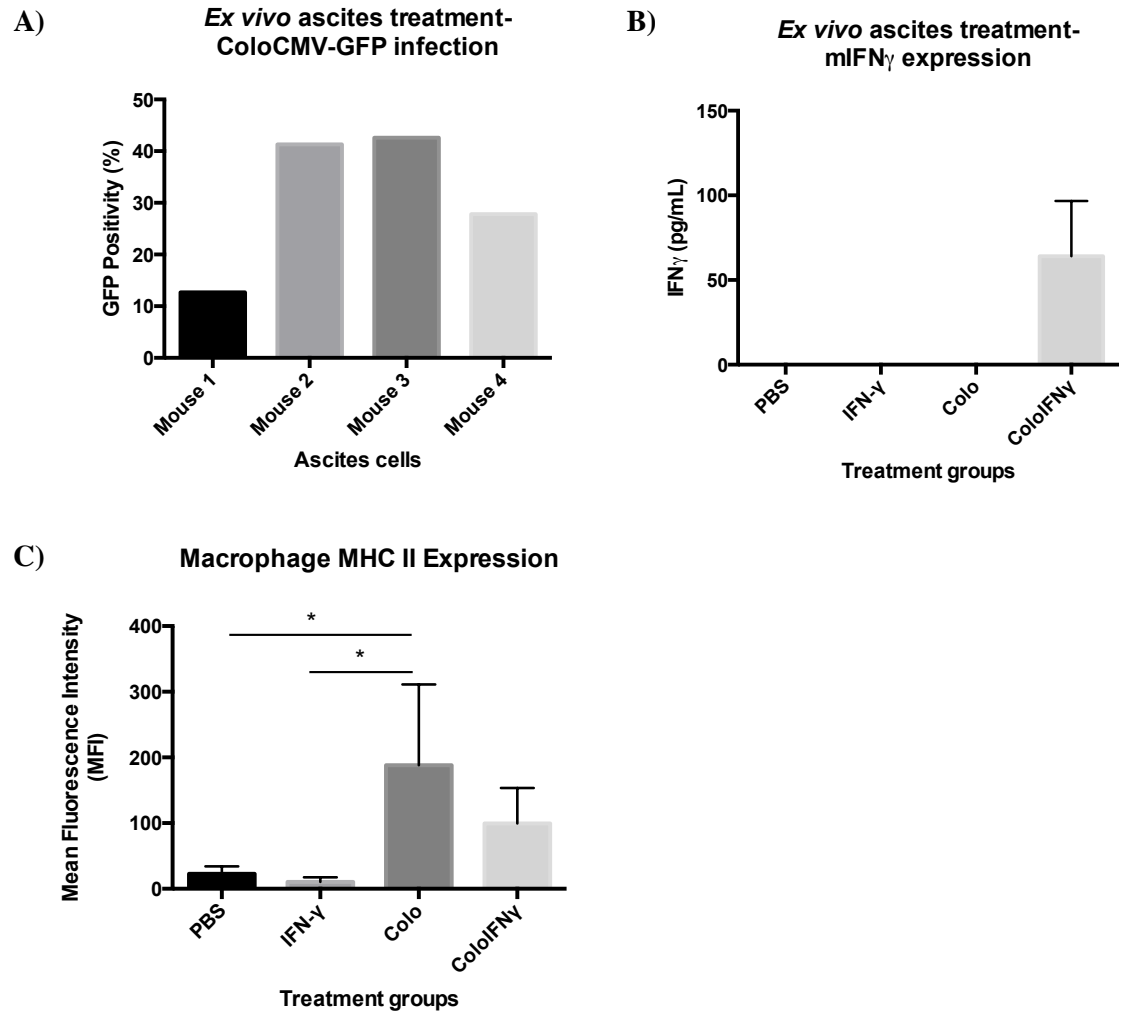


Figure 6.4 ***Ex vivo*** **treatment of peritoneal ascites**

Peritoneal ascites cells were obtained from mice that were allowed to develop ascites for 25 days. Cells were seeded at a concentration of 2 x 10^5 cells per well in 48 well plates in RPMI (2% FBS). Cells were treated with PBS (control), 10ng/ml murine IFNγ, ColoAd1-GFP ($8x10^{10}$ VP/mL) or, ColoAd1-mIFNγ ($8x10^{10}$ VP/mL) for seven days. Cells were harvested using non-enzymatic methods, stained for F4/80 and MHC II and analysed by flow cytometry, whilst supernatants were probed for levels of mIFNγ by ELISA. **A)** GFP positivity was assessed as a surrogate for virus infection by flow cytometry. **B)** To assess virus produced mIFN-γ, an ELISA was performed to look at relative levels of mIFN-γ in samples. **C)** Macrophages were stained with F4/80, and their expression of MHC II was assessed by mean fluorescence intensity using a FACS Calibur™. Results represent n=4 (where n corresponds to the number of animals per group), with errors bars indicating SD. Statistical analysis of significance was performed by one-way ANOVA, with a Tukey post-test. $P<0.05$ (*)

6.2.1.5 IGROV IP Pilot study: *in vivo* treatments

Having demonstrated that macrophages from murine ascites can have levels of MHC II changed by therapeutic treatment *ex vivo*, the xenograft experiment was expanded to allow study of possible macrophage activation *in vivo*. Mice were given an intraperitoneal injection of IGROV-1 cells, with ascites allowed to form for 25 days. At this stage, mice were treated with a further intraperitoneal injection of PBS, mIFN-γ, ColoAd1 or ColoAd1- mIFNγ for a week.

Treatment with ColoAd1-mIFNγ seemingly caused an increased total number of cells in the tumour ascites, although this result was not significant (*Figure 6.5A*). Assessing the composition of the ascites demonstrated significant increases in the macrophage content (% total cells) in all treatment groups relative to PBS controls (*Figure 6.5B*). Tumour cells were shown to constitute approximately 40% of the total cellular content in untreated mice (PBS control) however, all treatment groups showed a reduction in EpCAM positivity (*Figure 6.5C*). Whilst the decrease in tumour cell number upon mIFN-γ treatment was not significant, both ColoAd1 and ColoAd1-mIFNγ treatments were able to significantly reduce the number of IGROV cells to less than 5% of the total cells, most likely indicating successful oncolysis by these viruses.

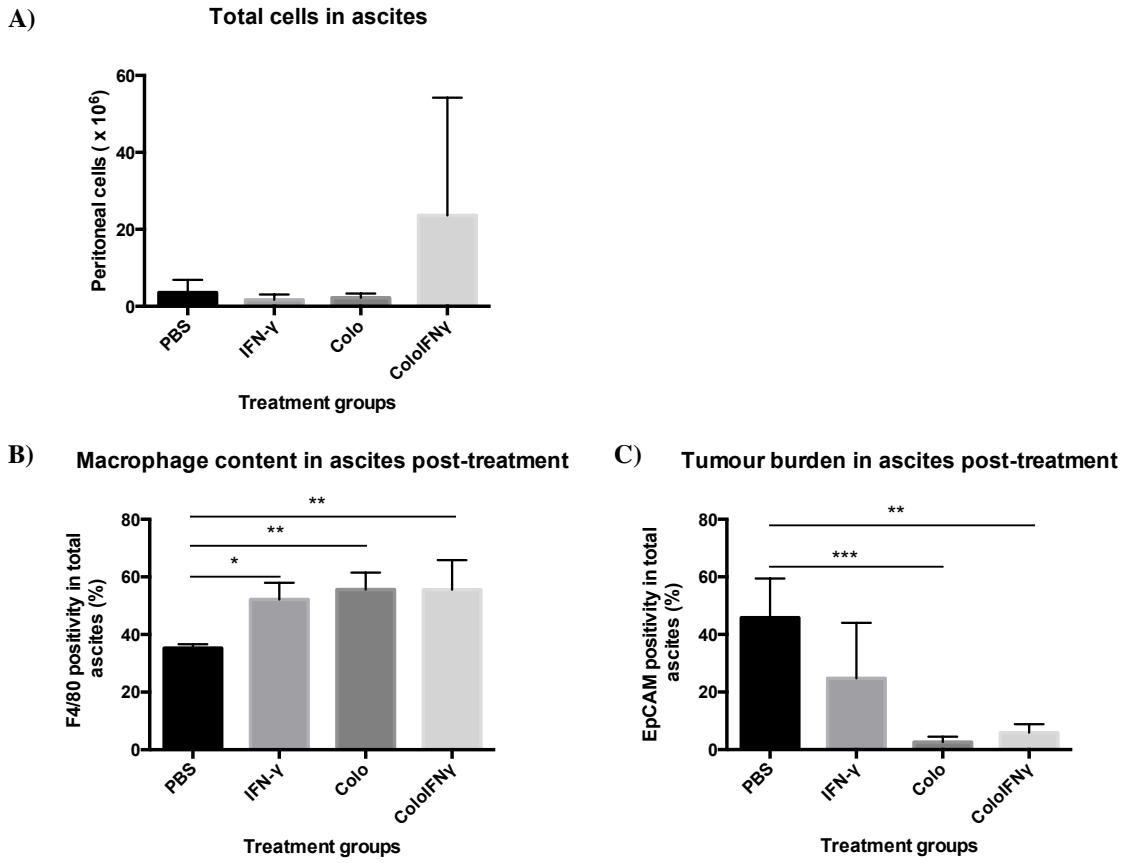


Figure 6.5 Effects of *in vivo* treatment on the composition of murine peritoneal ascites

Balb/c Nude mice were injected I.P. with 2 x 10^6 IGROV-1 human tumour cells, and ascites were allowed to form. After 25 days mice were injected I.P. with 500 µL of PBS (control), murine IFNγ (10ng/ml), ColoAd1-GFP (8x10^{10} VP/mL) or, ColoAd1- mIFNγ (8x10^{10} VP/mL) for 7 days. Cells were harvested by peritoneal lavage with PBS in final volume of 5 mL. **A)** Total cell numbers were determined using the Countess automated cell counter (Life Technologies ™). Cells were incubated with an Fc block, stained with a Live/dead cell stain before staining for **B)** F4/80 or **C)** EpCAM, to assess the number of macrophage and tumour cells respectively. Receptor positivity was determined using a FACS Calibur™ . Results represent n=6 (where n corresponds to the number of animals per group), with errors bars indicating SD. Statistical analysis of significance was performed by one-way ANOVA, with a Tukey post-test. $P<0.05$ (*)

6.2.1.6 IGROV IP Pilot study: *in vivo* re-education of macrophages in murine ascites

To assess whether the increased macrophage infiltrate caused by various treatments correlated with a change in polarisation state, macrophages were stained for expression of CD64, CD80, CD86 and MHC II expression (*Figure 6.6*). ColoAd1-mIFNγ-treated macrophages showed significant increases in MHC II expression relative to PBS, and ColoAd1 treatment. ColoAd1-mIFNγ also increased MHC II levels relative to mIFN-γ alone, but this change was not significant. There were some subtle increases in the levels of CD86 for the IFN-γ and ColoAd1-mIFNγ treated groups as compared to control, however, the increases observed were not significant. CD64 receptor levels appeared to be higher for both groups.

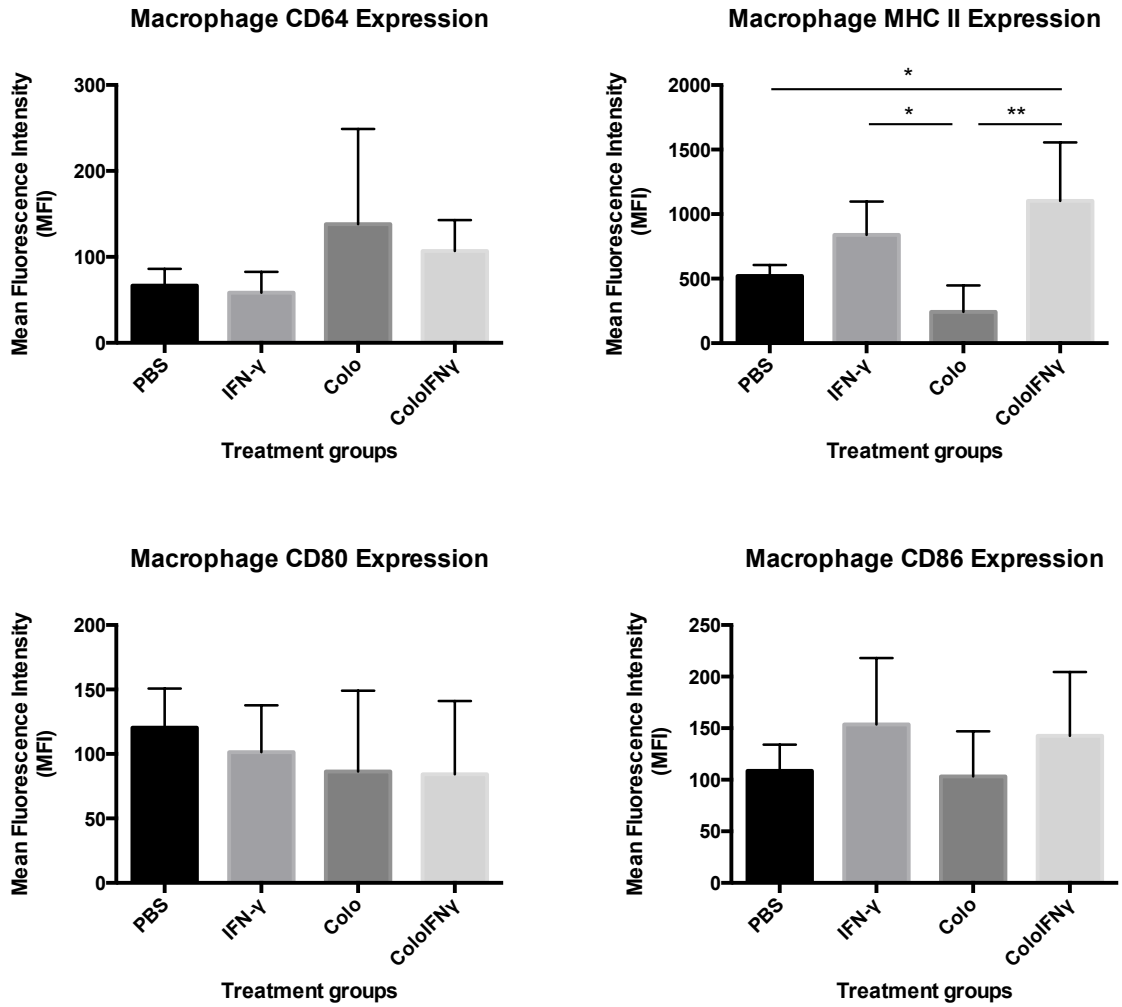


Figure 6.6 Phenotype of murine ascitic macrophages after treatment *in vivo*

Balb/c Nude mice were injected I.P. with 2 x 10^6 IGROV-1 human tumour cells, and ascites were allowed for form. After 25 days mice were injected I.P. with 500 µL of PBS (control), mIFNγ (10ng/ml), ColoAd1-GFP ($8x10^{10}$ VP/mL) or, ColoAd1- mIFNγ ($8x10^{10}$ VP/mL) for 7 days. Cells were harvested by peritoneal lavage with PBS in final volume of 5 mL, incubated with an Fc block, stained with a Live/dead cell stain before co-staining cells with F4/80 in combination with MHC II, CD64, CD80 or CD86. Receptor intensity was measured by MFI using a FACS Calibur™. Results represent n=6 (where n corresponds to the number of animals per group), with errors bars indicating SD. Statistical analysis of significance was performed by one-way ANOVA, with a Tukey post-test. $P<0.05$ (*),$P<0.01$ (**)

6.2.2 Studies into human macrophage polarisation using the ascitic fluid from patients with ovarian cancer

6.2.2.1 Polarisation with ovarian ascitic fluid gives a mixed phenotype of macrophages

Having shown that receptor expression by murine macrophages from malignant peritoneal ascites can be modulated *in vivo*, this work was extended into clinical samples of human ovarian cancer. Human THP-1 macrophages were cultured with human ascites samples for 24 hours and stained for various immune receptors to assess their polarisation state (*Figure 6.7*). For a number of receptors, the pattern of expression was consistent with what would be expected for a suppressive environment. For example the patterns of expression of CD40, CD80, CD86 and MHC II, were similar between ascites-polarised and M2 macrophages, and were significantly decreased relative to their M1 and hIFN-γ-polarised counterparts. MHC I expression was particularly variable between patient samples. Macrophages treated with ascites from patient 36 showed significantly reduced levels of MHC I relative to M2-polarised cells, whilst for patients 35 and 37, expression levels more closely resembled that of M1- or hIFN-γ-polarised macrophages. A similar pattern was observed for CD169 expression, with levels of this receptor on patients 35 and 37 resembling closely the hIFN-γ-polarised macrophages, whilst levels were reduced for patient 36 akin to the expression demonstrated by M2-polarised cells. SIRP-1α expression was maximal in patients 35 and 36, with levels of this receptor appearing marginally higher than the IFN-γ-polarised macrophages. Encompassing all the data from these receptor profiles, it could be inferred that macrophages from these patients display no consistent pro- or anti-inflammatory profile, instead they display a heterogeneous phenotype. Whether this

varied receptor profile correlates with a heterogeneous profile of behaviour was evaluated in the next section.

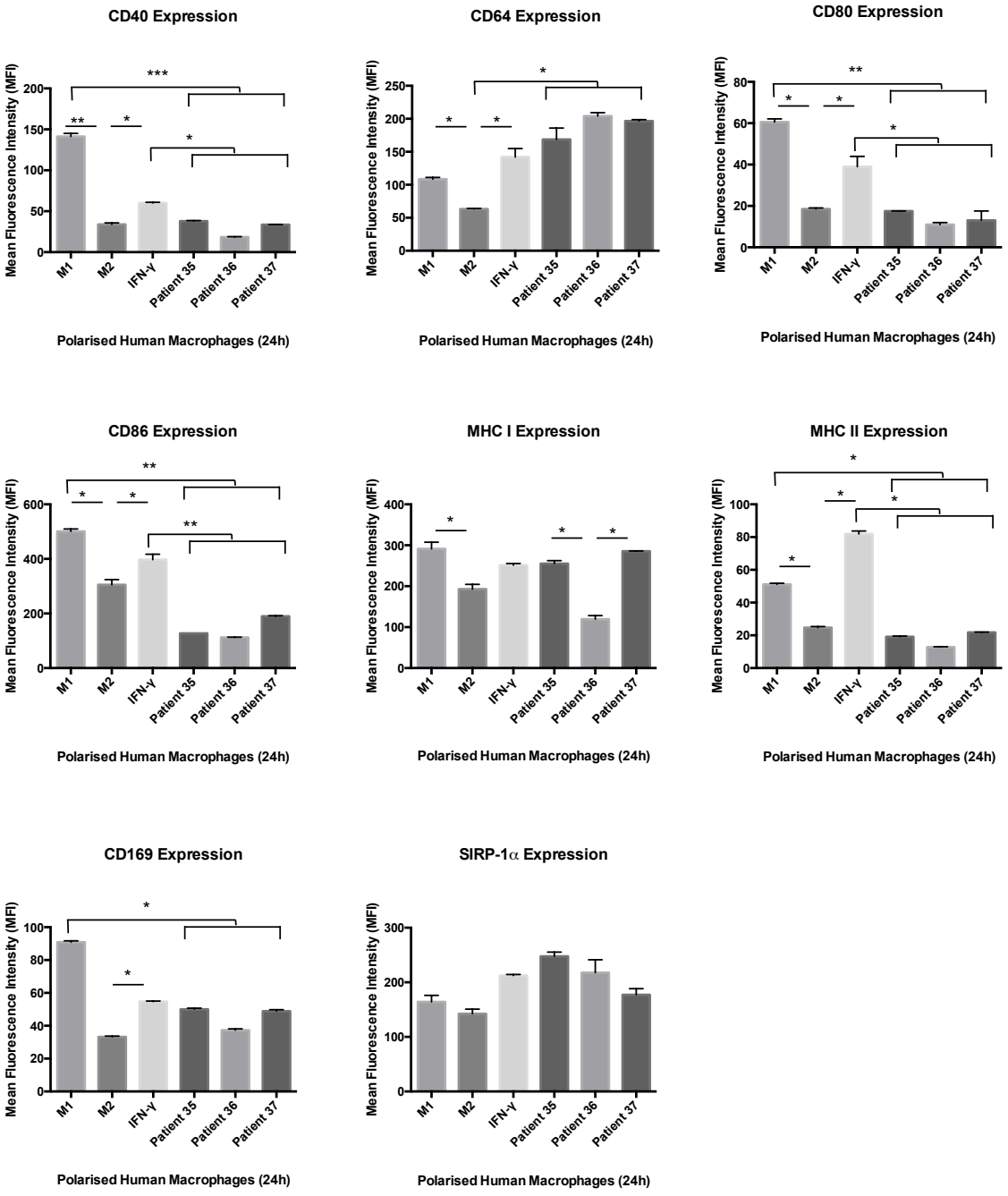


Figure 6.7 Receptor profiles of macrophages polarised with ovarian ascitic fluid

THP-1 macrophages were cultured for 24 hours with M1 media (LPS 1 ng/mL) and hIFN-γ (10 ng/mL), hIFN-γ alone media (10 ng/mL), M2 media (IL-4, 10 ng/mL) or with an acellular fluid obtained from samples of human ovarian ascites. Cells were harvested using non-enzymatic methods, stained for various cell surface receptors, and analysed for mean fluorescence intensity using a FACS Calibur™. Results represent n=3, with errors bars indicating SD. Statistical analysis of significance was performed by one-way ANOVA, with a Tukey post-test. P<0.05 (*), P<0.01 (**), P<0.001 (***) or non-significant (ns)

6.2.2.2 Macrophages polarised by ovarian ascitic fluid can be re-educated using hIFN-γ

Patient ascites samples were used to polarise THP-1 macrophages for 24 hours before media was replaced with either fresh RPMI, or RPMI containing either LPS + hIFN-γ ("M1") or hIFN-γ alone ("hIFN-γ") (*Figure 6.8A*). For CD64 and MHC II expression, treatment with hIFN-γ alone was able to significantly increase receptor levels above non-treated or M1 media treated samples. hIFN-γ treatment was also able to significantly increase CD80 expression in all patient samples above the non-treated control, however, treatment with M1 media induced significantly higher CD80 expression in Patient 35 and 36 samples. There was no significant difference between CD80 levels for M1 or hIFN-γ treated samples for Patient 37. These results follow the pattern previously observed in Chapter 2 when re-educating M2- or tumour supernatant polarised macrophages.

To confirm that these changes in receptor expression represent a change in polarisation state of the macrophages, cytokine analysis was performed by ELISA to probe for levels of TNF-α, IL-12 and IL-10 (*Figure 6.8B*). Treatment of ascites-conditioned macrophages with M1 or IFN-γ gave major increases in TNF-α production in all patient samples. For IL-12 however, only M1 media was able to induce increases in cytokine production for Patient samples 35 and 36. Ascites from Patient 37 caused very high levels of IL12 production by THP-1 cells and this made the attempted re-education hard to interpret. Finally, IL-10 levels were extremely low and pushed the limits of detection for the assay. Interestingly the levels measured for ascites from patients 35 and 37 were

highest in cells that were not exposed to the re-education conditions, although the changes were not statistically significant. Ideally, these experiments would be extended to include re-education by supplementation of IFN-γ or virus to compare with these data where media is replaced. Unlike IFN-γ protein which can be diluted from a stock to a desired final concentration with which to re-educate macrophage, virus lysates cannot be concentrated to the same degree. Thus, it would be hard to compare the efficacy of a small volume of viral lysate added as a supplement in these re-education experiments relative to neat IFN-γ. For these reasons, the efficacy of virus produced IFN-γ in the context of ovarian ascitic fluid was instead evaluated in *ex-vivo* patient samples (later in this chapter).

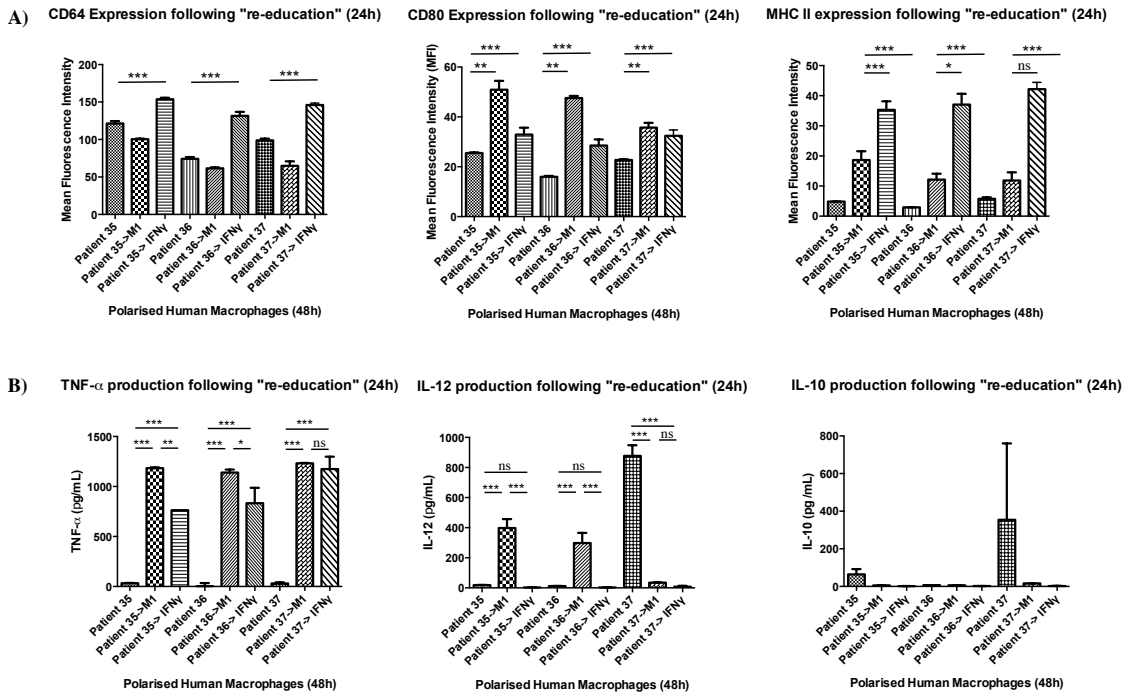


Figure 6.8 Re-education of ascites polarised macrophages

THP-1 macrophages were cultured for 24 hours with M1 media (LPS 1 ng/mL) and hIFN-γ (10 ng/mL), hIFN-γ alone media (10 ng/mL), M2 media (IL-4, 10 ng/mL) or with in acellular fluid obtained from samples of patients with ovarian ascites. After 24 hours media was exchanged for fresh RPMI, M1 media (LPS 1 ng/mL) and hIFN-γ (10 ng/mL), hIFN-γ alone media (10 ng/mL) or with IFN-γ alone media (10 ng/mL) for an additional 24 hours. **A)** Cells were harvested using non-enzymatic methods, stained for various cell surface receptors and analysed for mean fluorescence intensity using a FACS Calibur™ . **B)** Supernatants were harvested from these samples and cytokine levels of TNF-α, IL-12 (p40) and IL-10 were probed for using an ELISA. Results represent n=3, with errors bars indicating SD. Statistical analysis of significance was performed by one-way ANOVA, with a Tukey post-test. $P<0.05$ (*), $P<0.01$ (**), $P<0.001$ (***) or non-significant (ns)

6.2.2.3 Macrophages polarised by ovarian ascitic fluid can be re-educated by ColoAd1- hIFN-γ

We have shown earlier in this thesis that supernatants from cells infected with oncolytic adenoviruses can shift the polarisation state of either M2- or tumour supernatant-polarised murine macrophages toward a more pro-inflammatory state. Having shown that inflammatory media can similarly re-polarise human macrophages that had been pre-conditioned in human ascitic fluid, it was important to determine whether the same results could be obtained using supernatants from virus-infected tumour cells. Use of ColoAd1-hIFN-γ provides an interesting opportunity to examine if there are any differences between treatments with commercially available hIFN-γ compared to hIFN-γ produced by an oncolytic virus.

In the same experimental design as above, THP-1 macrophages were cultured for 24 hours in patient ascites samples. Media was then replaced with supernatants from IGROV-1 cells that had been infected with either ColoAd1 or ColoAd1-hIFN-γ for 3 days. After 24 hours cell surface receptors were analysed for expression of CD64, CD80 and MHC II (*Figure 6.9A*). The receptor data for re-education gained in this part of the study were largely negative. For example CD64 expression was unexpectedly decreased in all groups that had been subject to re-education conditions, for all patient samples. Similarly, with the exception of the ColoAd1 treated patient 35 sample, CD80 expression showed no significant differences between treated samples and non-treated controls. Levels of MHC II provided the most promising indication of re-education. Treatment with ColoAd1-IFN-γ supernatant was able to increase the levels of MHC II above control in all ascites samples used. Similarly, treatment of macrophages with

ColoAd1 supernatant was able to increase MHC II levels above control for Patient 35, but this effect was not seen in other patient samples.

Whilst the results of the receptor analysis were rather disappointing, supernatants from these samples were still probed for TNF-a, IL-12 and IL-10 as with previous re-education experiments (*Figure 6.9B*). Surprisingly, TNF-α levels for virus treatment groups increased above the non-treated control in all patient samples studied; however, significant increases were only observed for samples treated with ColoAd1-IFN-γ supernatants. The levels of IL-12 and IL-10 within the samples were largely undetectable with only a few exceptions, which are perhaps anecdotal at best. Levels of IL-12 peaked in the non-treated control for patients 35 and 36, with the addition of ColoAd1 supernatant appearing to decrease the levels of IL-12 for patient 36. IL-10 was only detected in the non-treated control of patient 36.

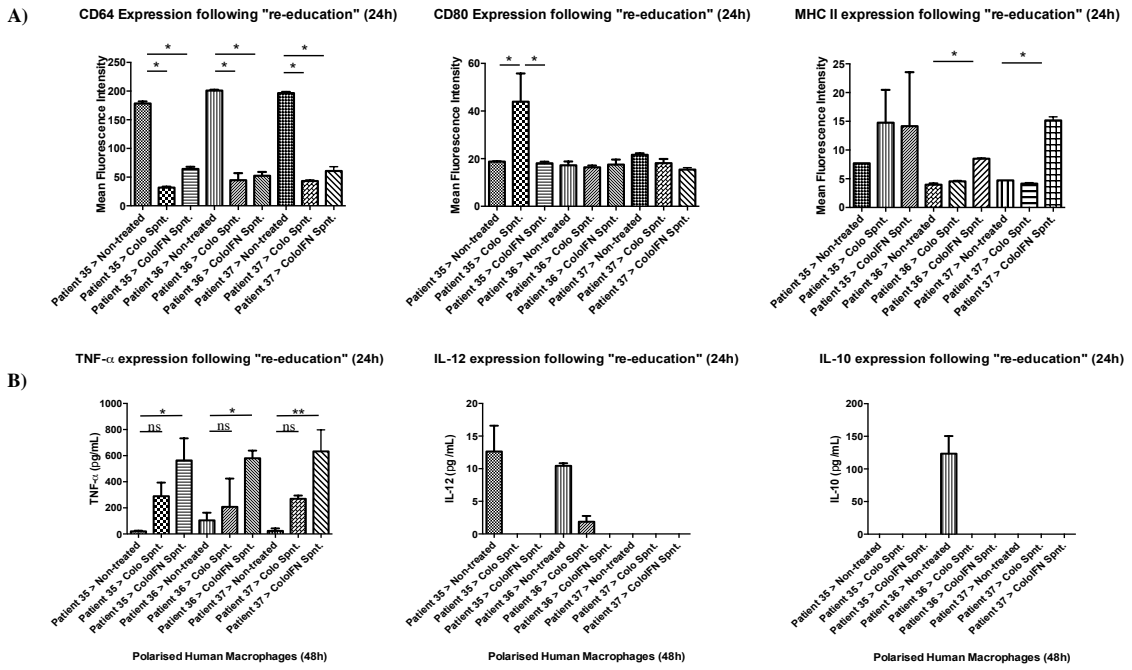


Figure 6.9 Re-education of ascites-polarised THP-1 macrophage with supernatant from virus- lysed tumour cells

Virus supernatants were generated by infecting confluent T175 flasks of IGROV-1 cells with 1 x 10^8 VP /mL of ColoAd1 or ColoAd1-hIFNγ, in 12 mL of RPMI. After 72 hours, virus infected media was harvested and cell-free supernatants were generated. THP-1 macrophages were cultured for 24 hours in acellular fluid obtained from samples of patients with ovarian ascites. After 24 hours media was exchanged for fresh RPMI, or supernatants from ColoAd1 or ColoAd1-hIFN γ infected cells for an additional 24 hours. **A)** Cells were harvested using non-enzymatic methods, stained for various cell surface receptors and analysed for mean fluorescence intensity using a FACS Calibur™ . **B)** Supernatants were harvested from these samples and cytokine levels of TNF-α, IL-12 (p40) and IL-10 were probed for using an ELISA. Baseline levels of these cytokines present in virus-infected media were subtracted from readings, to yield the concentrations produced by THP-1 cells. Results represent n=3, with errors bars indicating SD. Statistical analysis of significance was performed by one-way ANOVA, with a Tukey post-test. P<0.05 (*), P<0.01 (**), P<0.001 (***) or non-significant (ns)

6.2.2.4 Macrophages polarised by ovarian ascitic fluid can display a similar functional phenotype to M2 macrophages

In Chapter 4, the functional consequences of differentially polarised macrophages were evaluated and NO production was identified as a good marker for M1-type human macrophages. This functional assay was designed to illustrate whether changes in receptor expression on macrophages were correlating with changes in behaviour of the cells; an important factor when comparing macrophages that may only exhibit small changes in receptor expression.

This previously optimised assay was used here, to confirm the phenotype of ascitic-fluid polarised macrophages by functional readouts. No significant differences were observed in NO production between M2-polarised or ascitic fluid sample-polarised macrophages (*Figure 6.10A*). These levels of NO were also significantly different from those seen in IFN-γ-polarised macrophages. Such results demonstrate that whilst receptor data from study of the ascites-polarised macrophages does not follow the pattern of M2-polarised macrophages identically, these macrophages are characterised mainly by M2-type behaviour. Such results illustrate the importance of studying functional readouts in macrophage polarisation.

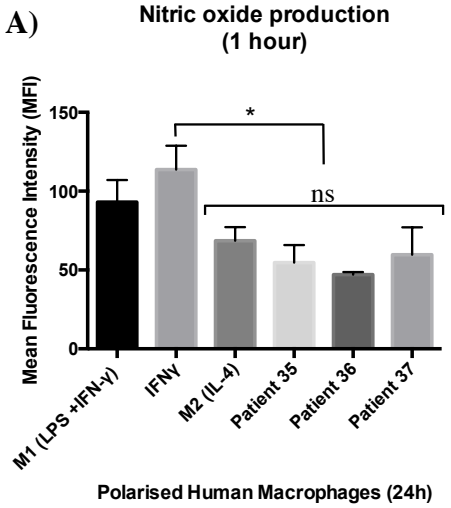


Figure 6.10 Ascites polarised macrophages display a similar functional behaviour profile to that of M2 macrophages

THP-1 macrophages were cultured for 24 hours with acellular fluid obtained from samples of patients with ovarian ascites. **A)** Nitric oxide was measured using DAF-FM Diacetate (Life Technologies™), with cells incubated at 5μM DAF-FM in 0.5 mL of RPMI for one hour at 37°C, washed 3 times with PBS, and incubated with 1 mL RPMI for an additional 15 minutes to allow complete de-esterification of intracellular esterases. Cells were harvested using non-enzymatic dissociation buffer and analysed for fluorescence using a FACS Calibur™ to determine the extent of nitric oxide production. Results represent n=3, with errors bars indicating SD. Statistical analysis of significance was performed by one-way ANOVA, with a Tukey post-test. $P<0.05$ (*) or non-significant (ns)

6.2.2.5 Virus can mediate macrophage re-education as evidenced by NO production

In Chapter 4, NO provided a functional marker to distinguish macrophages re-educated by exposure to oncolytic viruses. These experiments were extended here to confirm whether re-education of ovarian ascites-polarised human macrophages correlated with a change in functional phenotype, as evidence by change in NO production. As with previous re-education experiments, THP-1 macrophages were cultured for 24 hours in acellular ascitic fluid from patients with ovarian cancer before being treated with

ColoAd1 or ColoAd1-IFN-γ virus alone, or supernatants from virus-infected IGROV-1 cells.

After 48 hours, macrophages cultured in ascitic fluid demonstrated significantly decreased levels of NO production relative to M1- and hIFN-γ polarised macrophages (*Figure 6.11A*). Exchanging ascites for the supernatants of virally lysed cells induced significant increases in NO for both ColoAd1 and ColoAd1-hIFN-γ lysates, indicating a functional change in polarisation (*Figure 6.11 B and C*). Treatment with virus particles alone was also shown to induce increases in NO relative to control, however significant results were only obtained for ColoAd1. The ability of virus-produced hIFN-γ to re-educate macrophages was compared against hIFN-γ alone (*Figure 6.11D*). In two thirds of the patient samples studied, ColoAd1-hIFN-γ supernatants increased NO production significantly more than hIFN-γ alone, whilst for the ascites sample of Patient 31, there were no significant differences in NO production between ColoAd1-hIFN-γ supernatant and hIFN-γ alone. These data indicate that NO provides a useful marker for identifying functional re-education of human macrophages. These data further show that virus alone, or together with production of hIFN-γ, can mediate such functional re-education of macrophages to greater levels than with IFN-γ alone.

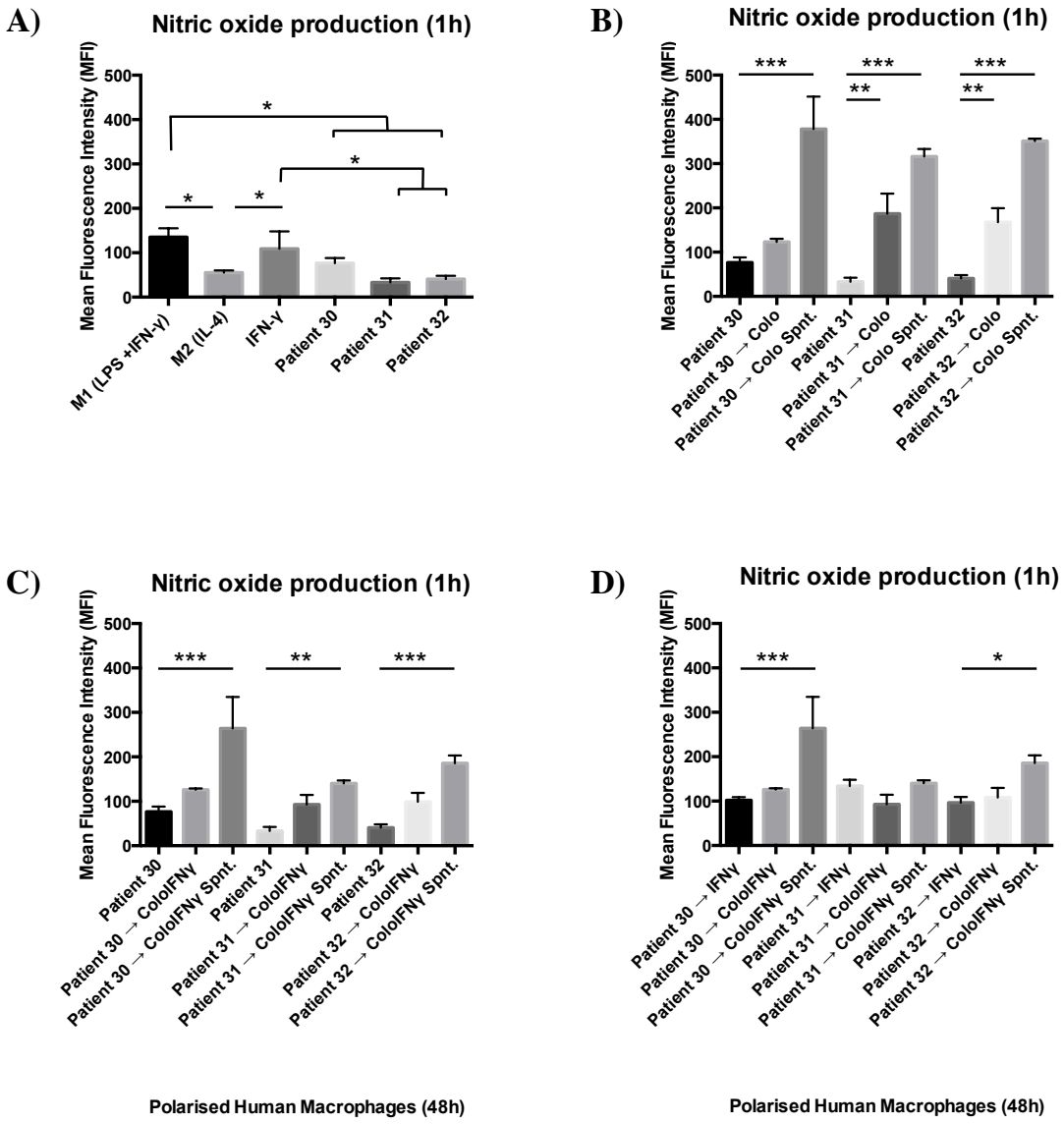


Figure 6.11 Virus can mediated macrophage re-education from ascites treated macrophages through NO induction.

A) THP-1 macrophages cells were plated out at 2 x 10^5 cells per well in 12 well plates in 0.5 mL of RPMI (10% FBS) alone, M1 media (LPS 1 ng/mL) and IFN-γ (10 ng/mL) or M2 media (IL-4, 10 ng/mL) or ascites for 48 hours. After 24 hours media was replenished with new M1or M2 media or ascites respectively and incubated for an additional 24 hours. **B) and C)** In parallel, ascites-treated cells had media removed, washed 2x PBS and had media replaced with supernatants of ColoAd1 or ColoAd1-IFNγ virus-infected DLD-1 cells (1000 Vp/cell) for 24 hours. Alternatively, supernatants from non-treated DLD cells as a base media, supplemented with ascites IFNγ (10 ng/mL), free ColoAd1 or free ColoAd1-IFNγ virus (1000 Vp/cell) for 24 hours. D) comparison of differing IFN-γ treatments. NO was measured using DAF-FM Diacetate (Life Technologies™), as previously described in this chapter. Level of NO production is demonstrated by mean fluorescence intensity. Results represent n=3, with errors bars indicating SD. Statistical analysis of significance was performed by one-way ANOVA, with a Tukey post-test. P<0.05 (*), P<0.01 (**), P<0.001 (***)

6.2.3 *Ex vivo* treatments of human ovarian ascites

6.2.3.1 Ascitic fluid can inhibit oncolytic virus infection

It was noted above that levels of infection achieved using the GFP reporter virus at normal virus concentrations (1-100 VPC) in experiments involving human ascites were consistently lower than would be expected in typical *in vitro* experiments. Several variables might be contributing to this reduced efficiency of virus infection, including the possibility of poor methodological set-up or neutralization of the virus by the ascites.

To determine whether ascites fluid itself may impact on virus efficacy, a series of infections of cancer cells were performed in the presence of human ascitic fluid obtained. For these studies, the lung cancer cell line A549 was chosen as these cells are readily infected by ColoAd1-CMV-GFP to very high levels, enabling clear definition of changes in infectivity that may be induced by the presence of ascitic fluid. A549 cells were infected with 100 VPC of ColoAd1-GFP in the presence of ascitic fluid from three different patients, with infection assessed by fluorescence at 72 hours post-infection. As shown (*Figure 6.12*) infection was almost entirely attenuated in the presence of ascitic fluid across all patient samples relative to cells infected in DMEM alone, suggesting that there are inhibitory factors present within ascites fluid that can antagonise virus infection.

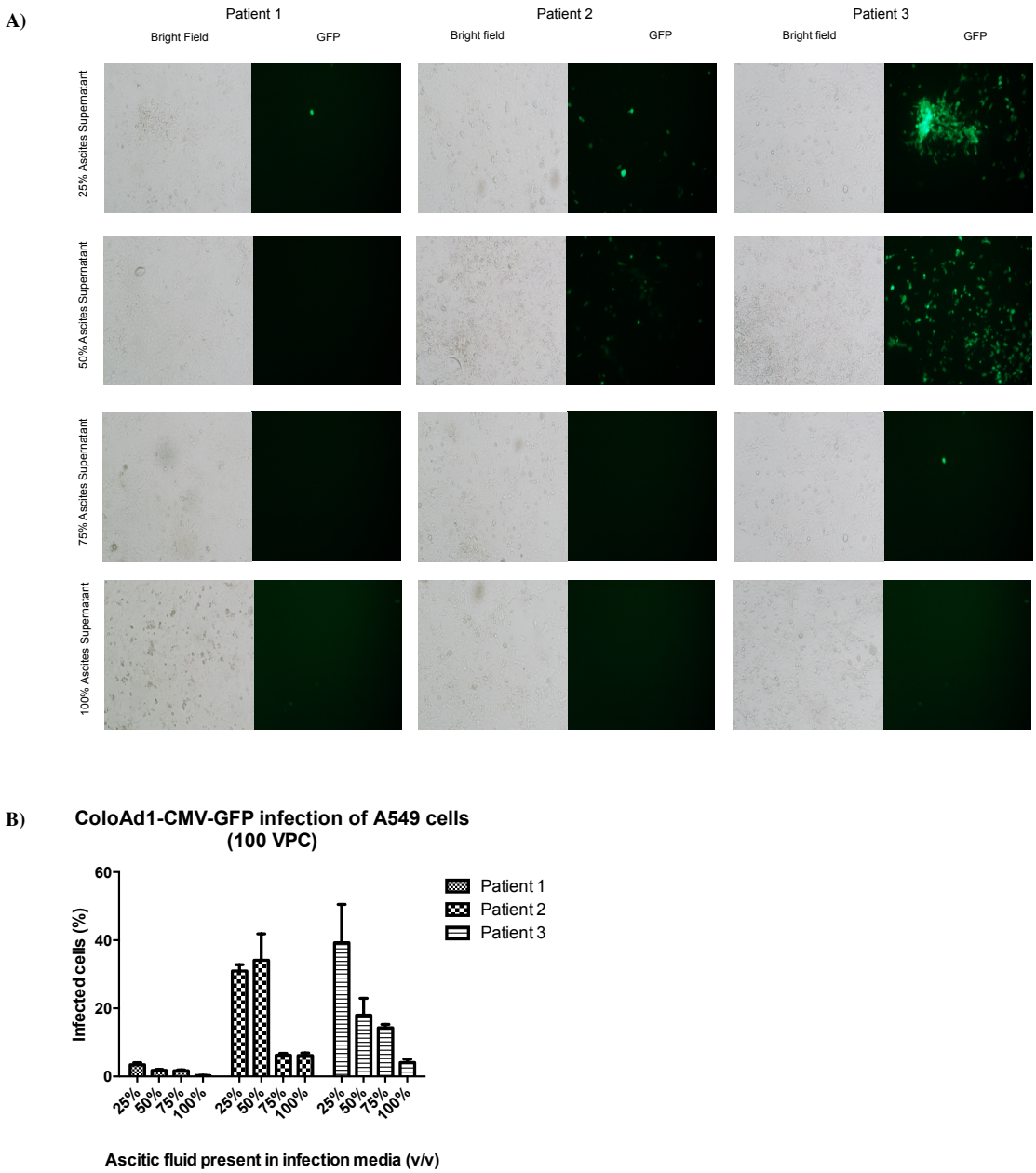


Figure 6.12 Fluid from malignant ascites inhibits infection of A549 cells

A549 cancer cell lines were seeded at $5x10^4$ cells per well in 24 well plates. Cells were infected with ColoAd1-CMV-GFP for 72 hours in 0.3 mL of DMEM medium, supplemented with 25%, 50%, 75% or 100% ascitic fluid. **A)** Infection of cells was assessed by fluorescence microscopy. **B)** Quantitative assessment of GFP-positive cells was obtained by flow cytometry. Values were normalised against a control group, infecting cells in the absence of ascitic fluid to give a "maximal infection" value. Results represent n=3, with errors bars indicating SD

Whilst 100 VPC is normally an excess in cell culture-based infections, it could well be that such doses are not effective for clinical experimentation. Indeed, an upcoming

clinical trial delivering ColoAd1 will aim to administer 1 x 10^{13} virus particles in a volume of 500ml into the peritoneal cavity of patients with cancer. To see whether inhibition of virus infection could be overcome by increasing virus concentrations, the experiment was repeated to include 100-, 1000- and 10000-virus particles per cell (VPC) in a range of volumes of ascitic media (*Figure 6.13*). The results of the lowest virus concentration largely follow the pattern observed previously; that the percentage of tumour cells infected by virus decreased with increasing concentrations of ascitic fluid. With the exception of Patient 2, all samples showed a complete lack of GFP positive cells when infections were performed in 90% ascites. For Patient 3, infection at 100 VPC the total percentage of infected cells was lower than previously observed (*Figure 6.12*), however the pattern of infection was the same, with increasing ascitic fluid decreasing percentage of infected cells. Such experimentation should be repeated to establish if the pattern remains. Perhaps more surprising was that this attenuation of GFP expression was consistent across infections performed in 30% and 60% ascitic fluid, with the exception of Patient 3 (at 30% ascites) and Patient 2 (all concentrations of ascites). Increasing virus concentration 10-fold restored infection to near-maximal levels in the 30% ascites samples with the exception of Patient 4. For samples infected at 60% and 90% ascites, all but two samples had GFP expression restored to at least 50%. Increasing virus concentration another 10-fold restored infection to near-maximal levels across all ascites concentrations and across all patients except Patients 1 and 4. Despite the ascitic fluid of patient 4 remaining the most resistant to virus infection, increasing concentrations of virus correlated with increased infection across all amounts of ascitic fluid. Such results suggest that the inhibitory effects of ascites can largely be overcome by increasing virus dose. On a per milliliter basis, the maximal virus

concentration used here would still be 100-fold lower than the proposed dosage for an intraperitoneal adenovirus study.

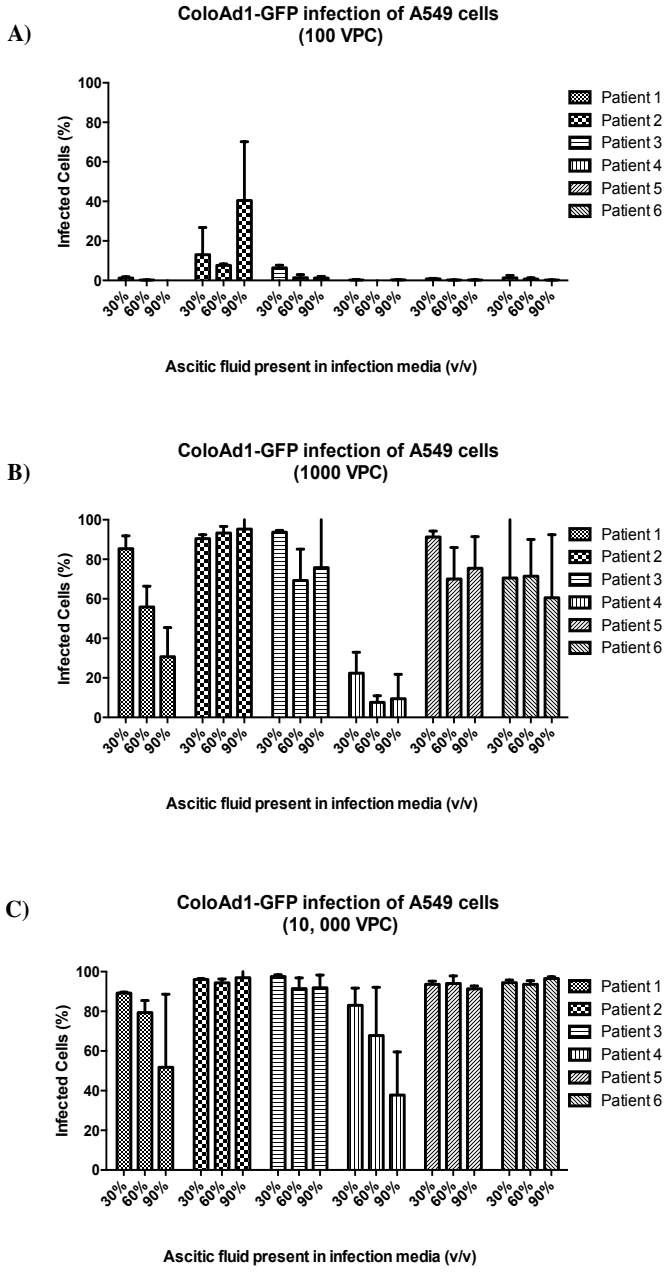


Figure 6.13 Inhibitory effects of ascites are concentration dependent

A549 cancer cell lines were seeded at $5x10^4$ cells per well in 24 well plates. Cells were infected with ColoAd1-CMV-GFP in 0.3 mL of RPMI medium, supplemented with 30%, 60%, or 90% of ascitic fluid obtained from patients with ovarian cancer. Infection was determined by GFP fluorescence using flow cytometry after 72 hours.Cells were infected with ColoAd1-CMV-GFP at a concentration of **A)** 100, **B)** 1000 or **C)** 10000 virus particles per cell. After 72 hours of infection, cells were harvested using non-enzymatic dissociation buffer and analysed for fluorescence using a FACS Calibur™ . For each concentration of virus, values were normalised against a control group of virus infection in the absence of ascitic fluid to give a percentage of infection relative to a "maximal infection" value. Results represent n=3, with errors bars indicating SD

There are a number of potential explanations for the decreased viral infection of tumour cells in the presence of human ascitic fluid. These include neutralisation of virus particles by pre-existing antibodies, or factors present within the ascitic fluid might be inducing suppressive, anti-viral signalling in tumour cells or even blocking CD46. For example, the Notch protein family member Jagged has been shown to interact with CD46 (Le Friec et al., 2012). To explore whether factors present in ascitic fluid were able to induce anti-viral signalling in tumour cells, virus infections were performed on tumour cells conditioned with cell-free ascites either pre- or post-infection (*Figure 6.14A and B*). In parallel, virus was administered to cells in the presence of ascitic fluid to examine whether neutralisation of virus particles is a key factor (*Figure 6.14C*).

At the lower concentration of virus, pre-conditioning of cells or infection in the presence of ascites resulted in the maximal inhibition of virus infection, with infection rates below 40% in almost all samples for both treatment groups. Increasing the virus concentration 10-fold was able to restore infection to near maximal levels for cell pre-treated with ascites. However, for cells treated with virus in the presence of ascitic fluid, increased viral dose was only able to increase infection by 10-20% overall. Whilst ascitic fluid is clearly mediating some anti-viral effects on cancer cells themselves, comparing these two experiments suggests that neutralisation of virus may prove to be a larger barrier for successful infection in ascites. For tumour cells conditioned with ascites after infection, there was only a marginal decrease in infectivity for most samples treated at the lower dose, which was completely restored by increasing the virus concentration 10-fold. Such data might indicate that the effect of ascitic fluid on tumour cells is only at the initial level of permissivity to infection.

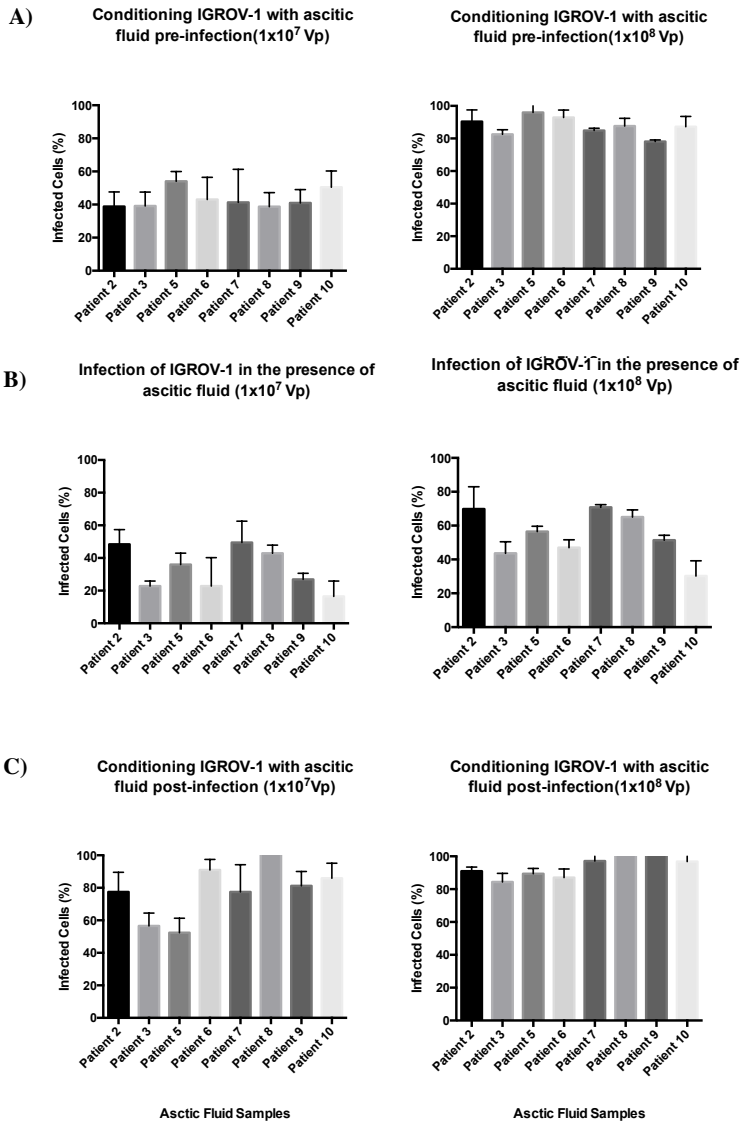


Figure 6.14 Inhibitory effects are mediated through neutralisation and pre-conditioning of cells

IGROV-1 cancer cells were seeded at $5x10^4$ cells per well in 24 well plates. Cells were infected with ColoAd1-CMV-GFP in 0.3 mL of DMEM medium, supplemented 90% of ascitic fluid obtained from patients with ovarian cancer. Cells were infected with either 1 x 10^7 (**left panels**) or 1 x 10^8 virus particles per ml (**right panels**) for 90 minutes in DMEM alone (**A** and **C**) or DMEM supplemented with 90% ascitic fluid. Virus-containing media was aspirated and cells were washed 3 x with PBS before replacing media with DMEM alone (**A** and **B**) or DMEM supplemented with 90% ascitic fluid (**C**). 72 hours post-infection, assessment of GFP levels was determined by flow cytometry. Cells were conditioned with ascitic fluid 24 hours prior to (**A**)- or immediately after virus infection (**C**). For each concentration of virus, values were normalised against a control group of virus infection in the absence of ascitic fluid to give a percentage of infection relative to a "maximal infection" value. Results represent n=3, with errors bars indicating SD

6.2.4 Short term *ex vivo* infection of ascitic cells from patients

This *ex vivo* methodology for study of patient ascites samples provided an important opportunity to

- assess successful infection of ascites tumour cells
- detect transgene production in ascites cells
- see whether production of transgene could re-educate ascites macrophages

Data from three patient samples are presented, representing some of the most complete data sets for patient samples that were obtained. As an initial assessment to examine whether samples were suitable for study, ascites cells were stained for EpCAM and CD68. EpCAM is a prevalent marker on ovarian cancer cells and was therefore used to identify tumour cells within the samples, which would be required to support virus infection and replication. The macrophage marker CD68 was utilised to identify macrophages present in the sample. To be able to demonstrate virus-mediated re-education of tumour-associated macrophages, there was a prerequisite that samples should express both EpCAM and CD68 before beginning experimentation. Additionally, cells were stained with antibodies recognizing CD4 and CD8 to identify T cell populations present within the samples, as these markers have clinical significance and would be important for future experimentation.

6.2.4.1 Composition of ascites cells

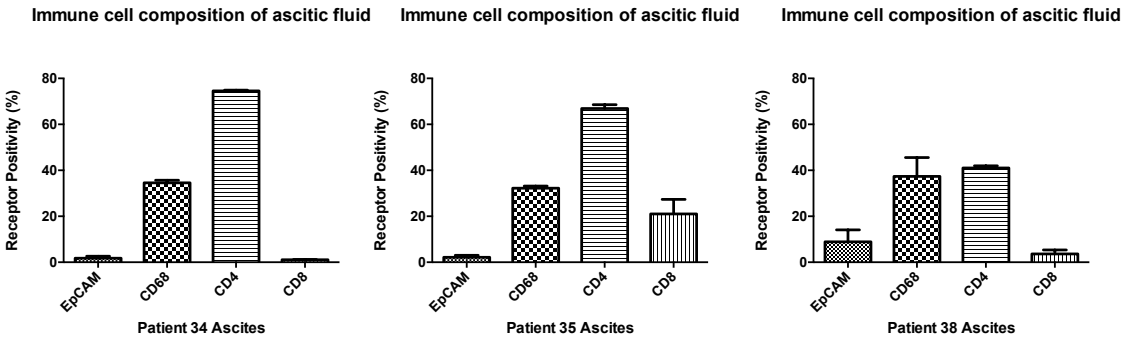


Figure 6.15 Immune profiling of Ascitic cells

Cells were purified from ascitic fluid and stained for EpCAM, CD68, CD4 and CD8, analysed using a using a FACS Calibur™. Results represent n=3 (triplicate samples generated per patient, performed across 3 separate patients), with errors bars indicating SD

The results of the cell profiling show that in each case, CD4 positive cells represent the most prevalent cell type, constituting over half of the ascites sample. Macrophages appeared to be the second more prevalent cell type, with CD68 positivity constituting 30-40% of cells across all the samples studied. In these three patients examined, the levels of tumour cells appeared to be low, with EpCAM staining below 10% in all samples. CD8 positivity was more variable however, ranging between 3-20% in the samples stained. Such immune profiling data is consistent with existing literature (Milliken et al., 2002). Macrophages have often been reported as a predominant infiltrate within ovarian ascites. The high CD4/CD8 ratio has been documented in a number of tumour types, and its observation in ovarian ascites has been correlated with a negative prognosis, largely attributed to the high presence of Treg cells.

6.2.4.2 Viruses successfully infect ascites cells and express h IFNγ from ColoAd1-hIFN-γ

As a surrogate for infection with ColoAd1-hIFN-γ, samples were infected with ColoAd1-CMV-GFP as a reporter. Flow cytometry results indicate that successful virus infection was achieved in all samples, with the peak in GFP observed at 72 hours most likely correlating with virus replication. The decrease in GFP expression at 120 hours perhaps represents lysis of infected cells, or decreased total cell viability. A major advantage of using the GFP expressing virus is the ability to assess what types of cells are being infected. At 72 hours where virus infection appeared maximal, cells were co-stained for the tumour marker EpCAM, or the pan-leukocyte marker, CD45, to ascertain whether the virus was infecting tumour or immune cells respectively. The levels of GFP infection in EpCAM positive cells was low, however this correlated with the low levels of EpCAM positivity observed, suggesting that all tumour cells present were infected. Surprisingly, the majority of the GFP was localised to CD45 positive-cells. This may be indicative of the CMV promoter driven GFP expression and the disproportionate number of immune cells to tumour cells present within the samples.

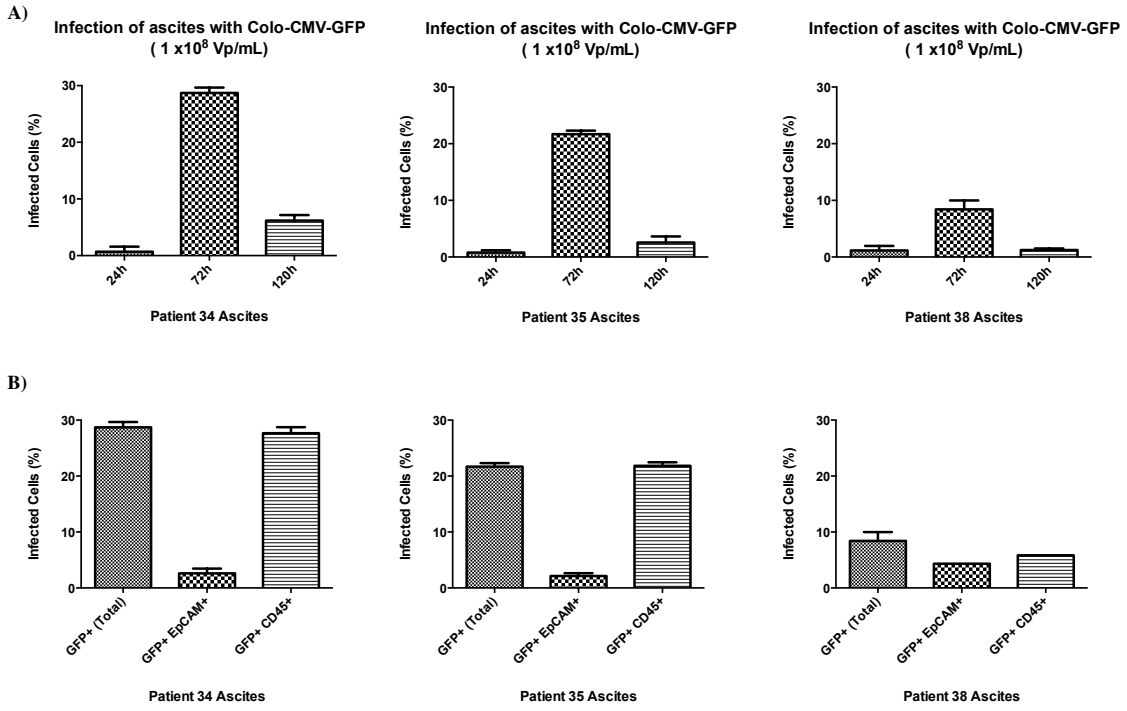


Figure 6.16 GFP infection of patient samples

Patient samples were infected with 1 x10 ^{8} vp/ mL of ColoAdGFP for 5 days, with samples taken at days 1, 3 and 5. Cells were co-stained with CD45 and EpCAM to identify the location of GFP expression. Cells were analysed by flow cytometry as previously described. N =3 (triplicate samples generated per patient, performed across 3 separate patients)

In parallel to ColoAd1-CMV-GFP treatment, patient samples were also infected with human IFN-γ encoding ColoAd1 virus. To assess whether transgene production was successful, samples were stained for hIFN-γ by ELISA. In all samples treated with the ColoAd1-hIFNγ virus, hIFN-γ production was detectable at good levels of expression and was significantly higher than other treatment groups both at 72- and 120-hours Importantly, hIFN-γ production was significantly higher than in the group treated with hIFN-γ alone, and was sustained throughout the 120 hours, consistent with prolonged virus infection and transgene expression.

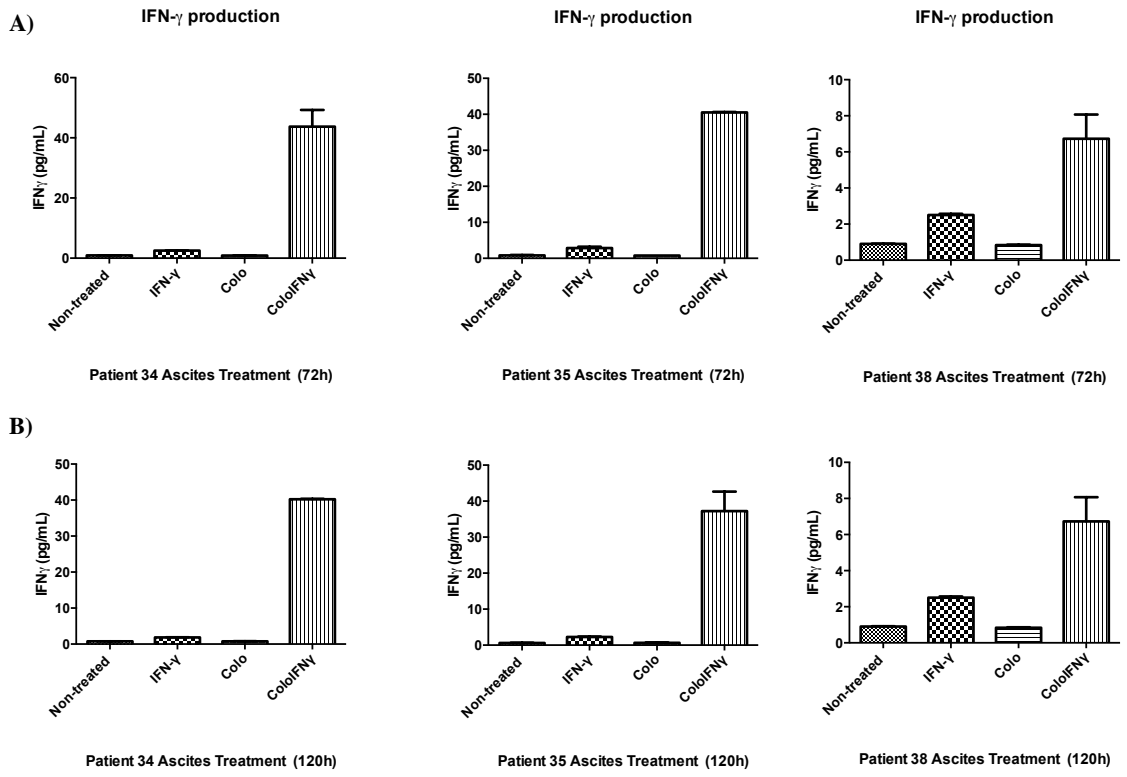


Figure 6.17 IFNγ production by infection of patient samples with ColoAd-hIFNγ

Patient samples were infected with 1 x10 ^{8} vp/ mL of ColoAdGFP for 5 days, with samples taken at days 1, 3 and 5. Cells were co-stained with CD45 and EpCAM to identify the location of GFP expression. Cells were analysed by flow cytometry as previously described. N =3 (triplicate samples generated per patient, performed across 3 separate patients)

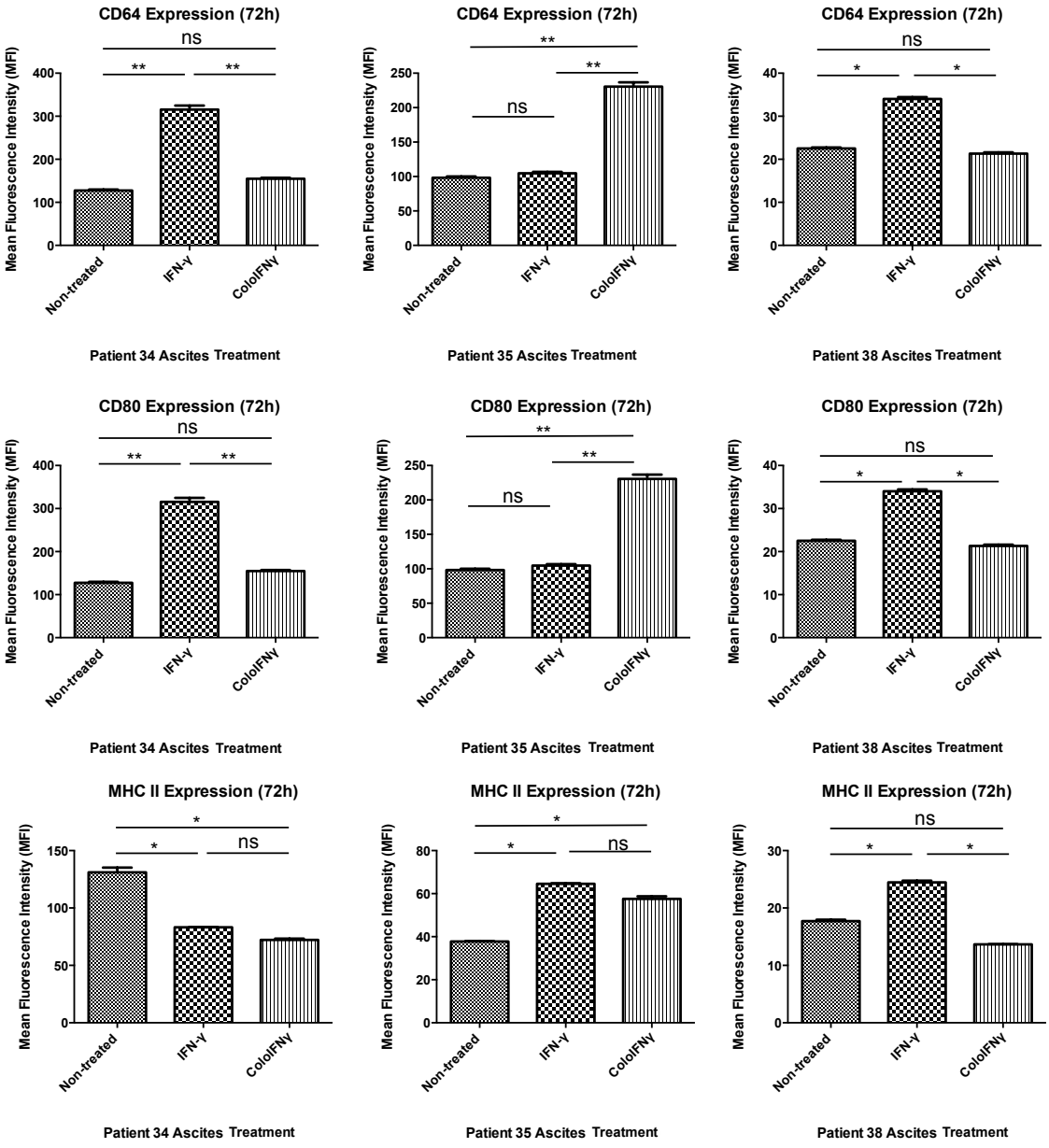


Figure 6.18 Immune modulation of macrophage phenotypes *ex vivo*

Patient samples were non-treated, infected with 1 x10 ^{8} vp/ mL of ColoAd1-hIFNγ, or given IFNγ for 5 days, with samples taken at day three. Cells were co-stained with CD68 and either MHC II, CD80 or CD64 to determine changes in phenotype. Cells were analysed by flow cytometry as previously described. N =3 (triplicate samples generated per patient, performed across three separate patients) with errors bars indicating SD. Statistical analysis of significance was performed by one-way ANOVA, with a Tukey post-test. P<0.05 (*), P<0.01 (**) or non-significant (ns)

Having demonstrated successful infection and expression of hIFN-γ, any correlation with changes in macrophage phenotype was assessed (*Figure 6.18*). Macrophages were stained by CD68 and subsequently stained for levels of CD64, CD80 and MHC II, which have previously been some of the most definitive markers of a pro-inflammatory, M1-type phenotype. Non-treated sample, those treated with hIFN-γ, or infected with ColoAd1-hIFN-γ were harvested at 72 hours (in keeping with maximal virus GFP expression) and studied for their marker expression.

Marker expression was variable among the patient samples, with varying patterns exhibited between treatment groups. For CD64, hIFN-γ treatment produced significantly higher expression in patients 34 and 38 relative to virus and control, whilst induced no increase above control in patient 35. ColoAd1-hIFN-γ induced significantly higher CD64 expression in patient 35 relative to control and hIFN-γ alone.

Similarly, for MHC II expression, treatment with hIFN-γ or virus showed decreased levels of MHC II relative to control for Patient 34. For Patient 35, both hIFN-γ or virus were able to induce significant increases in expression relative to control, with no significant differences between the two treatments in MHC II levels. For Patient 38, hIFN-γ treatment induced the highest levels of MHC II expression, with no differences observed between the control and virus treated sample.

6.3 Discussion of results

In this chapter, an *in vivo* murine model of malignant ascites was successfully developed and was able to support virus infection *in vivo* and *ex vivo* to evaluate human tropic adenovirus in xenografted cancer cells. Despite significant presence of tumour cells at the later stages of ascites, the receptor phenotype (as assessed by flow cytometry) of murine peritoneal macrophages was mixed; CD64 and CD86 expression closely resembled an M2 phenotype, whilst MHC II and CD80 resembled a phenotype closer to M1. This mixed phenotype might reflect the nature of the xenograft model, as many cytokines attributed with TAM polarisation are tumour cell- derived, requiring human cytokines produced by IGROV cells to polarise murine macrophage. Thus, a number of key cytokines may not cross the species barrier and would be unable to induce formation of suppressive macrophages. Alternatively, these models may represent an accurate depiction of TAM, as it is becoming increasingly apparent that macrophages isolated from many tumour contexts will most likely represent a heterogeneous mixture of cells (Reinartz et al., 2013).

Given the mixed phenotypes of murine ascites macrophages, it was perhaps not surprising that trying to re-educate them yielded a mixture of results. Following treatment *ex vivo*, an increase in MHC II expression was clear for macrophages exposed to ColoAd1 both expressing and not expressing murine IFN-γ, suggesting that exposure to virus particles could cause a rise in cellular markers associated with the pro-inflammatory M1 phenotype.

In vivo, whilst there was no significant increase in the percentage of F4/80-positive macrophages between mice treated I.P. with ColoAd1-mIFN-γ and the other treatment

groups, there was a striking increase in total ascites cells elicited by ColoAd1-mIFN-γ. MHC II expression proved again to be a reliable marker of re-education, demonstrating that ColoAd1-mIFNγ could induce significant increases in MHC II expression. Performing this in combination with a functional assay such as NO production might help to identify whether these macrophages have had their phenotype modulated *in vivo* toward a pro-inflammatory state.

Extending these studies into human patients samples, polarisation of THP-1 macrophages by ovarian ascites fluid show that these human macrophages demonstrate a receptor profile more similar to M2 (IL-4) treated cells. Decreased expression of MHC II complexes along with reduced CD80 and CD86 is in keeping with previous data published on macrophages from patients with ovarian cancer (Kryczek et al., 2006). There are a couple of surprising results however. For example, whilst ascitic fluid was able to significantly reduce expression of MHC II, MHC I expression actually increased above levels induced by hIFN-γ-polarisation in some patient samples. It would be interesting to examine whether this has functional significance on the cells themselves. It has been shown that dendritic cells have a reduced capacity for antigen presentation within tumours, with similar assertions being made for macrophages. Little is currently known about the level at which antigen presentation is disrupted in macrophages. We have shown in this thesis using *in vitro* model systems that M1-polarised macrophages can cross-present peptide antigen better than M2 counterparts, however conclusive evidence of tumour antigen cross -presentation or cross-presentation of cell-associated antigen has yet to be demonstrated. Perhaps the lack of obvious decreases in MHC I levels on ascites-polarised macrophages are indicative that the cross presentation process is not completely disrupted for macrophages from human ovarian ascites.

Previous studies into soluble macrophage-active factors present in ascites fluid have largely focused on factors promoting recruitment of macrophages, such as CCL-2, -3, -4 and 5 (Milliken et al., 2002), with the mediators that promoting suppressive macrophage polarisation as yet un-defined. Profiling the acellular components of ascitic samples have previously identified increased amounts of certain anti-inflammatory cytokines such as IL-10 (Matte et al., 2012), however, there have been few previous studies investigating whether soluble components from ascitic fluid have the potential to drive tumour-associated macrophage formation. One such example is in the case of CA-125, a tumoural mucin shown to be abundant in ovarian ascites and able to engage with the macrophage mannose receptor to induce production of IL-10 (Allavena et al., 2010).

The clear differences in expression of CD80 and MHC II in M1- or IFN-γ compared to M2 or ascites polarised cells provides validation for the usage of these markers for future experimentation. Whilst expression of CD64 in ascites polarised cells might suggest that it is not the most useful of markers for TAM identification, the results of re-polarising experiments highlights its utility in identifying "re-education". However, the result of the ascites polarisation perhaps illustrate a bigger point about the nature of receptor staining when phenotyping tumour-associated macrophages. Based on M1 and M2 profiles, CD64, CD169 and MHC I alone could have easily been selected as the panel for phenotyping. However, in so doing one could conclude that macrophages from ascites display an inflammatory profile akin to M1-type cells. Similarly, basing characterisation on MHC I alone, one might have concluded that phenotypes of ascitic macrophages are variable; with levels of MHC I ranging from highly suppressed, M2-like or M1-like. Such observations illustrate the requirement for using multiple markers

in macrophage phenotyping but also serve as a reminder of the difficulties in identifying different cell subsets.

The results for re-education of human ascites-polarised macrophages treated with M1 media or hIFN-γ are very encouraging, with significant increases in CD80 and MHC II observed for all re-polarising conditions. It would be good to expand these experiments to a larger number of patient samples to see if the same results, or at-least the same pattern of results is observed. To make a more stringent test of re-education, it would be wise to repeat the experiments in the presence of ascitic fluid to see whether M1- or hIFN-γ treatments can overcome the inherently suppressive environments, as was performed earlier in this thesis for murine macrophages using both M2 media and tumour supernatants.

An interesting finding is in the expression of IL-12 by re-educated human macrophages. hIFN-γ alone was unable induce production of IL-12, whilst significant levels of IL-12 produced when treated with hIFN-γ in combination with LPS. When human macrophages were exposed to virus particles, as part of a re-education approach, no IL-12 was produced. Together, these data may imply a requirement for TLR stimulation to induce IL-12 production in previously suppressed macrophages and may indicate that soluble mediators released in the course of virus infection are unable to provide this stimulation.

In the *ex vivo* treatments of ovarian samples with hIFN-γ or ColoAd1- hIFN-γ, an obvious trend did not emerge in the phenotypes of the macrophages following treatment. Future work should continue this experimentation into larger numbers of

patient samples to see if any trends emerge - in particular it would be useful to stratify samples based on the number of tumour cells identified such as to ensure of source of cells for the oncolytic viruses to produce transgene. Including parental virus within future studies would be an essential control in separating the effects of virus from IFN-γ. In these studies, the GFP expressing ColoAd1 was used as the "wild-type" virus to act as a control, but also to act as an easy way to assess whether successful infection had occurred; a choice largely decided by limited sample sizes for these patients. Unfortunately, the GFP expression from virus gave complications for fluorescence compensation on the flow cytometer when dual-staining for macrophage phenotypes. As such, the receptor levels for the macrophages treated with parental virus (GFP expressing ColoAd1) could not be accurately included for comparison.

In this chapter, for earlier experimentation with THP-1 cells virus treatment was administered by virus particles per cell, whilst in later experimentation virus particles were administered per unit volume (particles per mL). Whilst such a decision may appear counter-intuitive as to be inconsistent with the rest of the thesis, the rationale to change to particles per mL was so that data may be more comparable with the current ovarian clinical trial. By using doses of virus in ascites experiments at doses that are clinically relevant and directly comparable to the level of virus being added intraperitoneally to patients with ovarian cancer in the Psioxus clinical trial (OCTAVE study, trial identifier: NCT02028117, https://clinicaltrials.gov/). Further, the virus particle per cell units assumes a uniform sample of cancer cell lines – here the number of virus particles directly relates to cancer cells. This is not the case in the clinical samples where ascites contain a mixture of tumour and immune cells; as such, the usage of virus particles per cell as a unit is perhaps less relevant here.

The disparity in receptor expression between "classically" suppressive M2 macrophages and ascites polarised macrophages re-emphasises the importance of functional assays as a means to more accurately ascertain the behaviour of a given macrophage. Support for this concept is provided in the NO oxide production assay. Whereas comparing suppressive M2 macrophages and ascites polarised macrophages at the level of receptor expression can provide conflicting data, the pattern of NO expression is similar for both, indicating that they behave in a similar manner. NO can be further used to confirm that re-education of ascites polarised macrophages is inducing a substantive change in the phenotype of the cells. Virus (with or without encoded IFN-γ) was shown to induce changes in receptor expression, but perhaps more importantly was confirmed to induce a change in functional phenotype through measuring NO production.

Whilst the results of the NO are promising for virus re-education, interpreting the differences between treatment groups mechanistically is difficult. For example it is hard to delineate the effects of virus produced IFNγ compared to IFNγ- alone because of the plethora of factors released from cells upon virus infection, which may act to stimulate pro-inflammation and NO production. Second, the fact that virus particles themselves can induce NO production makes it hard to accurately identify the impact of virus produced IFNγ on macrophages in comparison with IFNγ treatments; supernatants from ColoAd1- IFNγ-treated cells will also contain free virus particles. Seemingly, the ColoAd1- IFNγ virus alone treatments should act as a control to resolves this issue, however the concentration of free virus particles may not be the same as the concentration in the supernatant of infected cells. Although the overall result of these data has been to suggest that IFNγ armed-virus has the potential to re-educate

suppressive macrophages, determining the relative impact of free virus particles, therapeutic transgene produced and the inflammatory nature of virus lysate on NO production in macrophages will require careful study. Careful study will be of particular importance is explaining the differences in re-education observed between the armed and un-armed ColoAd1. As earlier work in this thesis has demonstrated that ColoAd1-IFNγ virus (both free virus and supernatants) is better-able to induce NO production in macrophages than parental virus, so it is surprising that this effect is diminished in ascites-polarised macrophages. It might well be that increased NO production of ColoAd1-IFNγ virus particles relative to parental virus were a result of small amount of "contaminant" IFN-γ which could exert large effects in simple model systems such M2 stimulation of macrophages, which are lost under the more immunosuppressive environment created by ascites. If contaminant IFN-γ were the explanation of increased NO production in simple macrophage polarisation experiments, it does not explain why parental virus would induce higher levels of NO relative to the armed virus. Whilst both viruses have demonstrated similar infectivity of tumour cells, it might be that parental viruses produces more progeny virus per cell infected, which, in the context of NO production would provide more virus particles to stimulate CD46. Further experimentation should characterise progeny virus production for the two viruses to assess any potential differences.

The experiments described here were the first to study the activity of ColoAd1 using ascitic fluid from patient samples. The main conclusion from these studies was that neutralisation of virus by the ascitic fluid could inhibit virus infection, although there was clearly a threshold effect that could be easily overcome at clinical dose levels. The concept of a "threshold" over which virus increased virus infection can overcome

existing blood-based barriers has been explored documented for this virus in the context of human blood (Di et al., 2014). Previous studies using type 5 adenovirus (Ad5) in the context of ascitic fluid have implicated neutralising antibodies to prevalent Ad5 epitopes (notably hexon protein) as a limiting factor for adenoviral delivery (Hemminki et al., 2002). To confirm whether there is complement or pre-existing antibody-mediated sequestering of virus particles by ascitic fluid, it would useful to repeat these experiments with ascitic fluid that has been heat treated at 56 degrees. It was interesting to note that the pattern of infection observed (*Figure 6.16*) in patient samples suggested that virus predominantly infected CD45-positive immune cells. It could well have been informative to further profile which specific immune subsets were infected by ColoAdGFP by combining the staining panel used earlier in the chapter (*Figure 6.15*) to investigate whether infection was localised to lymphoid or myeloid subsets. Such an experiment provides a technical challenge with our flow cytometer owing to high bleed through of GFP into other channels, which can often limit the number of simultaneous markers studied. Whilst this can be circumvented *in vitro* by increasing the number of cells and splitting samples into distinct panels that can co-stain for GFP and other markers, the finite number of ascites cells within patient samples can often preclude this. Future experimentation should also focus on using an alternative GFP-reporter virus that utilises a more tumour-specific promoter to drive GFP expression (which has now been developed but was not available during my thesis). Whilst the CMV driven virus used in my thesis to drive either GFP or IFN-γ expression was useful to investigate the effects of IFN-γ expression as a proof-of-principle, a tumour-specific promoter would restrict expression to tumour cells and limit replication in immune cells and alter the pattern of expression seen here (recent unpublished observation in the laboratory).

The immune profile of the cells in samples of patient ascites is comparable with previous studies examining the immune composition of ascitic fluid. In particular, the high CD4/CD8 ratio has been demonstrated in a number of patient samples and has been shown to correlate with a negative prognosis. This factor has largely been attributed to the presence of CD4+ regulatory T cells. Many of the immunosuppressive functions attributed to Treg cells have been shown to shared by tumour-associated macrophages, particularly at the level of T cell inhibition (Kryczek et al., 2006). Further study in this model should aim to provide a more comprehensive immune cell analysis that allows profiling of the different subtypes of the resident immune cells and most importantly, look for markers of their activation status. In particular, it would be beneficial and completely novel to provide a comprehensive analysis of macrophage receptor expression within ovarian ascites by flow cytometry. Tailoring a multi-colour flow cytometry panel to encompass the study of all the major immune-regulatory receptors might provide resolution as to the role that these macrophages may play in immunosuppression in this environment.

Whilst the composition of immune cells within ascitic fluid may have been comparable to other studies, the level of tumour cells identified by EpCAM-positivity was seemingly low however the proportion of tumour cells in ascites is notoriously variable (Kipps et al., 2013). Previous staining within the laboratory has shown larger numbers of tumour cells within patient samples however, the markers used are not also kept consistent; this could potentially be a reflection of the marker chosen, and may have been resolved were the samples co-stained with an additional tumour marker such as EGFR. Often however patient samples limit the extent of staining that can be performed

using the laboratory flow cytometer. Alternatively, this may be a reflection on the patient's treatment history. Indeed, all three patients used in the cell composition experiment had received chemotherapy in the preceding 10 days before sample collection. As such, these results might represent a transient depletion in tumour cell numbers following therapy. Importantly, with increased samples a more representative figure of the tumour content within ascites can be established and this can be integrated into other *in vitro* studies that study macrophage – tumour interactions, such that the ratio of tumour cells to macrophage is representative of the clinical setting. For example, in early polarisation experiments within this thesis tumour cells and macrophages were cultured at 1:1 ratios based on extent of M2 polarisation observed across different ratios, but also guided by prior studies within this laboratory in colorectal cancer. By more accurately determining the tumour to macrophage ratio in ascites samples, this can be used to make *in vitro* models that better capitulate the clinical setting.

7 General discussion and conclusions

7.1 Principal findings

- M2-polarised macrophages display a phenotype that is reversible and can be therapeutically modulated by IFN-γ towards a more M1, classically-activated macrophage profile associated with enhanced NO production, and increased expression of CD80 and MHC II.

- Morphological characterisation of human ovarian cancer ascites-polarised macrophages shows a profile of receptor expression that does not fully conform to the idealized profile of either M1 or M2 cells, with particular discrepancies in CD64, CD169 and MHC I. However, the functional behaviour of the cells (as assessed by NO production) is essentially consistent with an M2 phenotype, and this can be switched to resemble M1 phenotype by re-education with IFN-γ. This provides a simple yet useful assay of functional re-education.

- ColoAd1 armed with hIFN-γ can mediate morphological re-education of M2-polarised human macrophages and human ovarian cancer ascites-polarised as evidenced by MHC II and TNF-α expression. Most importantly, ColoAd1-hIFN-γ re-educates ascites-polarised macrophages at the functional level, with virus-treated macrophages demonstrating increased NO production relative to those re-educated using hIFN-γ alone

7.2 General discussion

This thesis establishes, for the first time, that the plasticity of macrophages may be exploited by oncolytic viruses expressing IFN-γ, to convert M2 macrophages more to an M1 phenotype. This raises the possibility that such viruses might be developed and used to activate TAMs to a more tumouricidal phenotype, providing an additional therapeutic angle to the use of oncolytic viruses. The effects of macrophage activation within the tumour could be additive or even synergistic with the direct anticancer effects of the virus. This is an enticing possibility since TAMs often constitute a major fraction of the cells within solid tumours, and engaging them in a therapeutic effort could provide a powerful therapeutic innovation.

Macrophages are usually well differentiated and exhibit relatively low growth rates, providing major limitations to the availability of relevant cells for *in vitro* experimentation. As a result, most of the work in this thesis has been performed using cell line models of murine and human macrophages, rather than macrophages directly isolated or cultured from mice or humans. However, given the amount of optimisation and the number of macrophages required, using freshly-derived macrophages throughout would be a major challenge. Peritoneal lavage is a common method for macrophage isolation from mice, however cell numbers are low (approximately 1 $x10^5$ - 1 $x10^6$ cells per mouse). To overcome this issue, peritoneal elicitation of murine macrophages using beads of materials thioglycollate or gelatin can generate higher numbers of macrophages within the peritoneal cavity (approximately 1 $x10^6$ - 1 $x10^7$ cells per mouse). However, such materials often pre-polarise macrophages, typically displaying highly inflammatory properties which would skew baselines levels of receptor expression more toward an M1-type and would be incompatible with my studies (Zhang et al., 2001). In humans, macrophages are generated most commonly by

monocyte isolation from blood samples, followed by 5-7 day culture with M-CSF or GM-CSF and further differentiation using M1- or M2- polarising signals for 1-3 days. Again, cell numbers were a limiting factor from laboratory donations of peripheral blood, and significant variation in both the type and quality of macrophages generated from leukocyte or buffy coats obtained from the NHS blood service proved prohibitory for consistent research. From the outset, the cell line models were therefore used as a means to perform initial hypothesis testing, generating proof-of-concept data which could be expanded upon later using more clinically relevant models, to assess whether the hypotheses still held.

The significance of working with more clinically obtained cells is that they have not been subject to an immortalisation process that may affect the plasticity and polarisation of macrophages. As such, TAMs isolated from ovarian ascites have been utilised as early as possible during the course of this research and are central to future investigations, however they are themselves limited by availability and variability; collection of ascites can often be a sporadic process, a problem compounded by variability in sample quality in size. Thus, significant flexibility is required in the design of experiments and, conversely, maintaining consistent experimentation can often be challenging.

There is however an overwhelming imperative to work with more clinically relevant polarisation conditions. In Chapter 3 and 4, a large amount of this work has relied on very defined polarisation culture media, consisting of one or two cytokines alone that are probably not representative of the wider cytokine milieu to which macrophages are exposed *in vivo*. This issue has been addressed, at least in part, by using tumour cell line

supernatants and ascitic fluid as polarisation media, and these have been incorporated where possible and found to influence even the most fundamental aspects of polarisation. Receptor expression illustrate this point well in the context of ascitic fluid, where CD86 expression can be significantly lower in ascites-polarised macrophages than in M2 medium-polarised macrophages, whilst CD64 expression in ascites-polarised macrophages is higher than classically activated M1 macrophages; Such findings have profound implications for choices of markers in identifying TAM from clinical samples and in assessing re-education.

Such data also re-emphasises the requirement for functional assays in studies of macrophage polarisation, as means to assess changes in behaviour of macrophages. NO production has been widely utilised in this thesis to study functional changes in macrophages exposed to traditional and complex models of polarization, and to assess re-education in these settings. Cross-presentation of antigen arises as an attractive avenue of research to pursue following the preliminary findings in this thesis that M1-type macrophages are more efficient cross-presenters than M2-type. Study of cross presentation processes is particularly limited in the context of oncolytic adenovirus; in animal models there is a requirement for such studies to be performed in human tumour xenografts in immune-incompetent animals, while studies in human systems are currently limited by the paucity of antigen-presentation models.

7.3 Future work

To validate the findings with the morphological and functional markers identified in Chapters 3 and 4, it would be useful to repeat the polarisation and re-education

experiments using monocyte-derived macrophages from blood donors and in bone-marrow derived macrophages. To assess whether such re-education events are indicative of a more global change in macrophage phenotype, it would be useful to combine these experiments with analysis of changes in gene expression across a number of "known" M1/ M2 gene expression profiles (such as performed by Martinez et al (Martinez et al., 2013)). In such experiments it would be interesting to compare the differences in gene expression between macrophages re-educated with IFN-γ alone, or IFN-γ produced by oncolytic virus. Arguably, the most realistic model would be macrophages isolated from solid tumours or malignant ascites. In addition to the *ex vivo* method described in this thesis, it would be useful to perform a more simplistic *ex vivo* model, isolating the macrophages within the ascites by plastic adherence or magnetic sorting as previously described (Duluc et al., 2009), then trying to re-educate the cells using the *in vitro* methods described earlier. With the success of the NO assay in this thesis, it would be both interesting and important to assess whether it could work in such an *ex vivo* setting for macrophage re-education, as previous attempts have largely been limited by the quality and quantity of cells within the ascites samples (in both human and mouse settings).

A major focus of the functional assays studied in this thesis was the difference in cross presentation between differentially polarised macrophages. To study the impact of virally lysed B16OVA cells on the ability to induce tumouricidal CD8 T cells would require an immunocompetent mouse model, which would be incompatible with the human-specificity of ColoAd1. Therefore, as a means to study the induction of adaptive anti-tumour immunity following tumour cell lysis by an oncolytic virus expressing IFN-γ, the laboratory has engineered an oncolytic herpes virus expressing IFN-γ, which is

capable of infecting, replicating within and lysing murine tumour cells. This virus will provide a versatile model system and will be utilised in *in vivo* tumour experiments to examine both macrophage re-education and the induction of adaptive anti-tumour responses.

This thesis has focused on the ability of IFN-γ alone, or produced by an oncolytic adenovirus, to mediate changes in phenotype of macrophages, although relatively little attention was paid the little attention to the impact of virus alone. From clinical trials using oncolytic viruses, the interaction of viruses with macrophages seems to be of particular importance; macrophages have been identified as a predominant inflammatory infiltrate following successful oncolytic therapy, associated with tumour regression and induction of anti-tumour immune responses (Jakeman et al., 2015a). Future work should include focus on the reciprocal interactions between viruses and macrophages, in particular expanding on the immunomodulatory impact of CD46 ligation by ColoAd1 in inducing NO and pro-inflammatory cytokine production. Equally, work could focus on how macrophages may impact on virus infection and consequent oncolysis. A number of M2-associated secreted factors (such as TGF-β) have been shown to sensitise tumour cells to oncolytic virotherapy when produced by stromal cells such as fibroblasts, in a mechanism involving down-regulation of anti-viral gene expression (Ilkow et al., 2015). It would interesting to investigate whether M2 macrophages can elicit similar sensitising effects on tumour cells as this would have considerable therapeutic implications.

7.4 Conclusions

This thesis has demonstrated that the plasticity of macrophages can be modulated therapeutically by treatment with IFN-γ alone, or through IFN-γ produced by the oncolytic adenovirus, ColoAd1. Oncolytic virus-mediated delivery of IFN-γ represents a novel approach to macrophage re-education and further, provides a solution to the problems of limited half-life associated with IFN-γ administered as a free agent. Importantly, the changes in morphological and functional phenotypes of macrophages have been achieved in translationally-relevant settings, where macrophages were previously suppressed by IL-4, tumour cell line supernatants or by the fluid of malignant ascites.

Whether the re-education of macrophage phenotype observed in response to IFN-γ alone or ColoAd1-IFNγ will correlate with significant changes to tumour growth or the induction of anti-tumour immunity will require considerable experimentation. However, this thesis has demonstrated that macrophage re-education is a plausible hypothesis and provides proof of principle that such re-polarisation can be achieved by viral-mediated delivery of IFN-γ.

8 References

Ahmed, N., Stenvers, K.L., 2013. Getting to Know Ovarian Cancer Ascites: Opportunities for Targeted Therapy-Based Translational Research. Front. Oncol. 3, 256. doi:10.3389/fonc.2013.00256

Ahn, G.O., Ahn, G.-O., Tseng, D., Tseng, D., Liao, C.-H., Liao, C.H., Dorie, M.J., Dorie, M.J., Czechowicz, A., Czechowicz, A., Brown, J.M., Brown, J.M., 2010. Inhibition of Mac-1 (CD11b/CD18) enhances tumor response to radiation by reducing myeloid cell recruitment. Proc. Natl. Acad. Sci. U.S.A. 107, 8363–8368. doi:10.1073/pnas.0911378107

Aki, M., Shimbara, N., Takashina, M., Akiyama, K., Kagawa, S., Tamura, T., Tanahashi, N., Yoshimura, T., Tanaka, K., Ichihara, A., 1994. Interferon-gamma induces different subunit organizations and functional diversity of proteasomes. J. Biochem. 115, 257–269.

Allavena, P., Chieppa, M., Bianchi, G., Solinas, G., Fabbri, M., Laskarin, G., Mantovani, A., 2010. Engagement of the mannose receptor by tumoral mucins activates an immune suppressive phenotype in human tumor-associated macrophages. Clin. Dev. Immunol. 2010, 547179–10. doi:10.1155/2010/547179

Allavena, P., Germano, G., Marchesi, F., Mantovani, A., 2011. Chemokines in cancer related inflammation. Experimental Cell Research 317, 664–673. doi:10.1016/j.yexcr.2010.11.013

Allavena, P., Mantovani, A., 2012. Immunology in the clinic review series; focus on cancer: tumour-associated macrophages: undisputed stars of the inflammatory tumour microenvironment. Clinical & Experimental Immunology 167, 195–205. doi:10.1111/j.1365-2249.2011.04515.x

Allavena, P., Peccatori, F., Maggioni, D., Erroi, A., Sironi, M., Colombo, N., Lissoni, A., Galazka, A., Meiers, W., Mangioni, C., 1990. Intraperitoneal recombinant gamma-interferon in patients with recurrent ascitic ovarian carcinoma: modulation of cytotoxicity and cytokine production in tumor-associated effectors and of major histocompatibility antigen expression on tumor cells. Cancer Res. 50, 7318–7323.

Angell, T.E., Lechner, M.G., Jang, J.K., LoPresti, J.S., Epstein, A.L., 2014. MHC class I loss is a frequent mechanism of immune escape in papillary thyroid cancer that is reversed by interferon and selumetinib treatment in vitro. Clin. Cancer Res. 20, 6034–6044. doi:10.1158/1078-0432.CCR-14-0879

Arellano-Garcia, M.E., Misuno, K., Tran, S.D., Hu, S., 2014. Interferon-γ induces immunoproteasomes and the presentation of MHC I-associated peptides on human salivary gland cells. PLoS ONE 9, e102878. doi:10.1371/journal.pone.0102878

Asano, K., Nabeyama, A., Miyake, Y., Qiu, C.-H., Kurita, A., Tomura, M., Kanagawa, O., Fujii, S.-I., Tanaka, M., 2011. CD169-positive macrophages dominate antitumor immunity by crosspresenting dead cell-associated antigens. Immunity 34, 85–95. doi:10.1016/j.immuni.2010.12.011

Bak, S.P., Bak, S.P., Walters, J.J., Walters, J.J., Takeya, M., Takeya, M., Conejo-Garcia, J.R., Conejo-Garcia, J.R., Berwin, B.L., Berwin, B.L., 2007. Scavenger Receptor-A-Targeted Leukocyte Depletion Inhibits Peritoneal Ovarian Tumor Progression. Cancer Res. 67, 4783–4789. doi:10.1158/0008-5472.CAN-06-4410

Barleon, B., SOZZANI, S., Zhou, D., Weich, H.A., Mantovani, A., Marmé, D., 1996. Migration of human monocytes in response to vascular endothelial growth factor (VEGF) is mediated via the VEGF receptor flt-1. Blood 87, 3336–3343.

Beatty, G.L., Beatty, G.L., Chiorean, E.G., Chiorean, E.G., Fishman, M.P., Fishman, M.P., Saboury, B., Saboury, B., Teitelbaum, U.R., Teitelbaum, U.R., Sun, W., Sun, W., Huhn, R.D., Huhn, R.D., Song, W., Song, W., Li, D., Li, D., Sharp, L.L., Sharp, L.L., Torigian, D.A., Torigian, D.A., O'Dwyer, P.J., O'Dwyer, P.J., Vonderheide, R.H., Vonderheide, R.H., 2011. CD40 Agonists Alter Tumor Stroma and Show Efficacy Against Pancreatic Carcinoma in Mice and Humans. Science 331, 1612–1616. doi:10.1126/science.1198443

Bennett, E.M., Bennink, J.R., Yewdell, J.W., Brodsky, F.M., 1999. Cutting edge: adenovirus E19 has two mechanisms for affecting class I MHC expression. J. Immunol. 162, 5049–5052.

Bernhard, C.A., Ried, C., Kochanek, S., Brocker, T., 2015. CD169+ macrophages are sufficient for priming of CTLs with specificities left out by cross-priming dendritic cells. Proc. Natl. Acad. Sci.

U.S.A. 112, 5461–5466. doi:10.1073/pnas.1423356112
Bingle, L., Brown, N.J., Lewis, C.E., 2002. The role of tumour-associated macrophages in tumour progression: implications for new anticancer therapies. J. Pathol. 196, 254–265. doi:10.1002/path.1027
Biswas, S.K., Mantovani, A., 2010. Macrophage plasticity and interaction with lymphocyte subsets: cancer as a paradigm. Nat. Immunol. 11, 889–896. doi:10.1038/ni.1937
Biswas, S.K., Sica, A., Lewis, C.E., 2008. Plasticity of macrophage function during tumor progression: regulation by distinct molecular mechanisms. J. Immunol. 180, 2011–2017.
Boes, B., Hengel, H., Ruppert, T., Multhaup, G., Koszinowski, U.H., Kloetzel, P.M., 1994. Interferon gamma stimulation modulates the proteolytic activity and cleavage site preference of 20S mouse proteasomes. Journal of Experimental Medicine 179, 901–909.
Bonapace, L., Coissieux, M.-M., Wyckoff, J., Mertz, K.D., Varga, Z., Junt, T., Bentires-Alj, M., 2014. Cessation of CCL2 inhibition accelerates breast cancer metastasis by promoting angiogenesis. Nature 515, 130–133. doi:10.1038/nature13862
Boruchov, A.M., Boruchov, A.M., Heller, G., Veri, M.-C., Bonvini, E., Ravetch, J.V., Young, J.W., 2005. Activating and inhibitory IgG Fc receptors on human DCs mediate opposing functions. J. Clin. Invest. 115, 2914–2923. doi:10.1172/JCI24772
Brown, J.M., Giaccia, A.J., 1998. The unique physiology of solid tumors: opportunities (and problems) for cancer therapy. Cancer Res. 58, 1408–1416.
Brown, J.M., Wilson, W.R., 2004. Exploiting tumour hypoxia in cancer treatment. Nat. Rev. Cancer 4, 437–447. doi:10.1038/nrc1367
Brucet, M., Marqués, L., Sebastián, C., Lloberas, J., Celada, A., 2004. Regulation of murine Tap1 and Lmp2 genes in macrophages by interferon gamma is mediated by STAT1 and IRF-1. Genes Immun. 5, 26–35. doi:10.1038/sj.gene.6364035
Buhtoiarov, I.N., Lum, H., Berke, G., Paulnock, D.M., Sondel, P.M., Rakhmilevich, A.L., 2005. CD40 ligation activates murine macrophages via an IFN-gamma-dependent mechanism resulting in tumor cell destruction in vitro. J. Immunol. 174, 6013–6022.
Buhtoiarov, I.N., Sondel, P.M., Wigginton, J.M., Buhtoiarova, T.N., Yanke, E.M., Mahvi, D.A., Rakhmilevich, A.L., 2010. Anti-tumour synergy of cytotoxic chemotherapy and anti-CD40 plus CpG-ODN immunotherapy through repolarization of tumour-associated macrophages. Immunology 132, 226–239. doi:10.1111/j.1365-2567.2010.03357.x
Burgdorf, S., Burgdorf, S., Kautz, A., Kautz, A., Böhnert, V., Bohnert, V., Knolle, P.A., Knolle, P.A., Kurts, C., Kurts, C., 2007. Distinct Pathways of Antigen Uptake and Intracellular Routing in CD4 and CD8 T Cell Activation. Science 316, 612–616. doi:10.1126/science.1137971
Burgdorf, S., Schölz, C., Kautz, A., Tampé, R., Kurts, C., 2008. Spatial and mechanistic separation of cross-presentation and endogenous antigen presentation. Nat. Immunol. 9, 558–566. doi:10.1038/ni.1601
Cao, X., Cao, X., Leonard, K., Leonard, K., Collins, L.I., Collins, L.I., Cai, S.F., Cai, S.F., Mayer, J.C., Mayer, J.C., Payton, J.E., Payton, J.E., Walter, M.J., Walter, M.J., Piwnica-Worms, D., Piwnica-Worms, D., Schreiber, R.D., Schreiber, R.D., Ley, T.J., Ley, T.J., 2009. Interleukin 12 Stimulates IFN- -Mediated Inhibition of Tumor-Induced Regulatory T-Cell Proliferation and Enhances Tumor Clearance. Cancer Res. 69, 8700–8709. doi:10.1158/0008-5472.CAN-09-1145
Castillo-Avila, W., Piulats, J.M., Garcia Del Muro, X., Vidal, A., Condom, E., Casanovas, O., Mora, J., Germà, J.R., Capellà, G., Villanueva, A., Viñals, F., 2009. Sunitinib inhibits tumor growth and synergizes with cisplatin in orthotopic models of cisplatin-sensitive and cisplatin-resistant human testicular germ cell tumors. Clin. Cancer Res. 15, 3384–3395. doi:10.1158/1078-0432.CCR-08-2170
Chao, M.P., Alizadeh, A.A., Tang, C., Myklebust, J.H., Varghese, B., Gill, S., Jan, M., Cha, A.C., Chan, C.K., Tan, B.T., Park, C.Y., Zhao, F., Kohrt, H.E., Malumbres, R., Briones, J., Gascoyne, R.D., Lossos, I.S., Levy, R., Weissman, I.L., Majeti, R., 2010. Anti-CD47 antibody synergizes with rituximab to promote phagocytosis and eradicate non-Hodgkin lymphoma. Cell 142, 699–713. doi:10.1016/j.cell.2010.07.044
Chao, M.P., Weissman, I.L., Majeti, R., 2012. The CD47-SIRPα pathway in cancer immune evasion and potential therapeutic implications. Curr. Opin. Immunol. 24, 225–232. doi:10.1016/j.coi.2012.01.010
Chao, Y., Karmali, P.P., Simberg, D., 2012. Role of carbohydrate receptors in the macrophage uptake of dextran-coated iron oxide nanoparticles. Adv. Exp. Med. Biol. 733, 115–123. doi:10.1007/978-94-007-2555-3_11
Chartier, C., Degryse, E., Gantzer, M., Dieterle, A., Pavirani, A., Mehtali, M., 1996. Efficient generation of recombinant adenovirus vectors by homologous recombination in Escherichia coli. J. Virol. 70, 4805–4810.
Chen, C., Pore, N., Behrooz, A., Ismail-Beigi, F., Maity, A., 2001. Regulation of glut1 mRNA by

hypoxia-inducible factor-1. Interaction between H-ras and hypoxia. Journal of Biological Chemistry 276, 9519–9525. doi:10.1074/jbc.M010144200
Coffelt, S.B., Chen, Y.-Y., Muthana, M., Welford, A.F., Tal, A.O., Scholz, A., Plate, K.H., Reiss, Y., Murdoch, C., De Palma, M., Lewis, C.E., 2011. Angiopoietin 2 stimulates TIE2-expressing monocytes to suppress T cell activation and to promote regulatory T cell expansion. J. Immunol. 186, 4183–4190. doi:10.4049/jimmunol.1002802
Condeelis, J., Pollard, J.W., 2006. Macrophages: obligate partners for tumor cell migration, invasion, and metastasis. Cell 124, 263–266. doi:10.1016/j.cell.2006.01.007
Cook, K.W., Letley, D.P., Ingram, R.J.M., Staples, E., Skjoldmose, H., Atherton, J.C., Robinson, K., 2014. CCL20/CCR6-mediated migration of regulatory T cells to the Helicobacter pylori-infected human gastric mucosa. Gut 63, 1550–1559. doi:10.1136/gutjnl-2013-306253
Cramer, L.A., Klemsz, M.J., 1997. Altered kinetics of Tap-1 gene expression in macrophages following stimulation with both IFN-gamma and LPS. Cell. Immunol. 178, 53–61. doi:10.1006/cimm.1997.1118
Curiel, T.J., Coukos, G., Zou, L., Alvarez, X., Cheng, P., Mottram, P., Evdemon-Hogan, M., Conejo-Garcia, J.R., Zhang, L., Burow, M., Zhu, Y., Wei, S., Kryczek, I., Daniel, B., Gordon, A., Myers, L., Lackner, A., Disis, M.L., Knutson, K.L., Chen, L., Zou, W., 2004. Specific recruitment of regulatory T cells in ovarian carcinoma fosters immune privilege and predicts reduced survival. Nat Med 10, 942–949. doi:10.1038/nm1093
Dannenmann, S.R., Thielicke, J., Stöckli, M., Matter, C., Boehmer, von, L., Cecconi, V., Hermanns, T., Hefermehl, L., Schraml, P., Moch, H., Knuth, A., van den Broek, M., 2014. Tumor-associated macrophages subvert T-cell function and correlate with reduced survival in clear cell renal cell carcinoma. OncoImmunology 2, e23562. doi:10.4161/onci.23562
Daurkin, I., Daurkin, I., Eruslanov, E., Eruslanov, E., Stoffs, T., Stoffs, T., Perrin, G.Q., Perrin, G.Q., Algood, C., Algood, C., Gilbert, S.M., Gilbert, S.M., Rosser, C.J., Rosser, C.J., Su, L.-M., Su, L.M., Vieweg, J., Vieweg, J., Kusmartsev, S., Kusmartsev, S., 2011. Tumor-Associated Macrophages Mediate Immunosuppression in the Renal Cancer Microenvironment by Activating the 15-Lipoxygenase-2 Pathway. Cancer Res. 71, 6400–6409. doi:10.1158/0008-5472.CAN-11-1261
de Graaf, N., van Helden, M.J.G., Textoris-Taube, K., Chiba, T., Topham, D.J., Kloetzel, P.M., Zaiss, D.M.W., Sijts, A.J.A.M., 2011. PA28 and the proteasome immunosubunits play a central and independent role in the production of MHC class I-binding peptides in vivo. Eur. J. Immunol. 41, 926–935. doi:10.1002/eji.201041040
De Palma, M., Venneri, M.A., Galli, R., Sergi, L.S., Sergi Sergi, L., Politi, L.S., Sampaolesi, M., Naldini, L., 2005. Tie2 identifies a hematopoietic lineage of proangiogenic monocytes required for tumor vessel formation and a mesenchymal population of pericyte progenitors. Cancer Cell 8, 211–226. doi:10.1016/j.ccr.2005.08.002
Denning, T.L., Wang, Y.-C., Patel, S.R., Williams, I.R., Pulendran, B., 2007. Lamina propria macrophages and dendritic cells differentially induce regulatory and interleukin 17–producing T cell responses. Nat. Immunol. 8, 1086–1094. doi:10.1038/ni1511
Deshmane, S.L., Kremlev, S., Amini, S., Sawaya, B.E., 2009. Monocyte Chemoattractant Protein-1 (MCP-1): An Overview. Journal of Interferon & Cytokine Research 29, 313–326. doi:10.1089/jir.2008.0027
Di, Y., Seymour, L., Fisher, K., 2014. Activity of a group B oncolytic adenovirus (ColoAd1) in whole human blood. Gene Ther. 21, 440–443. doi:10.1038/gt.2014.2
Dickensheets, H.L., Venkataraman, C., Schindler, U., Donnelly, R.P., 1999. Interferons inhibit activation of STAT6 by interleukin 4 in human monocytes by inducing SOCS-1 gene expression. Proc. Natl. Acad. Sci. U.S.A. 96, 10800–10805.
Doedens, A.L., Doedens, A.L., Stockmann, C., Stockmann, C., Rubinstein, M.P., Rubinstein, M.P., Liao, D., Liao, D., Zhang, N., Zhang, N., DeNardo, D.G., Denardo, D.G., Coussens, L.M., Coussens, L.M., Karin, M., Karin, M., Goldrath, A.W., Goldrath, A.W., Johnson, R.S., Johnson, R.S., 2010. Macrophage Expression of Hypoxia-Inducible Factor-1 Suppresses T-Cell Function and Promotes Tumor Progression. Cancer Res. 70, 7465–7475. doi:10.1158/0008-5472.CAN-10-1439
Duluc, D., Corvaisier, M., Blanchard, S., Catala, L., Descamps, P., Gamelin, E., Ponsoda, S., Delneste, Y., Hebbar, M., Jeannin, P., 2009. Interferon-gamma reverses the immunosuppressive and protumoral properties and prevents the generation of human tumor-associated macrophages. Int. J. Cancer 125, 367–373. doi:10.1002/ijc.24401
Dunn, G.P., Sheehan, K.C.F., Old, L.J., Schreiber, R.D., 2005. IFN unresponsiveness in LNCaP cells due to the lack of JAK1 gene expression. Cancer Res. 65, 3447–3453. doi:10.1158/0008-5472.CAN-04-4316
Eggerding, F.A., Pierce, W.C., 1986. Molecular biology of adenovirus type 2 semipermissive infections.

I. Viral growth and expression of viral replicative functions during restricted adenovirus infection. Virology 148, 97–113.
Ehling, J., Ehling, J., Bartneck, M., Bartneck, M., Wei, X., Wei, X., Gremse, F., Gremse, F., Fech, V., Fech, V., Möckel, D., Mockel, D., Baeck, C., Baeck, C., Hittatiya, K., Hittatiya, K., Eulberg, D., Eulberg, D., Luedde, T., Luedde, T., Kiessling, F., Kiessling, F., Trautwein, C., Trautwein, C., Lammers, T., Lammers, T., Tacke, F., Tacke, F., 2014. CCL2-dependent infiltrating macrophages promote angiogenesis in progressive liver fibrosis. Gut 63, 1960–1971. doi:10.1136/gutjnl-2013-306294
Ellis, L.M., Hicklin, D.J., 2008. VEGF-targeted therapy: mechanisms of anti-tumour activity. Nat. Rev. Cancer 8, 579–591. doi:10.1038/nrc2403
Ferracini, M., Rios, F.J.O., Pecenin, M., Jancar, S., 2013. Clearance of Apoptotic Cells by Macrophages Induces Regulatory Phenotype and Involves Stimulation of CD36 and Platelet-Activating Factor Receptor. Mediators of Inflammation 2013, 1–8. doi:10.1155/2013/950273
Fleetwood, A.J., Lawrence, T., Hamilton, J.A., Cook, A.D., 2007. Granulocyte-macrophage colony-stimulating factor (CSF) and macrophage CSF-dependent macrophage phenotypes display differences in cytokine profiles and transcription factor activities: implications for CSF blockade in inflammation. J. Immunol. 178, 5245–5252.
Fletcher, M., Fletcher, M., Ramirez, M.E., Ramirez, M.E., Sierra, R.A., Sierra, R.A., Raber, P., Raber, P., Thevenot, P., Thevenot, P., Al-Khami, A.A., Al-Khami, A.A., Sanchez-Pino, D., Sanchez-Pino, D., Hernandez, C., Hernandez, C., Wyczechowska, D.D., Wyczechowska, D.D., Ochoa, A.C., Ochoa, A.C., Rodriguez, P.C., Rodriguez, P.C., 2015. L-Arginine Depletion Blunts Antitumor T-cell Responses by Inducing Myeloid-Derived Suppressor Cells. Cancer Res. 75, 275–283. doi:10.1158/0008-5472.CAN-14-1491
Fridman, W.-H., Pagès, F., Sautès-Fridman, C., Galon, J., 2012. The immune contexture in human tumours: impact on clinical outcome. Nat. Rev. Cancer 12, 298–306. doi:10.1038/nrc3245
Fritz, J.M., Tennis, M.A., Orlicky, D.J., Lin, H., Ju, C., Redente, E.F., Choo, K.S., Staab, T.A., Bouchard, R.J., Merrick, D.T., Malkinson, A.M., Dwyer-Nield, L.D., 2014. Depletion of Tumor-Associated Macrophages Slows the Growth of Chemically Induced Mouse Lung Adenocarcinomas. Front Immunol 5, 2893. doi:10.3389/fimmu.2014.00587
Fueyo, J., Gomez-Manzano, C., Alemany, R., Lee, P.S., McDonnell, T.J., Mitlianga, P., Shi, Y.X., Levin, V.A., Yung, W.K., Kyritsis, A.P., 2000. A mutant oncolytic adenovirus targeting the Rb pathway produces anti-glioma effect in vivo. Oncogene 19, 2–12. doi:10.1038/sj.onc.1203251
Gajewski, T.F., Meng, Y., Blank, C., Brown, I., Kacha, A., Kline, J., Harlin, H., 2006. Immune resistance orchestrated by the tumor microenvironment. Immunol. Rev. 213, 131–145. doi:10.1111/j.1600-065X.2006.00442.x
Galarneau, H., Villeneuve, J., Gowing, G., Julien, J.-P., Vallières, L., 2007. Increased glioma growth in mice depleted of macrophages. Cancer Res. 67, 8874–8881. doi:10.1158/0008-5472.CAN-07-0177
Gantner, B.N., Simmons, R.M., Canavera, S.J., Akira, S., Underhill, D.M., 2003. Collaborative induction of inflammatory responses by dectin-1 and Toll-like receptor 2. Journal of Experimental Medicine 197, 1107–1117. doi:10.1084/jem.20021787
Garbán, H.J., Garbán, H.J., Bonavida, B., Bonavida, B., 1999. Nitric Oxide Sensitizes Ovarian Tumor Cells to Fas-Induced Apoptosis. Gynecologic Oncology 73, 257–264. doi:10.1006/gyno.1999.5374
Germano, G., Frapolli, R., Belgiovine, C., Anselmo, A., Pesce, S., Liguori, M., Erba, E., Uboldi, S., Zucchetti, M., Pasqualini, F., Nebuloni, M., van Rooijen, N., Mortarini, R., Beltrame, L., Marchini, S., Fuso Nerini, I., Sanfilippo, R., Casali, P.G., Pilotti, S., Galmarini, C.M., Anichini, A., Mantovani, A., D'Incalci, M., Allavena, P., 2013. Role of macrophage targeting in the antitumor activity of trabectedin. Cancer Cell 23, 249–262. doi:10.1016/j.ccr.2013.01.008
Giraudo, E., Inoue, M., Hanahan, D., 2004. An amino-bisphosphonate targets MMP-9–expressing macrophages and angiogenesis to impair cervical carcinogenesis. J. Clin. Invest. 114, 623–633. doi:10.1172/JCI22087
Goerdt, S., Orfanos, C.E., 1999. Other functions, other genes: alternative activation of antigen-presenting cells. Immunity 10, 137–142.
Gordon, S., 2003. Alternative activation of macrophages. Nat. Rev. Immunol. 3, 23–35. doi:10.1038/nri978
Gowing, G., Vallières, L., Julien, J.-P., 2006. Mouse model for ablation of proliferating microglia in acute CNS injuries. Glia 53, 331–337. doi:10.1002/glia.20288
Groettrup, M., Ruppert, T., Kuehn, L., Seeger, M., Standera, S., Koszinowski, U., Kloetzel, P.M., 1995. The interferon-gamma-inducible 11 S regulator (PA28) and the LMP2/LMP7 subunits govern the peptide production by the 20 S proteasome in vitro. Journal of Biological Chemistry 270, 23808–23815.

Grugan, K.D., Grugan, K.D., McCabe, F.L., McCabe, F.L., Kinder, M., Kinder, M., Greenplate, A.R., Greenplate, A.R., Harman, B.C., Harman, B.C., Ekert, J.E., Ekert, J.E., van Rooijen, N., van Rooijen, N., Anderson, G.M., Anderson, G.M., Nemeth, J.A., Nemeth, J.A., Strohl, W.R., Strohl, W.R., Jordan, R.E., Jordan, R.E., Brezski, R.J., Brezski, R.J., 2012. Tumor-Associated Macrophages Promote Invasion while Retaining Fc-Dependent Anti-Tumor Function. J. Immunol. 189, 5457–5466. doi:10.4049/jimmunol.1201889

Guiducci, C., Vicari, A.P., Sangaletti, S., Trinchieri, G., Colombo, M.P., 2005. Redirecting in vivo elicited tumor infiltrating macrophages and dendritic cells towards tumor rejection. Cancer Res. 65, 3437–3446. doi:10.1158/0008-5472.CAN-04-4262

Gutiérrez-Martínez, E., Planès, R., Anselmi, G., Reynolds, M., Menezes, S., Adiko, A.C., Saveanu, L., Guermonprez, P., 2015. Cross-presentation of cell-associated antigens by MHC class I in dendritic cell subsets. Front Immunol 6, 363. doi:10.3389/fimmu.2015.00363

Hagemann, T., Hagemann, T., Biswas, S.K., Biswas, S.K., Lawrence, T., Lawrence, T., SICA, A., Sica, A., Lewis, C.E., Lewis, C.E., 2009. Regulation of macrophage function in tumors: the multifaceted role of NF- B. Blood 113, 3139–3146. doi:10.1182/blood-2008-12-172825

Hagemann, T., Lawrence, T., McNeish, I., Charles, K.A., Kulbe, H., Thompson, R.G., Robinson, S.C., Balkwill, F.R., 2008. “Re-educating” tumor-associated macrophages by targeting NF-kappaB. J. Exp. Med. 205, 1261–1268. doi:10.1084/jem.20080108

Hagemann, T., Wilson, J., Burke, F., Kulbe, H., Li, N.F., Plüddemann, A., Charles, K., Gordon, S., Balkwill, F.R., 2006. Ovarian cancer cells polarize macrophages toward a tumor-associated phenotype. J. Immunol. 176, 5023–5032.

Hait, W.N., 2010. Anticancer drug development: the grand challenges. Nat Rev Drug Discov 9, 253–254. doi:10.1038/nrd3144

Hanada, T., Nakagawa, M., Emoto, A., Nomura, T., Nasu, N., Nomura, Y., 2000. Prognostic value of tumor-associated macrophage count in human bladder cancer. International journal of urology : official journal of the Japanese Urological Association 7, 263–269.

Hanahan, D., Weinberg, R.A., 2011. Hallmarks of Cancer: The Next Generation. Cell 144, 646–674. doi:10.1016/j.cell.2011.02.013

Hanahan, D., Weinberg, R.A., 2000. The hallmarks of cancer. Cell 100, 57–70.

Hardison, J.L., Wrightsman, R.A., Carpenter, P.M., Lane, T.E., Manning, J.E., 2006. The chemokines CXCL9 and CXCL10 promote a protective immune response but do not contribute to cardiac inflammation following infection with Trypanosoma cruzi. Infect. Immun. 74, 125–134. doi:10.1128/IAI.74.1.125-134.2006

Harris, A.L., 2002. Hypoxia--a key regulatory factor in tumour growth. Nat. Rev. Cancer 2, 38–47. doi:10.1038/nrc704

Harris, N.L., Harris, N.L., Ronchese, F., Ronchese, F., 1999. The role of B7 costimulation in T-cell immunity. Immunol Cell Biol 77, 304–311. doi:10.1046/j.1440-1711.1999.00835.x

Hay, J.G., 2003. “Man's best friend”: a new model system for cancer therapeutics? Mol. Ther. 7, 144–145.

He, S., Cao, Q., Yoneyama, H., Ge, H., Zhang, Y., Zhang, Y., 2008. MIP-3alpha and MIP-1alpha rapidly mobilize dendritic cell precursors into the peripheral blood. J. Leukoc. Biol. 84, 1549–1556. doi:10.1189/jlb.0708420

Hemminki, A., Wang, M., Desmond, R.A., Strong, T.V., Alvarez, R.D., Curiel, D.T., 2002. Serum and Ascites Neutralizing Antibodies in Ovarian Cancer Patients Treated with Intraperitoneal Adenoviral Gene Therapy. Human Gene Therapy 13, 1505–1514. doi:10.1089/10430340260185139

Herrero, C., Hu, X., Li, W.P., Samuels, S., Sharif, M.N., Kotenko, S., Ivashkiv, L.B., 2003. Reprogramming of IL-10 activity and signaling by IFN-gamma. J. Immunol. 171, 5034–5041.

Hibbs, J.B., Taintor, R.R., Vavrin, Z., 1987. Macrophage cytotoxicity: role for L-arginine deiminase and imino nitrogen oxidation to nitrite. Science (New York, NY) 235, 473–476.

Hiraoka, K., Zenmyo, M., Watari, K., Iguchi, H., Fotovati, A., Kimura, Y.N., Hosoi, F., Shoda, T., Nagata, K., Osada, H., Ono, M., Kuwano, M., 2008. Inhibition of bone and muscle metastases of lung cancer cells by a decrease in the number of monocytes/macrophages. Cancer Science 99, 1595–1602. doi:10.1111/j.1349-7006.2008.00880.x

Hiroishi, K., Tüting, T., Lotze, M.T., 2000. IFN-alpha-expressing tumor cells enhance generation and promote survival of tumor-specific CTLs. J. Immunol. 164, 567–572.

Hoelder, S., Clarke, P.A., Workman, P., 2012. Discovery of small molecule cancer drugs: successes, challenges and opportunities. Mol Oncol 6, 155–176. doi:10.1016/j.molonc.2012.02.004

Honeychurch, J., Glennie, M.J., Johnson, P.W.M., Illidge, T.M., 2003. Anti-CD40 monoclonal antibody therapy in combination with irradiation results in a CD8 T-cell-dependent immunity to B-cell lymphoma. Blood 102, 1449–1457. doi:10.1182/blood-2002-12-3717

Hood, J.D., Meininger, C.J., Ziche, M., Granger, H.J., 1998. VEGF upregulates ecNOS message, protein, and NO production in human endothelial cells. Am. J. Physiol. 274, H1054–8.
Hoshino, K., Kaisho, T., Iwabe, T., Takeuchi, O., Akira, S., 2002. Differential involvement of IFN-beta in Toll-like receptor-stimulated dendritic cell activation. Int. Immunol. 14, 1225–1231.
Hristodorov, D., Mladenov, R., Felbert, von, V., Huhn, M., Fischer, R., Barth, S., Thepen, T., 2015. Targeting CD64 mediates elimination of M1 but not M2 macrophages in vitro and in cutaneous inflammation in mice and patient biopsies. MAbs 7, 853–862. doi:10.1080/19420862.2015.1066950
Huang, S., Van Arsdall, M., Tedjarati, S., McCarty, M., Wu, W., Langley, R., Fidler, I.J., 2002. Contributions of stromal metalloproteinase-9 to angiogenesis and growth of human ovarian carcinoma in mice. J. Natl. Cancer Inst. 94, 1134–1142.
Hughes, R., Hughes, R., Qian, B.Z., Qian, B.-Z., Rowan, C., Rowan, C., Muthana, M., Muthana, M., Keklikoglou, I., Keklikoglou, I., Olson, O.C., Olson, O.C., Tazzyman, S., Tazzyman, S., Danson, S., Danson, S., Addison, C., Addison, C., Clemons, M., Clemons, M., Gonzalez-Angulo, A.M., Gonzalez-Angulo, A.M., Joyce, J.A., Joyce, J.A., De Palma, M., De Palma, M., Pollard, J.W., Pollard, J.W., Lewis, C.E., Lewis, C.E., 2015. Perivascular M2 Macrophages Stimulate Tumor Relapse after Chemotherapy. Cancer Res. 75, 3479–3491. doi:10.1158/0008-5472.CAN-14-3587
Hume, D.A., 2008. Macrophages as APC and the dendritic cell myth. The Journal of Immunology 181, 5829–5835.
Hume, D.A., Hume, D.A., MacDonald, K.P.A., MacDonald, K.P.A., 2012. Therapeutic applications of macrophage colony-stimulating factor-1 (CSF-1) and antagonists of CSF-1 receptor (CSF-1R) signaling. Blood 119, 1810–1820. doi:10.1182/blood-2011-09-379214
Ibe, S., Qin, Z., Schüler, T., Preiss, S., Blankenstein, T., 2001. Tumor rejection by disturbing tumor stroma cell interactions. J. Exp. Med. 194, 1549–1559.
Ichihashi, T., Satoh, T., Sugimoto, C., Kajino, K., 2013. Emulsified Phosphatidylserine, Simple and Effective Peptide Carrier for Induction of Potent Epitope-Specific T Cell Responses. PLoS ONE 8, e60068. doi:10.1371/journal.pone.0060068
Ilkow, C.S., Marguerie, M., Batenchuk, C., Mayer, J., Ben Neriah, D., Cousineau, S., Falls, T., Jennings, V.A., Boileau, M., Bellamy, D., Bastin, D., de Souza, C.T., Alkayyal, A., Zhang, J., Le Boeuf, F., Arulanandam, R., Stubbert, L., Sampath, P., Thorne, S.H., Paramanthan, P., Chatterjee, A., Strieter, R.M., Burdick, M., Addison, C.L., Stojdl, D.F., Atkins, H.L., Auer, R.C., Diallo, J.-S., Lichty, B.D., Bell, J.C., 2015. Reciprocal cellular cross-talk within the tumor microenvironment promotes oncolytic virus activity. Nat Med 21, 530–536. doi:10.1038/nm.3848
Ilkow, C.S., Swift, S.L., Bell, J.C., Diallo, J.-S., 2014. From scourge to cure: tumour-selective viral pathogenesis as a new strategy against cancer. PLoS Pathog. 10, e1003836. doi:10.1371/journal.ppat.1003836
Jaiswal, S., Chao, M.P., Majeti, R., Weissman, I.L., 2010. Macrophages as mediators of tumor immunosurveillance. Trends Immunol. 31, 212–219. doi:10.1016/j.it.2010.04.001
Jaiswal, S., Jamieson, C.H.M., Pang, W.W., Park, C.Y., Chao, M.P., Majeti, R., Traver, D., van Rooijen, N., Weissman, I.L., 2009. CD47 is upregulated on circulating hematopoietic stem cells and leukemia cells to avoid phagocytosis. Cell 138, 271–285. doi:10.1016/j.cell.2009.05.046
Jakeman, P.G., Hills, T.E., Fisher, K.D., Seymour, L.W., 2015a. Macrophages and their interactions with oncolytic viruses. Curr Opin Pharmacol 24, 23–29. doi:10.1016/j.coph.2015.06.007
Jakeman, P.G., Hills, T.E., Tedcastle, A.B., Di, Y., Fisher, K.D., Seymour, L.W., 2015b. Improved In VitroHuman Tumor Models for Cancer Gene Therapy. Human Gene Therapy 26, 249–256. doi:10.1089/hum.2015.028
Jiang, H., Clise-Dwyer, K., Ruisaard, K.E., Fan, X., Tian, W., Gumin, J., Lamfers, M.L., Kleijn, A., Lang, F.F., Yung, W.-K.A., Vence, L.M., Gomez-Manzano, C., Fueyo, J., 2014. Delta-24-RGD oncolytic adenovirus elicits anti-glioma immunity in an immunocompetent mouse model. PLoS ONE 9, e97407. doi:10.1371/journal.pone.0097407
Jiang, Y., Li, Y., Zhu, B., 2015. T-cell exhaustion in the tumor microenvironment. Cell Death Dis 6, e1792. doi:10.1038/cddis.2015.162
Johnson, V.A., Nara, P.L., 2003. Quantitative Assays for virus infectivity, in: Techniques in HIV Research. pp. 71–86.
Josephs, D.H., Bax, H.J., Karagiannis, S.N., 2015. Tumour-associated macrophage polarisation and re-education with immunotherapy. Frontiers in bioscience (Elite edition) 7, 334–351.
Kakinoki, Y., Kubota, H., Yamamoto, Y., 2004. CD64 surface expression on neutrophils and monocytes is significantly up-regulated after stimulation with granulocyte colony-stimulating factor during CHOP chemotherapy for patients with non-Hodgkin's lymphoma. Int. J. Hematol. 79, 55–62.
Kamba, T., McDonald, D.M., 2007. Mechanisms of adverse effects of anti-VEGF therapy for cancer. Br J Cancer 96, 1788–1795. doi:10.1038/sj.bjc.6603813

Kant, A.M., De, P., Peng, X., Yi, T., Rawlings, D.J., Kim, J.S., Durden, D.L., 2002. SHP-1 regulates Fcgamma receptor-mediated phagocytosis and the activation of RAC. Blood 100, 1852–1859.
Kaplan, D.H., Shankaran, V., Dighe, A.S., Stockert, E., Aguet, M., Old, L.J., Schreiber, R.D., 1998. Demonstration of an interferon gamma-dependent tumor surveillance system in immunocompetent mice. Proc. Natl. Acad. Sci. U.S.A. 95, 7556–7561.
Karagiannis, S.N., Bracher, M.G., Beavil, R.L., Beavil, A.J., Hunt, J., McCloskey, N., Thompson, R.G., East, N., Burke, F., Sutton, B.J., Dombrowicz, D., Balkwill, F.R., Gould, H.J., 2007. Role of IgE receptors in IgE antibody-dependent cytotoxicity and phagocytosis of ovarian tumor cells by human monocytic cells. Cancer Immunol Immunother 57, 247–263. doi:10.1007/s00262-007-0371-7
Karwacz, K., Bricogne, C., MacDonald, D., Arce, F., Bennett, C.L., Collins, M., Escors, D., 2011. PD-L1 co-stimulation contributes to ligand-induced T cell receptor down-modulation on CD8+ T cells. EMBO Mol Med 3, 581–592. doi:10.1002/emmm.201100165
Kaufman, H.L., Kohlhapp, F.J., Zloza, A., 2015. Oncolytic viruses: a new class of immunotherapy drugs. Nat Rev Drug Discov 14, 642–662. doi:10.1038/nrd4663
Kees, T., Kees, T., Lohr, J., Lohr, J., Noack, J., Noack, J., Mora, R., Mora, R., Gdynia, G., Gdynia, G., Tödt, G., Todt, G., Ernst, A., Ernst, A., Radlwimmer, B., Radlwimmer, B., Falk, C.S., Falk, C.S., Herold-Mende, C., Herold-Mende, C., Régnier-Vigouroux, A., Regnier-Vigouroux, A., 2011. Microglia isolated from patients with glioma gain antitumor activities on poly (I:C) stimulation. Neuro-oncology 14, 64–78. doi:10.1093/neuonc/nor182
Keller, R., Keist, R., Wechsler, A., Leist, T.P., van der Meide, P.H., 1990. Mechanisms of macrophage-mediated tumor cell killing: a comparative analysis of the roles of reactive nitrogen intermediates and tumor necrosis factor. Int. J. Cancer 46, 682–686.
Kelly, B., O'Neill, L.A.J., 2015. Metabolic reprogramming in macrophages and dendritic cells in innate immunity. Cell Res 25, 771–784. doi:10.1038/cr.2015.68
Keskinen, P., Ronni, T., Matikainen, S., Lehtonen, A., Julkunen, I., 1997. Regulation of HLA class I and II expression by interferons and influenza A virus in human peripheral blood mononuclear cells. Immunology 91, 421–429.
Kimura, Y.N., Watari, K., Fotovati, A., Hosoi, F., Yasumoto, K., Izumi, H., Kohno, K., Umezawa, K., Iguchi, H., Shirouzu, K., Takamori, S., Kuwano, M., Ono, M., 2007. Inflammatory stimuli from macrophages and cancer cells synergistically promote tumor growth and angiogenesis. Cancer Science 98, 2009–2018. doi:10.1111/j.1349-7006.2007.00633.x
Kinugasa, N., Higashi, T., Nouso, K., Nakatsukasa, H., Kobayashi, Y., Ishizaki, M., Toshikuni, N., Yoshida, K., Uematsu, S., Tsuji, T., 1999. Expression of membrane cofactor protein (MCP, CD46) in human liver diseases. Br J Cancer 80, 1820–1825. doi:10.1038/sj.bjc.6690604
Kioi, M., Vogel, H., Schultz, G., Hoffman, R.M., Harsh, G.R., Brown, J.M., 2010. Inhibition of vasculogenesis, but not angiogenesis, prevents the recurrence of glioblastoma after irradiation in mice. J. Clin. Invest. 120, 694–705. doi:10.1172/JCI40283
Kipps, E., Tan, D.S.P., Kaye, S.B., 2013. Meeting the challenge of ascites in ovarian cancer: new avenues for therapy and research. Nat. Rev. Cancer 13, 273–282. doi:10.1038/nrc3432
Klampfer, L., Huang, J., Corner, G., Mariadason, J., Arango, D., Sasazuki, T., Shirasawa, S., Augenlicht, L., 2003. Oncogenic Ki-ras inhibits the expression of interferon-responsive genes through inhibition of STAT1 and STAT2 expression. Journal of Biological Chemistry 278, 46278–46287. doi:10.1074/jbc.M304721200
Kloetzel, P.M., Ossendorp, F., 2004. Proteasome and peptidase function in MHC-class-I-mediated antigen presentation. Curr. Opin. Immunol. 16, 76–81.
Klotz, L., Klotz, L., Hucke, S., Hucke, S., Thimm, D., Thimm, D., Classen, S., Classen, S., Gaarz, A., Gaarz, A., Schultze, J., Schultze, J., Edenhofer, F., Edenhofer, F., Kurts, C., Kurts, C., Klockgether, T., Klockgether, T., Limmer, A., Limmer, A., Knolle, P., Knolle, P., Burgdorf, S., Burgdorf, S., 2009. Increased Antigen Cross-Presentation but Impaired Cross-Priming after Activation of Peroxisome Proliferator-Activated Receptor Is Mediated by Up-Regulation of B7H1. J. Immunol. 183, 129–136. doi:10.4049/jimmunol.0804260
Klug, F., Prakash, H., Huber, P.E., Seibel, T., Bender, N., Halama, N., Pfirschke, C., Voss, R.H., Timke, C., Umansky, L., Klapproth, K., Schäkel, K., Garbi, N., Jäger, D., Weitz, J., Schmitz-Winnenthal, H., Hämmerling, G.J., Beckhove, P., 2013. Low-Dose Irradiation Programs Macrophage Differentiation to an iNOS+/M1 Phenotype that Orchestrates Effective T Cell Immunotherapy. Cancer Cell 24, 589–602. doi:10.1016/j.ccr.2013.09.014
Koong, A.C., Mehta, V.K., Le, Q.T., Fisher, G.A., Terris, D.J., Brown, J.M., Bastidas, A.J., Vierra, M., 2000. Pancreatic tumors show high levels of hypoxia. Int. J. Radiat. Oncol. Biol. Phys. 48, 919–922.
Korkolopoulou, P., Kaklamanis, L., Pezzella, F., Harris, A.L., Gatter, K.C., 1996. Loss of antigen-presenting molecules (MHC class I and TAP-1) in lung cancer. Br J Cancer 73, 148–153.

Kozin, S.V., Kozin, S.V., Kamoun, W.S., Kamoun, W.S., Huang, Y., Huang, Y., Dawson, M.R., Dawson, M.R., Jain, R.K., Jain, R.K., Duda, D.G., Duda, D.G., 2010. Recruitment of Myeloid but not Endothelial Precursor Cells Facilitates Tumor Regrowth after Local Irradiation. Cancer Res. 70, 5679–5685. doi:10.1158/0008-5472.CAN-09-4446

König, S., Nitzki, F., Uhmann, A., Dittmann, K., Theiss-Suennemann, J., Herrmann, M., Reichardt, H.M., Schwendener, R., Pukrop, T., Schulz-Schaeffer, W., Hahn, H., 2014. Depletion of Cutaneous Macrophages and Dendritic Cells Promotes Growth of Basal Cell Carcinoma in Mice. PLoS ONE 9, e93555. doi:10.1371/journal.pone.0093555

Kryczek, I., Kryczek, I., Wei, S., Wei, S., Zhu, G., Zhu, G., Myers, L., Myers, L., Mottram, P., Mottram, P., Cheng, P., Cheng, P., Chen, L., Chen, L., Coukos, G., Coukos, G., Zou, W., Zou, W., 2007. Relationship between B7-H4, Regulatory T Cells, and Patient Outcome in Human Ovarian Carcinoma. Cancer Res. 67, 8900–8905. doi:10.1158/0008-5472.CAN-07-1866

Kryczek, I., Zou, L., Rodriguez, P., Zhu, G., Wei, S., Mottram, P., Brumlik, M., Cheng, P., Curiel, T., Myers, L., Lackner, A., Alvarez, X., Ochoa, A., Chen, L., Zou, W., 2006. B7-H4 expression identifies a novel suppressive macrophage population in human ovarian carcinoma. J. Exp. Med. 203, 871–881. doi:10.1084/jem.20050930

Kuang, D.-M., Kuang, D.M., Zhao, Q., Zhao, Q., Peng, C., Peng, C., Xu, J., Xu, J., Zhang, J.P., Zhang, J.-P., Wu, C., Wu, C., Zheng, L., Zheng, L., 2009. Activated monocytes in peritumoral stroma of hepatocellular carcinoma foster immune privilege and disease progression through PD-L1. Journal of Experimental Medicine 206, 1327–1337. doi:10.1084/jem.20082173

Kuhn, I., Harden, P., Bauzon, M., Chartier, C., Nye, J., Thorne, S., Reid, T., Ni, S., Lieber, A., Fisher, K., Seymour, L., Rubanyi, G.M., Harkins, R.N., Hermiston, T.W., 2008. Directed Evolution Generates a Novel Oncolytic Virus for the Treatment of Colon Cancer. PLoS ONE 3, e2409. doi:10.1371/journal.pone.0002409

LaBarre, D.D., Lowy, R.J., 2001. Improvements in methods for calculating virus titer estimates from TCID50 and plaque assays. J. Virol. Methods 96, 107–126.

Lanier, L.L., Lanier, L.L., 2001. A renaissance for the tumor immunosurveillance hypothesis. Nat Med 7, 1178–1180. doi:10.1038/nm1101-1178

Lapaque, N., Walzer, T., Méresse, S., Vivier, E., Trowsdale, J., 2009. Interactions between human NK cells and macrophages in response to Salmonella infection. J. Immunol. 182, 4339–4348. doi:10.4049/jimmunol.0803329

Latchman, Y., Wood, C.R., Chernova, T., Chaudhary, D., Borde, M., Chernova, I., Iwai, Y., Long, A.J., Brown, J.A., Nunes, R., Greenfield, E.A., Bourque, K., Boussiotis, V.A., Carter, L.L., Carreno, B.M., Malenkovich, N., Nishimura, H., Okazaki, T., Honjo, T., Sharpe, A.H., Freeman, G.J., 2001. PD-L2 is a second ligand for PD-1 and inhibits T cell activation. Nat. Immunol. 2, 261–268. doi:10.1038/85330

Le Friec, G., Sheppard, D., Whiteman, P., Karsten, C.M., Shamoun, S.A.-T., Laing, A., Bugeon, L., Dallman, M.J., Melchionna, T., Chillakuri, C., Smith, R.A., Drouet, C., Couzi, L., Fremeaux-Bacchi, V., Köhl, J., Waddington, S.N., McDonnell, J.M., Baker, A., Handford, P.A., Lea, S.M., Kemper, C., 2012. The CD46-Jagged1 interaction is critical for human TH1 immunity. Nat. Immunol. 13, 1213–1221. doi:10.1038/ni.2454

Leblond, M.M., Gérault, A.N., Corroyer-Dulmont, A., MacKenzie, E.T., Petit, E., Bernaudin, M., Valable, S., 2016. Hypoxia induces macrophage polarization and re-education toward an M2 phenotype in U87 and U251 glioblastoma models. OncoImmunology 5, e1056442. doi:10.1080/2162402X.2015.1056442

Lee, A.Y.S., Eri, R., Lyons, A.B., Grimm, M.C., Korner, H., 2013. CC Chemokine Ligand 20 and Its Cognate Receptor CCR6 in Mucosal T Cell Immunology and Inflammatory Bowel Disease: Odd Couple or Axis of Evil? Front Immunol 4, 194. doi:10.3389/fimmu.2013.00194

Leek, R.D., Hunt, N.C., Landers, R.J., Lewis, C.E., Royds, J.A., Harris, A.L., 2000. Macrophage infiltration is associated with VEGF and EGFR expression in breast cancer. J. Pathol. 190, 430–436. doi:10.1002/(SICI)1096-9896(200003)190:4<430::AID-PATH538>3.0.CO;2-6

Leek, R.D., Lewis, C.E., Whitehouse, R., Greenall, M., Clarke, J., Harris, A.L., 1996. Association of macrophage infiltration with angiogenesis and prognosis in invasive breast carcinoma. Cancer Res. 56, 4625–4629.

Lefèvre, L., Galès, A., Olagnier, D., Bernad, J., Perez, L., Burcelin, R., Valentin, A., Auwerx, J., Pipy, B., Coste, A., 2010. PPARγ Ligands Switched High Fat Diet-Induced Macrophage M2b Polarization toward M2a Thereby Improving Intestinal Candida Elimination. PLoS ONE 5, e12828. doi:10.1371/journal.pone.0012828

Lesinski, G.B., Trefry, J., Brasdovich, M., Kondadasula, S.V., Sackey, K., Zimmerer, J.M., Chaudhury, A.R., Yu, L., Zhang, X., Crespin, T.R., Walker, M.J., Carson, W.E., 2007. Melanoma cells exhibit

variable signal transducer and activator of transcription 1 phosphorylation and a reduced response to IFN-alpha compared with immune effector cells. Clin. Cancer Res. 13, 5010–5019. doi:10.1158/1078-0432.CCR-06-3092
Lewis, C., Murdoch, C., 2005. Macrophage responses to hypoxia: implications for tumor progression and anti-cancer therapies. Am. J. Pathol. 167, 627–635. doi:10.1016/S0002-9440(10)62038-X
Lewis, C.E., Lewis, C.E., Pollard, J.W., 2006. Distinct Role of Macrophages in Different Tumor Microenvironments. Cancer Res. 66, 605–612. doi:10.1158/0008-5472.CAN-05-4005
Lewis, J.S., Landers, R.J., Underwood, J.C.E., Underwood, J.C., Harris, A.L., Lewis, C.E., 2000. Expression of vascular endothelial growth factor by macrophages is up-regulated in poorly vascularized areas of breast carcinomas. J. Pathol. 192, 150–158. doi:10.1002/1096-9896(2000)9999:9999<::AID-PATH687>3.0.CO;2-G
Li, J., Wang, L., Cong, N., Shi, C., Bu, W., Song, J., Chen, H., 2014. Efficacy of Sorafenib for Advanced Hepatocellular Carcinoma and Prognostic Factors. Hepatogastroenterology 61, 954–957.
Lin, E.Y., Li, J.-F., Gnatovskiy, L., Deng, Y., Zhu, L., Grzesik, D.A., Qian, H., Xue, X.-N., Pollard, J.W., 2006. Macrophages regulate the angiogenic switch in a mouse model of breast cancer. Cancer Res. 66, 11238–11246. doi:10.1158/0008-5472.CAN-06-1278
Lin, E.Y., Nguyen, A.V., Russell, R.G., Pollard, J.W., 2001. Colony-stimulating factor 1 promotes progression of mammary tumors to malignancy. J. Exp. Med. 193, 727–740.
Lissbrant, I.F., Stattin, P., Wikstrom, P., Damber, J.E., Egevad, L., Bergh, A., 2000. Tumor associated macrophages in human prostate cancer: relation to clinicopathological variables and survival. Int J Oncol 17, 445–451.
Liu, J., Wang, L., Zhao, F., Tseng, S., Narayanan, C., Shura, L., Willingham, S., Howard, M., Prohaska, S., Volkmer, J., Chao, M., Weissman, I.L., Majeti, R., 2015. Pre-Clinical Development of a Humanized Anti-CD47 Antibody with Anti-Cancer Therapeutic Potential. PLoS ONE 10, e0137345. doi:10.1371/journal.pone.0137345
Lomonosova, E., Subramanian, T., Chinnadurai, G., 2005. Mitochondrial localization of p53 during adenovirus infection and regulation of its activity by E1B-19K. Oncogene 24, 6796–6808. doi:10.1038/sj.onc.1208836
Lortat-Jacob, H., Baltzer, F., Grimaud, J.A., 1996. Heparin decreases the blood clearance of interferon-gamma and increases its activity by limiting the processing of its carboxyl-terminal sequence. J. Biol. Chem. 271, 16139–16143.
Lum, H.D., Buhtoiarov, I.N., Schmidt, B.E., Berke, G., Paulnock, D.M., Sondel, P.M., Rakhmilevich, A.L., 2006. Tumoristatic effects of anti-CD40 mAb-activated macrophages involve nitric oxide and tumour necrosis factor-alpha. Immunology 118, 261–270. doi:10.1111/j.1365-2567.2006.02366.x
MacMicking, J., MacMicking, J., Xie, Q.W., Xie, Q.-W., Nathan, C., Nathan, C., 1997. NITRIC OXIDE AND MACROPHAGE FUNCTION. Annu. Rev. Immunol. 15, 323–350. doi:10.1146/annurev.immunol.15.1.323
Mancardi, D.A., Albanesi, M., Jönsson, F., Iannascoli, B., van Rooijen, N., Kang, X., England, P., Daëron, M., Bruhns, P., 2013. The high-affinity human IgG receptor FcγRI (CD64) promotes IgG-mediated inflammation, anaphylaxis, and antitumor immunotherapy. Blood 121, 1563–1573. doi:10.1182/blood-2012-07-442541
Mantovani, A., Allavena, P., 2015. The interaction of anticancer therapies with tumor-associated macrophages. J. Exp. Med. 212, 435–445. doi:10.1084/jem.20150295
Mantovani, A., Biswas, S.K., Galdiero, M.R., Sica, A., Locati, M., 2012. Macrophage plasticity and polarization in tissue repair and remodelling. J. Pathol. 229, 176–185. doi:10.1002/path.4133
Mantovani, A., Mantovani, A., SICA, A., Sica, A., Sozzani, S., SOZZANI, S., Allavena, P., Allavena, P., Vecchi, A., VECCHI, A., Locati, M., LOCATI, M., 2004. The chemokine system in diverse forms of macrophage activation and polarization. Trends Immunol. 25, 677–686. doi:10.1016/j.it.2004.09.015
Mantovani, A., Sica, A., 2010. Macrophages, innate immunity and cancer: balance, tolerance, and diversity. Curr. Opin. Immunol. 22, 231–237. doi:10.1016/j.coi.2010.01.009
Mantovani, A., Sozzani, S., Locati, M., Allavena, P., Sica, A., 2002. Macrophage polarization: tumor-associated macrophages as a paradigm for polarized M2 mononuclear phagocytes. Trends Immunol. 23, 549–555.
Martin, M.E., Berk, A.J., 1998. Adenovirus E1B 55K represses p53 activation in vitro. J. Virol. 72, 3146–3154.
Martinez, F.O., Gordon, S., 2014. The M1 and M2 paradigm of macrophage activation: time for reassessment. F1000 Prime Rep 6, 13. doi:10.12703/P6-13
Martinez, F.O., Gordon, S., Locati, M., Mantovani, A., 2006. Transcriptional profiling of the human monocyte-to-macrophage differentiation and polarization: new molecules and patterns of gene

expression. J. Immunol. 177, 7303–7311.
Martinez, F.O., Helming, L., Gordon, S., 2009. Alternative Activation of Macrophages: An Immunologic Functional Perspective. Annu. Rev. Immunol. 27, 451–483. doi:10.1146/annurev.immunol.021908.132532
Martinez, F.O., Helming, L., Milde, R., Varin, A., Melgert, B.N., Draijer, C., Thomas, B., Fabbri, M., Crawshaw, A., Ho, L.P., Hacken, Ten, N.H., Cobos Jiménez, V., Kootstra, N.A., Hamann, J., Greaves, D.R., Locati, M., Mantovani, A., Gordon, S., 2013. Genetic programs expressed in resting and IL-4 alternatively activated mouse and human macrophages: similarities and differences. Blood 121, e57–69. doi:10.1182/blood-2012-06-436212
Martinez, F.O., Sica, A., Mantovani, A., Locati, M., 2008. Macrophage activation and polarization. Frontiers in bioscience : a journal and virtual library 13, 453–461.
Matte, I., Lane, D., Laplante, C., Rancourt, C., Piché, A., 2012. Profiling of cytokines in human epithelial ovarian cancer ascites. American journal of cancer research 2, 566–580.
McCart, J.A., Ward, J.M., Lee, J., Hu, Y., Alexander, H.R., Libutti, S.K., Moss, B., Bartlett, D.L., 2001. Systemic cancer therapy with a tumor-selective vaccinia virus mutant lacking thymidine kinase and vaccinia growth factor genes. Cancer Res. 61, 8751–8757.
Melcher, A., Parato, K., Rooney, C.M., Bell, J.C., 2011. Thunder and lightning: immunotherapy and oncolytic viruses collide. Mol. Ther. 19, 1008–1016. doi:10.1038/mt.2011.65
Miguel, R.D.V., Vicetti Miguel, R.D., Cherpes, T.L., Cherpes, T.L., Watson, L.J., Watson, L.J., McKenna, K.C., McKenna, K.C., 2010. CTL Induction of Tumoricidal Nitric Oxide Production by Intratumoral Macrophages Is Critical for Tumor Elimination. J. Immunol. 185, 6706–6718. doi:10.4049/jimmunol.0903411
Milliken, D., Scotton, C., Raju, S., Balkwill, F., Wilson, J., 2002. Analysis of chemokines and chemokine receptor expression in ovarian cancer ascites. Clin. Cancer Res. 8, 1108–1114.
Minard-Colin, V., Xiu, Y., Poe, J.C., Horikawa, M., Magro, C.M., Hamaguchi, Y., Haas, K.M., Tedder, T.F., 2008. Lymphoma depletion during CD20 immunotherapy in mice is mediated by macrophage FcgammaRI, FcgammaRIII, and FcgammaRIV. Blood 112, 1205–1213. doi:10.1182/blood-2008-01-135160
Miron, M.-J., Blanchette, P., Groitl, P., Dallaire, F., Teodoro, J.G., Li, S., Dobner, T., Branton, P.E., 2009. Localization and importance of the adenovirus E4orf4 protein during lytic infection. J. Virol. 83, 1689–1699. doi:10.1128/JVI.01703-08
Mizutani, K., Sud, S., McGregor, N.A., Martinovski, G., Rice, B.T., Craig, M.J., Varsos, Z.S., Roca, H., Pienta, K.J., 2009. The chemokine CCL2 increases prostate tumor growth and bone metastasis through macrophage and osteoclast recruitment. Neoplasia (New York, NY) 11, 1235–1242.
Mortier, E., Advincula, R., Kim, L., Chmura, S., Barrera, J., Reizis, B., Malynn, B.A., Ma, A., 2009. Macrophage- and dendritic-cell-derived interleukin-15 receptor alpha supports homeostasis of distinct CD8+ T cell subsets. Immunity 31, 811–822. doi:10.1016/j.immuni.2009.09.017
Mosser, D.M., 2003. The many faces of macrophage activation. J. Leukoc. Biol. 73, 209–212.
Mosser, D.M., Edwards, J.P., 2008. Exploring the full spectrum of macrophage activation. Nat. Rev. Immunol. 8, 958–969. doi:10.1038/nri2448
Movahedi, K., Movahedi, K., Laoui, D., Laoui, D., Gysemans, C., Gysemans, C., Baeten, M., Baeten, M., Stange, G., Stangé, G., Van den Bossche, J., Van den Bossche, J., Mack, M., Mack, M., Pipeleers, D., Pipeleers, D., In't Veld, P., In't Veld, P., De Baetselier, P., De Baetselier, P., Van Ginderachter, J.A., Van Ginderachter, J.A., 2010. Different Tumor Microenvironments Contain Functionally Distinct Subsets of Macrophages Derived from Ly6C(high) Monocytes. Cancer Res. 70, 5728–5739. doi:10.1158/0008-5472.CAN-09-4672
Munz, M., Baeuerle, P.A., Gires, O., 2009. The emerging role of EpCAM in cancer and stem cell signaling. Cancer Res. 69, 5627–5629. doi:10.1158/0008-5472.CAN-09-0654
Murdoch, C., Murdoch, C., Giannoudis, A., Lewis, C.E., 2004. Mechanisms regulating the recruitment of macrophages into hypoxic areas of tumors and other ischemic tissues. Blood 104, 2224–2234. doi:10.1182/blood-2004-03-1109
Murdoch, C., Muthana, M., Coffelt, S.B., Lewis, C.E., 2008. The role of myeloid cells in the promotion of tumour angiogenesis. Nat. Rev. Cancer 8, 618–631. doi:10.1038/nrc2444
Murdoch, C., Tazzyman, S., Webster, S., Lewis, C.E., 2007. Expression of Tie-2 by human monocytes and their responses to angiopoietin-2. J. Immunol. 178, 7405–7411.
Nagai, T., Tanaka, M., Tsuneyoshi, Y., Xu, B., Michie, S.A., Hasui, K., Hirano, H., Arita, K., Matsuyama, T., 2009. Targeting tumor-associated macrophages in an experimental glioma model with a recombinant immunotoxin to folate receptor β. Cancer Immunol Immunother 58, 1577–1586. doi:10.1007/s00262-009-0667-x
Nagy, J.A., Chang, S.-H., Dvorak, A.M., Dvorak, H.F., 2009. Why are tumour blood vessels abnormal

and why is it important to know? Br J Cancer 100, 865–869. doi:10.1038/sj.bjc.6604929
Naidoo, J., Page, D.B., Wolchok, J.D., 2014. Immune modulation for cancer therapy. Br J Cancer 111, 2214–2219. doi:10.1038/bjc.2014.348
Negus, R.P., Stamp, G.W., Hadley, J., Balkwill, F.R., 1997. Quantitative assessment of the leukocyte infiltrate in ovarian cancer and its relationship to the expression of C-C chemokines. Am. J. Pathol. 150, 1723–1734.
Niewerth, D., Kaspers, G.J., Kaspers, G.J.L., Assaraf, Y.G., van Meerloo, J., Kirk, C.J., Anderl, J., Blank, J.L., van de Ven, P.M., Zweegman, S., Jansen, G., Cloos, J., 2014. Interferon-γ-induced upregulation of immunoproteasome subunit assembly overcomes bortezomib resistance in human hematological cell lines. J Hematol Oncol 7, 7. doi:10.1186/1756-8722-7-7
Nimmerjahn, F., Ravetch, J.V., 2008. Fcγ receptors as regulators of immune responses. Nat. Rev. Immunol. 8, 34–47. doi:10.1038/nri2206
Nishie, A., Ono, M., Shono, T., Fukushi, J., Otsubo, M., Onoue, H., Ito, Y., Inamura, T., Ikezaki, K., Fukui, M., Iwaki, T., Kuwano, M., 1999. Macrophage infiltration and heme oxygenase-1 expression correlate with angiogenesis in human gliomas. Clin. Cancer Res. 5, 1107–1113.
O'Hagan, H.M., Ljungman, M., 2004. Nuclear accumulation of p53 following inhibition of transcription is not due to diminished levels of MDM2. Oncogene 23, 5505–5512. doi:10.1038/sj.onc.1207709
O'Reilly, M.S., Holmgren, L., Shing, Y., Chen, C., Rosenthal, R.A., Moses, M., Lane, W.S., Cao, Y., Sage, E.H., Folkman, J., 1994. Angiostatin: a novel angiogenesis inhibitor that mediates the suppression of metastases by a Lewis lung carcinoma. Cell 79, 315–328.
O'Shea, C., Klupsch, K., Choi, S., Bagus, B., Soria, C., Shen, J., McCormick, F., Stokoe, D., 2005. Adenoviral proteins mimic nutrient/growth signals to activate the mTOR pathway for viral replication. EMBO J. 24, 1211–1221. doi:10.1038/sj.emboj.7600597
O'Shea, C.C., Johnson, L., Bagus, B., Choi, S., Nicholas, C., Shen, A., Boyle, L., Pandey, K., Soria, C., Kunich, J., Shen, Y., Habets, G., Ginzinger, D., McCormick, F., 2004. Late viral RNA export, rather than p53 inactivation, determines ONYX-015 tumor selectivity. Cancer Cell 6, 611–623. doi:10.1016/j.ccr.2004.11.012
Oldenborg, P.A., Gresham, H.D., Lindberg, F.P., 2001. CD47-signal regulatory protein alpha (SIRPalpha) regulates Fcgamma and complement receptor-mediated phagocytosis. Journal of Experimental Medicine 193, 855–862.
Paludan, S.R., Ellermann-Eriksen, S., Malmgaard, L., Mogensen, S.C., 2000. Herpes simplex virus type 2 infection of macrophages impairs IL-4-mediated inhibition of NO production through TNF-alpha-induced activation of NF-kappaB. Arch. Virol. 145, 575–591.
Papadopoulos, N., Martin, J., Ruan, Q., Rafique, A., Rosconi, M.P., Shi, E., Pyles, E.A., Yancopoulos, G.D., Stahl, N., Wiegand, S.J., 2012. Binding and neutralization of vascular endothelial growth factor (VEGF) and related ligands by VEGF Trap, ranibizumab and bevacizumab. Angiogenesis 15, 171–185. doi:10.1007/s10456-011-9249-6
Parker, J.N., Gillespie, G.Y., Love, C.E., Randall, S., Whitley, R.J., Markert, J.M., 2000. Engineered herpes simplex virus expressing IL-12 in the treatment of experimental murine brain tumors. Proc. Natl. Acad. Sci. U.S.A. 97, 2208–2213. doi:10.1073/pnas.040557897
Parker, L.C., Whyte, M.K.B., Vogel, S.N., Dower, S.K., Sabroe, I., 2004. Toll-like receptor (TLR)2 and TLR4 agonists regulate CCR expression in human monocytic cells. J. Immunol. 172, 4977–4986.
Paulus, P., Paulus, P., Stanley, E.R., Schäfer, R., Abraham, D., Aharinejad, S., 2006. Colony-Stimulating Factor-1 Antibody Reverses Chemoresistance in Human MCF-7 Breast Cancer Xenografts. Cancer Res. 66, 4349–4356. doi:10.1158/0008-5472.CAN-05-3523
Petrillo, M., Zannoni, G.F., Martinelli, E., Pedone Anchora, L., Ferrandina, G., Tropeano, G., Fagotti, A., Scambia, G., 2015. Polarisation of Tumor-Associated Macrophages toward M2 Phenotype Correlates with Poor Response to Chemoradiation and Reduced Survival in Patients with Locally Advanced Cervical Cancer. PLoS ONE 10, e0136654. doi:10.1371/journal.pone.0136654
Platanias, L.C., 2005. Mechanisms of type-I- and type-II-interferon-mediated signalling. Nat. Rev. Immunol. 5, 375–386. doi:10.1038/nri1604
Platzer, B., Stout, M., Fiebiger, E., 2014. Antigen Cross-Presentation of Immune Complexes. Front Immunol 5, 77. doi:10.3389/fimmu.2014.00140
Poon, I.K.H., Lucas, C.D., Rossi, A.G., Ravichandran, K.S., 2014. Apoptotic cell clearance: basic biology and therapeutic potential. Nat. Rev. Immunol. 14, 166–180. doi:10.1038/nri3607
Porta, C., Porta, C., Rimoldi, M., Rimoldi, M., Raes, G., Raes, G., Brys, L., Brys, L., Ghezzi, P., Ghezzi, P., Di Liberto, D., Di Liberto, D., Dieli, F., Dieli, F., Ghisletti, S., Ghisletti, S., Natoli, G., Natoli, G., De Baetselier, P., De Baetselier, P., Mantovani, A., Mantovani, A., SICA, A., Sica, A., 2009. Tolerance and M2 (alternative) macrophage polarization are related processes orchestrated by p50 nuclear factor B. Proc. Natl. Acad. Sci. U.S.A. 106, 14978–14983. doi:10.1073/pnas.0809784106

Pozzi, L.-A.M., Maciaszek, J.W., Rock, K.L., 2005. Both dendritic cells and macrophages can stimulate naive CD8 T cells in vivo to proliferate, develop effector function, and differentiate into memory cells. J. Immunol. 175, 2071–2081.

Priceman, S.J., Priceman, S.J., Sung, J.L., Sung, J.L., Shaposhnik, Z., Shaposhnik, Z., Burton, J.B., Burton, J.B., Torres-Collado, A.X., Torres-Collado, A.X., Moughon, D.L., Moughon, D.L., Johnson, M., Johnson, M., Lusis, A.J., Lusis, A.J., Cohen, D.A., Cohen, D.A., Iruela-Arispe, M.L., Iruela-Arispe, M.L., Wu, L., Wu, L., 2010. Targeting distinct tumor-infiltrating myeloid cells by inhibiting CSF-1 receptor: combating tumor evasion of antiangiogenic therapy. Blood 115, 1461–1471. doi:10.1182/blood-2009-08-237412

Pyonteck, S.M., Akkari, L., Schuhmacher, A.J., Bowman, R.L., Sevenich, L., Quail, D.F., Olson, O.C., Quick, M.L., Huse, J.T., Teijeiro, V., Setty, M., Leslie, C.S., Oei, Y., Pedraza, A., Zhang, J., Brennan, C.W., Sutton, J.C., Holland, E.C., Daniel, D., Joyce, J.A., 2013. CSF-1R inhibition alters macrophage polarization and blocks glioma progression. Nat Med 19, 1264–1272. doi:10.1038/nm.3337

Querido, E., Teodoro, J.G., Branton, P.E., 1997. Accumulation of p53 induced by the adenovirus E1A protein requires regions involved in the stimulation of DNA synthesis. J. Virol. 71, 3526–3533.

Ravichandran, K.S., 2010. Find-me and eat-me signals in apoptotic cell clearance: progress and conundrums. J. Exp. Med. 207, 1807–1817. doi:10.1084/jem.20101157

Reeh, M., Bockhorn, M., Görgens, D., Vieth, M., Hoffmann, T., Simon, R., Izbicki, J.R., Sauter, G., Schumacher, U., Anders, M., 2013. Presence of the coxsackievirus and adenovirus receptor (CAR) in human neoplasms: a multitumour array analysis. Br J Cancer 109, 1848–1858. doi:10.1038/bjc.2013.509

Reinartz, S., Schumann, T., Finkernagel, F., Wortmann, A., Jansen, J.M., Meissner, W., Krause, M., Schwörer, A.-M., Wagner, U., Müller-Brüsselbach, S., Müller, R., 2013. Mixed-polarization phenotype of ascites-associated macrophages in human ovarian carcinoma: Correlation of CD163 expression, cytokine levels and early relapse. Int. J. Cancer 134, 32–42. doi:10.1002/ijc.28335

Robertson, J.M., Jensen, P.E., Evavold, B.D., 2000. DO11.10 and OT-II T cells recognize a C-terminal ovalbumin 323-339 epitope. J. Immunol. 164, 4706–4712.

Roca, H., Roca, H., Varsos, Z.S., Varsos, Z.S., Sud, S., Sud, S., Craig, M.J., Craig, M.J., Ying, C., Ying, C., Pienta, K.J., Pienta, K.J., 2009. CCL2 and Interleukin-6 Promote Survival of Human CD11b+ Peripheral Blood Mononuclear Cells and Induce M2-type Macrophage Polarization. Journal of Biological Chemistry 284, 34342–34354. doi:10.1074/jbc.M109.042671

Rogers, H., Williams, D.W., Feng, G.-J., Lewis, M.A.O., Wei, X.-Q., 2013. Role of bacterial lipopolysaccharide in enhancing host immune response to Candida albicans. Clin. Dev. Immunol. 2013, 320168–9. doi:10.1155/2013/320168

Ruffell, B., Affara, N.I., Coussens, L.M., 2012a. Differential macrophage programming in the tumor microenvironment. Trends Immunol. 33, 119–126. doi:10.1016/j.it.2011.12.001

Ruffell, B., Ruffell, B., Au, A., Au, A., Rugo, H.S., Rugo, H.S., Esserman, L.J., Esserman, L.J., Hwang, E.S., Hwang, E.S., Coussens, L.M., Coussens, L.M., 2012b. Leukocyte composition of human breast cancer. Proc. Natl. Acad. Sci. U.S.A. 109, 2796–2801. doi:10.1073/pnas.1104303108

Russell, S.J., Peng, K.-W., Bell, J.C., 2012. Oncolytic virotherapy. Nat. Biotechnol. 30, 658–670. doi:10.1038/nbt.2287

Rutschman, R., Lang, R., Hesse, M., Ihle, J.N., Wynn, T.A., Murray, P.J., 2001. Cutting edge: Stat6-dependent substrate depletion regulates nitric oxide production. J. Immunol. 166, 2173–2177.

Sabatino, R., Antonelli, A., Battistelli, S., Schwendener, R., Magnani, M., Rossi, L., 2014. Macrophage Depletion by Free Bisphosphonates and Zoledronate-Loaded Red Blood Cells. PLoS ONE 9, e101260. doi:10.1371/journal.pone.0101260

Saccani, A., Saccani, A., Schioppa, T., Schioppa, T., Porta, C., Porta, C., Biswas, S.K., Biswas, S.K., Nebuloni, M., Nebuloni, M., Vago, L., Vago, L., Bottazzi, B., Bottazzi, B., Colombo, M.P., Colombo, M.P., Mantovani, A., Mantovani, A., Sica, A., SICA, A., 2006. p50 Nuclear Factor- B Overexpression in Tumor-Associated Macrophages Inhibits M1 Inflammatory Responses and Antitumor Resistance. Cancer Res. 66, 11432–11440. doi:10.1158/0008-5472.CAN-06-1867

Sadler, A.J., Williams, B.R.G., 2008. Interferon-inducible antiviral effectors. Nat. Rev. Immunol. 8, 559–568. doi:10.1038/nri2314

Sandler, A., Gray, R., Perry, M.C., Brahmer, J., Schiller, J.H., Dowlati, A., Lilenbaum, R., Johnson, D.H., 2006. Paclitaxel-carboplatin alone or with bevacizumab for non-small-cell lung cancer. N. Engl. J. Med. 355, 2542–2550. doi:10.1056/NEJMoa061884

Saric, T., Chang, S.-C., Hattori, A., York, I.A., Markant, S., Rock, K.L., Tsujimoto, M., Goldberg, A.L., 2002. An IFN-gamma-induced aminopeptidase in the ER, ERAP1, trims precursors to MHC class I-presented peptides. Nat. Immunol. 3, 1169–1176. doi:10.1038/ni859

Sarkar, S., Döring, A., Zemp, F.J., Silva, C., Lun, X., Wang, X., Kelly, J., Hader, W., Hamilton, M., Mercier, P., Dunn, J.F., Kinniburgh, D., van Rooijen, N., Robbins, S., Forsyth, P., Cairncross, G., Weiss, S., Yong, V.W., 2013. Therapeutic activation of macrophages and microglia to suppress brain tumor-initiating cells. Nat Neurosci 17, 46–55. doi:10.1038/nn.3597

Sasieni, P.D., Shelton, J., Ormiston-Smith, N., Thomson, C.S., Silcocks, P.B., 2011. What is the lifetime risk of developing cancer?: the effect of adjusting for multiple primaries. Br J Cancer 105, 460–465. doi:10.1038/bjc.2011.250

Savage, N.D.L., de Boer, T., Walburg, K.V., Joosten, S.A., van Meijgaarden, K., Geluk, A., Ottenhoff, T.H.M., 2008. Human anti-inflammatory macrophages induce Foxp3+ GITR+ CD25+ regulatory T cells, which suppress via membrane-bound TGFbeta-1. J. Immunol. 181, 2220–2226.

Schindler, H., Lutz, M.B., Röllinghoff, M., Bogdan, C., 2001. The production of IFN-gamma by IL-12/IL-18-activated macrophages requires STAT4 signaling and is inhibited by IL-4. J. Immunol. 166, 3075–3082.

Schreiber, R.D., 1984. Identification of gamma-interferon as a murine macrophage-activating factor for tumor cytotoxicity. Contemporary topics in immunobiology 13, 171–198.

Schroder, K., Schroder, K., Hertzog, P.J., Ravasi, T., Hume, D.A., 2003. Interferon- : an overview of signals, mechanisms and functions. J. Leukoc. Biol. 75, 163–189. doi:10.1189/jlb.0603252

Selby, M.J., Selby, M.J., Engelhardt, J.J., Engelhardt, J.J., Quigley, M., Quigley, M., Henning, K.A., Henning, K.A., Chen, T., Chen, T., Srinivasan, M., Srinivasan, M., Korman, A.J., Korman, A.J., 2013. Anti-CTLA-4 Antibodies of IgG2a Isotype Enhance Antitumor Activity through Reduction of Intratumoral Regulatory T Cells. Cancer Immunology Research 1, 32–42. doi:10.1158/2326-6066.CIR-13-0013

Semenza, G.L., Jiang, B.H., Leung, S.W., Passantino, R., Concordet, J.P., Maire, P., Giallongo, A., 1996. Hypoxia response elements in the aldolase A, enolase 1, and lactate dehydrogenase A gene promoters contain essential binding sites for hypoxia-inducible factor 1. Journal of Biological Chemistry 271, 32529–32537.

Seymour, L.W., Fisher, K.D., 2016. Oncolytic viruses: finally delivering. Br J Cancer 114, 357–361. doi:10.1038/bjc.2015.481

Shaw, T.J., Senterman, M.K., Dawson, K., Crane, C.A., Vanderhyden, B.C., 2004. Characterization of intraperitoneal, orthotopic, and metastatic xenograft models of human ovarian cancer. Mol. Ther. 10, 1032–1042. doi:10.1016/j.ymthe.2004.08.013

Shen, L., Shen, L., Rock, K.L., Rock, K.L., 2004. Cellular protein is the source of cross-priming antigen in vivo. Proc. Natl. Acad. Sci. U.S.A. 101, 3035–3040. doi:10.1073/pnas.0308345101

Shmulevitz, M., Pan, L.-Z., Garant, K., Pan, D., Lee, P.W.K., 2010. Oncogenic Ras promotes reovirus spread by suppressing IFN-beta production through negative regulation of RIG-I signaling. Cancer Res. 70, 4912–4921. doi:10.1158/0008-5472.CAN-09-4676

Shree, T., Shree, T., Olson, O.C., Olson, O.C., Elie, B.T., Elie, B.T., Kester, J.C., Kester, J.C., Garfall, A.L., Garfall, A.L., Simpson, K., Simpson, K., Bell-McGuinn, K.M., Bell-McGuinn, K.M., Zabor, E.C., Zabor, E.C., Brogi, E., Brogi, E., Joyce, J.A., Joyce, J.A., 2011. Macrophages and cathepsin proteases blunt chemotherapeutic response in breast cancer. Genes & Development 25, 2465–2479. doi:10.1101/gad.180331.111

Sica, A., Allavena, P., Mantovani, A., 2008. Cancer related inflammation: The macrophage connection. Cancer Letters 267, 204–215. doi:10.1016/j.canlet.2008.03.028

Sica, A., Mantovani, A., 2012. Macrophage plasticity and polarization: in vivo veritas. J. Clin. Invest. 122, 787–795. doi:10.1172/JCI59643

SICA, A., Saccani, A., Bottazzi, B., Bernasconi, S., Allavena, P., Gaetano, B., Fei, F., LaRosa, G., Scotton, C., Balkwill, F., Mantovani, A., 2000. Defective expression of the monocyte chemotactic protein-1 receptor CCR2 in macrophages associated with human ovarian carcinoma. J. Immunol. 164, 733–738.

Sierra-Filardi, E., Sierra-Filardi, E., Nieto, C., Nieto, C., Domínguez-Soto, A., Dominguez-Soto, A., Barroso, R., Barroso, R., Sánchez-Mateos, P., Sanchez-Mateos, P., Puig-Kroger, A., Puig-Kroger, A., López-Bravo, M., Lopez-Bravo, M., Joven, J., Joven, J., Ardavin, C., Ardavín, C., Rodríguez-Fernández, J.L., Rodriguez-Fernandez, J.L., Sanchez-Torres, C., Sánchez-Torres, C., Mellado, M., Mellado, M., Corbi, A.L., Corbí, A.L., 2014. CCL2 Shapes Macrophage Polarization by GM-CSF and M-CSF: Identification of CCL2/CCR2-Dependent Gene Expression Profile. J. Immunol. 192, 3858–3867. doi:10.4049/jimmunol.1302821

Simpson, T.R., Simpson, T.R., Li, F., Li, F., Montalvo-Ortiz, W., Montalvo-Ortiz, W., Sepulveda, M.A., Sepulveda, M.A., Bergerhoff, K., Bergerhoff, K., Arce, F., Arce, F., Roddie, C., Roddie, C., Henry, J.Y., Henry, J.Y., Yagita, H., Yagita, H., Wolchok, J.D., Wolchok, J.D., Peggs, K.S., Peggs, K.S., Ravetch, J.V., Ravetch, J.V., Allison, J.P., Allison, J.P., Quezada, S.A., Quezada, S.A., 2013. Fc-

dependent depletion of tumor-infiltrating regulatory T cells co-defines the efficacy of anti-CTLA-4 therapy against melanoma. Journal of Experimental Medicine 210, 1695–1710. doi:10.1084/jem.20130579

Sindrilaru, A., Peters, T., Wieschalka, S., Baican, C., Baican, A., Peter, H., Hainzl, A., Schatz, S., Qi, Y., Schlecht, A., Weiss, J.M., Wlaschek, M., Sunderkötter, C., Scharffetter-Kochanek, K., 2011. An unrestrained proinflammatory M1 macrophage population induced by iron impairs wound healing in humans and mice. J. Clin. Invest. 121, 985–997. doi:10.1172/JCI44490

Singh, R., Cresswell, P., 2010. Defective cross-presentation of viral antigens in GILT-free mice. Science 328, 1394–1398. doi:10.1126/science.1189176

Sinha, P., Clements, V.K., Ostrand-Rosenberg, S., 2005. Reduction of myeloid-derived suppressor cells and induction of M1 macrophages facilitate the rejection of established metastatic disease. J. Immunol. 174, 636–645.

Small, E.J., Carducci, M.A., Burke, J.M., Rodriguez, R., Fong, L., van Ummersen, L., Yu, D.C., Aimi, J., Ando, D., Working, P., Kirn, D., Wilding, G., 2006. A phase I trial of intravenous CG7870, a replication-selective, prostate-specific antigen-targeted oncolytic adenovirus, for the treatment of hormone-refractory, metastatic prostate cancer. Mol. Ther. 14, 107–117. doi:10.1016/j.ymthe.2006.02.011

Solinas, G., Germano, G., Mantovani, A., Allavena, P., 2009. Tumor-associated macrophages (TAM) as major players of the cancer-related inflammation. J. Leukoc. Biol. 86, 1065–1073. doi:10.1189/jlb.0609385

Stein, M., Keshav, S., Harris, N., Gordon, S., 1992. Interleukin 4 potently enhances murine macrophage mannose receptor activity: a marker of alternative immunologic macrophage activation. J. Exp. Med. 176, 287–292.

Stessels, F., Van den Eynden, G., Van der Auwera, I., Salgado, R., Van den Heuvel, E., Harris, A.L., Jackson, D.G., Colpaert, C.G., van Marck, E.A., Dirix, L.Y., Vermeulen, P.B., 2004. Breast adenocarcinoma liver metastases, in contrast to colorectal cancer liver metastases, display a non-angiogenic growth pattern that preserves the stroma and lacks hypoxia. Br J Cancer 90, 1429–1436. doi:10.1038/sj.bjc.6601727

Stojdl, D.F., Lichty, B.D., tenOever, B.R., Paterson, J.M., Power, A.T., Knowles, S., Marius, R., Reynard, J., Poliquin, L., Atkins, H., Brown, E.G., Durbin, R.K., Durbin, J.E., Hiscott, J., Bell, J.C., 2003. VSV strains with defects in their ability to shutdown innate immunity are potent systemic anti-cancer agents. Cancer Cell 4, 263–275.

Stout, R.D., Jiang, C., Matta, B., Tietzel, I., Watkins, S.K., Suttles, J., 2005. Macrophages sequentially change their functional phenotype in response to changes in microenvironmental influences. J. Immunol. 175, 342–349.

Stout, R.D., Stout, R.D., Watkins, S.K., Watkins, S.K., Suttles, J., Suttles, J., 2009. Functional plasticity of macrophages: in situ reprogramming of tumor-associated macrophages. J. Leukoc. Biol. 86, 1105–1109. doi:10.1189/jlb.0209073

Swann, J.B., Hayakawa, Y., Zerafa, N., Sheehan, K.C.F., Scott, B., Schreiber, R.D., Hertzog, P., Smyth, M.J., 2007. Type I IFN contributes to NK cell homeostasis, activation, and antitumor function. J. Immunol. 178, 7540–7549.

Talks, K.L., Turley, H., Gatter, K.C., Maxwell, P.H., Pugh, C.W., Ratcliffe, P.J., Harris, A.L., 2000. The expression and distribution of the hypoxia-inducible factors HIF-1alpha and HIF-2alpha in normal human tissues, cancers, and tumor-associated macrophages. Am. J. Pathol. 157, 411–421.

Tang, X., Mo, C., Wang, Y., Wei, D., Xiao, H., 2013. Anti-tumour strategies aiming to target tumour-associated macrophages. Immunology 138, 93–104. doi:10.1111/imm.12023

Tao, N., Gao, G.P., Parr, M., Johnston, J., Baradet, T., Wilson, J.M., Barsoum, J., Fawell, S.E., 2001. Sequestration of adenoviral vector by Kupffer cells leads to a nonlinear dose response of transduction in liver. Mol. Ther. 3, 28–35. doi:10.1006/mthe.2000.0227

Theocharides, A.P.A., Theocharides, A.P.A., Jin, L., Jin, L., Cheng, P.Y., Cheng, P.-Y., Prasolava, T.K., Prasolava, T.K., Malko, A.V., Malko, A.V., Ho, J.M., Ho, J.M., Poeppl, A.G., Poeppl, A.G., van Rooijen, N., van Rooijen, N., Minden, M.D., Minden, M.D., Danska, J.S., Danska, J.S., Dick, J.E., Dick, J.E., Wang, J.C.Y., Wang, J.C.Y., 2012. Disruption of SIRP signaling in macrophages eliminates human acute myeloid leukemia stem cells in xenografts. Journal of Experimental Medicine 209, 1883–1899. doi:10.1084/jem.20120502

Thorsteinsson, L., O'Dowd, G.M., Harrington, P.M., Johnson, P.M., 1998. The complement regulatory proteins CD46 and CD59, but not CD55, are highly expressed by glandular epithelium of human breast and colorectal tumour tissues. APMIS 106, 869–878.

Tirapu, I., Huarte, E., Guiducci, C., Arina, A., Zaratiegui, M., Murillo, O., Gonzalez, A., Berasain, C., Berraondo, P., Fortes, P., Prieto, J., Colombo, M.P., Chen, L., Melero, I., 2006. Low surface

expression of B7-1 (CD80) is an immunoescape mechanism of colon carcinoma. Cancer Res. 66, 2442–2450. doi:10.1158/0008-5472.CAN-05-1681
Tridandapani, S., Tridandapani, S., Siefker, K., Siefker, K., Teillaud, J.L., Teillaud, J.-L., Carter, J.E., Carter, J.E., Wewers, M.D., Wewers, M.D., Anderson, C.L., Anderson, C.L., 2002. Regulated Expression and Inhibitory Function of Fc RIIb in Human Monocytic Cells. Journal of Biological Chemistry 277, 5082–5089. doi:10.1074/jbc.M110277200
Turner, L., Scotton, C., Negus, R., Balkwill, F., 1999. Hypoxia inhibits macrophage migration. Eur. J. Immunol. 29, 2280–2287. doi:10.1002/(SICI)1521-4141(199907)29:07<2280::AID-IMMU2280>3.0.CO;2-C
van Den Broek, M., Bachmann, M.F., Köhler, G., Barner, M., Escher, R., Zinkernagel, R., Kopf, M., 2000. IL-4 and IL-10 antagonize IL-12-mediated protection against acute vaccinia virus infection with a limited role of IFN-gamma and nitric oxide synthetase 2. J. Immunol. 164, 371–378.
Van Overmeire, E., Laoui, D., Keirsse, J., Van Ginderachter, J.A., 2014. Hypoxia and tumor-associated macrophages: A deadly alliance in support of tumor progression. OncoImmunology 3, e27561. doi:10.4161/onci.27561
Varela, J.C., Atkinson, C., Woolson, R., Keane, T.E., Tomlinson, S., 2008. Upregulated expression of complement inhibitory proteins on bladder cancer cells and anti-MUC1 antibody immune selection. Int. J. Cancer 123, 1357–1363. doi:10.1002/ijc.23676
Vargo-Gogola, T., Fingleton, B., Crawford, H.C., Matrisian, L.M., 2002. Matrilysin (matrix metalloproteinase-7) selects for apoptosis-resistant mammary cells in vivo. Cancer Res. 62, 5559–5563.
Veillette, A., Thibaudeau, E., Latour, S., 1998. High expression of inhibitory receptor SHPS-1 and its association with protein-tyrosine phosphatase SHP-1 in macrophages. Journal of Biological Chemistry 273, 22719–22728.
Venneri, M.A., De Palma, M., Ponzoni, M., Pucci, F., Scielzo, C., Zonari, E., Mazzieri, R., Doglioni, C., Naldini, L., 2007. Identification of proangiogenic TIE2-expressing monocytes (TEMs) in human peripheral blood and cancer. Blood 109, 5276–5285. doi:10.1182/blood-2006-10-053504
Vonderheide, R.H., 2015. CD47 blockade as another immune checkpoint therapy for cancer. Nat Med 21, 1122–1123. doi:10.1038/nm.3965
Wakim, L.M., Bevan, M.J., 2011. Cross-dressed dendritic cells drive memory CD8+ T-cell activation after viral infection. Nature 471, 629–632. doi:10.1038/nature09863
Wang, X., Zhang, Y., Zhang, X., Tian, W., Feng, W., Chen, T., 2011. The curcumin analogue hydrazinocurcumin exhibits potent suppressive activity on carcinogenicity of breast cancer cells via STAT3 inhibition. Int J Oncol 40, 1189–1195. doi:10.3892/ijo.2011.1298
Wang, Y., Hallden, G., Hill, R., Anand, A., Liu, T.-C., Francis, J., Brooks, G., Lemoine, N., Kirn, D., 2003. E3 gene manipulations affect oncolytic adenovirus activity in immunocompetent tumor models. Nat. Biotechnol. 21, 1328–1335. doi:10.1038/nbt887
Watkins, S.K., Egilmez, N.K., Suttles, J., Stout, R.D., 2007. IL-12 rapidly alters the functional profile of tumor-associated and tumor-infiltrating macrophages in vitro and in vivo. J. Immunol. 178, 1357–1362.
West, L.C., Cresswell, P., 2013. Expanding roles for GILT in immunity. Curr. Opin. Immunol. 25, 103–108. doi:10.1016/j.coi.2012.11.006
Whyte, P., Williamson, N.M., Harlow, E., 1989. Cellular targets for transformation by the adenovirus E1A proteins. Cell 56, 67–75.
Wolkers, M.C., Wolkers, M.C., Brouwenstijn, N., Bakker, A.H., Toebes, M., Schumacher, T.N.M., 2004. Antigen Bias in T Cell Cross-Priming. Science 304, 1314–1317. doi:10.1126/science.1096268
Wu, C., Molavi, O., Zhang, H., Gupta, N., Alshareef, A., Bone, K.M., Gopal, K., Wu, F., Lewis, J.T., Douglas, D.N., Kneteman, N.M., Lai, R., 2015. STAT1 is phosphorylated and downregulated by the oncogenic tyrosine kinase NPM-ALK in ALK-positive anaplastic large-cell lymphoma. Blood 126, 336–345. doi:10.1182/blood-2014-10-603738
Wu, X., Schulte, B.C., Zhou, Y., Haribhai, D., Mackinnon, A.C., Plaza, J.A., Williams, C.B., Hwang, S.T., 2014. Depletion of M2-Like Tumor-Associated Macrophages Delays Cutaneous T-Cell Lymphoma Development In Vivo. Journal of Investigative Dermatology 134, 2814–2822. doi:10.1038/jid.2014.206
Wu, Y.-Y., Tsai, H.-F., Lin, W.-C., Hsu, P.-I., Shun, C.-T., Wu, M.-S., Hsu, P.-N., 2007. Upregulation of CCL20 and recruitment of CCR6+ gastric infiltrating lymphocytes in Helicobacter pylori gastritis. Infect. Immun. 75, 4357–4363. doi:10.1128/IAI.01660-06
Wunder, T., Schmid, K., Wicklein, D., Groitl, P., Dobner, T., Lange, T., Anders, M., Schumacher, U., 2013. Expression of the coxsackie adenovirus receptor in neuroendocrine lung cancers and its implications for oncolytic adenoviral infection. Cancer Gene Ther. 20, 25–32.

doi:10.1038/cgt.2012.80
Wyckoff, J.B., Wyckoff, J.B., Wang, Y., Wang, Y., Lin, E.Y., Lin, E.Y., Li, J.F., Li, J.-F., Goswami, S., Goswami, S., Stanley, E.R., Stanley, E.R., Segall, J.E., Segall, J.E., Pollard, J.W., Pollard, J.W., Condeelis, J., Condeelis, J., 2007. Direct Visualization of Macrophage-Assisted Tumor Cell Intravasation in Mammary Tumors. Cancer Res. 67, 2649–2656. doi:10.1158/0008-5472.CAN-06-1823
Xin, H., Xin, H., Zhang, C., Zhang, C., Herrmann, A., Herrmann, A., Du, Y., Du, Y., Figlin, R., Figlin, R., Yu, H., Yu, H., 2009. Sunitinib Inhibition of Stat3 Induces Renal Cell Carcinoma Tumor Cell Apoptosis and Reduces Immunosuppressive Cells. Cancer Res. 69, 2506–2513. doi:10.1158/0008-5472.CAN-08-4323
Xu, M., Xu, M., Liu, M., Liu, M., Du, X., Du, X., Li, S., Li, S., Li, H., Li, H., Li, X., Li, X., Li, Y., Li, Y., Wang, Y., Wang, Y., Qin, Z., Qin, Z., Fu, Y.X., Fu, Y.-X., Wang, S., Wang, S., 2015. Intratumoral Delivery of IL-21 Overcomes Anti-Her2/Neu Resistance through Shifting Tumor-Associated Macrophages from M2 to M1 Phenotype. J. Immunol. 194, 4997–5006. doi:10.4049/jimmunol.1402603
Xu, W., Liu, L.Z., Loizidou, M., Ahmed, M., Charles, I.G., 2002. The role of nitric oxide in cancer. Cell Res 12, 311–320. doi:10.1038/sj.cr.7290133
Yamazaki, T., Yang, X.O., Chung, Y., Fukunaga, A., Nurieva, R., Pappu, B., Martin-Orozco, N., Kang, H.S., Ma, L., Panopoulos, A.D., Craig, S., Watowich, S.S., Jetten, A.M., Tian, Q., Dong, C., 2008. CCR6 regulates the migration of inflammatory and regulatory T cells. J. Immunol. 181, 8391–8401.
Yan, H., Kamiya, T., Suabjakyong, P., Tsuji, N.M., 2015. Targeting C-Type Lectin Receptors for Cancer Immunity. Front Immunol 6, 408. doi:10.3389/fimmu.2015.00408
Yin, Y., Yin, Y., Huang, X., Huang, X., Lynn, K.D., Lynn, K.D., Thorpe, P.E., Thorpe, P.E., 2013. Phosphatidylserine-Targeting Antibody Induces M1 Macrophage Polarization and Promotes Myeloid-Derived Suppressor Cell Differentiation. Cancer Immunology Research 1, 256–268. doi:10.1158/2326-6066.CIR-13-0073
York, I.A., Chang, S.-C., Saric, T., Keys, J.A., Favreau, J.M., Goldberg, A.L., Rock, K.L., 2002. The ER aminopeptidase ERAP1 enhances or limits antigen presentation by trimming epitopes to 8-9 residues. Nat. Immunol. 3, 1177–1184. doi:10.1038/ni860
Zaidi, M.R., Zaidi, M.R., Merlino, G., Merlino, G., 2011. The Two Faces of Interferon- in Cancer. Clin. Cancer Res. 17, 6118–6124. doi:10.1158/1078-0432.CCR-11-0482
Zamanian, M., La Thangue, N.B., 1992. Adenovirus E1a prevents the retinoblastoma gene product from repressing the activity of a cellular transcription factor. EMBO J. 11, 2603–2610.
Zeisberger, S.M., Odermatt, B., Marty, C., Zehnder-Fjällman, A.H.M., Ballmer-Hofer, K., Schwendener, R.A., 2006. Clodronate-liposome-mediated depletion of tumour-associated macrophages: a new and highly effective antiangiogenic therapy approach. Br J Cancer 95, 272–281. doi:10.1038/sj.bjc.6603240
Zhang, K.-X., Matsui, Y., Hadaschik, B.A., Lee, C., Jia, W., Bell, J.C., Fazli, L., So, A.I., Rennie, P.S., 2010. Down-regulation of type I interferon receptor sensitizes bladder cancer cells to vesicular stomatitis virus-induced cell death. Int. J. Cancer 127, 830–838. doi:10.1002/ijc.25088
Zhang, Q.-W., Liu, L., Gong, C.-Y., Shi, H.-S., Zeng, Y.-H., Wang, X.-Z., Zhao, Y.-W., Wei, Y.-Q., 2012. Prognostic Significance of Tumor-Associated Macrophages in Solid Tumor: A Meta-Analysis of the Literature. PLoS ONE 7, e50946. doi:10.1371/journal.pone.0050946
Zhang, W., Zhang, W., Zhu, X.-D., Zhu, X.D., Sun, H.-C., Sun, H.C., Xiong, Y.-Q., Xiong, Y.Q., Zhuang, P.-Y., Zhuang, P.Y., Xu, H.X., Xu, H.-X., Kong, L.Q., Kong, L.-Q., Wang, L., Wang, L., Wu, W.Z., Wu, W.-Z., Tang, Z.-Y., Tang, Z.Y., 2010. Depletion of Tumor-Associated Macrophages Enhances the Effect of Sorafenib in Metastatic Liver Cancer Models by Antimetastatic and Antiangiogenic Effects. Clin. Cancer Res. 16, 3420–3430. doi:10.1158/1078-0432.CCR-09-2904
Zhang, X., Goncalves, R., Mosser, D.M., 2001. The Isolation and Characterization of Murine Macrophages. John Wiley & Sons, Inc., Hoboken, NJ, USA. doi:10.1002/0471142735.im1401s83
Zhang, X., Hussain, R., Turnell, A.S., Mymryk, J.S., Gallimore, P.H., Grand, R.J.A., 2005. Accumulation of p53 in response to adenovirus early region 1A sensitizes human cells to tumor necrosis factor alpha-induced apoptosis. Virology 340, 285–295. doi:10.1016/j.virol.2005.06.020
Zhang, X., Tian, W., Cai, X., Wang, X., Dang, W., Tang, H., Cao, H., Wang, L., Chen, T., 2013. Hydrazinocurcumin Encapsuled Nanoparticles "Re-Educate" Tumor-Associated Macrophages and Exhibit Anti-Tumor Effects on Breast Cancer Following STAT3 Suppression. PLoS ONE 8, e65896. doi:10.1371/journal.pone.0065896
Zhao, X.W., Zhao, X.W., van Beek, E.M., van Beek, E.M., Schornagel, K., Schornagel, K., Van der Maaden, H., Van der Maaden, H., Van Houdt, M., Van Houdt, M., Otten, M.A., Otten, M.A., Finetti, P., Finetti, P., Van Egmond, M., Van Egmond, M., Matozaki, T., Matozaki, T., Kraal, G., Kraal, G.,

Birnbaum, D., Birnbaum, D., van Elsas, A., van Elsas, A., Kuijpers, T.W., Kuijpers, T.W., Bertucci, F., Bertucci, F., van den Berg, T.K., van den Berg, T.K., 2011. CD47-signal regulatory protein- (SIRP) interactions form a barrier for antibody-mediated tumor cell destruction. Proc. Natl. Acad. Sci. U.S.A. 108, 18342–18347. doi:10.1073/pnas.1106550108

Zheng, Y., Manzotti, C.N., Liu, M., Burke, F., Mead, K.I., Sansom, D.M., 2004. CD86 and CD80 differentially modulate the suppressive function of human regulatory T cells. J. Immunol. 172, 2778–2784.

Zhu, X.-D., Zhu, X.D., Zhang, J.B., Zhang, J.-B., Zhuang, P.Y., Zhuang, P.-Y., Zhu, H.-G., Zhu, H.G., Zhang, W., Zhang, W., Xiong, Y.Q., Xiong, Y.-Q., Wu, W.Z., Wu, W.-Z., Wang, L., Wang, L., Tang, Z.-Y., Tang, Z.Y., Sun, H.C., Sun, H.-C., 2008. High Expression of Macrophage Colony-Stimulating Factor in Peritumoral Liver Tissue Is Associated With Poor Survival After Curative Resection of Hepatocellular Carcinoma. Journal of Clinical Oncology 26, 2707–2716. doi:10.1200/JCO.2007.15.6521

Zou, W., 2005. Immunosuppressive networks in the tumour environment and their therapeutic relevance. Nat. Rev. Cancer 5, 263–274. doi:10.1038/nrc1586